

# **Oncolytic Adenovirus Vectors for Nitroreductase Suicide Gene Therapy of Prostate Cancer**

**Morgan Reece Herod**

A thesis submitted to the School of Cancer Sciences  
of the University of Birmingham  
for the degree of  
DOCTOR OF PHILOSOPHY

School for Cancer Sciences  
College of Medical and Dental Sciences  
University of Birmingham  
June 2010

UNIVERSITY OF  
BIRMINGHAM

**University of Birmingham Research Archive**

**e-theses repository**

This unpublished thesis/dissertation is copyright of the author and/or third parties. The intellectual property rights of the author or third parties in respect of this work are as defined by The Copyright Designs and Patents Act 1988 or as modified by any successor legislation.

Any use made of information contained in this thesis/dissertation must be in accordance with that legislation and must be properly acknowledged. Further distribution or reproduction in any format is prohibited without the permission of the copyright holder.

## **Abstract**

Prostate cancer is the most common male cancer in the UK and USA, with a 1/13 chance of diagnosis and a 1/30 lifetime risk of death from the disease. Current treatment options include radiotherapy, surgery and hormone therapy, however 1/3 patients escape from all therapies and novel therapies are urgently required for this patient group. The University of Birmingham gene therapy group constructed two oncolytic adenovirus vectors, CRAd-NTR and vNR6, both of which contained the E1B-55K deletion and expressed the transgene nitroreductase for combined oncolytic virotherapy and enzyme/prodrug gene therapy. The latter of these two vectors, vNR6, expressing nitroreductase from the pIX virus promoter demonstrated the greatest cytotoxicity at low virus concentrations however also showed some lytic activity to non-transformed human fibroblasts. Our collaborators at the Institut Català d'Oncologia designed a panel of oncolytic adenovirus vectors with the E1A CR2  $\Delta$ 24 deletion and the E1A promoter replaced by an insulated E2F-1 promoter. The latest two in this series of vectors, termed ICOVIR-5 and ICOVIR-7, provide potential oncolytic backbones for the introduction of the therapeutic transgene nitroreductase. The aim of this thesis was therefore to 'arm' the ICOVIR based vectors with nitroreductase for combined oncolytic virotherapy and enzyme/prodrug therapy. At the beginning of this study no reports were published with either ICOVIR-5 or ICOVIR-7 based vectors. It was therefore first decided to construct both vectors expressing the marker transgene eGFP. These vectors were characterised in terms of cytotoxicity, transgene expression, DNA replication and E1A expression. Furthermore, these vectors were compared to the vNR3, an E1B-55K deleted virus similar to vNR6, but the eGFP ORF replacing that of pIX. The ICOVIR-7 based vectors were identified as being the most tumour selective vectors and demonstrated no cytotoxicity to non-transformed human fibroblasts, and were therefore chosen for the

introduction of the therapeutic transgenes. The new ICOVIR-7 based vectors were constructed to express either wildtype, double mutant or triple mutant nitroreductase. Double and triple mutant nitroreductase are two previously characterised mutant nitroreductases, which show enhanced catalytic activity for the prodrug CB1954. The new nitroreductase expressing ICOVIR-7 vectors were characterised in terms of virus mediated cytotoxicity, tumour selectivity, E1A and NTR expression and cytotoxicity with the prodrug CB1954. One vector, expressing double mutant nitroreductase, showed the highest tumour selectivity and greatest combined cytotoxicity with the prodrug CB1954. Furthermore, this vector showed greater tumour selectivity and combined cytotoxicity than the E1B-55K deleted vector vNR6.

## **Acknowledgements**

I would like to thank my supervisors Drs Vivien Mautner and Peter Searle for their guidance throughout my PhD, the critical reading of this thesis and being excellent mentors through the three years. I would also like to thank the gene therapy group for providing a pleasurable and stimulating working environment and supplying three years worth of good times outside the lab. In particular, I would like to mention David Onion and Simon Vass for their generous support and help in the lab.

## Table of Contents

<b>CHAPTER 1</b>	<b>Introduction .....</b>	<b>1</b>
<b>1.1</b>	<b>Gene Therapy .....</b>	<b>2</b>
<b>1.1.1</b>	<b>Monogenic Diseases .....</b>	<b>2</b>
1.1.1.1	Cystic Fibrosis .....	3
1.1.1.2	SCID-X1 .....	4
1.1.1.3	Adenosine Deaminase (ADA) Deficiency .....	5
<b>1.1.2</b>	<b>Other Gene Therapy Targets.....</b>	<b>6</b>
<b>1.1.3</b>	<b>Cancer Gene Therapy.....</b>	<b>7</b>
1.1.3.1	Cancer Gene Therapy Vectors .....	8
1.1.3.1.1	Non-Viral Vectors.....	9
1.1.3.1.2	Viral Vectors .....	9
1.1.3.1.2.1	Retrovirus.....	9
1.1.3.1.2.2	Herpes Simplex Virus .....	12
1.1.3.1.2.3	Adeno-Associated Virus .....	15
1.1.3.1.2.4	Adenovirus .....	18
<b>1.2</b>	<b>Adenovirus.....</b>	<b>19</b>
<b>1.2.1</b>	<b>Capsid Structure and Organisation .....</b>	<b>20</b>
<b>1.2.2</b>	<b>Core Structure and Genome Organisation.....</b>	<b>25</b>
1.2.2.1	Early Gene Expression.....	26
1.2.2.1.1	E1 .....	26
1.2.2.1.2	E2 .....	31
1.2.2.1.3	E3 .....	32
1.2.2.1.4	E4 .....	35
1.2.2.2	Intermediate Gene Expression .....	39
1.2.2.3	Late Gene Expression .....	41
<b>1.2.3</b>	<b>Adenovirus Lytic Life Cycle .....</b>	<b>45</b>
<b>1.2.4</b>	<b>Current Adenovirus Cancer Gene Therapy Strategies.....</b>	<b>55</b>
1.2.4.1	Replication Deficient Adenovirus Vectors .....	56
1.2.4.1.1	p53 Tumour Suppressor Replacement .....	58
1.2.4.1.2	Enzyme – Prodrug Therapy .....	59
1.2.4.1.2.1	Herpes Simplex Virus Thymidine Kinase – Ganciclovir .....	60
1.2.4.1.2.2	Cytosine deaminase – 5-Fluorocytosine .....	63
1.2.4.1.2.3	Nitroreductase – CB1954.....	63
1.2.4.2	Oncolytic Adenoviruses .....	66
1.2.4.2.1	Adenovirus Gene Deletions .....	66
1.2.4.2.2	Promoter Replacements .....	70
1.2.4.3	Oncolytic Adenoviruses Carrying Transgenes .....	73
1.2.4.4	Improved Adenovirus Systems .....	74
1.2.4.4.1	Retargeting to Tumours .....	74
1.2.4.4.2	Improving Tumour Specificity .....	78
1.2.4.4.3	Improving Enzyme-Prodrug Systems .....	82
<b>1.3</b>	<b>Prostate Cancer Gene Therapy .....</b>	<b>84</b>

1.3.1	The Prostate and Prostate Cancer.....	84
1.3.2	Molecular Mechanisms of Prostate Cancer.....	85
1.3.3	Current Prostate Cancer Therapy.....	87
1.3.4	Gene Thereapy Strategies for Prostate Cancer.....	88
1.4	Aims of Thesis.....	90
<b>CHAPTER 2 Materials and Methods.....</b>		<b>91</b>
2.1	Suppliers of Materials.....	92
2.2	Molecular Cloning.....	92
2.2.1	Restriction Endonuclease Digestion of DNA.....	92
2.2.2	Phenol/Chloroform Extraction.....	92
2.2.3	Precipitation of DNA.....	93
2.2.4	Agarose Gel Electrophoresis.....	93
2.2.5	Gel Purification of DNA Fragments.....	94
2.2.6	Quantitation of DNA.....	94
2.2.7	DNA Ligations.....	94
2.2.8	Polymerase Chain Reaction (PCR).....	95
2.2.9	DNA Sequencing.....	98
2.2.10	Preparation of Chemically Competent Cells.....	99
2.2.11	Bacterial Transformation.....	99
2.2.12	Small Scale Preparation of Plasmid DNA.....	100
2.2.13	Large Scale Preparation of Plasmid DNA.....	101
2.3	Tissue Culture.....	102
2.3.1	Maintenance of Cell Lines.....	102
2.3.2	Cell Counting.....	103
2.3.3	Cryogenic Preservation of Cell Lines.....	104
2.4	Adenovirus Methods.....	104
2.4.1	Adenovirus Rescue by Calcium Phosphate Co-Precipitation.....	105
2.4.2	Harvesting of Adenovirus Seed Stocks.....	105
2.4.3	Infecting Tissue Culture Cells with Adenovirus Seed Stock.....	106
2.4.4	Plaque Purification of Adenovirus.....	106
2.4.5	Caesium Chloride Purification of Adenovirus.....	107
2.4.6	Plaque Assay for Quantitation of Infectious Viral Particles.....	107
2.4.7	Quantitation of Virus Particle Number by PicoGreen Assay.....	108
2.4.8	Infecting Monolayers with Banded Virus Stocks.....	108
2.5	Measurement of Cell Viability.....	109
2.5.1	Acid Phosphatase Cell Viability Assay.....	109
2.5.2	MTS Cell Viability Assay.....	109
2.6	Extraction of DNA and RNA.....	110
2.6.1	Extraction of DNA from Virus Seed stocks.....	110
2.6.2	Extraction of DNA from CsCl Purified Virus.....	110
2.6.3	Extraction of Total DNA.....	110

2.6.4	Extraction of Total RNA .....	111
2.7	DNA and RNA Detection.....	111
2.7.1	Quantitative-PCR (Q-PCR) .....	111
2.7.2	Production of cDNA by Reverse Transcription .....	113
2.7.3	Relative Quantification.....	114
2.8	Detection of Proteins by Western Blotting .....	115
2.8.1	Preparation of Protein Samples.....	115
2.8.2	Protein Quantitation by Bradford Assay.....	115
2.8.3	SDS-Polyacrylamide Gel Electrophoresis (SDS-PAGE) .....	115
2.8.4	Western Blotting .....	116
2.9	Imaging Techniques.....	118
2.9.1	Flow Cytometry.....	118
2.9.1.1	GFP Sample Preparation and Antibody Staining.....	118
2.9.1.2	Analysis of Cells by Flow Cytometry.....	119
2.9.2	Microscopy.....	120
2.10	Graph Plotting and Statistical Analysis .....	120
<b>CHAPTER 3</b>	<b>vMH Vector Construction .....</b>	<b>121</b>
3.1	Introduction.....	122
3.2	Aim of Chapter.....	124
3.3	Overview of Vector Design.....	124
3.4	Virus Cloning Strategy .....	126
3.5	Virus Recovery and Verification .....	132
3.6	Discussion.....	139
3.6.1	Virus Construction and Screening .....	139
3.6.2	Virus Titres and Particle to Infectivity Ratios .....	139
3.7	Summary.....	140
<b>CHAPTER 4</b>	<b>Characterisation of vMH Viruses.....</b>	<b>141</b>
4.1	Introduction.....	142
4.2	Aims of Chapter .....	143
4.3	Results .....	143
4.3.1	CAR and Integrin Expression.....	143
4.3.2	Cytotoxicity of vMH Vectors .....	145
4.3.3	eGFP Transgene Expression with vMH Vectors .....	152

4.3.4	DNA Replication with vMH Vectors.....	156
4.3.5	E1A Expression .....	159
4.3.6	DNA Replication and Transgene Expression in HEK293 Cells .....	165
4.3.7	Cytotoxicity of vMH Vectors in HEK293 Cells.....	169
4.3.8	Sequencing the ICOVIR-7 Promoter in vMH6 and vMH7 .....	171
4.3.9	Lytic Timecourse in DU145.....	172
4.3.10	Effect of Transgene Insertion .....	174
4.3.10.1	Comparison of vMH6 and vMH7 with vICOVIR-7.....	174
4.3.10.1.1	Cytotoxicity of vICOVIR-7 vs vMH6 and vMH7 .....	174
4.3.10.1.2	Restriction Profiling and PCR Screening of vICOVIR-7 .....	177
4.3.10.2	Cytotoxicity of vPS1393 vs vMH Vectors .....	184
4.3.11	Transduction of Carcinoma Cell Lines.....	189
4.3.12	Virus Dissemination in Monolayers .....	191
4.4	Discussion.....	197
4.4.1	Lytic Activity and Therapeutic Index .....	197
4.4.2	E1A Expression in vMH Viruses .....	201
4.4.3	Effect of Transgene Insertion .....	204
4.4.4	RGD-Retargeted Fibre .....	205
4.4.5	Virus Dissemination in Monolayers .....	206
4.5	Summary.....	207
<b>CHAPTER 5 Characterisation of NTR Expressing Vectors .....</b>		<b>208</b>
5.1	Introduction.....	209
5.2	Aim of Chapter.....	210
5.3	Construction of NTR Expressing ICOVIR-7 Vectors .....	210
5.4	Results .....	214
5.4.1	vPS1361 and vPS1362 DNA replication.....	214
5.4.2	Cytotoxicity of vPS136X Vectors.....	216
5.4.3	vMH6/7 vs vPS136X Vectors .....	221
5.4.4	vPS136X NTR Expression.....	223
5.4.5	vPS136X E1A Expression.....	225
5.4.6	vPS136X ICOVIR-7 Promoter Sequencing.....	227
5.4.7	Cytotoxicity of vPS136X Vectors with CB1954.....	227
5.5	Discussion.....	236
5.5.1	Construction of vPS136X Vectors and P:I Ratios .....	236
5.5.2	vPS136X Cytotoxicity and Therapeutic Index .....	239
5.5.3	E1A Expression and Promoter Sequencing.....	242
5.5.4	NTR Expression and NTR/CB1954 Mediated Cytotoxicity.....	244
5.6	Summary.....	248

<b>CHAPTER 6</b>	<b>Summary and Future Work.....</b>	<b>249</b>
------------------	-------------------------------------	------------

## List of Figures

Figure 1-1. Gene therapy trials by target .....	7
Figure 1-2. Vectors used in gene therapy clinical trials.....	9
Figure 1-3. Organisation of adenovirus capsid .....	21
Figure 1-4. Cryo-electron microscopy of polypeptide IX location.....	23
Figure 1-5. Ad 5 genome schematic .....	26
Figure 1-6. Ad E1A protein-protein interactions .....	28
Figure 1-7. Function of the E3 region.....	33
Figure 1-8. Functions of the E4 proteins .....	36
Figure 1-9. Transcription from the major late promoter.....	41
Figure 1-10. PKR inhibition by adenovirus VA RNA.....	45
Figure 1-11. Adenovirus fibre and knob domain structure.....	47
Figure 1-12. Adenovirus DNA replication model .....	50
Figure 1-13. CB1954 reduction by nitroreductase.....	64
Figure 3-1. Schematic of the ICOVIR-5 and ICOVIR-7 promoters.....	123
Figure 3-2. Schematic of vMH viruses .....	126
Figure 3-3. vMH Virus construction ‘road map’ .....	129
Figure 3-4. PCR screening vMH vectors for E1A CR2 $\Delta$ 24 deletion .....	134
Figure 3-5. PCR screening vMH vectors for eGFP insertion .....	136
Figure 4-1. Surface CAR and integrin expression of the cells used in this study.....	144
Figure 4-2. Dose response curves for vMH cytotoxicity .....	148
Figure 4-3. Therapeutic indices for vMH vectors.....	151
Figure 4-4. eGFP percentage positive with vMH vectors.....	153
Figure 4-5. eGFP MFI with vMH vectors .....	156
Figure 4-6. DNA replication of vMH vectors.....	158
Figure 4-7. Western blots for E1A expression with vMH vectors .....	161
Figure 4-8. rtQ-PCR for E1A expression with vMH vectors .....	164
Figure 4-9. DNA replication of vMH vectors in HEK293 cells .....	166
Figure 4-10. vMH eGFP expression in HEK293 cells .....	168
Figure 4-11. Dose response curves for vMH cytotoxicity in HEK293 cells .....	170
Figure 4-12. Lytic timecourse for vMH vectors .....	173
Figure 4-13. Dose response curves for vMH6 and vMH7 vs vICOVIR-7 cytotoxicity .....	176
Figure 4-14. Restriction enzyme profile of Ad5 wt and vICOVIR-7 .....	178
Figure 4-15. Schematic of PCR primers covering E1A and its promoter region .....	180
Figure 4-16. E1A PCR screening of vICOVIR-7 .....	180
Figure 4-17. SacII restriction enzyme profile of vICOVIR-7MHB1 .....	184
Figure 4-18. Dose response curves for vPS1393 cytotoxicity .....	186
Figure 4-19. Dose response curves for vPS1393 cytotoxicity in HEK293 cells .....	188
Figure 4-20. Transduction of CAR negative cells by vMH vectors .....	190
Figure 4-21. Infectious centre assays for vMH vectors in DU145 cells.....	192
Figure 4-22. Fluorescence microscopy images of representative vMH vector plaques .....	194
Figure 4-23. Infectious centre assays for vMH vectors in MRC5 cells.....	196
Figure 5-1. Schematic of vPS136X Vectors .....	211
Figure 5-2. DNA replication profile of vPS1361 and vPS1362 .....	215
Figure 5-3. Dose response curves for vPS136X cytotoxicity .....	218
Figure 5-4. Therapeutic index values for vPS136X vectors .....	220
Figure 5-5. Cytotoxicity of vPS136X vs vMH6 and vMH7 in DU145 cells.....	222

Figure 5-6. Western blot of NTR expression in vPS136X and vNR6 .....	224
Figure 5-7. Western blot for E1A expression in vPS136X vectors .....	226
Figure 5-8. Dose response curves for 16 hour CB1954 exposure .....	229
Figure 5-9. Dose response curves for combined cytotoxicity with 16 hour CB1954 exposure .....	231
Figure 5-10. Dose response curves for 4 hour CB1954 exposure .....	234
Figure 5-11. Dose response curves for combined cytotoxicity with 4 hour CB1954 exposure .....	235
Figure 5-12. Scatter plot of vector size vs P:I ratio .....	238

## List of Tables

Table 1-1. Adenovirus type classification and associated disease.....	20
Table 1-2. Clinical trials since 2000 using replication deficient Ad – HSVtk-GCV.....	62
Table 1-3. Clinical trials with ONYX-015 from 2002 onwards .....	69
Table 1-4. CRAd promoter replacements .....	71
Table 1-5. CRAd with tissue specific promoters .....	80
Table 1-6. Prostate cancer gene therapy trials reported ongoing.....	89
Table 2-1. PCR primers used for cloning, screening and sequencing .....	97
Table 2-2. Bacterial growth medium .....	99
Table 2-3. Cell lines and culture media .....	103
Table 2-4. Primers and probes for Q-PCR.....	112
Table 2-5. E1A primers and probe.....	114
Table 2-6. Antibodies used in western blotting .....	117
Table 2-7. Antibodies used for flow cytometry .....	119
Table 3-1. Starting plasmids used in the study .....	127
Table 3-2. Virus recovery combinations.....	133
Table 3-3. Virus particle count, plaque count and P:I ratios. ....	138
Table 4-1. EC50 values with 95% C.I. (PFU/cell) for vMH cytotoxicity .....	149
Table 4-2. EC50 values with 95% C.I. (PFU/cell) in HEK293 cells.....	170
Table 4-3. EC50 values with 95% C.I. for vMH6 and vMH7 vs vICOVIR-7 .....	177
Table 4-4. Predicted PCR bands with E1A screening primes .....	180
Table 4-5. EC50 values with 95% C.I. (PFU/cell) for vMH vectors and vPS1393.....	187
Table 4-6. EC50 values with 95% C.I. (PFU/cell) for cytotoxicity in HEK293 .....	188
Table 4-7. Rank scoring from 1 - 7 (most - least) of vMH vectors .....	198
Table 4-8. p53, pRb, E2F and Ad receptor levels of prostate cancer cell lines.....	200
Table 5-1. Particle count, plaque count and P:I ratios of NTR expressing vectors .....	213
Table 5-2. EC50 values with 95% C.I. (PFU/cell) for vPS136X induced cytotoxicity.....	219
Table 5-3. EC50 values with 95% C.I. (PFU/cell) for vPS136X vs vMH6 and vMH7 .....	222
Table 5-4. EC50 values with 95% C.I. (PFU/cell) after 16 hours CB1954 exposure .....	230
Table 5-5. EC50 values with 95% C.I. (PFU/cell) for 4 hour CB1954 exposure.....	234
Table 5-6. Rank scoring from 1 - 7 (most - least) of vPS136X vectors .....	240

## Abbreviations

<b>5-FC</b>	5-fluorocytosine
<b>5-FU</b>	5-fluorouracil
<b>50x TAE</b>	242g of Tris.HCl, 57.1ml of glacial acetic acid, 18.2g of disodium EDTA in 1 litre of ddH <sub>2</sub> O
<b>AAV</b>	Adeno-associated virus
<b>Ab</b>	Antibody
<b>Ad</b>	Adenovirus
<b>ADA</b>	Adenosine demaninase
<b>ADP</b>	Adenovirus death protein
<b>AP</b>	Acid phosphatase
<b>APS</b>	Ammonium persulphate
<b>AR1</b>	Auxiliary region 1
<b>AR2</b>	Auxiliary region 2
<b>ATP</b>	Adenosine triphosphate
<b>BAC</b>	Bacterial artificial chromosome
<b>bp</b>	Base pair
<b>CAR</b>	Coxsackievirus and adenovirus receptor
<b>CD</b>	Cytosine deaminase
<b>CF</b>	Cystic fibrosis
<b>CFTR</b>	CF transmembrane conductance regulator
<b>CIAP</b>	Calf intestine alkaline phosphatase
<b>CMV</b>	Cytomegalovirus
<b>CPE</b>	Cytopathic effect
<b>CRAd</b>	Conditionally replicating adenovirus
<b>DBP</b>	DNA binding protein
<b>dCMP</b>	Deoxycytidine monophosphate
<b>ddH<sub>2</sub>O</b>	Double de-ionised water
<b>DM-1</b>	Myotonic dystrophy locus
<b>DME</b>	Dulbecco's modified Eagle medium
<b>DMSO</b>	Dimethyl sulphoxide
<b>EDTA</b>	ethylenediamine tetra-acetic acid
<b>eGFP</b>	Green fluorescent protein
<b>ER</b>	Endoplasmic reticulum
<b>FCS</b>	Foetal calf serum
<b>FITC</b>	Fluorescein isothiocyanate
<b>FX</b>	Factor X
<b>g</b>	Gravity
<b>GON</b>	Groups of nine
<b>HEPES</b>	N-(2-hydroxyethyl)piperazine-N'-(2ethanesulphonicacid);4-(2-hydroxyethyl)piperazine-1-ethanesulphonic acid
<b>HIV</b>	Human immunodeficiency virus
<b>HLA</b>	Human leukocyte antigen
<b>HRP</b>	Horse radish peroxidase
<b>HSPG</b>	Heparan sulphate proteoglycans
<b>HSV</b>	Herpes simplex virus
<b>hTERT</b>	human telomerase reverse transcriptase

<b>II</b>	Polypeptide II
<b>III</b>	Polypeptide III
<b>IIIa</b>	Polypeptide IIIa
<b>IFN</b>	Interferon
<b>Ig(G)</b>	Immunoglobulin (G)
<b>IRES</b>	Internal ribosome entry site
<b>ITR</b>	Inverted terminal repeat
<b>IV</b>	Polypeptide IV
<b>IVa2</b>	Polypeptide IVa2
<b>K</b>	Kozak sequence
<b>kb</b>	Kilo-base
<b>kDa</b>	Kilo-Dalton
<b>LATs</b>	Latence-associated transcripts
<b>LB</b>	Luria Bertani medium
<b>LTR</b>	Long terminal repeat
<b>M</b>	Molar
<b>MFI</b>	Mean fluorescent intensity
<b>mg</b>	Milligram
<b>MHC</b>	Major histocompatibility complex
<b>ml</b>	Millilitre
<b>MLP</b>	Major late promoter
<b>MLTU</b>	Major late transcription unit
<b>mM</b>	Millimolar
<b>MOI</b>	Multiplicity of infection
<b>MoMLV</b>	Mouse moloney leukemia virus
<b>µg</b>	Microgram
<b>µl</b>	Microlitre
<b>µm</b>	Micrometer
<b>µM</b>	Micromolar
<b>NF-I</b>	Nuclear factor I
<b>NF-II</b>	Nuclear factor II
<b>NF-III</b>	Nuclear factor III
<b>ng</b>	Nanogram
<b>nm</b>	Nanometer
<b>nM</b>	Nanomolar
<b>NTR</b>	Nitroreductase
<b>O.D.</b>	Optical density
<b>ORF</b>	Open reading frame
<b>p</b>	Precursor protein
<b>P:I</b>	Particle to infectivity ratio
<b>PBS</b>	Phosphate buffered saline
<b>PCR</b>	Polymerase chain reaction
<b>PFU</b>	Plaque forming unit(s)
<b>PI</b>	Post infection
<b>PIN</b>	Prostatic intraepithelial neoplasia
<b>PKC</b>	Protein kinase C
<b>PKR</b>	Protein kinase R
<b>PMT</b>	Photo multiplier tube

<b>Pol</b>	Ad encoded DNA polymerase
<b>pRb</b>	Retinoblastoma protein
<b>PSA</b>	Prostate specific antigen
<b>Q-PCR</b>	Quantitative polymerase chain reaction
<b>RID</b>	Receptor internalisation and degradation
<b>rpm</b>	Revolutions per minute
<b>RT</b>	Room temperature
<b>rtQ-PCR</b>	Reverse transcriptase Q-PCR
<b>S.D.</b>	Standard deviation
<b>S.E.M.</b>	Standard error of the mean
<b>SCID</b>	Severe combined immunodeficiencies
<b>SDS</b>	Sodium dodecyl sulphate
<b>SIN</b>	Self inactivating
<b>SOC</b>	Super optimal broth with Catabolite repression
<b>SOB</b>	Super optimal broth
<b>solution 1</b>	50mM glucose, 25mM Tris pH8, 10mM EDTA
<b>solution 2</b>	0.2M NaOH, 1% (w/v) SDS
<b>solution 3</b>	147g potassium acetate and 57.5ml glacial acetic acid in 500ml ddH <sub>2</sub> O
<b>STAT</b>	Signal transduction and activation of transcription
<b>T<sub>10</sub>E<sub>1</sub></b>	10mM Tris, 1mM EDTA, pH 8
<b>T<sub>10</sub>E<sub>1</sub>N<sub>100</sub></b>	10mM Tris, 1mM EDTA, 100mM NaCl, pH 8
<b>T<sub>10</sub>E<sub>5</sub>N<sub>100</sub></b>	10mM Tris, 5mM EDTA, 100mM NaCl, pH 8
<b>TAF</b>	TBP associated factors
<b>TBP</b>	TATA binding protein
<b>TEMED</b>	N,N,N',N'-tetramethylethylenediamine
<b>TI</b>	Therapeutic index
<b>tk</b>	thymidine kinase
<b>TNF</b>	Tumour necrosis factor
<b>TP</b>	Terminal protein
<b>TPL</b>	Tripartite leader
<b>TRAIL</b>	TNF related apoptosis-inducing ligand
<b>Tris</b>	Tris(hydroxymethyl)methylamine
<b>Tween</b>	Polyoxyethylene-sorbitan monooleate
<b>UV</b>	Ultraviolet
<b>UXP</b>	U exon protein
<b>V</b>	Volts
<b>v/v</b>	Volume by volume
<b>VA RNA</b>	Virus associated RNA
<b>VDEPT</b>	Virus directed enzyme prodrug therapy
<b>VP</b>	Virus particles
<b>w/v</b>	Weight by volume
<b>wt</b>	Wildtype
<b>X</b>	Polypeptide X
<b>X-SCID</b>	X-linked severe combined immunodeficiency syndrome

# **CHAPTER 1**

## **Introduction**

## **1.1 Gene Therapy**

Gene therapy is the therapeutic delivery of exogenous genetic material including DNA, RNA or oligonucleotides, into the cells of an organism for the treatment of a disease. Over the past 50 years gene therapy has progressed from a theoretical principle into clinical trials, with over 1000 clinical trials completed to date [www.wiley.co.uk, Dec. 09]. In 2004 China became the first country to approve a commercial gene therapy product for the treatment of cancer patients [Peng, 2005].

The primary objective of this study is the development of adenovirus vectors for cancer gene therapy. However initial gene therapy attempts focused on treating single gene defects, an approach which is still in trial and has had impact on the gene therapy of cancer. This introduction will therefore briefly review some key examples of gene therapy of single gene defects, before discussing some of the viral vectors used for cancer gene therapy. The biology of adenoviruses will be discussed in greater detail, before reviewing the application of adenoviruses for cancer gene therapy.

### **1.1.1 Monogenic Diseases**

The single gene defects that give rise to monogenic diseases provide a relatively easy target for gene therapy by simply introducing the wildtype gene into the cells with the mutant version. Thus monogenic diseases were the first targets for gene therapy. This next section will cover some of the efforts to treat monogenic diseases, which have had implications for the treatment of more complex diseases such as cancer.

### 1.1.1.1 Cystic Fibrosis

With a prevalence of approximately 1 in 2000, cystic fibrosis (CF) is the most common lethal hereditary disease among Caucasians. The disease presents itself as chronic lung inflammation, chronic pulmonary infection and digestive problems and at best reduces life expectancy to 45 years [Bobadilla et al, 2002; FitzSimmons, 1993]. CF is the result of a mutation within the cystic fibrosis transmembrane conductance regulator (*cftr*) gene, which produces a mutant CFTR protein with a defective cAMP-regulated chloride channel function [Bear et al, 1992; Riordan et al, 1989]. This is located on the long arm of chromosome 7 [Knowlton et al, 1985] and the most common mutation was shown to be a whole codon deletion resulting in the loss of phenylalanine at position 505 [Kerem et al, 1989].

CF is a good target for gene therapy as the single gene defect makes it easy to replace, the mutant *cftr* gene is recessive suggesting gene dose is not critical and the accessibility of the lung should make it easy to treat. Furthermore the progressive nature of the disease means that a normal phenotype is present at birth, providing a window for treatment [Lee et al, 2005].

Gene therapy has focused on using adenovirus (Ad), adeno-associated virus (AAV) or cationic liposomes to deliver the entire 6.5kb wildtype *cftr* gene or 4.45kb *cftr* cDNA [reviewed by Lee et al, 2005].

The first gene therapy trial for CF was conducted in 1993 using a replication deficient Ad vector [Wilson et al, 1994] and many subsequent trials using Ad vectors have been conducted. Unfortunately multiple groups have identified several limitations with Ad based delivery. The thick bacterially infected mucus that covers the CF airway presents a barrier for gene delivery [Stern et al, 1998]. Inflammatory responses have consistently been

identified with Ad vectors due to innate immunity, cell-mediated immunity and humoral immune responses [Lee et al, 2005; Schwiebert, 2004]. Poor *cfr* gene transduction has been observed with Ad vectors, in part due to the lack of the primary adenovirus receptor CAR, on the luminal surface of respiratory cells. However CF still remains one of the primary targets for gene therapy and different strategies are being investigated to overcome the limitations and setbacks identified so far [review by Mueller and Flotte, 2008].

#### **1.1.1.2 SCID-X1**

X-linked severe combined immunodeficiency (SCID-X1) disease is caused by mutations within the cytokine receptor common gamma chain ( $\gamma_c$ ). The  $\gamma_c$  cytokine receptor subunit forms part of the receptor complex for cytokines such as interleukins 2, 4, 7, 9, 15 and 21, and its functional loss is characterised by a complete block in T and NK lymphocytes differentiation. Patients with SCID-X1 or so-called 'Bubble babies' suffer severe clinical infections and have exceptionally low life expectancies [Cavazzana-Calvo and Fischer, 2007; Fischer, 2000].

Gene therapy trials of SCID-X1 commenced in 1999 in London and Paris, using a non-replicating retroviral vector expressing the  $\gamma_c$  cDNA from the long terminal repeat (LTR) in CD34+ haematopoietic cells. Nine out of 10 patients from the Paris trial showed emergence of gene-corrected T and NK cells, with 7 of these 9 patients reaching normal T cell counts. Even after 8 years these patients remain immunocompetent [Cavazzana-Calvo and Fischer 2007; Hacein-Bey-Abina et al, 2002].

Unfortunately 4 patients from this trial have developed lymphoproliferative disease from clonal T cell proliferation, leading to the death of one patient, with the remaining 3 under chemotherapy and in complete remission. In three of the 4 patients the disease was the result of a single retroviral integration event, causing aberrant expression of the LIM

domain only 2 (*LMO2*) proto-oncogene. From the London trial one of ten patients developed leukaemia post treatment, also associated with insertional activation of the *LMO2* gene, but is now in complete remission. Unfortunately *LMO2* mediated oncogenesis is poorly understood and it is not clear whether retroviral insertion alone accounts for the malignant transformation [Hacein-Bey-Abina et al, 2003; reviewed by Qasim et al, 2009].

Extensive efforts have been made by researchers to improve the safety of viral vectors that function by genome insertions, such as inhibiting unwanted expression and promoting site directed integration (see section 1.1.3.1.2.1). However the use of integrating vectors may be essential for the long-term expression of therapeutic genes.

### **1.1.1.3 Adenosine Deaminase (ADA) Deficiency**

ADA deficiencies contribute to approximately 20% of all severe combined immunodeficiencies (SCID). The ubiquitous enzyme ADA reversibly converts adenosine and 2'-deoxyadenosine to inosine and 2'-deoxyinosine, respectively. ADA patients have mutations within the ADA gene, resulting in a build-up of adenosine and deoxyadenosine both of which are indirectly toxic to lymphocytes. In most cases ADA deficiency results in very low T and B cell counts, which can be accompanied by skeletal abnormalities and neurological problems [Fischer 2000].

Gene therapy trials have been conducted for the treatment of ADA deficiency, through the *ex vivo* transduction of autologous T cells and haematopoietic stem cells with a retrovirus expressing ADA followed by re-infusion [Cavazzana-Calvo and Fischer 2007]. In general, gene therapy trials using this system in conjunction with replacement ADA (either bovine ADA or PEG-ADA) were not greatly successful. It would seem that the treatment with replacement ADA negated the selective advantage of transduced cells over un-transduced cells. However no toxicity was observed, and in many patients the transduced T cells

persisted for several years. Since the initial attempts clinical trials have been more successful by using improved gene transfer protocols and no PEG-ADA. Combined results from three trials treating over 20 patients have shown limited toxicity and at least a partial recovery of immune function. Taken together these trials demonstrate direct clinical benefit from gene therapy of ADA deficiency. In comparison to previous SCID-X1 trials no patients in ADA deficiency trails showed problems from retroviral integration into known oncogene sequences, demonstrating the future potential of ADA gene therapy [reviewed by Gaspar et al, 2009].

### **1.1.2 Other Gene Therapy Targets**

Following the initial gene therapy trial for ADA deficiency in 1990 it was quickly realised gene therapy held potential for the treatment of a wide range of diseases. Since then clinical trails have been initiated for cardiovascular, infectious, neurological and ocular diseases plus 17 other monogenic disease (summarised in Figure 1-1), all of which are outside the scope of this work, but have been extensively reviewed previously [Edelstein et al, 2004]. Over recent years the greatest effort has been focused on gene therapy of cancer diseases.

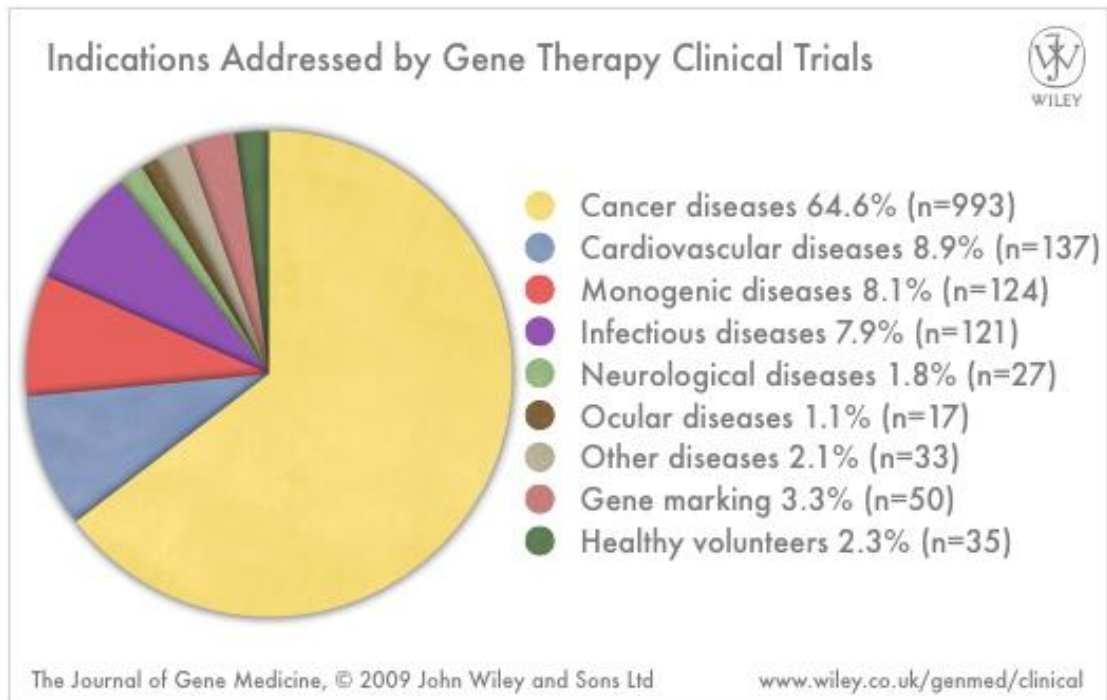


**Figure 1-1. Gene therapy trials by target**

Worldwide gene therapy trials by disease. [www.wiley.co.uk, Dec. 09].

### 1.1.3 Cancer Gene Therapy

Over the past three decades worldwide efforts have led to an increase in our understanding of the molecular mechanisms and pathogenesis of cancer. Whereas cancer incidence rates have increased over the past 38 years, mortalities due to all cancers have decreased. Still more than 155,000 (>30% of the total deaths) people died from cancer in 2007 in the UK alone [www.statistics.gov.uk/statbase/, Dec. 09].

Current treatments for cancer comprise surgery, chemotherapy, radiotherapy and hormone therapy. However, current treatments often have unwanted side effects and do not guarantee a cure. This emphasises the need for new cancer therapies, reflected in the fact that over 60% of all gene therapy trials conducted to date are for the treatment of cancer (Figure 1-1).

Currently several gene therapy strategies have been investigated for the treatment of cancer. All gene therapy strategies require a vector to deliver the therapeutic nucleic acids into target cells. This next part covers some vectors that have been investigated for cancer gene therapy; briefly addressing non-viral vectors before reviewing the more frequently used viral gene delivery vectors. Following this general introduction adenovirus will be discussed in more detail, first by summarising the adenovirus lifecycle before focusing on how these viruses are used for cancer gene therapy.

### **1.1.3.1 Cancer Gene Therapy Vectors**

Two thirds of all ongoing gene therapy clinical trials use viral vectors for the delivery of genetic material. This can be sub-divided into 6 main virus vectors, summarised in Figure 1-2, demonstrating the wide range of vectors, which have been used for the delivery of therapeutic genes. In addition to these vectors several non-viral methods have been investigated, including physical, chemical and bacterial vectors.

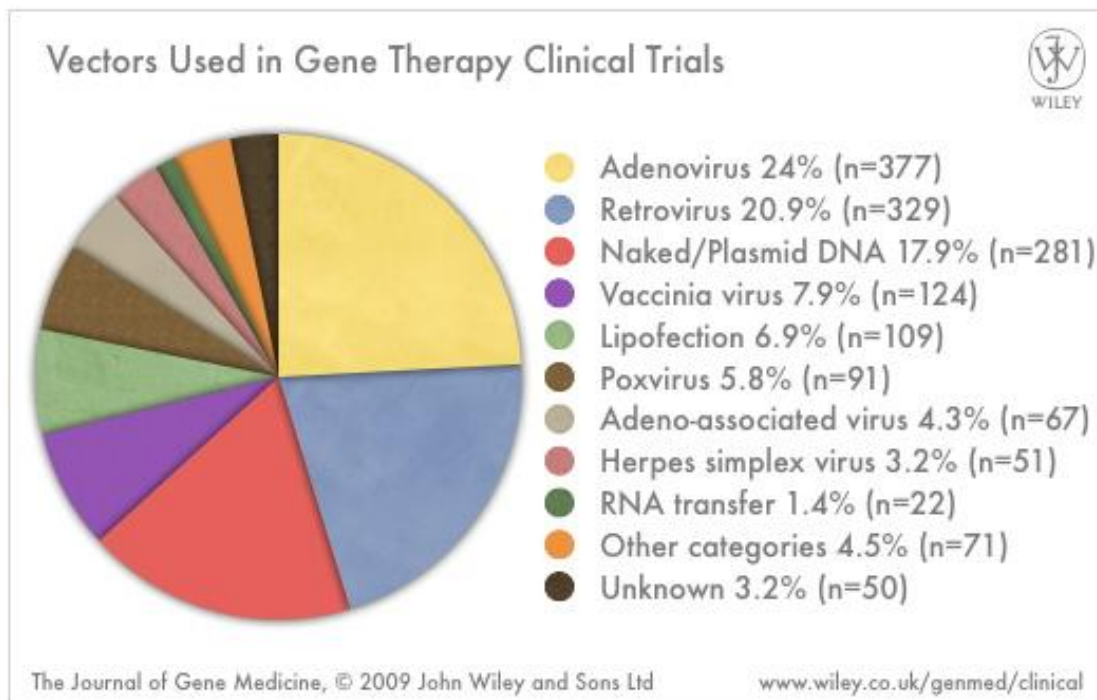


**Figure 1-2. Vectors used in gene therapy clinical trials**  
Gene therapy trials by vector. [www.wiley.co.uk, Dec. 09].

### 1.1.3.1.1 Non-Viral Vectors

The non-viral gene delivery vectors can be divided into three sub-groups; physical gene delivery, chemical gene delivery and non-viral biological gene delivery. Numerous studies have investigated methods for non-viral gene delivery, all of which are outside the scope of this thesis, however the more advanced ones have been reviewed previously [Gao et al, 2007; Niidome and Huang, 2002; Seow and Wood, 2009].

### 1.1.3.1.2 Viral Vectors

#### 1.1.3.1.2.1 Retrovirus

*Retroviridae* are a large family of viruses split into two subfamilies; *Orthoretrovirinae* which contains 6 recognised genera (*alpharetrovirus*, *betaretrovirus*, *deltaretrovirus*,

*epsilonretrovirus, gammaretrovirus and lentivirus*) and *Spumaretrovirinae* which only contains one recognised genera (*spumavirus*) [www.ictvonline.org, Dec. 09]. All retroviruses are lipid enveloped single-stranded RNA viruses with a genome of 7-13kb and contain long terminal repeat sequences (LTR), which flank retroviral genomes of varied complexity. The simplest retroviral genomes encode just 3 genes: *gag*, *pol* and *env*, which can be found in all retroviral genomes. More complex retroviruses, such as the lentivirus HIV-1, can encode multiple accessory proteins, which have added functions in the viral life cycle [Hu and Pathak, 2000].

Retroviral infection starts with entry of the virion core into the host cell. The viral RNA genome is reverse-transcribed into a linear dsDNA genome by the viral encoded reverse transcriptase. The dsDNA genome is transported to the nucleus where it is integrated into the host cell genome. The integrated virus, termed provirus, is transcribed by cellular RNA polymerase II. A fraction of transcribed viral RNA is translated by cellular machinery to produce the viral proteins. The remaining full length viral RNA assemble with viral proteins to form the progeny virions, which bud out of host cells [Hu and Pathak 2000].

Many of the initial cancer gene therapy studies used retroviral vectors. To date retroviruses remain the second most used vector for gene therapy (see Figure 1-2). Most cancer gene therapy studies use non-replicating retroviruses, in which up to 8kb of transgenes are flanked by LTR sequences. Virion packaging is enabled by the packaging sequences, generally located within or near the LTR. Production of such gutted vectors requires the essential viral genes (*gag*, *pol* and *env*) to be supplied in *trans*, normally from a packaging cell line.

Most early studies used the Moloney murine leukaemia virus (MoMuLV), with transgene expression from the promoter/enhancer elements present in the U3 region of the 5' LTR,

which is copied from the 3' LTR upon reverse transcription. Self inactivating or SIN vectors were developed, which have the promoter/enhancer elements within the U3 region of the 3' LTR deleted, thus upon reverse transcription and provirus formation, the resulting 5' LTR also lacks these transcriptional regulatory sites. Transgene expression is then driven from specific promoter/enhancer elements inserted upstream of the transgene, but outside the LTR regions. SIN vectors therefore allow greater regulation of transgene expression and also greater safety by reducing the possibility of activating adjacent cellular oncogenes [Yu et al, 1986].

MoMuLV cannot cross the nuclear membrane and therefore can only transduce dividing cells. This can be a significant disadvantage since at any one time not all tumour cells will be dividing. It is worth noting that some groups have found this an advantage, when the requirement is to target dividing cells [Liu and Deisseroth, 2006].

To overcome this problem new generations of lentivirus vectors were created, generally based around human immunodeficiency virus 1 (HIV-1). These vectors are able to transduce both dividing and non-dividing cells, greatly widening the target cell types. Extensive work has since been performed using lentiviral vectors to improve production, transduction and transgene expression [review by Delenda, 2004; and Liu and Deisseroth 2006].

Multiple studies have used pseudotyped lentiviral vectors to expand upon the natural cellular tropism. Pseudotyping is achieved by incorporating heterologous viral glycoproteins into the viral envelope and has been performed with both lentiviral and non-lentiviral glycoproteins [reviewed by Cronin et al, 2005].

All retroviral vectors are able to support long-term transgene expression, often a requirement for a gene therapy vector. However, retrovirus integration favours

transcriptional active gene regions, leading to the possibility oncogenesis [Ciuffi et al, 2005; Ciuffi et al, 2006]. However by using SIN and non-integrating vectors these dangers can be reduced.

Retroviral vectors have been used extensively *in vitro* with several different strategies for cancer gene therapy [and by Dalba et al, 2007; reviewed by Kafri, 2004]. These have translated into over 20 phase II trials using different strategies, however only the thymidine kinase – ganciclovir system has been put into phase III clinical trails [www.wiley.co.uk, Dec. 09].

#### **1.1.3.1.2.2 Herpes Simplex Virus**

There are two types of herpes simplex virus, type 1 (HSV-1) and type 2 (HSV-2), which are part of the large family of *Herpesviridae* and fall into the genus *Simplexviruses* [www.ictvonline.org, Dec. 09]. HSV-1 is a large enveloped virus, with a dsDNA genome of approximately 150kb, and can undergo both a lytic and latent life cycle. HSV-1 lytic infection begins with entry into the host cell, where the viral dsDNA enters the nucleus along with the viral structural protein VP16. Following entry a cascade of gene expression is activated, starting with immediate-early gene expression that is activated by VP16. Immediate-early gene expression is followed by expression of early and late genes, which encode the proteins required for DNA replication and the viral structural proteins. New virions are assembled and released by lysis of the host cell [Burton et al, 2001; Shen and Nemunaitis, 2006].

Upon entry into neuronal cells, HSV-1 can undergo lytic infection, but can alternatively enter a latent infection. In latent infection the viral genome persists as a stable episomal unit that adopts a chromatin-like structure. During latency no immediate early, early or late genes are expressed, but a set of nontranslated RNA species termed the latency-associated

transcripts (LATs) are synthesised from the inverted repeat sequences. Latency can persist for many years, and sometimes the entire lifetime of the host. Alternatively latent infection can revert to lytic infection, typically following environmental stresses and immunosuppression [Burton et al, 2001; Shen and Nemunaitis 2006]. The exact mechanism behind the latent to lytic transition is unknown, however recent studies have implicated chromatin as an important factor in the switch from latent to lytic infection [reviewed by Knipe and Cliffe, 2008].

Gene therapy vectors based on HSV-1 were primarily developed for targeting the central nervous system. Initially HSV-1 vectors were developed into 2 different vector systems: recombinant and amplicon. More recently a third system has been developed using oncolytic HSV-1 vectors.

Recombinant HSV-1 are non-replicating vectors, which contain deletions in genes essential for virus replication. Use of packaging cell lines to complement the removal of essential genes allow relatively high titres of virus to be produced [Dobson et al, 1990]. Large deletions in essential genes can allow them to accommodate 30kb of transgenes inserts. Recombinant vectors retain most of the viral genome, leaving the possibility of low level viral gene expression, leading to an immune response and subsequent cytotoxicity [Burton et al, 2001].

HSV amplicons are non-replicating vectors, which contain no viral genes. Their genome consists of a circular DNA element, which contains one copy of the origin of replication and packaging sequences, leaving up to 130kb free for insertion of large or multiple transgenes. Production of amplicon vectors requires all the viral genes to be supplied in *trans*, since they contain no viral genes themselves. This can be achieved by using non-replicating helper viruses, which yield amplicon vector stocks contaminated with helper

viruses [Spaete and Frenkel, 1982]. Helper virus contamination can give rise to an unwanted HSV helper virus directed immune response, along with some associated toxicity. Helper virus contamination can be overcome by using a packaging defective, replication-defective helper HSV-1 genome. Alternatively, all the genes essential for virus replication can be supplied in *trans* from overlapping cosmid vectors or bacterial artificial chromosomes [Fraefel et al, 1996; Sena-Esteves et al, 2000]. Removal of helper virus contamination eliminates most of the associated immune response and toxic side effects. However, such methods are more complicated and yield lower virus titres [all reviewed by Epstein, 2005].

The first replication competent oncolytic herpes viruses were developed in 1991 and tested using subcutaneous and subrenal malignant gliomas in nude mice [Martuza et al, 1991]. Since then many conditionally replicating HSV-1 vectors have been constructed, for the treatment of a wide range of human cancers [reviewed by Varghese and Rabkin, 2002]. The first generation vectors contained single deletions or mutations in genes essential for viral replication in normal cell, but which could be partially substituted in cancer cells, (e.g. deletion of the HSV encoded thymidine kinase). These vectors were selective for replication in dividing cells, and were unable to replicate in non-dividing cells. However these vectors were found to be non-specific in their replication and showed associated neurotoxicity. Subsequent second and third generation conditionally replicating vectors were created which contained multiple deletions/mutations in viral genes.

More recently tumour or tissue targeted vectors have been engineered, by the insertion of tumour/tissue specific promoters and insulator elements. These vectors showed better tumour specificity and reduced neurovirulence [Ring, 2002; Varghese and Rabkin 2002]. All HSV-1 oncolytic vectors are able to carry very large transgene insertions (up to 30kb),

due to the large number of non-essential genes that can be removed. Furthermore many non-essential genes are associated with neurovirulence; hence their deletion can increase the safety of the vector, while also increasing the transgene capacity. These facts, coupled with their ability to replicate in a large range of tumour cell types, make them ideal for oncolytic cancer gene therapy.

HSV vectors have been tested in clinical trials for the treatment of a variety of cancers including glioma, melanoma, head-and-neck cancer, prostate cancer and mesothelioma, which have been previously reviewed [reviewed by Shen and Nemunaitis 2006].

#### **1.1.3.1.2.3 Adeno-Associated Virus**

Adeno-associated virus (AAV) was initially discovered in 1965 contaminating stocks of simian adenoviruses [Atchison et al, 1965]. Since then human AAV has emerged as a small collection of viruses, numbering only 7 species (11 serotypes) that belong to the genus of *Dependovirus*, within the family of *Parvoviridae* [Choi et al, 2005; www.ictvonline.org, Dec. 09]. AAV is one of the smallest viruses, with a non-enveloped capsid 22-26nm in diameter. AAV has an ssDNA genome, of approximately 4.7kb that contains two open reading frames (ORF) and inverted terminal repeat (ITR) sequences flanking either end of the genome. The two ORF, *rep* and *cap*, encode for all the 7 AAV proteins, through the use of alternative promoters and differential splicing. The *rep* ORF produces 4 proteins that are involved in viral DNA replication (Rep proteins), while the *cap* ORF produces the 3 viral capsid proteins (VP1-3) [Goncalves, 2005]. The ITR elements contain the minimal *cis*-acting sequences required for DNA replication and packaging. AAV can undergo two separate lifecycles: a lytic and a lysogenic [reviewed by Goncalves 2005].

AAV lytic growth requires co-infection with helper viruses such as adenovirus (mediated by the E1, E2A, VA RNA and E4orf6 proteins) or herpes simplex virus (mediated by the

Helicase/primase complex, DNA binding protein, ICP0, ICP4 and DNA polymerase complex). Helper virus infection activates the AAV gene expression cascade, which leads to Rep mediated provirus excision. Viral DNA replication and packaging follow, both of which require the viral ITR sequences. Stress conditions such as metabolic inhibitors and DNA damage have also been shown to induce low level AAV lytic growth, in the total absence of helper virus, demonstrating AAV is not absolutely replication defective [Yalkinoglu et al, 1988].

In absence of a helper virus AAV normally undergoes lysogenic infection. Within lysogenic infection minimal AAV gene expression acts to auto-repress full AAV gene expression and the genome is integrated into the host genome as a provirus. Viral genome integration preferentially targets a 2kb region on the long arm of human chromosome 19 [Kotin et al, 1990; Samulski et al, 1991]. Site specific integration requires *cis* components supplied by the ITRs and two viral encoded Rep proteins, Rep78 and Rep68; without these integration is random.

AAV are attractive gene therapy vectors because they can infect a wide range of cell types, both dividing and non-dividing, and can persist over several years, allowing long-term gene expression.

AAV vectors have all viral genes deleted, containing only transgenes flanked by the viral ITRs. Due to the comparatively small genome size up to 4.7kb of transgenes can be inserted, in comparison to other vectors that can carry much large inserts (such as herpes simplex virus) [Flotte, 2000]. Furthermore, transgene expression takes substantially longer than other vectors, requiring several weeks to months in certain situations [Fisher et al, 1997]. However studies using so called 'self-complementary' vectors, which form dimeric genomes to alleviate the requirement of host cell mediate second strand viral DNA

synthesis, have been shown to greatly reduce this time [McCarty et al, 2001]. Because AAV vectors are essentially 'guttled', vector production requires all viral genes to be supplied *in trans*, and can be done through co-infection with helper virus such as adenovirus. AAV vectors need to be separated from helper virus, bringing the possibility of helper virus contamination. Alternatively the AAV viral genes and essential helper viral genes can be expressed on plasmids. Whereas this method can eliminate helper virus contamination, it is substantially more complicated and harder to scale up for clinical applications [Goncalves 2005]. Removal of all viral genes leaves open the possibility of insertional mutagenesis, as site direct integration requires the Rep proteins. Indeed integration seems to prefer transcriptionally active regions, however much also seems to remain as episomal concatemers [Nakai et al, 2003; Tenenbaum et al, 2003].

Several cancer gene therapy strategies have been tested *in vitro* and in mouse animal models, and such strategies have been reviewed several times previously [Coura and Nardi, 2007; for reviews see Li et al, 2005; and Park et al, 2008]. As yet no cancer gene therapy trials using AAV have been reported, but 15 clinical trials from phases I-III are ongoing for the treatment of prostate cancer [www.wiley.co.uk, Dec. 09]. A recent series of studies have used AAV vectors in *in vivo* mouse and rat models to treat retinitis pigmentosa and leber congenital amaurosis, both of which cause progressive visual loss and are caused by defects in AIPL1. This series of studies used AAV in gene replacement therapy and have demonstrated long-term rescue of these photoreceptor-specific defects, with a minimal immune response that allow repeat vector administration [Barker et al, 2009; Sun et al, 2010; Tan et al, 2009].

#### **1.1.3.1.2.4 Adenovirus**

To date over three hundred gene therapy trials have used adenovirus based vectors. These account for almost a quarter of all gene therapy clinical trials conducted worldwide (see Figure 1-2). Adenovirus vectors have been used in the gene therapy of many simple and complex diseases such as ornithine transcarbamylase deficiency, coronary heart disease, angina and cystic fibrosis. However, most adenovirus gene therapy has focused on the treatment of cancer, giving rise to several alternative strategies.

To further elaborate on how adenoviruses have been used in gene therapy, the next section will cover adenovirus in detail. The basic structure, gene expression and life cycle of adenovirus will be reviewed, before discussing adenovirus vectors for cancer gene therapy.

## 1.2 Adenovirus

Adenoviruses were first discovered over 50 years ago by two groups simultaneously. Rowe *et al*, investigating spontaneously degrading adenoids tissue, showed a transmissible agent was present in 62% of adenoid specimens [Rowe et al, 1953] . A second group studying an epidemic of respiratory disease in American army recruits recovered a new unidentified transmissible agent [Hilleman and Werner, 1954]. It soon became clear that both agents belonged to the same family, and the name of adenovirus (Ad) was put forward [Enders et al, 1956]. It was soon discovered that human adenoviruses form part of a large family of viruses, which are present in a range of vertebrates including primates, birds, reptiles, amphibians and fish.

Currently the *Adenoviridae* family is divided into five main genera, of which human adenoviruses fall into the *Mastadenoviridae* genus. The other main genera are *Aviadenoviridae*, *Atadenoviridae*, *Ichtadenovirus* and *Siadenoviridea* with recent suggestions to add other minor genus [Davison et al, 2003; www.ictvonline.org, Dec. 09].

To date there are 52 serotypes of human adenoviruses which fall into 7 species, named A-G, many of which cause a range of disease, summarised in Table 1-1.

Species	Types	Typical Associated Diseases
A	12, 18, 31	Gastroenteritis, hepatitis (Ad31)
B1	3, 7, 16, 21, 50	Acute respiratory infections, conjunctivitis (Ad3 and 7)
B2	11, 14, 34, 35	Renal infections (Ad11, 34 and 35) and some acute respiratory tract infections
C	1, 2, 5, 6	Respiratory tract infections
D	8, 9, 10, 13, 15, 17, 19, 20, 22-30, 32, 33, 36-39, 42-49, 51	Keratoconjunctivitis (Ad8, 19, 37)
E	4	Respiratory disease
F	40, 41	Infantile gastroenteritis
G	52	Gastroenteritis?

**Table 1-1. Adenovirus type classification and associated disease**

[Fields, 2007; www.ictvonline.org, Dec. 09]

### 1.2.1 Capsid Structure and Organisation

Adenoviruses are non-enveloped icosahedral shaped viruses measuring approximately 100nm in diameter. Their outer capsid has three principle components; hexon, penton base and fibre, along with several copies of 4 minor capsid components IIIa, VI, VIII and IX [recently reviewed by Russell, 2009]. The location of each capsid component can be seen in Figure 1-3.

Each capsid has 252 principle subunits; 240 of which are hexons that form the 20 facets with 12 hexons per facet. The remaining 12 subunits are comprised of penton base and fibre, which together form the pentons [Ginsberg et al, 1966], located at the apex of five facets, with the fibre projecting from the structural vertex.

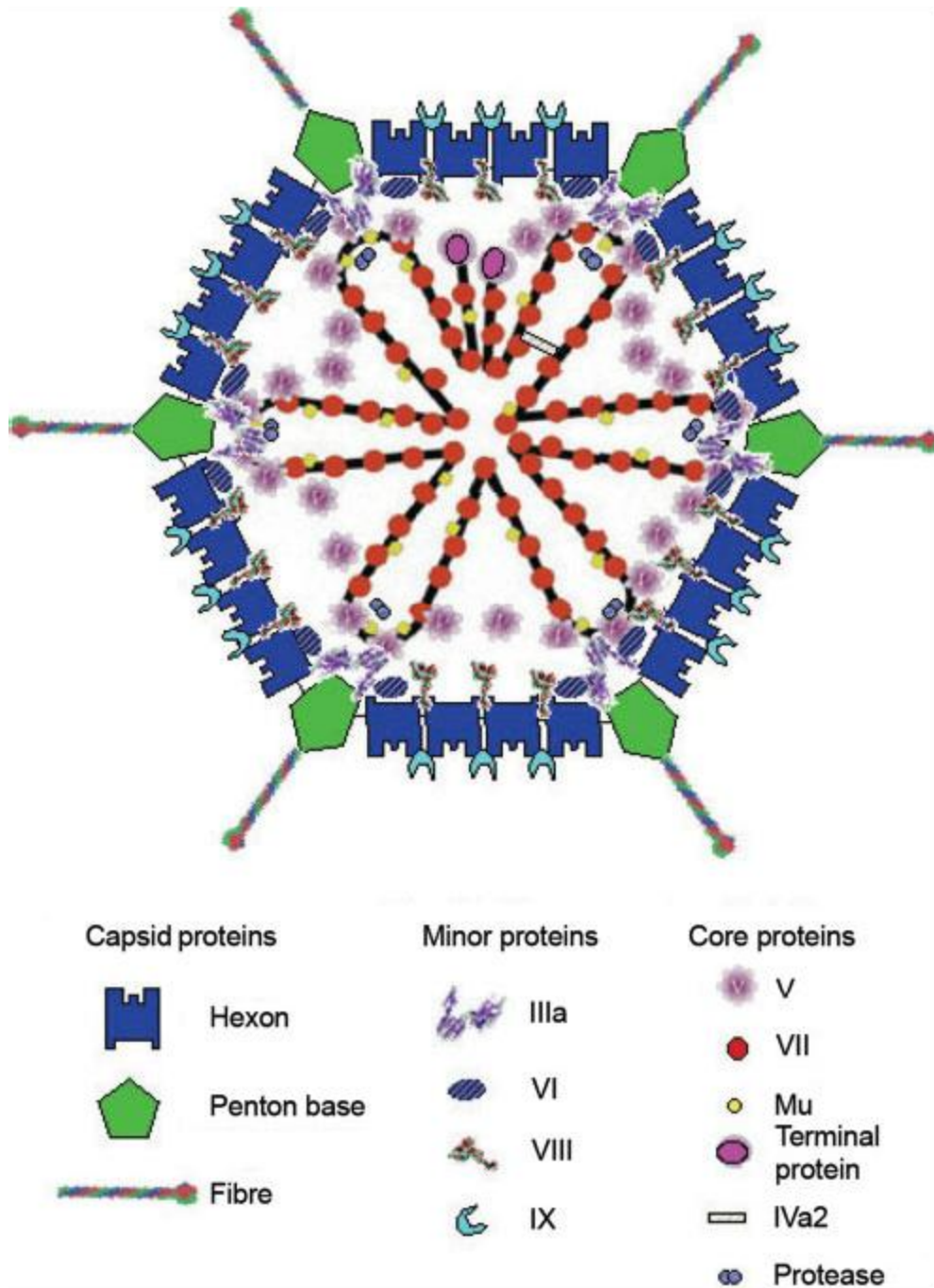


**Figure 1-3. Organisation of adenovirus capsid**

Diagrammatic representation of the adenovirus capsid structure. The outer capsid contains 3 major capsid proteins and 4 minor capsid proteins. The core structure contains 4 structural proteins as well as two non structural proteins: protease and IVa2 [taken from Russell 2009].

Each hexon protein consists of three closely associated molecules of polypeptide II (II) and each penton base consists of 5 copies of polypeptide III (III) [Boudin et al, 1979; Russell 2009]. Three copies of polypeptide IV (IV) form each fibre protein, which bind non-covalently via the N-terminus onto the top surface of penton base to form the pentons. A sequence near the N-terminus of each fibre polypeptide (FNPVYPY) has been shown to lie in a hydrophobic groove on the top surface of penton base. This interaction together with a number of hydrogen bonds and a salt bridge has been suggested to stabilise the fibre – penton base interaction [Zubieta et al, 2005]. All human adenoviruses encode one fibre protein which they use as the primary cell surface receptor, with the exception of species F adenoviruses that encode two separate fibres [Kidd et al, 1993].

Each capsid contains several copies of 4 minor capsid components, IIIa, VI, VIII and IX, the primary function of which is thought to be in stabilising the capsid structure [reviewed by Vellinga et al, 2005].

The minor capsid proteins IIIa, VI and VIII (along with the core proteins VII, TP and Mu) are first synthesised as precursor proteins, designated with a p prefix (i.e. pIIIa is cleaved into polypeptide IIIa). The precursor proteins are cleaved into their mature forms by the adenovirus encoded protease upon virion assembly, discussed further in section 1.2.3.

Each viral particle contains 240 copies of polypeptide IX (IX), which is thought to stabilise hexon-hexon interactions. Following mild dissociation conditions, virions break apart producing groups of nine (GON) hexon proteins, each of which derives from the central region of the capsids icosahedral facets [Colby and Shenk, 1981]. The current model positions the N-terminus of IX as a trimer in the centre of each facet, with the C termini forming a 4 helical bundle consisting of 3 copies of IX from the same facet but different trimers, and one copy of IX from the adjacent facet (see Figure 1-4). Some debate still

remains as to the exact position of IX C-terminus, however it has recently been shown using peptide tagging the IX C-termini associates in an antiparallel manner, most likely within the 4 helical bundles [Fabry et al, 2009; Marsh et al, 2006; Saban et al, 2006].

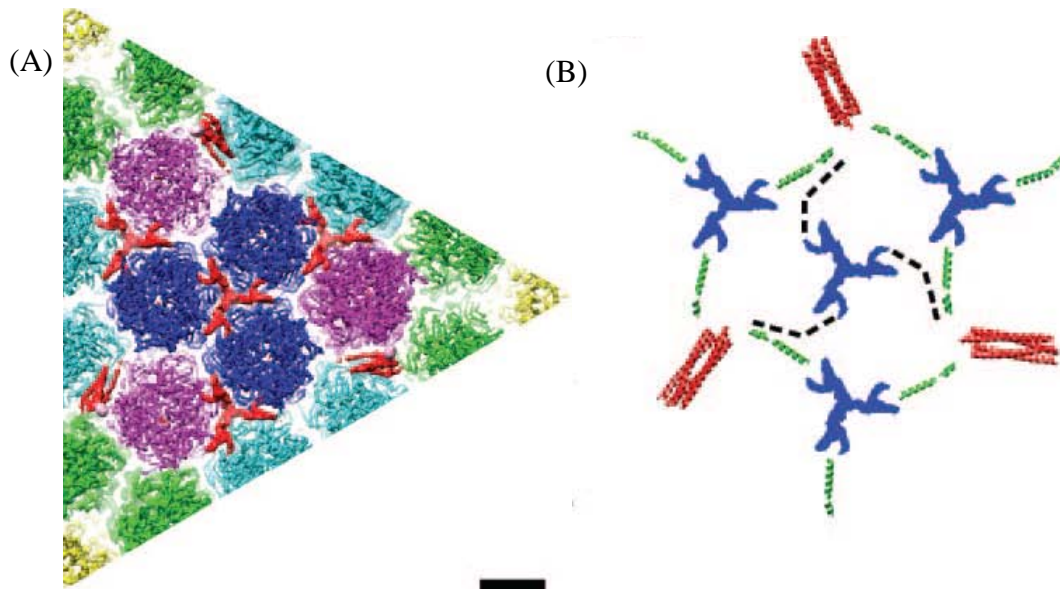


#### **Figure 1-4. Cryo-electron microscopy of polypeptide IX location**

Cryo-electron microscope location of polypeptide IX location in the Ad capsid. A region of a cryo-EM difference map (red) and pseudoatomic capsid showing hexons (green, cyan, blue, magenta), roughly corresponding to one icosahedral facet. Four trimeric density regions and three helix bundles of IX are observed in red (A). Diagram showing the interoperation of the difference map. The four trimeric density regions were assigned to the N-terminal domain of protein IX (blue), the weak density regions were assigned to the midsection of IX (green) and the helical bundles are assigned to the C-terminal  $\alpha$  helix region of IX. The black dotted lines indicated presumed extended connections between central trimeric region and helical bundles. Note, one of the 4 helices in each bundle appears to come from a copy of IX in an adjacent facet (B) [adapted from Saban et al, 2006].

It was shown that when pIX is deleted, virion particles are more heat sensitive and do not form GON under mild dissociation [Colby and Shenk 1981]. Polypeptide IX has also been shown to have additional minor functions in transcriptional regulation (see section 1.2.2.2.). Polypeptide IIIa (IIIa) was found to be an elongated monomer with 5 copies positioned below the penton base at each apex (thus 60 copies altogether) [Saban et al, 2006]. The N-

terminal region associates with penton base, hexons and VI, and has been shown to be positioned beneath the vertex complex, and in wedges at the interface between the penton base and peripentonal hexons [San Martin et al, 2008]. Older co-immunoprecipitation experiments showed that IIIa was in direct contact with the inner capsid protein V and VII [Boudin et al, 1980; Stewart et al, 1993]. It is thought that IIIa has a role in stabilising hexon assembly, and possibly a minor role in the splicing of late gene products, [Molin et al, 2002; Stewart et al, 1993]. However more recent data has pointed to a role in stabilisation of the vertex and the packaged genome.

The exact location of VI in the capsid is still not fully known. However it appears to be in direct contact with the hexon inner cavity, IIIa and penton base, and core protein V [Fabry et al, 2005; Matthews and Russell, 1998; Stewart et al, 1993]. When the virion particle is internalised into the endosome the acidic environment causes a conformational change in virion structure, which allows release of VI from the partially disassembled virus particle. Free VI mediates disruption of the endosomal membrane, releasing the virus for nuclear transport [Wiethoff et al, 2005]. Furthermore, the VI precursor protein (pVI) facilitates the nuclear import of newly synthesised hexon protein [Wodrich et al, 2003] and the C-terminal domain of cleaved pIV acts as a cofactor for the Ad protease, allowing full protease activity [Honkavuori et al, 2004] (discussed in section 1.2.3.).

Polypeptide VIII (VIII) is the least studied minor viral capsid protein. Polypeptide VIII is a 15kDa protein located on the inner capsid surface, both as a ring around peripentonal hexons connecting them to the GONs and in rings stabilising the GONs. In this manner VIII is thought to help stabilize the viral capsid [Liu et al, 1985; Stewart et al, 1993].

### **1.2.2 Core Structure and Genome Organisation**

Adenovirus has a double stranded DNA genome of approximately 36kb, which is located within the virion capsid with 4 virus proteins; VII, V, Mu, and TP (plus also IVa2 and the adenovirus protease) (see Figure 1-3)

Polypeptide VII (VII) is the major core protein and acts like a histone protein, around which the viral genome is wrapped [Chatterjee et al, 1986]. Polypeptide V has been shown to associate loosely with VII and virus DNA and tightly with VI and is thought to be a bridge between core and capsid [Everitt et al, 1975; Russell 2009]. Polypeptide X, also known as Mu, has no clear function. The Mu precursor, pMu, was shown to be required for expression of the pre-terminal protein (pTP) from the E2B region [Lee et al, 2004]. The least abundant protein constituent in the viral core is the Terminal Protein (TP). This protein is present in two copies that are covalently attached to the 5' ends of the viral genome. The TP is essential for viral DNA replication (discussed in section 1.2.3), but also can assist in attachment of the viral genome to the nuclear matrix [Schaack et al, 1990].

The Ad5 genome produces over 50 proteins via convergent transcription from both strands of the viral genome as illustrated in Figure 1-5.

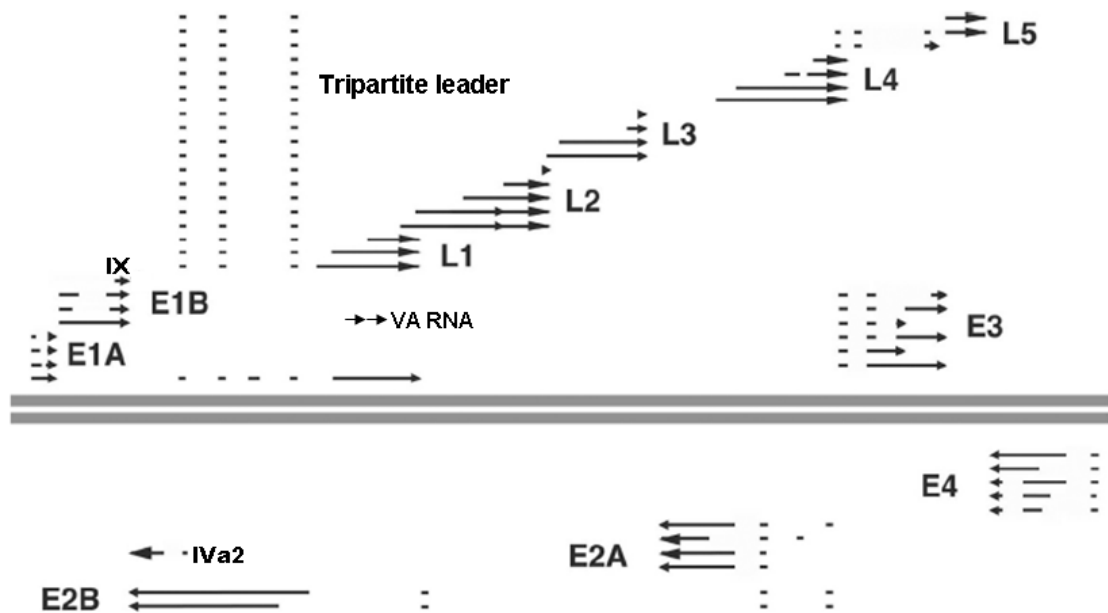


**Figure 1-5. Ad 5 genome schematic**

Adenovirus transcription map. Arrows indicate the direction of transcription [adapted from Wold and Gooding, 1991]

The genome is flanked by inverted terminal repeat (ITR) sequences of 93-371bp (103bp for Ad2 and Ad5), which are essential in viral DNA replication (see section 1.2.3). Adenovirus gene expression is divided into 3 stages; early, intermediate and late, each one of which is discussed in the following sections.

### 1.2.2.1 Early Gene Expression

Early adenovirus gene transcription is divided into 5 transcription units E1A, E1B, E2, E3 and E4.

#### 1.2.2.1.1 E1

The E1A region is the first to be expressed upon viral entry into a cell, from a promoter found immediately downstream of the left ITR. The E1A region is transcribed into 5 mRNA species through differential splicing, two of which are found from early times of

infection with the remaining three accumulating at later times [Chow et al, 1979; Stephens and Harlow, 1987]. The two early expressed mRNA species, 13S and 12S, encode proteins of 289 and 243 amino acids, respectively, commonly referred to as E1A-13S and E1A-12S. A third mRNA species 9S encodes for the E1A-9S protein, which accumulates later in infection.

Upon comparing E1A proteins from a variety of adenovirus serotypes, it became clear that they contain four conserved regions (CR1, 2, 3 and 4, respectively). Further analysis also revealed the N terminus to be important for a wide variety of E1A functions [Berk, 2005]. The 12S and 13S-E1A proteins have identical CR1, 2, 4 and N terminal regions, with only the 13S protein possessing CR3 (see Figure 1-6). The 9S protein only contains the N-terminus and CR1 [Spector et al, 1978].

To date E1A has not be shown to bind any DNA elements, however it has been demonstrated to bind to an extensive range of viral and host proteins, which are mostly involved in modifying gene expression [and Berk 2005; reviewed by Gallimore and Turnell, 2001], summarised in Figure 1-6.

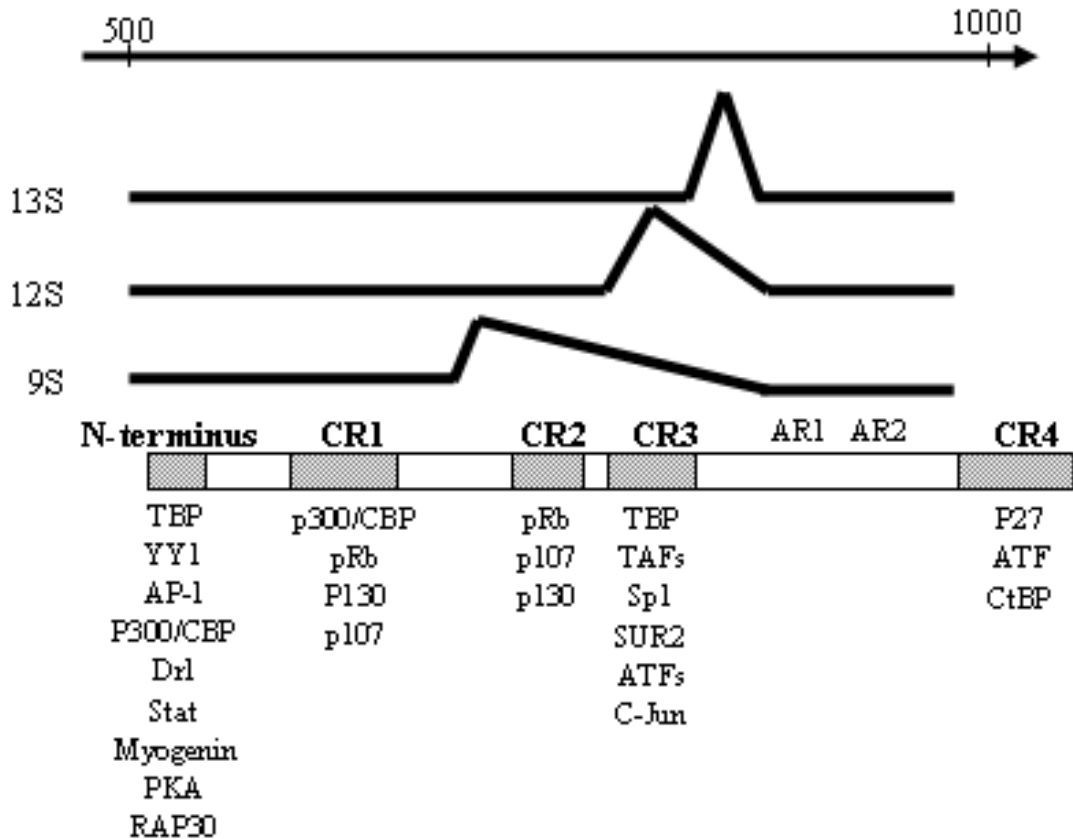


### Figure 1-6. Ad E1A protein-protein interactions

Linear representation of the Ad2/5 E1A 13S protein showing the 13S, 12S and 9S splice variants. Known regions of conservation between serotypes are shaded in grey and some of the known E1A-interacting proteins are shown [and Berk 2005; adapted from Gallimore and Turnell 2001].

Both E1A 12S and 13S proteins can bind to the retinoblastoma (pRb) family of proteins through interactions with the CR1 and CR2 regions [Dyson et al, 1992; Whyte et al, 1988]. The pRb family of tumour suppressor proteins act to regulate gene expression and the cell cycle by sequestering the E2F family of transcription factors. E2F upregulates expression of proteins essential for cell cycle progression (such as DNA polymerase A and c-myc), and facilitates the transition from late G1 phase into S phase. The CR1 and CR2 regions bind to

pRb, allowing the release of E2F and progression of the cell cycle [Bagchi et al, 1990; Bagchi et al, 1991].

Interactions between the CR3 region of E1A-13S and the TATA-binding protein (TBP) have been shown to modulate gene expression. TBP is an important part of TFIID, a transcription factor that can bind the TATA box and up-regulate transcription of many viral and cellular genes [Lee et al, 1991]. The tumour suppressor protein p53 can bind to and inactivate TBP and in doing so suppress transcription. Binding of E1A-13S to TBP blocks the repression by p53, allowing increased transcription [Horikoshi et al, 1995].

E1A can further modulate cellular gene expression through interactions with a wide range of cellular proteins, including: p300/CBP, TBP-associated factors (TAFs), TFIIF rap30 subunit, Sug1, Dr1 and Sur-2 proteins [Berk 2005; Gallimore and Turnell 2001; Turnell et al, 2005]. Early viral gene transcription is highly regulated by E1A. For example, the E2 promoter can be directly activated by E1A through its TATA site, ATF sites or E2F binding sites [reviewed by Shenk, 2001].

The N-terminal region of Ad5 E1A has been shown to directly subvert the host immune response. Signal transduction and activation of transcription (STAT) proteins represent an integral part of the intra-cellular pathway activated by the interferon (IFN) immune response. Upon IFN stimulation STATs activate transcription of cellular immune response genes, partly through recruitment of the p300/CBP complex [reviewed by Goodbourn et al, 2000]. Not only does E1A exhibit p300/CBP interactions, it has been shown to directly bind STATs and downregulate the IFN response [Look et al, 1998].

The E1B region encodes two proteins, 19kDa (E1B-19K) and 55kDa (E1B-55K), produced via differential splicing [Virtanen and Pettersson, 1985]. Embedded within the E1B region is the pIX gene, which is activated from a separate promoter, discussed in section 1.2.2.2.

E1B-19K was initially reported to have both a positive and negative effect on early viral gene transcription. It has since been discovered that E1B-19K is a Bcl-2 homologue, and has a role in blocking both p53-dependent and p53-independent apoptosis [Chiou et al, 1994a; Chiou et al, 1994b; Subramanian et al, 1995]. Bcl-2 is located in the outer mitochondrial membrane and blocks the translocation of cytochrome c from the mitochondrion to the cytoplasm. Upon translocation, cytochrome c activates caspase-9 leading to an apoptotic response [Chiou et al, 1994a; Cuconati et al, 2002].

E1B-55K binds to the amino-terminal activation domain of p53 and in conjunction with E4orf6 blocks p53 dependent apoptosis, relieves a p53 cell cycle block and blocks p53 activated transcription [Ornelles and Shenk, 1991]. In doing so E1B-55K helps create an environment primed for viral DNA replication and gene expression. Further investigation revealed that E1B-55K interacts with E4orf6 along with cellular proteins to form an E3 ubiquitin ligase complex [reviewed by Blackford and Grand, 2009]. This complex targets cellular proteins including p53 and Mre11 for proteasomal degradation and is important in mediating the E1B-55K protein functions. E1B-55K can also form a complex with E4orf3 which re-localises the Mre11 complex to cytoplasmic aggregates. Mre11 is part of the Mre11-Rad50-Nbs1 (MRN) complex responsible for the recognition and repair of DNA double strand breaks. The ends of adenovirus DNA would normally be recognised by the MRN complex as double strand breaks and subsequently “repaired” to form viral DNA concatemers. Thus E1B-55K in complexes with E4orf3 and E4orf6 stops the formation of viral DNA concatemers during infection [Stracker et al, 2002].

Late in infection the E1B-55K-E4orf6 E3 ubiquitin ligase complex is required for the export of late viral mRNA, while also blocking the export of cellular messages, thereby resulting in a cytoplasmic accumulation of late viral mRNA [review by Blackford and Grand 2009].

#### **1.2.2.1.2 E2**

The E2 region consists of the E2A gene, which codes the DNA binding protein (DBP), and the E2B genes, which codes for the pTP and DNA polymerase (Pol). The E2 transcription unit is driven by two promoters; early and late. The E2 early promoter is *trans*-activated early in infection by E1A. Basal activity of this promoter requires the transcription factors TBP, E2F and ATF. TBP and ATF bind their respective binding regions, found within the E2 early promoter at position -23 to -29 and -69 to -76 relative to the transcriptional start site. Located between these sites is the E2F binding palindrome, which binds two heterodimeric complexes of E2F/DP-1 which are dimerised by E4orf6/7. E1A targets all four transcription factors (TBP, ATF, E2F and DP-1) to greatly upregulate transcription [Kovesdi et al, 1987; Schaley et al, 2000; Swaminathan and Thimmapaya, 1996]. During intermediate times of infection the E1A *trans*-activation of the early E2 promoter is blocked, probably by E4orf4-PP2A mediated dephosphorylation of E1A, and the E2 late promoter is activated [Mannervik et al, 1999]. The E2 late promoter contains a TBP binding site, two SP-1 recognition sites and three CAAT boxes. Two CAAT boxes located at positions of -71 and -135 relative to the E2 late transcriptional start site are sufficient for promoter activity and bind the transcription factor YB-1 [Goding et al, 1987; Holm et al, 2002].

All three E2 proteins are primarily involved in viral DNA replication and can be mainly found associated with viral replication centres as infection proceeds (localized nuclear sites

of Ad transcription and DNA replication). The 80kDa pTP is found covalently attached to the 5' end of viral DNA, and is cleaved by the adenovirus protease to a 50kDa mature form (TP) upon viral assembly [Mangel et al, 2003]. The E2B encoded Pol is a distinct DNA polymerase which uses pTP as a protein primer and possesses both 5'-3' polymerase activity and 3'-5' exonuclease activity. The E2A encoded DBP unwinds dsDNA and is required for chain elongation and to stabilise the pTP-DNA interaction. A full description of the pTP, Pol and DBPs roles in the viral lifecycle will be discussed later in section 1.2.3.

Late in infection (following DNA replication) a novel transcription unit is activated, which runs in the same direction as the E2 and E4 early regions. The unit codes for the U exon protein (UXP), from an ORF overlapping with DBP and a small part of L4-100K. UXP expression is from a yet unidentified promoter; however there is a presumed promoter near the 5' end of the UXP mRNA. UXP localises to the nucleolus where it is localised with viral replication centres as infection proceeds. Aberrant DBP localization upon UXP deletion suggests UXP is required for establishment of viral replication centres. The exact function of UXP is currently not known, however deleting UXP seems to cause a mild growth defect and lower yields of progeny virions [Tollefson et al, 2007].

#### **1.2.2.1.3 E3**

The E3 region encodes for proteins involved in evading the host immune system and controlling apoptosis, summarised in Figure 1-7 [reviewed by Horwitz, 2004; and by Lichtenstein et al, 2004b]. The E3 region within species C adenoviruses can be divided into two parts; E3A and E3B, dependant on poly(A) site usage, and produces 7 proteins via differential splicing. At early times post infection expression of the E3 region is from the same E3 promoter region, which like the other early regions is activated by E1A. Several

binding regions for cellular transcription factors including ATF, AP-1 and NF-1 have been identified in the E3 promoter region. E1A can interact with the multiple components of the E3 basal promoter to upregulate E3 transcription [Garcia et al, 1987; Hurst and Jones, 1987; Kornuc et al, 1990]. During late times of infection E3 promoter activity is downregulated and expression of one E3 protein termed adenovirus death protein (ADP) is upregulated from the major late promoter (discussed further in section 1.2.2.3) [Tollefson et al, 1992].

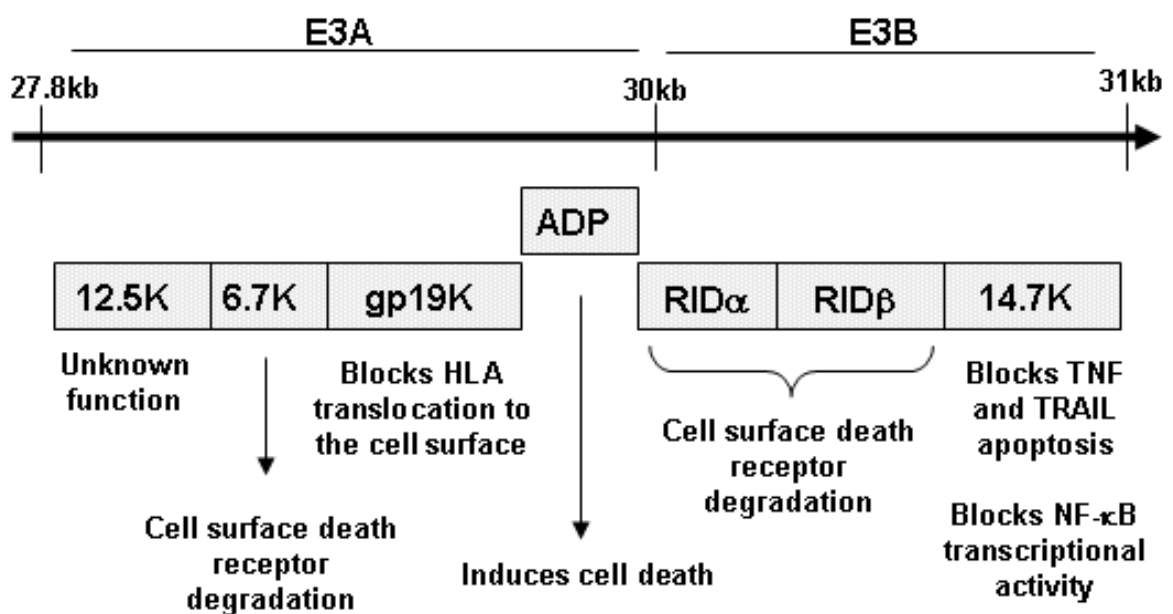


**Figure 1-7. Function of the E3 region**

Schematic representation of the E3 region with the approximate position in the Ad5 genome in kb (not to scale). The E3 region is divided into E3A and E3B, based on poly(A) usage, and is differentially spliced to produce 7 proteins. Proteins are shown as open boxes labelled with the primary functions. Late in infection the E3 promoter is downregulated and ADP is upregulated from the major late promoter.

Two E3 encoded genes, RIDα and RIDβ (also known as E3-14.5K and E3-10.4K, respectively) form a complex termed the receptor internalisation and degradation or RID complex [Tollefson et al, 1991]. The RID complex stimulates the internalisation and degradation of specific cell surface death receptors such as Fas and tumour necrosis factor

(TNF)-related apoptosis-inducing ligand (TRAIL) (including both TRAIL receptor one and two, TR1 and TR2 respectively) [Elsing and Burgert, 1998; Lichtenstein et al, 2002; Tollefson et al, 2001]. This prevents ligand-receptor binding and so blocks apoptosis. E3-6.7K has been shown to block apoptosis both independently and also in conjunction with the RID complex. E3-6.7K localises mainly to the endoplasmic reticulum (ER), with a small amount reaching the plasma membrane [Wilson-Rawls and Wold, 1993] and has been proposed to act in the ER as a general inhibitor of apoptosis, possibly by helping maintain cytosolic calcium homeostasis [Moise et al, 2002]. Furthermore, E3-6.7K can associate with the RID complex to assist in TR2 and possibly TR1 RID mediated degradation, but not Fas or EGFR degradation [Benedict et al, 2001; Lichtenstein et al, 2004a].

The two genes positioned at the ends of the E3 region encode for the distantly related E3-12.5K and E3-14.7K proteins. These are thought to have arisen via gene duplication at an early stage of *Mastadenoviridae* evolution and were subsequently lost in some lineages [Davison et al, 2003]. E3-14.7K can directly block TNF $\alpha$  and TRAIL induced apoptosis and has been linked to blocking Fas induced apoptosis [Chen et al, 1998; Horton et al, 1991; Schneider-Brachert et al, 2006; Tollefson et al, 2001]. More recent studies have suggested E3-14.7K can inhibit NF- $\kappa$ B transcriptional activity, by direct and selective targeting of NF- $\kappa$ B p50 [Carmody et al, 2006]. It is possible this interaction influences the E3-14.7K mediated anti-apoptotic response and expression of inflammatory cytokines such as IL-6 and IL-12.

E3-19K binds to cellular HLA class I molecules in the ER and in doing so prevents their translocation to the cell surface, thus avoiding cytotoxic T cell activated cell death [Burgert and Kvist, 1987; Burgert et al, 1987].

The E3 adenovirus death protein (ADP) or E3-11.6K is only produced in small amounts at early times of infection. ADP production is upregulated approximately 400-fold in late times of infection by expression from the major late promoter [Tollefson et al, 1992]. ADP deleted viruses are typically characterised by a small plaque phenotype, a feature that led to the discovery of ADP function [Tollefson et al, 1996a]. As the name suggests, ADP promotes cell death late in infection and thus aids in the release of progeny virions [Tollefson et al, 1996b]. ADP is a membrane glycoprotein that accumulates in the Golgi body and ER and eventually the nuclear membrane late in infection [Tollefson et al, 2003]. To date the exact mechanism of ADP action is unknown, however ADP must interact with membranes in order to function. Using yeast two hybrid screens ADP has been linked to MAD2B, a protein similar to the spindle assembly checkpoint protein MAD2, and suggests that this interaction is somehow relevant [Ying and Wold, 2003]. Furthermore, ADP can work in both a caspase-dependent and caspase-independent manner [Zou et al, 2004].

#### **1.2.2.1.4 E4**

The E4 region is located at the right hand end of the Ad genome and is transcribed in a leftward direction. This region produces at least 18 distinct mRNA from the same promoter through differential splicing [Virtanen et al, 1984]. These were predicted to produce 7 proteins, named after their corresponding open reading frame (E4orf1, E4orf2, E4orf3, E4orf4, E4orf3/4, E4orf6 and E4orf6/7), six of which have been identified in infected cells (shown in Figure 1-8).

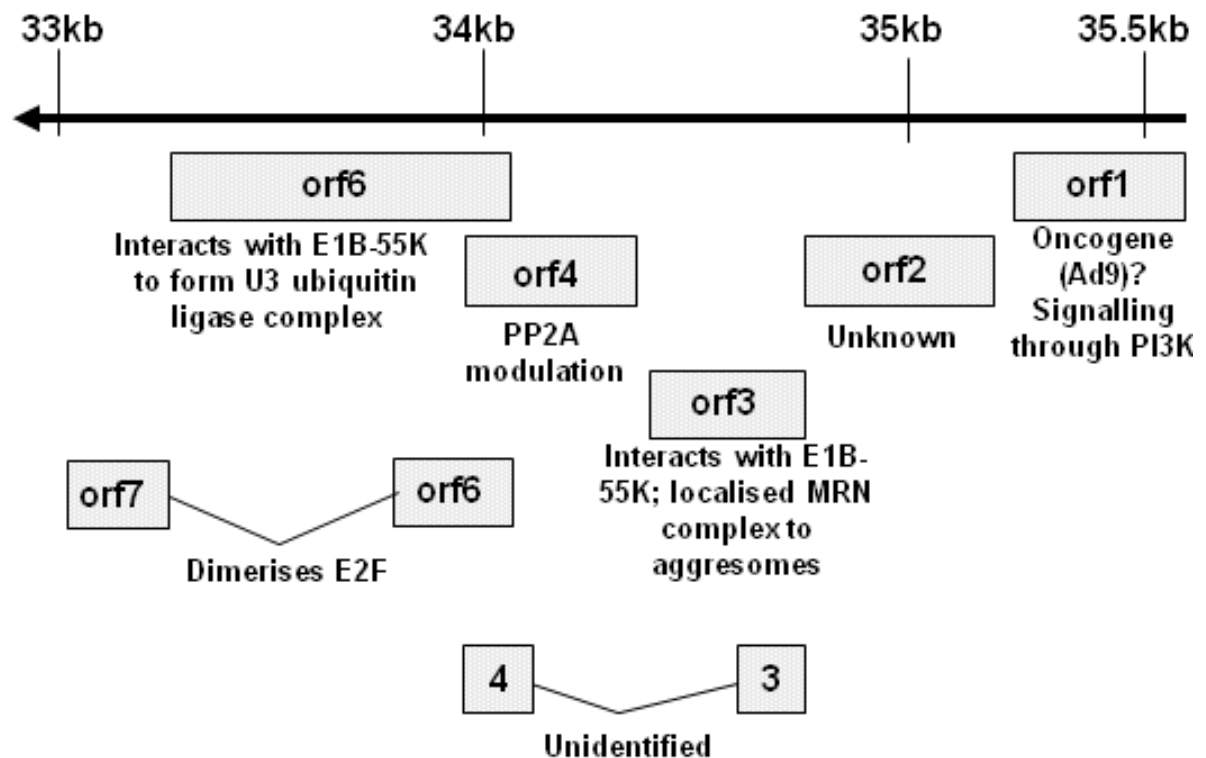


### Figure 1-8. Functions of the E4 proteins

Schematic representation of the E4 region with the approximate position in the Ad5 genome in kb (not to scale). The primary E4 transcript is spliced to produce 7 predicted proteins, shown as open boxes labelled with the known function of each protein. Proteins whose coding regions are split by intron sequences are shown as boxes linked by a line. Overlapping proteins have different polypeptide sequences unless they share the same number [adapted from Leppard, 1997].

Transcription of the E4 region occurs early in infection and is activated by the E1A-13S protein. The E4 promoter region contains binding sites for the transcription factors ATF and E4F. E1A interacts with both ATF and E4F to upregulate transcription, seemingly via two separate pathways. E4F mediated activation involves interaction with the E1A CR3 region, plus two C-terminal regions termed auxiliary regions 1 and 2 (AR-1 and AR-2) [Bondesson et al, 1992; Raychaudhuri et al, 1987]. The AR-1 and AR-2 regions have been suggested to be required for the phosphorylation of E4F, which in turn is required for E4F dependent upregulation [Raychaudhuri et al, 1989]. In contrast ATF mediated upregulation does not

seem to be AR dependent. However conflicting evidence has also demonstrated ATF alone can upregulate transcription independent of E1A [Jones and Lee, 1991; Liu and Green, 1990; Rooney et al, 1990; Strom et al, 1998]. Some of the E4 proteins have functions that are required for lytic growth in tissue culture, whereas others have no clear function [reviewed by Leppard 1997].

E4orf1 was discovered to be a major oncogenic factor of Ad9 in the presence of the E1 region [Javier, 1994]. Further investigations have suggested that E4orf1 from a variety of Ad serotypes has the ability to transform cells in the presence of the E1 region [Weiss and Javier, 1997; Weiss et al, 1997]. The C-terminal PDZ binding domain of E4orf1 was found to be responsible for the transforming activity, by interaction with phosphatidylinositol 3-kinase (PI3K), triggering a downstream signalling cascade to effectors such as protein kinase B (Akt) and mTOR. Through these effectors PI3K alters protein synthesis and cell survival [Frese et al, 2003; O'Shea et al, 2005]. A recent study has also demonstrated E4orf1 limits late viral mRNA translation in cells in G1 phase, and as a result reduces the progeny virus production in an E1B-55K deleted virus [Thomas et al, 2009].

The E4orf2 protein has been shown to be present in Ad infected cells [Dix and Leppard, 1995]. However as of yet no function has been defined for this protein.

The E4 products E4orf3 and E4orf6 are the most studied E4 proteins and can compensate for each other *in vitro*. Both proteins use post-transcriptional mechanisms to cause a cytoplasmic accumulation of late viral mRNAs, resulting in increased viral late proteins. Both proteins have also been shown to alter RNA splicing patterns thus modulating gene translation [Ohman et al, 1993]. E4orf6 interacts with the E1B-55K gene to form an E3 ubiquitin ligase complex which targets cellular proteins such as Mre11 and p53 for degradation. This complex helps to stop viral DNA concatemer formation, blocks the

export of cellular mRNA and increases the export of late viral mRNA [Gonzalez and Flint, 2002; Ornelles and Shenk 1991; Querido et al, 2001a; Querido et al, 2001b]. Older reports have also shown E4orf6 can directly bind p53, in the absence of E1B-55K, and in doing so repress p53 function as a transcriptional activator and block p53 dependent apoptosis [Dobner et al, 1996].

E4orf3 interacts with E1B-55K to relocalise the Mre11 complex to cytoplasmic aggregates to help stop viral concatemer formation [Araujo et al, 2005]. E4orf3 has been shown to reorganise an important group of nuclear transcription/replication factors [Carvalho et al, 1995; Evans and Hearing, 2005]. E4orf3 dependent relocalisation of these factors to virus replication centres helps modulate late viral transcription. Other studies have implicated E4orf3 in the enhancement of S-phase replication and in the repression of the interferon immune response, again by rearrangements of nuclear transcription bodies [Shepard and Ornelles, 2003; Ullman et al, 2007].

E4orf4 has been linked to several functions in the viral life cycle [reviewed by Branton and Roopchand, 2001]. E4orf4 interacts with the B $\alpha$  subunit of protein phosphatase 2A (PP2A), which result in the selective hypophosphorylation of viral and non-viral proteins [Kleinberger and Shenk, 1993; Muller et al, 1992], and it is this interaction which is thought to be responsible for all E4orf4 functions. E4orf4 has been shown to downregulate E1A transcription as well as inhibit E1A mediated transcriptional activation of E4, demonstrating an E1-E4 regulatory feedback loop [Bondesson et al, 1996]. E4orf4 can regulate alternative splicing of adenoviral L1 proteins [Estmer et al, 2001; Kanopka et al, 1998]. E4orf4 can induce p53-independent apoptosis, in both a caspase-dependent and caspase-independent manner, which is dependent on the interaction with the B $\alpha$  subunit of PP2A [Lavoie et al, 2000; Lavoie et al, 1998; Marcellus et al, 2000; Marcellus et al, 1996].

More recent work demonstrated E4orf4 induced a G2/M cell cycle arrest, resulting in cell death, by blocking the PP2A dependent dephosphorylation of proteins involved in cell cycle progression [Li et al, 2009a]. It also appears E4orf4 is targeted to the nucleus and localises primarily in viral replication centres, in nucleoli and in perinuclear bodies. Furthermore this targeting is important in E4orf4 induced cell death and export of late viral mRNAs [Li et al, 2009b; Miron et al, 2009; Miron et al, 2004].

E4orf6/7 is involved in the control of the cellular transcription factor E2F. E4orf6/7 dimerises to link two E2F molecules, which stabilises the binding to specific E2F DNA binding elements [Huang and Hearing, 1989; Obert et al, 1994]. Palindromic E2F binding motifs have been located within the Ad E2 early promoter as well as within the E2F-1 promoter itself. In this way E4orf6/7 helps to activate transcription of E2F responsive genes, such as Ad E2, E2F-1 as well as potentially many other cellular genes [Johnson et al, 1994; Schaley et al, 2005].

#### **1.2.2.2 Intermediate Gene Expression**

Intermediate gene expression coincides with the start of viral DNA replication, after the initiation of early genes but before the onset of late gene expression. There are two genes expressed at intermediate times of infection; protein IVa2 (IVa2) and polypeptide IX (IX).

IVa2 acts as a transcription factor and is important for activation of late gene expression from the major late promoter (MLP). IVa2 can bind a recognition sequence positioned +85 to +120 bases downstream of the MLP transcription start site [Lutz and Kedinger, 1996; Tribouley et al, 1994]. Once bound IVa2 can co-operate with enhancer elements upstream of the MLP to activate transcription, discussed in section 1.2.2.3. Activation of IVa2 transcription first requires removal of the transcriptional repressor IV-RF, which binds to elements downstream of the IVa2 promoter [Huang et al, 2003b]. The mechanism by which

transcriptional repression is removed is not entirely understood but a build-up of viral DNA aids in relieving this block, thus it is speculated IV-RF is titrated out upon viral genome amplification [Iftode and Flint, 2004]. An early viral gene product could also be involved in relieving IVa2 repression and subsequently activating late gene expression. In these models IVa2 acts as part of a 'timer' for virus replication and gene expression.

Polypeptide IX expression begins at intermediate times of infection and levels of pIX increase rapidly at late times of infection. IX is expressed from a separate promoter, embedded within the E1B region, and shares its poly(A) site with the E1B transcripts. During early phases of infection active transcription of E1B through the IX promoter blocks IX expression. Once E1B transcription declines during infection and following DNA replication, IX transcription is allowed to proceed [Fessler and Young, 1998; Vales and Darnell, Jr., 1989]. Outside its role as a structural protein, IX may have functions in transcriptional activation and nuclear reorganisation [reviewed by Parks, 2005; and Vellinga et al, 2005]. Transfection assays showed that IX can enhance expression of both adenoviral and non-adenoviral genes including: E1A, E4, MLP, HSV thymidine kinase and human  $\beta$ -globin. To date IX has not been shown to have any direct DNA binding activity. In addition, IX has been shown to homo-multimerize and has been suggested to interact with other DNA binding elements or transcription factors [Rosa-Calatrava et al, 2001]. More recently IX has been shown to co-localise with promyelocytic leukaemia protein (PML) and in doing so is thought to have a minor or backup role in regulating the cellular antiviral response [Rosa-Calatrava et al, 2003]. However, conflicting evidence using pIX deleted viruses and complementing pIX expression either *in trans* or with stably expressing

cell lines, showed pIX had no effect on E1A expression or virus DNA replication [Sargent et al, 2004].

### 1.2.2.3 Late Gene Expression

Late gene expression is controlled by the major late promoter (MLP), which when fully active produces a primary transcript approximately 29,000 nucleotides long. This primary transcription unit is differentially spliced into multiple mRNAs that are grouped into five families termed L1 to L5 [Nevins and Darnell, Jr., 1978] based on the utilization of common poly(A) sites (Figure 1-9), which encode 18 proteins.

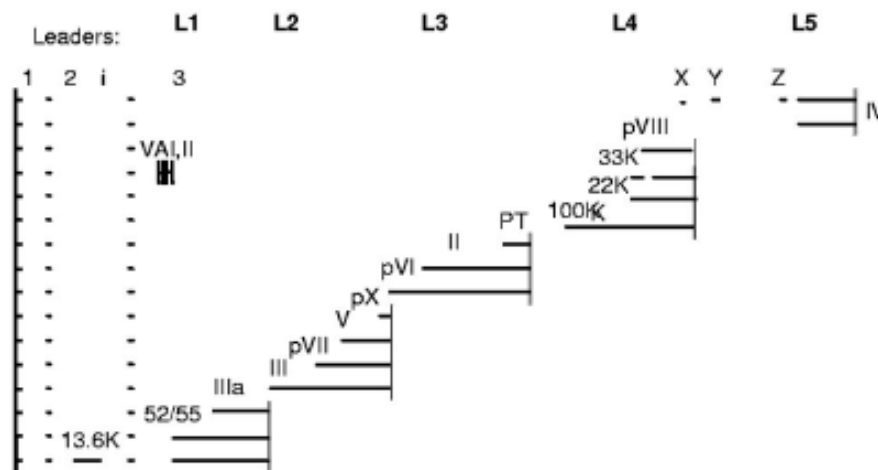


**Figure 1-9. Transcription from the major late promoter**

Schematic diagram of the Ad2/5 major late transcription unit, showing the alternatively spliced mRNAs and encoded proteins. The 5 families, L1-L5 are labelled along with the obligate leaders sequences; 1, 2, 3 and the optional leaders; i, x, y and z [adapted from Morris and Leppard, 2009].

All major late transcripts are spliced to start with the tripartite leader (TPL) sequence. The TPL consists of 3 small sequences, termed 1, 2, and 3, which are spliced to the 3' acceptor sites within the main MLTU body [Logan and Shenk, 1984]. The TPL is important for nuclear export, translation and major late mRNA stability [reviewed by Young, 2003]. In

addition to sequence 1, 2 and 3, which are present in all MLP transcripts four additional leader sequences have been identified; i, x, y and z, which are used less frequently. Despite the name, the MLP is active at low levels at early times of infection, producing transcripts which preferentially end at the L1 poly(A) site (and do not extend beyond the L3 poly(A) site) [Symington et al, 1986]. This results in production of large amounts of L1-52/55K mRNA, most of which use the optional i-leader sequence, inserted between leaders 2 and 3 [Nevins, 1981; Nevins and Wilson, 1981].

Post Ad DNA replication MLP promoter activity is upregulated by multiple factors which act on sequences both upstream and downstream of the transcriptional start site. E1A can strongly activate the MLP through binding the TATA motif and through interactions with Sp1/MAZ (with their binding sites upstream of the MLP) [Parks and Shenk, 1997]. Protein IVa2 has been shown to bind directly with elements downstream of the MLP, termed DE1 and DE2 (+86 to +96 and +101 to +116, respectively). DE1 and DE2 have been shown to bind a homodimer of IVa2, as well as a IVa2 heterodimer with a yet undefined viral protein, suggested to be L4-22K or L4-33K [Ali et al, 2007; Farley et al, 2004; Morris and Leppard 2009; Ostapchuk et al, 2006; Tribouley et al, 1994]. These proteins bind to factors upstream of the initiation codon, such as USF, to activate transcription [Mondesert and Kedinger, 1991; Mondesert et al, 1992; Toth et al, 1992]. Late upregulation from the MLP also requires *cis*-acting elements that must be activated in addition to the *trans*-acting factors [Thomas and Mathews, 1980].

Beyond encoding for structural proteins the major late transcripts produce several non-structural proteins with roles within the virus life cycle. L3 produces the adenovirus cysteine protease, which is required for cleavage of pVI, pVII, pIII and pTP into their mature forms, yielding infectious virus particles [Weber, 1976].

The L1 encoded 52/55kDa (L1-52/55K) proteins are essential for assembly of new virion particles. L1-52/55K binds to the viral genome packaging sequence and its deletion result in production of empty capsids [Hasson et al, 1992; Perez-Romero et al, 2006].

Two L4 encoded proteins (L4-33K and L4-22K) have been shown to be required for full length MLP activity via post transcriptional mechanisms. L4-33K is a viral splice factor which activates splicing to specific late 3' mRNA splice sites. It has recently been suggested L2-22K acts in a similar manner to L4-33K, however it complements L4-33K by activating splicing to alternative 3' mRNA [Farley et al, 2004; Morris and Leppard 2009; Tormanen et al, 2006].

The L4 encoded 100kDa protein (L4-100K) directly blocks cellular mRNA translation by disrupting the cap-initiation complex. Furthermore L4-100K binds to the Ad TPL sequence, (discussed above), allowing translation of late viral mRNA by a process called ribosome shunting [Xi et al, 2005; Yueh and Schneider, 1996].

All human adenoviruses produce short RNA polymerase III (pol III) transcribed non-coding RNA species, termed virus associated or VA RNAs. All human adenoviruses produce two distinct VA RNAs, a major species VA RNA<sub>I</sub>, and a minor species VA RNA<sub>II</sub>, with the exception of species F Ads that only produces VA RNA<sub>II</sub>. The two VA RNAs in species C Ads differ extensively in sequence; however both are highly GC rich and approximately 160 nucleotides in length. VA RNAs have specific secondary structures, with an apical and central domain that form a hairpin-loop like structure that is imperative for their function [Mellits et al, 1990; Mellits et al, 1992]. VA RNAs are produced early in infection with production rapidly accelerating during late infection. The pol III promoter elements are

found downstream of the transcriptional start site, and consist of two regions, an A box and a B box [Fowlkes and Shenk, 1980; Guilfoyle and Weinmann, 1981].

VA RNAs act to block an interferon (IFN) induced shut-off of cellular translation [Mathews and Shenk, 1991]. Upon stimulation by type I IFN, several anti-viral genes are upregulated, one of which is dsRNA activated protein kinase R (PKR). In Ad infected cells PKR is activated by the formation of dsRNA, produced from convergent transcription of the adenovirus genome. Upon activation PKR phosphorylates the  $\alpha$  subunit of eukaryotic translation initiation factor 2 (eIF-2). Phosphorylation of eIF-2 blocks translational initiation thus acting to shut down virally infected cells. VA RNA can bind to PKR in a manner similar to that of dsRNA, block PKR activation, yielding un-phosphorylated eIF-2 and relieving the block on translation (outlined in Figure 1-10).

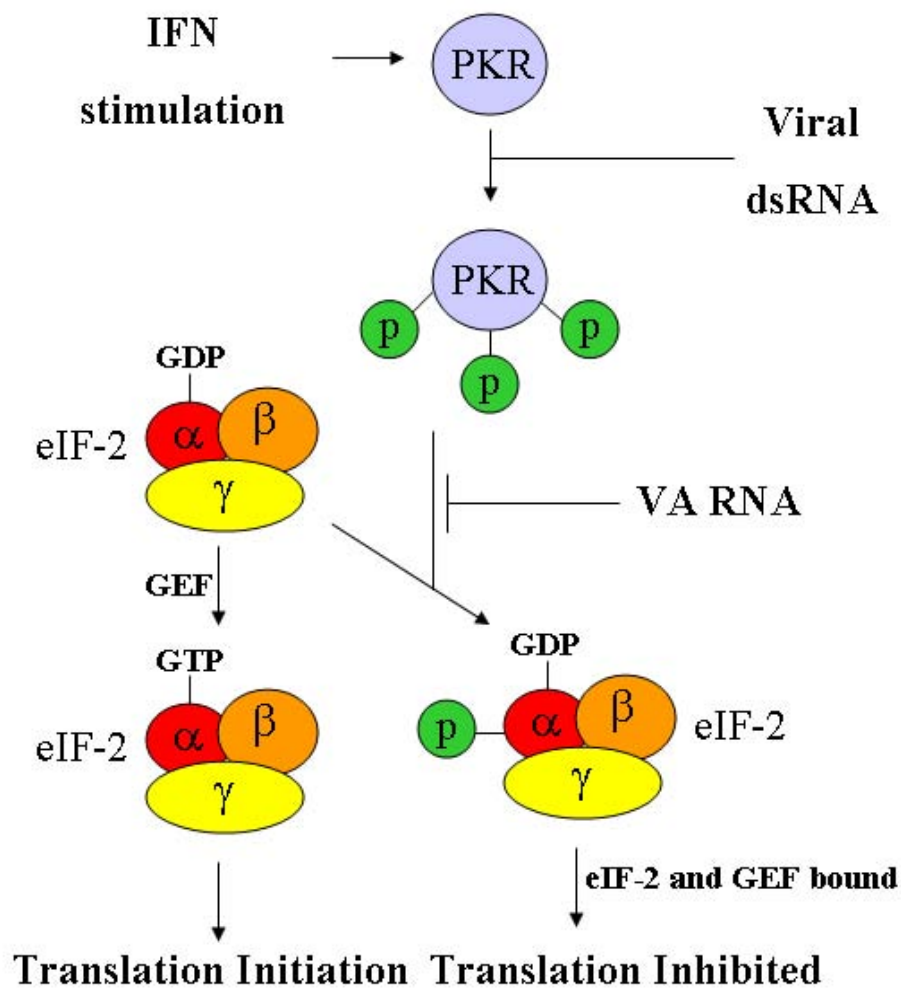


**Figure 1-10. PKR inhibition by adenovirus VA RNA**

Regulation of PKR by VA RNA. GDP is bound to the  $\alpha$ -subunit of eIF-2 following translation initiation, which is exchanged for a molecular of GTP in a reaction catalysed by GEF. Activation of PKR by viral dsRNA results in its autophosphorylation. Activated PKR phosphorylates the  $\alpha$ -subunit of eIF-2, which then forms a tight complex with GEF, preventing the exchange of GDP for GTP, thus blocking translation initiation. VA RNA binds to PKR to inhibit activation by dsRNA, thus allowing continued translation [adapted from Mathews and Shenk 1991].

### 1.2.3 Adenovirus Lytic Life Cycle

To date little is known about the Ad infectious lifecycle within the natural host. However there is detailed understanding of the virus lytic lifecycle in cultured cell lines.

The Ad cycle begins with the attachment of the virus to cell surface receptors mediated by the capsid proteins [reviewed by Arnberg, 2009; and by Nemerow et al, 2009]. Different

species of adenovirus use different cell surface receptors and subsequent internalisation pathways, however the species C attachment and internalisation pathway has been most well characterised. Initial interaction is generally mediated by the Ad fibre protein. Within species C Ads the distal C-terminal end of the fibre protein forms a knob domain, which contains the initial receptor-binding site. For Ad2 and Ad5 initial attachment is to the coxsackievirus and adenoviruses receptor (CAR) via the CAR binding site on the fibre knob domain (positioned within the loops between A and B strands, and slightly with the adjacent DE and FG loops, shown in Figure 1-11) [Bewley et al, 1999; Roelvink et al, 1999].

CAR has also been demonstrated to be the initial cell attachment receptor for a range of species A, E, D and F Ads. Some species B (plus possibly some species D) viruses have been shown to use CD46 as the primary receptor [Marttila et al, 2005; Segerman et al, 2003], but probably not Ad3 and Ad7. Some species B viruses may use CD80 and CD86 as receptors or co-receptors [Short et al, 2004], however this interaction has been recently disputed. Multiple species D viruses have been shown to enter cells after initial attachment to  $\alpha$ -linked sialic acid [Arnberg et al, 2000a; Arnberg et al, 2000b].

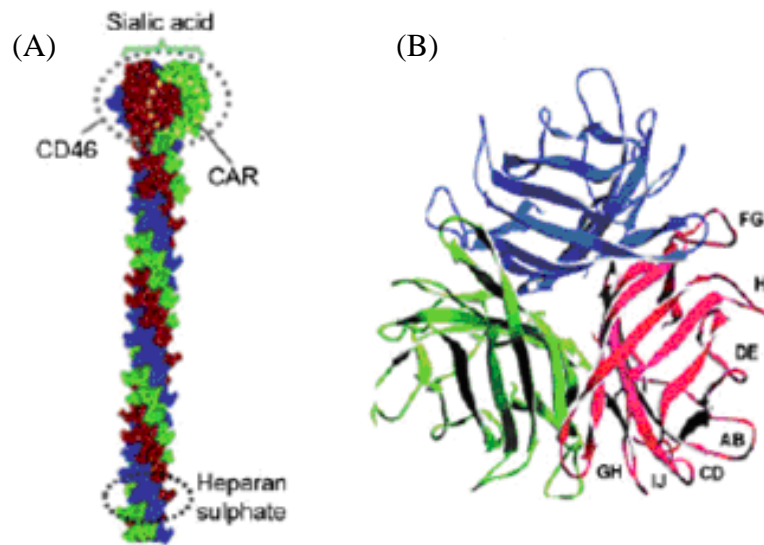


**Figure 1-11. Adenovirus fibre and knob domain structure**

A fibre space filling models indicating the sites for receptor attachment modelled from the atomic structure of Ad2 (A). A ribbon representation of the fibre knob of Ad35, showing the protruding loops with the agreed notations. All fibre knobs have a similar structure, with variations in the number and amino acid composition (B) [taken from Russell 2009].

Following initial attachment a second interaction is required for cell internalisation. This interaction is between an arg-gly-asp (RGD) binding motif, present on each copy of protein III (found on a flexible loop domain) in the penton base, with integrins, a large family of hetrodimeric cell surface receptors [Zubieta et al, 2005]. Several integrins have been suggested as secondary receptors; however two integrins;  $\alpha_v\beta_3$  and  $\alpha_v\beta_5$  have been directly shown to allow virus attachment and are sufficient for virus internalisation [Wickham et al, 1993].

Heparan sulphate proteoglycans (HSPG) have been shown to be receptors for species C adenoviruses, potentially via three independent mechanisms. Cell surface expression of HSPG has been shown to facilitate CAR independent binding and infection, potentially through interaction with a KKTK motif within the fibre shaft [Dehecchi et al, 2001;

Dechecchi et al, 2000; Smith et al, 2003]. However it has not been shown that mutation of this motif reduces the ability of the virus to directly bind to HSPG. Since then various coagulation factors have been shown to facilitate Ad attachment. Initially the Ad5 knob was shown to bind factor IX and C4BP (complement component C4 binding protein), and through these molecules to HSPG on hepatocytes [Shayakhmetov et al, 2005]. Subsequently it was shown coagulation factor X (FX) binds directly to the central depression in the Ad hexon protein, and ablation of this binding resulted in dramatically reduced hepatocyte transduction in murine models [Kalyuzhnyi et al, 2008a; Waddington et al, 2008]. All three potential HSPG interactions have to date not been investigated simultaneously and it would be interesting to investigate the HSPG-fibre interactions in light of the HSPG-hexon evidence.

Finally, dipalmitoyl phosphatidylcholine, lactoferrin, vascular cell adhesion molecular 1, scavenger receptors and MHC-1  $\alpha 2$  have all been implicated as receptors for adenovirus [reviewed by Arnberg 2009]. However debate still remains as to the exact *in vivo* order of importance of all the *in vitro* identified Ad receptors. *In vitro* attachment of the initial receptors normally occurs in concert with integrin binding [Mathias et al, 1994], allowing virus internalisation.

Species C adenoviruses are internalised into clathrin-coated pits via receptor mediated endocytosis [reviewed by Greber, 2002], triggered by penton base attachment to  $\alpha_v$  integrins. This process requires rearrangement of the actin cytoskeleton, the large GTPase dynamin, PI3K and several other cellular proteins [Varga et al, 1991; Wang et al, 1998; Wickham et al, 1993]. Sequential degradation of the viral capsid is initiated at internalisation starting with the fibre protein and continues in the endosome where IIIa and penton base are lost next. Structural studies have suggested integrin binding may induce a

conformational change in penton base, initiating the process of capsid disassembly and leading to the intracellular signalling required for internalisation [Lindert et al, 2009].

Once in the endosome the acidic conditions allow release of protein VI which facilitates the release of the viral particle into the cytosol. In the cytosol the partially disassembled capsid traffics to the nucleus via interactions between exposed hexons and the dynein/dynactin complex with the cellular microtubules. The partly disassembled capsid locates to a nuclear pore complex (NPC) and docks with the NCP filament protein Can/Nup214 [Trotman et al, 2001]. Import into the nucleus requires a number of cellular components including importins, histone H1, hsp70 and CRM1 [Saphire et al, 2000; Strunze et al, 2005; Trotman et al, 2001]. Recently protein VII has been suggested to be the major mediator of virus DNA import into the nucleus facilitated by interaction with transportin [Hindley et al, 2007; Wodrich et al, 2006]. In the nucleus TP associates with the nuclear matrix, a step which seems to be required for efficient gene transcription [Fredman and Engler, 1993]. Transcription of E1A plus several non-viral factors leads to the release of VII and remodelling of virus chromatin, allowing full viral transcription [Chen et al, 2007; Gyurcsik et al, 2006; Haruki et al, 2006; Johnson et al, 2004].

Gene expression then proceeds starting with the E1A region, followed by the remaining early transcription units, which generally block apoptosis and prime the cell for DNA replication (functions of early genes are described in section 1.2.2.1). DNA replication generally begins 5 to 8 hours post infection (in permissive cells such as HeLa or A529), as the E2 gene products accumulate. An overview of viral DNA replication is shown in Figure 1-12 [as reviewed by Shenk, 2001].

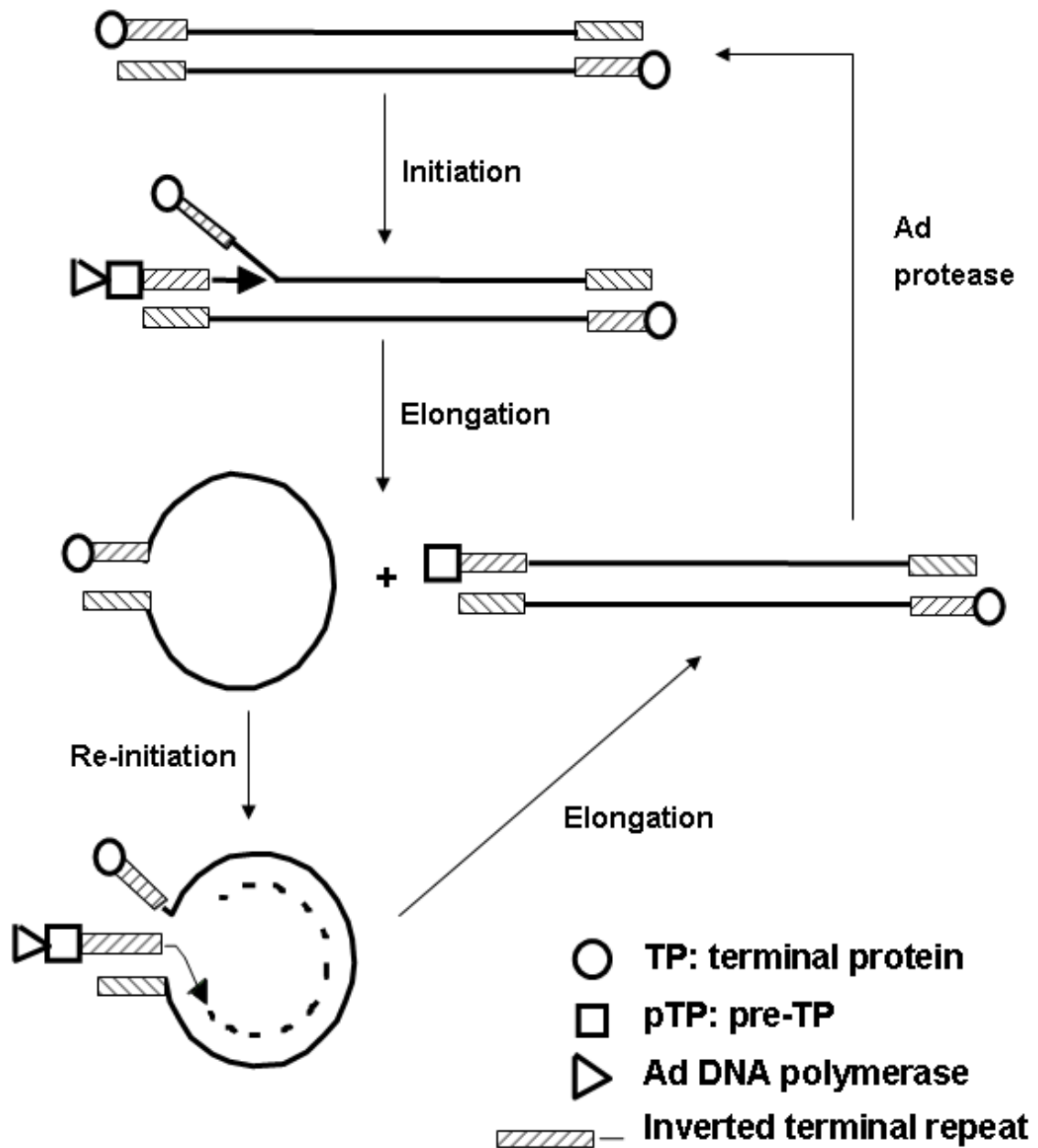


**Figure 1-12. Adenovirus DNA replication model**

Overview of the adenovirus DNA replication model. Replication is initiated using pTP as a protein primer from one strand of the genome, to produce one dsDNA consisting of one daughter and one parental strand. The ITRs of the second parental strand anneal to form a 'pan-handle' structure, which is then used for DNA replication via the same mechanism, resulting in the production of a second dsDNA genome. The Ad protease then cleaves pTP into the mature TP.

The first step is to initiate DNA synthesis from one strand of the linear dsDNA genome. This produces one dsDNA duplex, consisting of one parental strand and one daughter strand, plus one single strand of parental DNA. The latter parental ssDNA molecule is then free to go through the second step of DNA replication. In this process, the ssDNA circularises by annealing of the self-complementary ITR sequences. The resulting 'panhandle' structure possesses termini with the same structure as the original dsDNA viral genome. DNA synthesis can then take place using the first step machinery, again resulting in a dsDNA molecule consisting of one parental strand and one daughter strand, the final result being two dsDNA genomes, each one consisting of one parental strand and one daughter strand.

Viral DNA replication is initiated via a protein priming mechanism involving the pTP. The ITRs contain the *cis*-acting viral origins of replications essential for DNA replication. Each ITR consists of three functional domains, termed A, B and C. Domain A serves as a binding region of a heterodimeric complex of pTP and virus encoded DNA polymerase (pol) [Temperley and Hay, 1992]. Domain A is required for DNA replication, but by itself only supports minimal DNA replication. Efficient DNA synthesis requires domains B and C (located immediately downstream of domain A), which bind cellular factors that greatly enhance the efficacy of replication initiation. Domain B binds a dimer of nuclear factor I (NFI) and domain C binds nuclear factor III (NFIII), which together cause a bending in the DNA [Mysiak et al, 2004b] and bind to pol and pTP, helping to stabilize the pol-pTP complex [Mul and van der Vliet, 1992; Mul et al, 1990]. The heterodimeric pol-pTP complex covalently attaches a deoxycytidine monophosphate (dCMP) molecular to pTP [Mysiak et al, 2004a] ), which then uses nucleotides 4-6 (GTA) of the template DNA strand to form a pTP-CAT primer. This primer then jumps back to the nucleotides 1-3 of the

template strand, also GTA, [King and van der Vliet, 1994], where pol disassociates from pTP and commences strand elongation.

Chain elongation also requires the Ad encoded DNA binding protein (DBP) and nuclear factor II (NFII). DBP can tightly but non-specifically bind ssDNA molecules using the core globular domain and forms multimers using the hinged C-terminal hook domain, which hooks into another molecule of DBP. Multimerisation of individual DBPs to form long chains along dsDNA causes strand displacement, allowing efficient elongation of the daughter strand synthesis [van Breukelen et al, 2000].

Late gene expression is stimulated following the start of DNA replication, encoding for most of the Ad structural proteins (discussed in section 1.2.2.3), after which virion assembly can take place.

Capsid assembly takes place in the nucleus, thus requiring the import of all viral capsid proteins from the cytoplasm. L4-100K is required for II trimerisation to form the hexons in the cytoplasm, and may act as a scaffold for Ad assembly [Cepko and Sharp, 1982; Morin and Boulanger, 1986]. Precursor protein pVI contains two nuclear localisation and two nuclear export signals and is responsible for shuttling to and from the nucleus and in doing so transports hexons into the nucleus [Honkavuori et al, 2004; Wodrich et al, 2003]. The Ad protease is first activated by binding non-specifically to viral DNA [Gupta et al, 2004], which allows cleavage of pVI. Upon cleavage, the C-terminal domain of pIV (pVIc) acts as a co-factor for the Ad protease to allow full activity and mature VI can act as a capsid structural protein. It has been suggested this activated protease-pVIc complex then moves along the viral DNA, cleaving the other virion precursor proteins (pIIIa, pVII, pVIII, pIX, pTP and pMu) to their mature forms [Russell 2009].

Packaging of viral DNA requires recognition of *cis*-acting packaging sequences at the left end of the genome. The packaging sequence consists of 7 AT rich regions designated A repeats (A1-A7) which have the consensus sequence 5'-TTTG-(N<sub>8</sub>)-CG-3' [Hearing et al, 1987; Schmid and Hearing, 1997]. The exact mechanism of DNA packaging is unclear. Evidence exists which suggests that the viral DNA is packaged into ready-made capsids [Tibbetts and Giam, 1979] and that recognition of the packaging sequence is required first, before initiation of encapsidation around the viral DNA [Zhang and Imperiale, 2000]. DNA encapsidation has however been determined with the bacteriophage  $\phi$ 29, which resembles Ad in that it is a dsDNA phage that contains a packaging signal located at one end of the genome and a covalently linked 5' terminal protein. With  $\phi$ 29, stable capsid shells are produced first into which the phage DNA is inserted. and it is this mechanism which has been recently put forward for Ad [reviewed by Ostapchuk and Hearing, 2005]. Whatever the molecular mechanism behind DNA encapsidation, several host and viral proteins have been identified as essential.

IVa2 has been shown to directly bind the CG portion of the A repeats and interact with L1-52/55K, which also potentially binds the packaging sequence, and both are required for successful encapsidation [Gustin and Imperiale, 1998; Hasson et al, 1992] [Gustin et al, 1996; Perez-Romero et al, 2005]. L1-52/55K appears to be involved in serotype specific Ad packaging [Wohl and Hearing, 2008]. Cellular proteins have been reported to bind the packaging sequence, including the CCAAT displacement protein (CDP), which forms a complex with viral protein IVa2 [Ostapchuk et al, 2005; Tyler et al, 2007]. Furthermore L4-22K has been shown to be required for virus assembly or DNA packaging, binding the TTTG repeats in the packaging sequence, and is thought to assist binding of IVa2 to the packaging sequence [Ewing et al, 2007; Ostapchuk et al, 2006]. It is worth considering that

if the bacteriophage  $\phi$ 29 analogy is correct then an ATP-driven motor is required to move the viral DNA into the empty pro-capsid, and recently IVa2 has been shown to bind ATP *in vitro* [Ostapchuk and Hearing, 2008].

Release of virus particles is a multi-factor process that involves several viral and cellular proteins. Two systems have been identified that aid in escape of viral particles. One system centres on the E3 adenovirus death protein as discussed in section 1.2.2.1.

The second system centres on collapsing the cellular cytoskeleton; a process which involves the L3 encoded adenovirus protease. The L3 proteinase cleaves the cellular cytokeratin K18, rendering it unable to form filaments [Chen et al, 1993]. By both mechanisms the intermediate filament network is disrupted, rendering the cell more susceptible to lysis and subsequent release of viral progeny.

During infection a large excess of fibre is produced, in relation to the amount that can be incorporated into new virion particles. It has been hypothesised this large excess in fibre is to aid in viral escape and spread from the initial site of infection [Walters et al, 2002]. Excess fibres are secreted at the basolateral surface, which eventually migrate to cell-cell tight junctions where CAR is located. Fibre proteins subsequently bind to CAR and disrupt the intercellular CAR-CAR homodimers, which as a result opens up the tight junctions. This allows virions which have previously escaped the cell to migrate in between cells, towards the apical surface, and thus spread to surrounding cells.

#### **1.2.4 Current Adenovirus Cancer Gene Therapy Strategies**

A rapid increase in understanding the molecular mechanisms behind cancer has resulted in a large number of studies and clinical trials using Ad for cancer gene therapy. Between 1993 and 2008 the UK Gene Therapy Advisory Committee (GTAC) approved 126 clinical trials for cancer gene therapy alone, almost 20% of which use Ad based vectors [GTAC 14th Annual Report, 2008]. Multiple strategies have been studied *in vitro*, some of which have been investigated with *in vivo* murine models, of which a limited number have transferred into human clinical trials.

The most recent *in vitro* studies use Ad with multiple modifications to both increase tumour toxicity and improve vector safety. This next section covers some current cancer gene therapy strategies that use adenovirus vectors and reviews the latest vector developments and cancer gene therapy trials.

Adenoviruses have many attributes which make them good gene therapy vectors. Their life cycle and biology is well understood, allowing easy strategy design. High titres of virus can be readily produced. They can typically infect a broad range of cell types, including both actively dividing and non-dividing cells, in comparison to other vectors that have narrow tropisms (such as retroviruses for actively dividing cells). Finally integration into the human genome is rarely seen, eliminating the chance of insertional mutagenesis that is associated with some vectors e.g. retroviruses [Harui et al, 1999]. Disadvantages to adenoviruses include their non-integrating nature, which precludes long-term gene expression. The pre-existing immunity in the general population means adenovirus vectors may be rapidly cleared from the body, greatly reducing the therapeutic window.

Unfortunately ten years ago on the 17<sup>th</sup> of December 1999, Jesse Gelsinger died in the first OTC deficiency gene therapy trial. This patient suffered a severe inflammatory response

following administration of  $6 \times 10^{11}$  virus particle/kg of a replication deficient Ad vector via the right hepatic artery. It is thought this toxicity was due to an innate or humoral immune response primarily to the adenovirus capsid proteins [Raper et al, 2003], but trial protocol violations may have played a part in his death. This does however demonstrate how the immune response may limit the success of viral vectors.

#### **1.2.4.1 Replication Deficient Adenovirus Vectors**

The first adenovirus gene therapy vectors used were replication deficient vectors, with the entire E1 region and most or the entire E3 region deleted [reviewed by Danthinne and Imperiale, 2000]. The E1 deletion removes the E1A and E1B genes while keeping the IX gene and renders the virus replication deficient. The E3 region is not essential for replication (*in vitro*) and was therefore dispensed with to increase the transgene capacity. With the E1 and E3 regions deleted, first generation Ad vectors can incorporate approximately 8kb of insertion. Transgenes are normally inserted as expression cassettes, with expression controlled from foreign promoters and poly(A) sequences, generally within the E1 deletion and sometimes within the E3 region. Despite deleting the E1 and E3 regions first generations showed some level of 'autoreplication', particularly at very high multiplicities of infection, and was associated with transcriptional activity of several viral gene including DNA polymerase, DNA binding protein and E4 proteins. Transcriptional activity is probably as a result of basal promoter activity and possibly exogenous or cryptic promoters which may enhance transcriptional activity [Marienfeld et al, 1999]. Transgene expression from first generation vectors is normally shut down 2-3 weeks post infection in immuno-competent murine models. Transgene elimination is attributed to immune response raised against viral gene expression even in the E1 deleted background [Yang et al, 1996b]. Recent evidence has demonstrated leaky protein IX expression from the enhancer elements

in upstream transgene promoters, and IX co-expression may be one of the main causes of Ad induced immune response in a murine model. By using transgene promoters with weaker enhancer elements, transgene expression was considerably extended [Nakai et al, 2007].

Production of first generation replication deficient Ads requires helper cells lines such as 293 and 911, which expresses the E1 region allowing virus production [Fallaux et al, 1996; Graham et al, 1977]. With both cells lines there is the possibility of recombination between the E1-deleted viral genome and chromosomally integrated E1A DNA sequences, yielding batches of virus contaminated with replication competent virus. To circumvent this limitation a new cell line was created, PER.C6, which has a smaller E1 insertion that is under control of the human phosphoglycerate kinase promoter. By designing vectors with E1 deletions which do not overlap with the E1 sequences in PER.C6 cells, the chance of homologous recombination resulting in contaminated batches is reduced [Fallaux et al, 1998]. First generation Ad vectors are still widely used and are an important tool for cancer gene therapy, reflected in the fact two UK trials are still in progress for treatment of glioma and intra-abdominal, and one trial recently accepted for treatment of prostate cancer, all using an E1/E3 deleted Ad5 vector [GTAC 14th Annual Report 2008]

In response to the limitations observed with first generation Ad vectors, further genes were removed to give second-generation vectors. Second-generation vectors retain the E1 and E3 deletions and have additional deletions in any of the E2A, E2B, or E4 regions. The aim was to completely eliminate viral gene expression, thus reducing the immune response, while increasing the transgene capacity up to 14kb. Second generation vectors are however more difficult to produce, requiring relevant viral proteins to be supplied *in trans* [Krougliak and Graham, 1995; Nakai et al, 2007; Wang et al, 1995; Zhou et al, 1996]. In the UK two

clinical trials are underway using E1 and E4 deleted vectors for the treatment of critical limb ischemia and intermittent claudication. However no second generation vectors are being used in UK clinical trials for the treatment of cancer [GTAC 14th Annual Report 2008].

By taking the Ad genetic deletions to the extreme, so-called ‘gutless’ Ad vectors were produced, which only contain the viral ITR, required for DNA replication [reviewed by Alba et al, 2005]. Such a large deletion allows insertion of large or multiple transgenes up to 35kb. Furthermore, gutless vectors are highly attractive for gene therapy due to a reduction in the *in vivo* immune response in animal models compared to first and second generation vectors [Danthinne and Imperiale 2000]. Production of gutless Ad vectors requires all the Ad genes to be supplied *in trans*. This can be achieved by using helper viruses which have a system to remove helper virus packaging sequences (such as the Cre-loxP system), thus removing helper virus contamination. However levels of helper virus contamination are still too high for use in clinical trials [Alba et al, 2005].

All replication deficient virus vectors need to carry transgenes to elicit a therapeutic effect, some of which are discussed below.

#### **1.2.4.1.1 p53 Tumour Suppressor Replacement**

The p53 protein is an important tumour suppressor that is mutated or lost in approximately 50% of all human cancers. The initial studies using Ad expressing wildtype p53 (Ad-p53) showed inhibition of growth and induction of apoptosis in a range of cancer cell types [Liu et al, 1995; Yang et al, 1995]. Several phases I and I/II clinical trials have since demonstrated the safety of Ad-p53 both alone and in combination with radiotherapy, chemotherapy or surgery [Lang et al, 2003; Pagliaro et al, 2003; Shimada et al, 2006; Wolf et al, 2004]. Phase II/III studies are reported to be still ongoing [www.wiley.co.uk, Dec. 09]

and one phase III clinical trial has been commenced in the US and Europe by Invitrogen, for treatment of squamous cell carcinoma of the head and neck [reported by Invitrogen, 2007]. Despite this, it is worth noting a previous phase II/III clinical trial using Ad-p53 for the treatment of ovarian cancer was closed after the first interim analysis due to an inadequate therapeutic benefit, and it was thus suggested the complex nature of cancer means that a single gene repair may not be a suitable strategy for the treatment of some cancers [reviewed by Zeimet and Marth, 2003].

In 2004 China approved the use of a replication deficient Ad vector expressing wildtype p53 (Gendicine) from a rous sarcoma virus promoter, for the treatment of head and neck in conjunction with radiotherapy [reviewed by Peng 2005; and by Xin, 2006]. This represented the first commercial available gene therapy treatment for cancer.

#### **1.2.4.1.2 Enzyme – Prodrug Therapy**

Virus directed enzyme prodrug therapy (VDEPT) or suicide gene therapy uses a viral vector to administer a gene encoding an enzyme which can convert a non-toxic prodrug into a cytotoxic agent. Furthermore, the cytotoxic effects of the activated prodrug are transferred to neighbouring untransduced cells, in a phenomenon called the ‘bystander’ effect.

Because of the bystander effect, VDEPT is less dependent on complete tumour transduction, compared to other systems such as tumour suppressor replacement. VDEPT should also allow for localised high concentrations of cytotoxic agent within the tumour microenvironment, while avoiding high systemic concentrations. This is in comparison to conventional chemotherapy in which high systemic concentration of cytotoxic agent can cause significant side effects.

Whereas VDEPT has enjoyed great success *in vitro*, general *in vivo* limitations have been identified both in murine models and human trials. The requirement for efficient *in vivo*

gene transfer still raises problems even though VDEPT does not in theory require complete tumour transduction. Additionally, problems have been identified in achieving local concentrations of prodrug upon systemic delivery, to translate into high concentrations of cytotoxic agent [Chung-Faye et al, 2001; Jaberipour et al, 2010].

VDEPT has been used extensively in multiple studies with several different combinations of enzyme and prodrug. The three most common enzyme-prodrug systems used in Ad delivery are discussed in detail below.

#### **1.2.4.1.2.1 Herpes Simplex Virus Thymidine Kinase – Ganciclovir**

The herpes simplex virus thymidine kinase (HSVtk) – ganciclovir (GCV) VDEPT system is the most widely used system for suicide gene therapy. GCV is a drug commonly used for treatment of HSV infection (such as cold sores) and acute CMV infections. HSVtk can phosphorylate GCV into GCV-monophosphate, which is subsequently converted to GCV-diphosphate and tri-phosphate by cellular kinases. GCV-triphosphate (GCV-TP) is a nucleotide analogue of dGTP and competes for incorporation into DNA by cellular DNA polymerase  $\alpha$ . Once incorporated GCV-tp acts as a DNA chain terminator, thus inhibiting DNA synthesis and resulting in cell death [Cheng et al, 1983a; Cheng et al, 1983b].

*In vitro* and murine studies have revealed that cellular gap junctions, which aid the spread of phosphorylated GCV, are involved in the HSVtk-GCV bystander effect [Mesnil and Yamasaki, 2000; Princen et al, 1999; Touraine et al, 1998]. Whereas a wide variety of cells have shown a good bystander effect, many tumour cell lines show a reduce gap junction capacity and thus exhibit a poor bystander effect. This could potentially provide a hurdle for treatment of a variety of tumours. Since GCV-TP acts at DNA replication, this system can only target cells that are in S-phase. Arguably, this is the system's greatest disadvantage, as in most tumours only a small fraction may be in S-phase.

The HCVtk-GCV system has been extensively investigated *in vitro* and in animal models for the treatment of a variety of cancers. Multiple clinical trials have been reported on using this system in replication deficient Ad vectors, summarised in Table 1-2 , with more trials reported to be ongoing [[www.wiley.co.uk](http://www.wiley.co.uk), Dec. 09]. From all the reported trials the authors concluded the vector is safe and well tolerated alone and in combination with GCV. Signs of clinical efficacy were observed in most trials, however it has been postulated that any effect observed may be due to induction of an antitumour immune response [Sternan et al, 2005].

Target	Phase	Additional treatment	Authors conclusions	Reference
Malignant brain cancers	I		Vector and GCV were safely tolerated in all 13 patients up to the maximum virus dose of $2 \times 10^{12}$ VP.	[Trask et al, 2000]
Colorectal cancer	I		In all 16 patients the vector was safely administered up to maximum dose of $10^{13}$ VP in combination with GCV	[Sung et al, 2001]
Ovarian cancer	I	Topotecan	From a total of 10 patients the median survival was approximately 1/3 longer following gene therapy with topotecan and surgery	[Hasenbur g et al, 2001]
Malignant glioma	I		Vector and prodrug doses used in this study were safe. Ten of 11 patients survived >52 weeks post diagnosis.	[Germano et al, 2003]
Malignant glioma	I		Vector and prodrug combination was safely tolerated in all 14 patients, and maximum tolerated dose was not reached up to $4.6 \times 10^{11}$ VP.	[Smitt et al, 2003]
Prostate cancer	I		All 11 patients tolerated the therapy with no serious adverse events. Local cell death was observed in 7 out of 11 patients	[Kubo et al, 2003]
Prostate cancer	I/II	+/- radiotherapy and hormone therapy	All 59 patients tolerated the therapy. Combined therapy appeared to provide good locoregional control.	[Teh et al, 2001; Teh et al, 2004]
Malignant mesothelioma	I		In all 21 patients the therapy was safe and tolerated. Two patients receiving $> 1.6 \times 10^{13}$ VP therapy showed long-term responses	[Sberman et al, 2005; Sberman et al, 1998]
Prostate cancer	I/II	Docetaxel and estramustine	All 6 patients tolerated the therapy with no serious adverse events. 4 patients showed a partial response.	[Shirakawa et al, 2007]
Head and neck cancer and other malignant tumours	I		Of 18 patients 10 experienced transient fever and 10 local injection site reaction. One patient had a partial response, 1 had moderate response, 5 had stable disease and 10 had progressive disease	[Xu et al, 2009]

**Table 1-2. Clinical trials since 2000 using replication deficient Ad – HSVtk-GCV**

#### **1.2.4.1.2.2 Cytosine deaminase – 5-Fluorocytosine**

The bacterial and yeast enzyme cytosine deaminase (CD) has been used extensively in combination with the antifungal agent 5-fluorocytosine (5-FC). CD converts 5-FC into the chemotherapeutic agent 5-fluorouracil (5-FU), which is then converted by cellular enzymes into 5-F-UTP and 5-F-dUMP. 5-F-dUMP irreversibly inhibits thymidylate synthase preventing DNA synthesis, and is thought to be the main mechanism of 5-FC mediated toxicity. Additionally, 5-F-UTP can replace UTP in RNA synthesis resulting in the inhibition of nuclear mRNA transport. Furthermore, 5-FU molecules are able to diffuse through cell membranes without passing through gap junctions to give a powerful bystander effect [Lawrence et al, 1998] and 5-FU is also a strong radiosensitiser [Lawrence et al, 2003].

The CD-5-FC system has been used extensively both *in vitro* and *in vivo* murine models, however this has not transferred into any clinical trials with replication deficient Ad vectors. The furthest progress made is for the treatment of prostate cancer, in combination with the HSVtk-GCV system in an oncolytic Ad vector, discussed further in section 1.2.4.3.

#### **1.2.4.1.2.3 Nitroreductase – CB1954**

The nitroreductase (NTR)-CB1954 (5-aziridin-1-yl)-2,4-dinitrobenzamide) enzyme-prodrug system uses the *E.coli nfsB* encoded NTR enzyme in conjunction within the prodrug CB1954 (see Figure 1-13). CB1954 was initially used in a 1960s study of Walker rat carcinosarcoma that was sensitive to CB1954 killing [Cobb et al, 1969]. Nitroreductase reduces CB1954 into a bifunctional alkylating agent by reducing either nitro group to form a 2-hydroxylamino or a 4-hydroxylamino derivative, a step which requires either NADH or NADPH. Following the initial reduction the 4-hydroxylamino derivative is further

converted by cellular thioesters into a bifunctional alkylating agent [Knox et al, 1992], which causes interstrand DNA crosslinking, resulting in cell death.

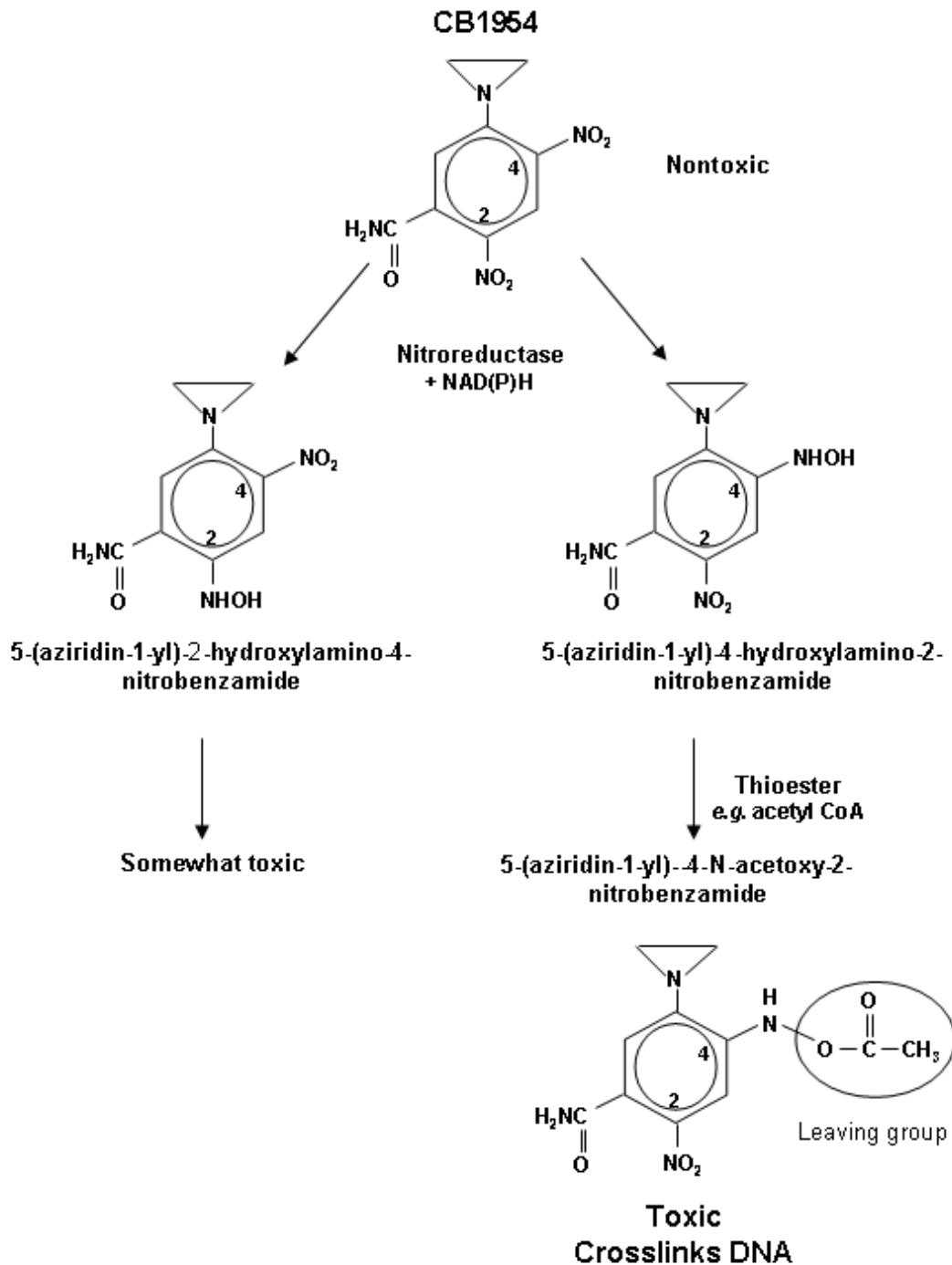


**Figure 1-13. CB1954 reduction by nitroreductase**

Reduction of CB1954 by nitroreductase into the activated cytotoxic agent (see text for details).

The mode of action of activated CB1954 means it is cytotoxic at any stage of the cell cycle. This is a distinct advantage over the HSVtk-GCV and CD-5-FC systems, which require the target cells to be in S-phase. Furthermore, the activated CB1954 is able to freely diffuse through cell membranes, independent of cellular gap junction, and in doing so elicits a powerful bystander effect [Bridgewater et al, 1997].

Two clinical trials have been completed using the NTR-CB1954 enzyme prodrug system, both using a replication deficient Ad vector [Palmer et al, 2004; Patel et al, 2009]. The latest of these was a phase I/II trial for treatment of prostate cancer. The vector, named CTL102, has a complete E1 and E3 deletion, and expresses NTR from the CMV immediate early promoter, inserted within the E1 deletion. This trial consisted of two arms; the first was a dose escalation study of the vector alone in patients with localised prostate cancer scheduled for radical prostatectomy. This was to establish vector safety, tolerability and NTR expression. The second arm consisted of patients with local failure following primary treatment options, who received virus plus prodrug, and was designed to establish safety and tolerability. Both arms demonstrated the vector was well tolerated with minimal side effects. Immunohistochemistry of resected prostates demonstrated NTR staining at all viral doses. 19 patients received virus plus prodrug, with minimal toxicity. Preliminary evidence suggested partial efficacy represented by a change in prostate specific antigen (PSA) kinetics, with 4/19 showing 0-50% decrease in PSA, and 2/19 showing >50% decrease in PSA, 6 months following treatment. Despite this, NTR staining of resected prostates showed only localised transgene expression thus demonstrating limited virus distribution due to the small number of infection sites and the fact the virus is unable to replicate and spread from the initial sites of infection. It is therefore likely enzyme-prodrug systems

would benefit from combination with CRAd vectors, which can spread the therapeutic transgenes from the initial sites of infection (discussed in section 1.2.4.3).

#### **1.2.4.2 Oncolytic Adenoviruses**

Conditionally replicating Ad (CRAd) vectors, otherwise known as oncolytic adenoviruses, contain gene mutations or deletions, which render them only capable of replicating in cancer cells. Over the past two decades multiple modifications have been investigated, which can roughly be divided into gene deletions and promoter replacements.

##### **1.2.4.2.1 Adenovirus Gene Deletions**

Of all CRAd modifications the two most studied are the E1B-55K gene deletion and the E1A CR2 24bp deletion.

An E1B-55K deleted Ad2/5 chimeric virus called *dl1520*, was initially generated to investigate E1B functions [Barker and Berk, 1987]. The virus, later referred to ONYX-015, was reported to replicate only in tumour cells, but not in normal cells [Heise et al, 1997]. Tumour selectivity was originally thought to be because E1B-55K is not present to bind to p53 in normal cells and release a p53 mediated block on the cell cycle. In cancer cells which have a broken p53 pathway, this function of E1B-55K is not required and the virus can proceed with DNA replication. However tumour selectivity was later shown to be independent of p53 status [Goodrum and Ornelles, 1998; Rothmann et al, 1998; Turnell et al, 1999]. Further investigations revealed the tumour selectivity was due to inhibition of late viral mRNA export in normal cells [O'Shea et al, 2004]. It is now widely accepted E1B-55K works in concert with E4orf6 to promote late viral mRNA export from the nucleus while inhibiting cellular mRNA export (discussed in section 1.2.2.1). In normal cells deletion of E1B-55K does not allow export of late viral mRNA thus no late viral proteins

are produced. Presumably cancer cells have mutations which allow viral mRNA export, despite the E1B-55K deletion.

ONYX-015 has been tested in multiple phase I and II clinical trials for a variety of cancer types, some in conjunction with other therapies. The trials up to 2002 were reviewed by Post and by Kirn [Kirn, 2001a; Kirn, 2001b; Post, 2002] and the trials from 2002 are summarised in Table 1-3. In 2005 a phase III clinical trial with ONYX-015 was stopped due to funding problems [Guo and Xin, 2006] however several phase II trials are still ongoing [www.wiley.co.uk, Dec. 09].

In 2005 China approved a second genetically engineered Ad vector, named H101, with an E1B-55K deletion and is similar to ONYX-015. H101 has been approved for head and neck cancers, after a phase III clinical trial conducted in China with 160 patients showed 74% of patients who received H101 and chemotherapy showed a reduction in tumour size compared to 40% receiving chemotherapy alone [reviewed by Guo and Xin 2006].

<b>Target</b>	<b>Phase</b>	<b>Additional treatment</b>	<b>Authors conclusions</b>	<b>Reference</b>
Recurrent/refractory epithelial ovarian cancer	Phase I	No	Maximum tolerated dose not reached at $10^{11}$ PFU and no significant toxicities observed	[Vasey et al, 2002]
Gastrointestinal cancer metastatic to the liver	Phase II	5-FU and leucovorin	Combination of virotherapy and chemotherapy showed some antitumoural activity in some chemotherapy-resistant colorectal tumours	[Reid et al, 2002]
Pancreatic cancer	Phase I/II	Gemcitabine	After combination therapy 2 patients had partial regression, 2 had minor response, 6 has stable disease and 11 has progressive disease	[Hecht et al, 2003]
Hepatobiliary cancer	Phase II	No	Treatment was safe and well tolerated. Of 20 patients enrolled 16 were evaluated for response. 1 patient had a partial response, 1 has prolonged stabilization and 8 had a >50% reduction in tumour markers.	[Makower et al, 2003]
Colorectal cancer	Phase II	No	Common toxicities including flu-like symptoms, nausea and emesis were observed in all 18 patients. All 18 patients had progressive disease.	[Hamid et al, 2003]
Advanced malignancy	Phase I pilot trial	Irinotecan and 5-FU or IL-2	Virus related toxicity was limited to transient fever. All patients demonstrated elevated neutralizing antibodies within 4 weeks of treatment.	[Nemunaitis et al, 2003]

Premalignant oral dysplasia	Phase I	No	No toxicities greater than grade 2 was observed. Histologic resolution of dysplasia was seen in 7 of 19 patients.	[Rudin et al, 2003]
Recurrent malignant gliomas	Phase I	No	No maximum tolerated dose reached at $1 \times 10^{10}$ PFU.	[Chiocca et al, 2004]
Advanced sarcomas	Phase I/II	MAP chemotherapy	No dose limiting toxicity observed. Evidence of antitumour activity in 1 out of 6 patients.	[Galanis et al, 2005]
Metastatic colorectal cancer	Phase I/II	No	No dose limiting toxicity observed. Of 24 patients included 11 had stable disease after 3 months.	[Reid et al, 2005]
Advanced cancers	Phase I	Enbrel	No significant adverse events were attributed to the experimental regimen.	[Nemunaitis et al, 2007]

**Table 1-3. Clinical trials with ONYX-015 from 2002 onwards**

The E1A CR2 24bp deletion (commonly referred to as E1A CR2  $\Delta$ 24) removes the region of E1A which binds with the highest affinity to the retinoblastoma protein (pRb). Binding of E1A to pRb via the CR2 region causes the release of the transcription factor E2F, allowing cell cycle progression and virus replication. In normal cells with an intact pRb pathway, the mutant E1A cannot bind pRb and release E2F thus virus replication is blocked. Within cancer cells with a mutant pRb pathway this function of E1A is redundant and the mutant virus is able to replicate and kill the cell.

Since the initial studies over a decade ago [Fueyo et al, 2000; Howe and Bayley, 1992] the E1A CR2  $\Delta$ 24 CRA<sub>d</sub> virus has been used extensively for *in vitro* studies and *in vivo* murine models to treat a variety of cancers [reviewed by Dobbelstein, 2004; and by Everts and van der Poel, 2005]. No clinical trials have been completed with an E1A CR2  $\Delta$ 24 vector,

however three clinical trials have been recently approved using  $\Delta 24$  vectors which contain additional mutations. Two trials use a  $\Delta 24$  vector which has been retargeted with either the RGD sequence or an Ad5/3 chimeric fibre and are discussed in section 1.2.4.4.1. The third trial also uses an RGD retargeted vector, but has insertions to enhance tumour specificity and will be discussed in section 1.2.4.4.2.

In addition to the E1B and E1A deletions, VA RNA deletions have also investigated for treatment of pancreatic tumours. VA RNA inactivates PKR to allow continued protein translation in virus infected cells. However the Ras pathway, which is active in pancreatic tumours, can inactivate PKR and thus dispensing for the need of VA RNA and allowing translation to continue [Cascallo et al, 2003].

#### **1.2.4.2.2 Promoter Replacements**

The second basic strategy for engineering CRAbs involves replacing natural viral promoters such as the E1A promoter with tumour or tissue specific promoters. Tumour specific promoters respond to factors found over-expressed in cancer cells, but not activated in normal cells, such as the E2F-1 promoter, which responds to free E2F generally found in most tumours [Jakubczak et al, 2003]. Tissue specific promoters respond to factors found only in specific target tissues and are typically upregulated in target cancers, such as the prostate specific antigen (PSA) promoter which is found upregulated in prostate cancer [Rodriguez et al, 1997]. Many tumour and tissue specific promoters have been investigated *in vitro*, some of which are summarised in Table 1-4, however this is by no means an exhaustive list.

Promoter Replaced	Inserted Promoter	Selectivity	Other Information	Reference:
E1 and E4	COX-2 and/or MK promoter	Colorectal and pancreatic cancer	Enhanced viral replication specificity observed with double COX-2/MK promoter over either single promoter alone	[Hoffmann and Wildner, 2006]
E1A and E4	pS2 promoter containing estrogen-responsive elements	Breast cancer	Estrogen receptor positive breast cancer cells killed as efficiently as wt Ad5 but has decreased cytotoxicity observed with receptor negative cells	[Hernandez-Alcoceba et al, 2000]
E1A	PSA promoter	Prostate cancer	E1A expression only observed in PSA positive prostate cell lines	[Rodriguez et al, 1997]
E1A	A33 antigen promoter	Colon cancer	Reduction in tumour growth in nude mice with colon cancer xenografts	[Cafferata et al, 2009]
E1A	hTERT promoter	Tumour specific	Inhibition of tumour growth in mice xenografts with absence of hepatotoxicity	[Huang et al, 2003a]
E1A	E2F-1 promoter	Tumour specific	Replication attenuated in non-proliferating normal cells	[Tsukuda et al, 2002]

**Table 1-4. CRAd promoter replacements**

From the various promoter replacement oncolytic strategies tested *in vitro* and in animal models, to date only two, the hTERT and the PSA promoter, have successfully transferred into clinical trial.

Transcriptional activation of the human telomerase reverse transcriptase (hTERT) promoter is a major mechanism for cancer specific activation of telomerase [reviewed by Kyo et al, 2008]. Telomerase activation is one mechanism used by tumour cells to prevent telomere loss, which is necessary to prevent eventual cell senescence. Nemunaitis *et al* recently completed a phase I clinical trail using Telomelysin, an oncolytic Ad vector with the E1A

and E1B genes under control of the hTERT promoter, has been tested in patients with advanced solid tumours [Nemunaitis et al, 2009]. The trial used a single intratumoural injection of the Telomelysin to 16 patients with a variety of solid tumours, which were split into three cohorts receiving  $1 \times 10^{10}$ ,  $1 \times 10^{11}$  or  $1 \times 10^{12}$  viral particles. The authors report that the vector was well tolerated at all dose levels with 1 patient having a partial response of the injected lesion and 7 patients having stable disease 56 days after treatment, suggesting antitumour activity.

Two PSA responsive oncolytic vectors have been tested in clinical trials; CV706 (also known as CN706) and CG7870. CV706 has the E1A promoter region replaced by the minimal 5' promoter/enhancer elements from the PSA gene, and has been in a phase I clinical trial for locally recurrent prostate cancer [Chen et al, 2001; DeWeese et al, 2001]. This trial demonstrated CV706 was safe and not associated with any irreversible grade 3 or any grade 4 toxicities, and some signs of efficacy were demonstrated by a 50% fall in serum PSA levels in 5 of 25 patients. The second vector, CG7870, has the E1A gene under control of the rat probasin promoter, the E1B gene under control of the PSA promoter and a full length E3 region. This vector has been tested in a phase I and phase I/II clinical trial for the treatment of hormone-refractory metastatic prostate cancer [Dilley et al, 2005; Small et al, 2006]. The most recent of these trials used a single intravenous dose of CG7870, in a dose escalation from  $1 \times 10^{10}$  to  $6 \times 10^{12}$  VP. The authors report good tolerance with 3 therapy related grade 3 events and no grade 4 events. No complete PSA responses were observed, however 5 patients of 23 showed signs of efficacy illustrated by a 25-50% drop in serum PSA levels.

Initially CRAd vectors contained large deletions within the E3 region. Suzuki *et al* demonstrated that retaining the wt E3 region improved the oncolytic activity of CRAd vectors [Suzuki et al, 2002]. It was later shown the oncolytic activity and spread of CRAd vectors could be increased by over-expressing the E3 encoded ADP [Doronin et al, 2003].

#### **1.2.4.3 Oncolytic Adenoviruses Carrying Transgenes**

The primary drawback with replication deficient Ad vectors is the impracticality of achieving complete delivery to every cell in the tumour. Only cells surrounding the immediate site of administration are susceptible to treatment, reducing potential efficacy.

Overall, clinical trials with oncolytic vectors indicate that while CRAd vectors are safe, they are unable to significantly alter the course of the disease. Many studies have demonstrated that 'arming' of CRAd vectors with additional cytotoxic functions can improve the lytic effect of the virus [reviewed by Cody and Douglas, 2009]. Furthermore, these vectors can replicate and disseminate from the initial site of administration, theoretically spreading the transgene(s) in the process. However the smaller deletions in CRAd vectors (compared to replication defective vectors) limit the size of transgene inserts.

All of the enzyme-prodrug systems described above have been combined with CRAd vectors to improve upon the oncolytic effect alone [reviewed by Cody and Douglas 2009]. To date the only CRAd/enzyme-prodrug combination put into clinical trial uses an E1B-55K deleted backbone, carrying an HSVtk-CD fusion gene, in so-called double suicide gene therapy. In a series of clinical trials for prostate cancer the safety was assessed alone and in combination with radiotherapy. Some signs of efficacy were observed indicated by transgene expression, needlecore biopsies and serum PSA levels. Furthermore an increase in the PSA doubling time from 17 to 31 months was observed at a 5 year follow-up

[Freytag et al, 2002; Freytag et al, 2007a; Freytag et al, 2007b; Freytag et al, 2003]. The latest of these studies used a yeast encoded CD (yCD), which is more catalytically active than the previously used bacterial CD (bCD), and a mutant HSVtk, HSVtk<sub>SR39</sub>, which is more catalytically active than the wildtype HSKtk. This vector, termed Ad5-yCD/*mutTK rep-hNIS*, also encoded the human sodium iodide symporter as a reporter gene system to allow imaging of virus dissemination by PET or SPECT. Again this phase I clinical trial was for prostate cancer, and demonstrated the vector safety in all 19 patients (3 grade three events and no grade 4 events) and feasibility of nuclear imaging adenovirus mediate gene expression and distribution [Barton et al, 2008].

#### **1.2.4.4 Improved Adenovirus Systems**

##### **1.2.4.4.1 Retargeting to Tumours**

It was hypothesised that poor virus infection of tumour tissue was one of the primary setbacks in Ad based cancer gene therapy. This hypothesis was supported by evidence showing the low and variable expression of CAR on cancer cells [Okegawa et al, 2004]. CAR is the primary cell surface receptor for species C Ad and is required for efficient Ad5 infection. In response, several strategies have been investigated using genetic or chemical modifications to retarget Ad, in attempts to improve infectivity.

Various modifications can be employed to genetically retarget Ads, including; pIX gene fusions, hexon modification, penton base gene fusions, fibre modifications and whole fibre replacements [reviewed by Mathis et al, 2005].

The simplest of these strategies is whole fibre replacement to generate so-called 'pseudotyped' or chimeric adenoviruses. This strategy is made possible by the high degree of structural similarity between Ad fibres and the identification of Ad serotypes whose native tropism is not CAR. Successful Ad fibre replacement was achieved in the mid

nineties, by replacement of the Ad5 fibre with that of Ad7 [Gall et al, 1996]. Since then, chimeric viruses have been constructed with the fibres from Ad35 (to target lymphoid cell lines) and Ad16 (to target cultured synovial cells) [Goossens et al, 2001; Nilsson et al, 2004], both of which increase target cell transduction. Replacement of the fibre with that of Ad37 (a species D virus) produces significantly less viral infection to rat liver *in vivo* [Denby et al, 2004]. Replacement of the entire Ad fibre is perhaps not as desirable as other genetic retargeting strategies. The length and flexibility of the fibre shaft appears to play a role in Ad cell entry and replacement of longer shafts (such as Ad5) with shorter shafts (as found in Ad37) may cause a steric hindrance problem resulting in reduced cell attachment [discussed by Nemerow et al, 2009].

Krasnykh *et al* employed a slight variation of this strategy, by replacing just the fibre knob domain of Ad5 with that of Ad3 and achieved an increase in transduction of ovarian, renal and squamous cell cancer cells [Haviv et al, 2002; Kanerva et al, 2002]. This strategy has also been shown possible with the Ad37 fibre knob domain, which uses sialic acid as a receptor [Cashman et al, 2004].

A more elegant approach to fibre retargeting is the genetic incorporation of targeting peptide within the fibre knob domain. Peptide binding motifs can be incorporated into both the C-terminal and HI loop of the fibre knob domain. The C-terminal additions were the first to be exploited, however this strategy is severely limited, since incorporation of 27 or more amino acids inhibits fibre trimerisation [Hong and Engler, 1996]. The HI loop can tolerate up to a 83 amino acid insertion, without affecting virion integrity or natural tropism [Belousova et al, 2002] and is thus more useful for peptide insertion.

The most common use of this strategy is insertion of the RGD integrin binding motif within the HI loop of the fibre knob domain. The RGD motif is found within the Ad penton base as

well as other viral proteins (such as the yellow fever virus envelope protein) and cellular proteins (such as fibronectin), and binds  $\alpha_v\beta_{3/5}$  integrins. By inserting the RGD motif within the Ad5 fibre knob the virus can use integrins as the primary cell attachment receptor [Dmitriev et al, 1998]. Integrins are generally highly expressed across many cell types and therefore represent a good candidate for virus retargeting. Indeed several groups have constructed RGD-retargeted Ad5 vectors, and have demonstrated improve transduction of a variety of CAR negative cell lines and primary tumour material [Mathis et al, 2005]. Retargeting in this way can be performed without affecting the natural CAR tropism.

Because of the large insertions tolerated in the HI loop, various peptides binding motifs have been successfully inserted. A series of investigations have inserted multiple immunoglobulin binding domains (also known as Affibodies) into knob-less fibre protein and within the fibre HI loop [Henning et al, 2005; Henning et al, 2002; Magnusson et al, 2007; Myhre et al, 2007]. Recently two immunoglobulin binding domains specific for HER2/neu and Taq polymerase, separated by a flexible linker domain, were inserted into the HI loop of the same virus. This study demonstrated two separate Affibody molecules can be inserted into the same HI-loop while retaining the target specific binding of both affinity proteins [Myhre et al, 2009].

Other studies have investigated virus retargeting using hexon, penton base and protein IX. The RGD motif has been inserted into the fifth hypervariable region of Ad5 hexon and has shown enhanced transduction to  $\alpha_v$  integrins [Mathis et al, 2005].

The C-terminal domain of protein IX has been fused to several peptides to modify the tropism of the virus. These include polylysine, the RGD motif and the c-Myc epitope [Dmitriev et al, 2002; Vellinga et al, 2004], however direct retargeting to cells has not been demonstrated for any of these peptides. The entire IX gene has been fused with a single-

chain antibody against  $\beta$ -galactosidase, via a spacer sequence. EM demonstrated the antibody was present on the outside of the capsid protein and available to its ligand, however this method has not been shown to directly retarget virus binding [Vellinga et al, 2007].

A recent series of studies has investigated liver detargeting by ablation of the hexon-FIX interaction, which was shown to mediate liver transduction via HSPG *in vitro* and *in vivo* mice models. Exchanging the hypervariable regions of hexon responsible for FIX binding with ones that do not bind FIX, or mutagenesis of the amino acids responsible for FIX binding, completely ablated liver transduction *in vitro* and *in vivo* murine models [Alba et al, 2009; Greig et al, 2009; Kalyuzhniy et al, 2008b].

To date no clinical trial has been completed with a retargeted virus. Two phase I trials have been recently approved for treatment of recurrent ovarian cancer, both of which use an Ad vector with the RGD insertion in the fibre HI loop. The first of these trials uses a replication deficient Ad vector expressing both the HSKtk gene for suicide gene therapy, and the human somatostatin receptor subtype-2 (hSSTR2) for imaging of virus distribution. This vector has been recently tested in a pre-clinical Syrian hamster model to provide justification for planned dosing, and insights into any anticipated toxicity [Matthews et al, 2009] The second of these trials uses an ‘un-armed’ oncolytic Ad vector containing the E1A CR2  $\Delta$ 24 deletion. Again a pre-clinical study of this vector has been completed in cotton rats to gain insights into clinical dosing and any anticipated toxicity [Page et al, 2007].

A phase I clinical trial has also been approved in the US using an Ad5 vector with a chimeric Ad3 fibre for the treatment of recurrent ovarian cancer. However no data has been published as yet [www.wiley.co.uk, Dec. 09].

Chemical modifications use synthetic polymers to evade the immune response and for tumour targeting. The use of chemical retargeting is outside the scope of this thesis, however has been extensively reviewed previously [Kreppel and Kochanek, 2008].

#### **1.2.4.4.2 Improving Tumour Specificity**

Increased understanding of cell biochemistry has helped develop more stringent tissue and tumour selective CRAd. Replacement of viral promoters with tumour or tissue specific promoters has been combined with the E1B-55K or E1A CR2  $\Delta$ 24 deletion to create an extensive variety of CRAd vectors.

In 2002 Johnson *et al* constructed an E1A CR2  $\Delta$ 24 vector which had both the E1A and E4 promoters replaced by the tumour selective E2F-1 promoter [Johnson et al, 2002]. This CRAd displaced potent cytotoxic activity against cancer cells but was essentially replication deficient in primary culture cells. Later the same vector was armed by replacing the E3B region with the NTR gene, to create ONYX-411<sup>NTR</sup>. In combination with the prodrug SN28343 this vector was able to eliminate H1299 tumour xenographs in 5 out of 8 (62.5%) mice [Singleton et al, 2007].

Majem *et al* constructed two vectors similar to ONYX-411, both of which contained the E1A CR2  $\Delta$ 24 deletion and an RGD motif inserted into the fibre HI-loop [Majem et al, 2006]; however these vectors retained the wildtype E4 promoter. The first, vICOVIR-1, had the natural E1A promoter replaced by the human E2F-1 promoter, preceded by a synthetic poly(A) sequence to insulate against transcription from non-selective endogenous viral transcription elements. In the second of these vectors, vICOVIR-2, the E2F-1 promoter has been additionally insulated using the 0.7kb insulator region from the myotonic dystrophy

locus (DM-1). This region contains CTG repeats and CTCF binding regions that together function as an insulator, blocking the interaction between promoter-enhancer elements. Both vectors expressed less E1A in normal cell lines and introduction of the tumour specific promoters did not show any significant loss of antitumour efficacy. Moreover introduction of the DM-1 insulator elements resulted in increased selectivity of E1A expression [Majem et al, 2006]. During the course of this thesis Alonso *et al* improved this vector by introducing a Kozak consensus sequence direct before the E1A translational start site for increased E1A expression. Three studies subsequently demonstrated this vector, termed vICOVIR-5, possessed potent anti glioma effect in *in vivo* mice models, alone and in combination with chemotherapy, and low systemic toxicity [Alonso et al, 2007a; Alonso et al, 2007b; Cascallo et al, 2007]. Furthermore, this vector has recently been approved for a phase I clinical study of gliomer [www.wiley.co.uk, Dec. 09]. Finally in 2009 Rojas *et al* modified the E2F-1 promoter in vICOVIR-5, by inserting an additional two E2F responsive regions (each one containing the two E2F binding palindromes), to create the vICOVIR-7 virus [Rojas et al, 2009]. The presence of these extra E2F binding palindromes caused increased tumour selectivity (i.e. reduced expression in normal cells), resulting in a low systemic toxicity at high doses in immuno-competent mice.

Within this series of vectors all the tumour selective modifications made centre on the pRb pathway. This could cause a problem, as loss of one control mechanism in normal cells would not be compensated for by the second. This is further complicated by presence of wildtype E4orf6/7 under control of the wildtype E4 promoter. E4orf6/7 is known to dimerise with E2F and activate transcription of E2F response elements, such as those found in the Ad5 E2 region and the E2F-1 promoter itself. Thus any leaky expression of E4orf6/7 could sequester any small amount of free E2F in normal cells and allow transcriptional

activation of E1A and E2F itself. More E2F could upregulate E1A transcription, which could in turn upregulate E4orf6/7 transcription and further enhance E2F and E1A transcription. The resultant positive feedback loop could reduce the normal cell attenuation and also cause increased E1A expression at late times of infection.

Increased replication selectivity has been achieved by combining the E1B-55K or E1A CR2 deletions with various tissue selective promoter replacements. Table 1-5 lists a selection of combinations which have been investigated; however this list is by no means exhaustive.

<b>Deletion</b>	<b>Promoter</b>	<b>Target</b>	<b>Conclusion</b>	<b>Reference</b>
E1B-55K	Carcinoembryonic antigen promoter	Colon cancer	Elimination of colon metastasis in mice xenograph model	[Sagawa et al, 2004]
E1A CR2 $\Delta$ 24 +/- $\Delta$ N-terminal	Long or short Cox2 promoter	Ovarian cancer	>10,000-fold growth attenuation in normal cells	[Bauerschmitz et al, 2006]
E1B	PPT promoter (PSA enhancer, PSMA enhancer and TARP promoter)	Prostate cancer	Suppressed growth of aggressively growing prostate tumour in mice	[Danielsson et al, 2008]
E1A CR2 $\Delta$ 24	E1A replaced with poly(A) sequence and tyrosinase enhancer/promoter	Malignant melanoma	100-1000 fold attenuation in non-melanocytic tissue	[Nettelbeck et al, 2002]

**Table 1-5. CRAd with tissue specific promoters**

Whereas introduction of tissue specific promoters can increase the replication selectivity, it of course narrows down the potential therapeutic targets to just one tissue. Additionally introduction of tissue specific promoters generally increases the size of the viral genome, reducing the space left for introduction of therapeutic transgenes.

Use of tissue selective promoters in CRAAd vectors has been taken to the extreme by replacing almost all the natural Ad promoters with foreign promoters. Fuerer and Iggo produced a series of Tcf responsive CRAAd vectors for treatment of colon cancer [Fuerer and Iggo, 2002]. The Tcf transcription factor is part of the wnt signalling pathway, which is pathologically activated in the majority of colon cancers. Mutations, at any one of several points in the wnt pathway, result in nuclear localisation of  $\beta$ -catenin where it associates with Tcf to activate transcription of wnt responsive genes such as c-myc, cyclin D1 and Tcf1. Thus the Tcf controlled viruses should only replicate in colon cancer, where the wnt pathway is activated. The panel of viruses created used Tcf responsive elements to control early viral gene transcription (including the E1A, E1B, E2 and E4 regions), with or without an E1A N-terminal deletion. This deletion removes the region of E1A responsible for interacting with p300/CBP, ablating the ability to activate viral transcription in normal cells. The CRAAd termed vCF62, in which the natural E1A, E1B, E2 and E4 promoters were all replaced with Tcf responsive elements, and the N-terminus of E1A deleted, demonstrated attenuated growth compared to Ad5 wt in all the cell lines tested. Several viral intermediates of vCF62 showed good replication selectivity for a range of colon cancer cell lines, and no attenuated growth compared to vCF62. This report not only demonstrates how tumour selective promoter can be used successfully, but how extreme modifications can result in less useful attenuated vectors.

The first CRAAd vectors contained deletions in the E3 region, which is dispensable for growth in tissue culture. However it was demonstrated by Suzuki et al that the presence of the E3 region improved lytic activity due to the activity of ADP [Suzuki et al, 2002]. Doronin *et al* over-expressed the ADP protein in a vector with a wt E1 region and all E3 genes deleted except for E3-12.K [Doronin et al, 2003]. This vector, VRX-007 and later

referred to as INGN-007, demonstrated improved oncolytic activity and has recently been approved for a phase I clinical trial [www.wiley.co.uk, Dec. 09]. In anticipation of this trial pre-clinical studies were completed to investigate toxicity and biodistribution in Syrian hamsters [Ying et al, 2009].

#### **1.2.4.4.3 Improving Enzyme-Prodrug Systems**

Chen *et al* at The University of Birmingham, School for Cancer Sciences –Gene Therapy group (SCS-GT group) developed an E1B-55K deleted CRAd vector expressing NTR, termed CRAd-NTR, for combined oncolytic and enzyme-prodrug therapy. NTR expression was under control of the CMV immediate early promoter, and had a downstream intron and 3'-end processing signals from the human  $\beta$ -globin and complement C2 genes, respectively [Chen et al, 2004]. This NTR expression cassette was inserted within the E1B-55K deletion. CRAd-NTR out-performed replication deficient vector expressing NTR from a similar expression cassette (CTL102), *in vitro* and in *in vivo* animal studies [Chen et al, 2004]. However, the early expression of NTR in combination with CB1954 had a detrimental effect on virus replication, reducing the natural oncolytic effect of the virus. In response, a second vector was constructed which replaced the pIX coding region with the NTR sequence for expression at intermediate times of replication [Roesen, 2006]. As expected this virus, vNR6, showed no reduction in virus replication in the presence of the prodrug CB1954. Additionally, this virus demonstrated increased *in vitro* cytotoxicity and greater vector spread through monolayer and three dimensional tissue culture models, however the level of NTR expression, and hence the degree of sensitisation to CB1954, was reduced compared to CRAd-NTR.

This work illustrates the balance required between viral lytic activity and enzyme-prodrug cytotoxicity. If enzyme expression is too high and early, treatment with prodrug can have a

detrimental effect of virus growth. However expression needs to be high enough to provide a therapeutic effect.

Studies using the NTR-CB1954 enzyme prodrug system in replication deficient vectors *in vitro* and *in vivo* demonstrated the extent of cell killing was dependent upon the level of expression (or viral dose) and prodrug concentration [Djeha et al, 2001; McNeish et al, 1998; Weedon et al, 2000]. These data imply that the rate of CB1954 activation is a significant limitation to the efficacy of the therapy and indeed CB1954 is a poor substrate for the enzyme NTR [Anlezark et al, 1992]. In response to these observations, mutagenesis has been used on the NTR gene, *nfsB*, to create NTR mutant variants, termed ‘turbo-NTR’. The first study used the crystal structure of NTR to identify 9 potential residues around the active site which could directly influence prodrug binding and catalysis. Selected mutations in 6 of these residues showed increase sensitivity to CB1954 compared to the wt enzyme [Grove et al, 2003]. Guise *et al* then developed a direct positive selection strategy to identify NTR mutants for improved CB1954 catalysis from a library of  $\sim 10^6$  possible combinations. This strategy identified a triple mutant NTR variant, T41Q/N71S/F124T, which conferred a 40- to 80-fold increase in CB1954 sensitivity to ovarian cancer cells [Guise et al, 2007]. The single mutations identified by Grove *et al* were also combined to give a panel of 53 double mutant ‘turbo-NTR’ variants, of which the best combination, T41L/N71S, showed a 14-17 fold increase in sensitisation to CB1954 compared to wt NTR, in ovarian cancer cells [Jaberipour et al, 2010].

Most studies using the NTR-CB1954 suicide gene therapy system have focused on using the minor *E.coli* NTR encoded by the *nfsB* gene. The major NTR variant encoded by the *nfsA* gene has also been investigated in combination with the prodrug CB1954. The wt

version of *nfsA* NTR shows a 3.5- to 8-fold greater sensitivity to CB1954 compared to the wt *nfsB* encoded NTR. Furthermore *nfsA* NTR was shown to have an increased bystander effect with CB1954 compared to *nfsB* NTR, due to selective reduction of the 2-NO<sub>2</sub> group of CB1954 [Vass et al, 2009].

## **1.3 Prostate Cancer Gene Therapy**

### **1.3.1 The Prostate and Prostate Cancer**

The prostate is a walnut sized gland situated directly below the bladder, in the pelvic cavity between the lower part of the pubic symphysis and the superior fascia of the urogenital diaphragm. The prostate is composed of approximately 70% glandular tissue and 30% fibromuscular stroma and in normal biology serves as an exocrine gland that produces upto 12% of semen by volume [Patel, 2006].

Prostate cancer accounts for almost a quarter of all new male cancers diagnosed, making it the most common cancer in men in the UK. Over the past 30 years better detection techniques have lead to an increase in prostate cancer incidence rates. However this increase has not translated into increased mortality, which has remained approximately constant since the mid 1970's [Patel 2006; Selley et al, 1997; [www.statistics.gov.uk/statbase/](http://www.statistics.gov.uk/statbase/), Dec. 09].

Incidence rates of prostate cancer are strongly associated with age, with little incidence in men under 50 and more than 60% of cases occurring in men over 70 years old. It has been estimated upto 30% of men over the age of 50 have histological evidence of prostate cancer, which rises to 60-70% of men by the age of 80. However still only 4% (approximately 1 in 25) of these men will die from this disease [Selley et al, 1997].

Prostate cancer has the highest prevalence rates in African-American men which is significantly higher than that of white Americans, with the lowest rates recorded in Asian men and men of South Asian origin [Patel 2006; www.cancer.gov, 09]. In addition to age and ethnicity, a family history of prostate cancer in a first degree relative (brother or father) also increases the risk of developing prostate cancer by 2 to 3 times [Monroe et al, 1995]. Furthermore, men whose families have a history of breast cancer, specifically associated with the BRCA2 gene, are also at high risk of prostate cancer. Several dietary factors have been associated with an increased risk of prostate cancer including alpha-linolenic acid, cholesterol, dairy products and alcohol [Patel 2006]. It has also been suggested the high incidence rates of prostate cancer found in developed countries is associated with the western diet, especially the high intake of animal fats.

### **1.3.2 Molecular Mechanisms of Prostate Cancer**

Prostate cancer is a highly heterogeneous disease which results from multiple complex genetic alterations [reviewed by Reynolds, 2008]. Prostate cancer is a disease of aging and is thought to begin with chronic accumulation of prostatic intraepithelial neoplasia (PIN) lesions which eventually develop into adenocarcinoma [Lawson, 1997]. Early genetic events in the development of prostate cancer are thought to be driven by the loss of tumour suppressor proteins such as PTEN, NKX3.1, P27, KLF5 and KLF6. It has been suggested these early genetic events, in particular loss of the tumour suppressors PTEN and NKX3.1, dysregulate cellular proliferation and drive benign to PIN transition [Reynolds 2008].

It would seem one of the major factors in the progression from PIN to adenocarcinoma is the development of gene fusions between TMPRESS2 and members of the oncogenic ETS family of transcription factors [reviewed by Morris et al, 2008]. This fusion joins the oncogenic ETS family members to the regulated promoter region of androgen-responsive

gene *TMPRSS2*, resulting in the direct androgen dependent upregulation of the ETS oncogenic factors.

Molecular techniques such as gene array profiling and rt-PCR identified the alpha-methyl CoA racemase (*AMACAR*) gene as being highly upregulated in 100% of prostate cancers and has subsequently been used as a marker for prostate cancer morphologies in prostate needle biopsies [Magi-Galluzzi et al, 2003; Reynolds 2008]. Histone deacetylases (HDAC) are frequently found upregulated in prostate cancer, particularly in hormone-refractory diseases. Histone acetylation is a major epigenetic modulation which facilitates transcriptional activation and the hypoacetylation of histones is highly associated with DNA methylation, which is believed to repress transcription of methylated promoters. Hypermethylation of *GSTP1*, a gene involved in carcinogen detoxification, is one of the most frequently observed modifications, in addition to the *MDR1* and *APC* genes [Bastian et al, 2005; Lodygin et al, 2005; Yegnasubramanian et al, 2004].

Androgen receptor gene reactivation is a central transformation event in the transition to hormone-refractory prostate cancer. There are several potential mechanisms behind androgen receptor reactivation including gene amplification, somatic mutations and epigenetic modifications. In addition to androgen receptor, *MYC* and *EIF3S3* have also been identified as undergoing frequent gene amplifications in hormone-refractory prostate cancers [Nupponen and Visakorpi, 1999].

Mutations in the p53 tumour suppressor gene are also commonly observed in prostate cancer, with an average frequency of 20-30%. Furthermore, p53 mutations are more frequently detected in more advanced prostate cancers and have been associated with locally advanced hormone-refractory diseases [Gao et al, 1997; Grignon et al, 1997; Quinn et al, 2000]. The insulin-like growth factor-binding protein 2 (*IGFBP2*) has been shown to

be overexpressed in 36% of primary prostate tumours and 100% of hormone-refractory prostate cancers, while expression is normal in benign prostate hyperplasia samples [Reynolds 2008]. When taken together both the p53 and IGFBP2 observations suggest a steady accumulation of genetic mutations during the development from benign to advanced hormone-refractory disease.

### **1.3.3 Current Prostate Cancer Therapy**

Treatment options for early localised prostate cancer comprise of surgery and radiotherapy, both of which demonstrate upto a 90% ten-year survival rate [Donovan et al, 1999; Patel 2006]. Following progression to locally advanced disease patients may receive radiotherapy or hormone therapy. Treatment of patients who are at high risk of advanced local recurrence with adjuvant radiotherapy following prostatectomy improves five year PSA relapse-free survival [Bolla et al, 2005a; Bolla et al, 2005b]. Approximately 30-60% of patients with local disease following local therapy go on to show PSA recurrence within 10 years of treatment. This rate is substantially higher with locally advanced disease [Patel 2006]. Treatment options for locally recurrent prostate cancer centre around surgery and radiotherapy, however the selection of treatment depends on many factors and individual patient consideration needs to be taken into account. Most patients with locally recurrent prostate cancer will fail surgery or radiotherapy with disseminated disease and are managed with hormone therapy. Whereas treatment of metastatic disease with hormone therapy gives good short-term control there is no curative option and in most cases the cancer begins to grow again. As a last resort chemotherapeutic agents such as mitoxantrone or docetaxel may be used to try and give a survival benefit; however any benefit has to be weighed against the associated toxicity [Tannock et al, 2004]. It is therefore essential novel therapies, such as gene therapy, are developed for the treatment of locally recurrent prostate

cancers as improved local control would be of major benefit by either postponing or avoiding completely the development of metastatic disease and need for systemic hormone treatments.

#### **1.3.4 Gene Therapy Strategies for Prostate Cancer**

Gene therapy was first used for prostate cancer in 1994 and since then 103 clinical trials have started of which 73 are reported to be ongoing [www.wiley.co.uk, Dec. 09]. A variety of viral vectors are undergoing clinical trial for prostate cancer including retrovirus, adeno-associated virus, pox viruses and vaccinia virus, however more than half of all prostate cancer gene therapy trials use adenovirus vectors. Several strategies have been employed using adenovirus delivery and are summarized in Table 1-6.

<b>Therapy</b>	<b>Gene delivery/modification</b>	<b>Number trials</b>
Tumour suppressor replacements	p53 p16	2 Phase I 1 Phase II 1 Phase I
Immunotherapy	IL-2 IL-12 TRAIL IFN- $\beta$ CD40 + prostate specific membrane antigen RTVP-1 p501 with p501 protein and adjuvant MUC1 PSA vaccine	2 Phase I 2 Phase I 1 Phase I 1 Phase I 1 Phase I/II 1 Phase I 1 Phase I 1 Phase I 1 Phase I 2 Phase II
Enzyme - prodrug therapies	HSVtk or HSVtk with CD Purine nucleoside phosphorylase Nitroreductase	5 Phase I 4 Phase I/II 1 Phase I 1 Phase I 1 Phase I/II
Oncolytic adenovirus	PSA promoter  Osteocalcin promoter	4 Phase I 2 Phase I/I 2 Phase II 1 Phase I
Radioisotope deliverey	Sodium iodide cymporter with radioiodine	1 Phase I
Combined theapies	GM-CSF + NT Oncolytic vector with combined HVtk and CD  Oncolytic vectors with sodium iodide smporter	1 Phase 3 Phase I 2 Phase I/II 1 Phase II 1 Phase III 1 Phase I

**Table 1-6. Prostate cancer gene therapy trials reported ongoing**

Whereas the use of immunotherapy for treatment of prostate cancer is outside the scope of this work the most recently clinical trials using tumour suppressor replacements, enzyme-prodrug systems, oncolytic adenoviruses and combined therapies have all been previously discussed (see sections 1.2.4.1.1 to 1.2.4.4). Of all the adenovirus strategies used oncolytic vectors combined with HSVtk and CD has arguably had the most success, demonstrated by the fact this is the only phase III clinical trial in progress.

## **1.4 Aims of Thesis**

The aim of this research was to construct improved oncolytic adenovirus vectors armed with NTR, for combinational oncolytic virotherapy and NTR/CB1954 enzyme/prodrug therapy, for the treatment of prostate cancer. The new oncolytic NTR viruses were based around the ICOVIR vectors designed by Dr R. Alemany and were compared to the E1B-55K deleted vNR vectors (vNR3 and vNR6)

To begin the ICOVIR-5 and ICOVIR-7 based vectors from Dr R. Alemany's lab were chosen for construction of new oncolytic adenovirus vectors expressing the marker transgene eGFP. These new oncolytic vectors were to be characterised and compared to the E1B-55K deleted vectors vNR3, in terms virus replication, transgene expression, cytotoxicity, tumour selectivity, DNA replication, transgene expression and any effect on transgene insertion on oncolytic activity.

Using this data the most tumour selective vector would be chosen of the introduction of the therapeutic transgene NTR. ICOVIR based vectors will be constructed which expresses either wt NTR, double mutant NTR or triple mutant NTR. These vectors will be subsequently characterised and compared to vNR6, in terms of oncolytic cytotoxicity, tumour selectivity, NTR/CB1954 mediate cytotoxicity and combined cytotoxicity. From this data the vector which showed the greatest tumour selectivity and combined cytotoxicity was to be identified as a potential future vector for prostate cancer gene therapy.

# **CHAPTER 2**

## **Materials and Methods**

## **2.1 Suppliers of Materials**

Unless otherwise stated all materials were supplied by Sigma-Aldrich (Poole, UK). De-ionised water (ddH<sub>2</sub>O) was obtained from a Maxima Ultrapure Water (ELGA, High Wycombe, UK).

## **2.2 Molecular Cloning**

Experiments involving bacteria were performed in a specific work area, within an ACGM containment level 2 room. Generally methods for molecular biology were based on “Molecular Cloning: A Laboratory Manual” [Sambrook et al, 1989] or “Current Protocols in Molecular Biology” [Ausubel et al, 1998], unless otherwise described. All position in the adenovirus type 5 genome were in reference to the published Ad5 sequence on GenBank, accession number AC\_000008 (reference sequence BK000408)

### **2.2.1 Restriction Endonuclease Digestion of DNA**

All enzymes were sourced from New England Biolabs (Hitchin, UK) or Roche Welwyn Garden City, UK). Reaction components and incubation conditions were all based on manufacturer’s instructions.

Where digestion with multiple enzymes was required, digestions were either carried out simultaneously (provided the reaction conditions were compatible) or DNA was purified following the first digestion before being digested with the second enzyme in a separate reaction.

### **2.2.2 Phenol/Chloroform Extraction**

Phenol/chloroform extraction was performed to purify DNA. Samples were made up to a convenient volume (e.g. 200µl) with T<sub>10</sub>E<sub>1</sub> or T<sub>10</sub>E<sub>1</sub>N<sub>100</sub> as appropriate, to which an equal

volume of 1:1 (v/v) phenol/chloroform was added. Samples were securely capped, thoroughly mixed by inversion or vortexing before being centrifuged (16,000g for 1 minute in a microcentrifuge) to separate the organic and aqueous phases. The DNA containing aqueous phase was transferred into a new tube and an equal volume of chloroform added. The mixing and centrifuge steps were repeated and the DNA containing aqueous phase transferred into a new tube. If residual ethidium bromide (EtBr) was still present multiple rounds of extraction were performed.

### **2.2.3 Precipitation of DNA**

For DNA precipitation samples were adjusted with T<sub>10</sub>E<sub>1</sub> and 5M NaCl to give a final NaCl concentration of 100mM. DNA was precipitated by the addition of 2-2.5 volumes of 100% ethanol or 1 volume of isopropanol and incubated for 30-60 minutes at -20°C. DNA was pelleted by centrifugation (16,000g for 10 minutes in a microcentrifuge), the supernatant removed by aspiration and DNA pellets air dried. DNA was resuspended in the required volume of T<sub>10</sub>E<sub>1</sub> or ddH<sub>2</sub>O.

### **2.2.4 Agarose Gel Electrophoresis**

0.6% to 2% (w/v) agarose gels were prepared in 1x TAE running buffer (diluted from a 50x TAE stock solution) and submerged in 1xTAE buffer in a horizontal gel electrophoresis tank. DNA samples were mixed with 5x glycerol loading buffer (50% (v/v) glycerol with bromophenol blue in ddH<sub>2</sub>O) and loaded into preformed wells. Commercial DNA ladders (100bp – 10kb) were used for measurement of band size.

Samples were run at 20-100V for 2-16 hours depending on band size and separation required. Gels were stained in 1xTAE containing 0.5µg/ml ethidium bromide (diluted from a 10 mg/ml stock) and visualised by UV illumination. If required, gels were destained in

1xTAE solution. Images were recorded using a Kodak DC290 camera (Kodak, Hemel Hempstead, UK) in combination with a Spectroline TVC312A UV transilluminator (Spectroline, Westbury, NY, USA).

### **2.2.5 Gel Purification of DNA Fragments**

0.6% to 1.5% (w/v) agarose gels were made using SeaKem GTG low melting point agarose (Lonza, Wokingham, UK) in 1xTAE solution. DNA samples were mixed with 5x glycerol loading buffer and 2µl of SYBR® Gold (Invitrogen, Paisley, UK) before being loaded into preformed wells and separated by electrophoresis. Bands were visualised on a blue light transilluminator and required bands excised from the gel using a scalpel.

DNA was extracted using a Qiaquick DNA Gel Extraction Kit (QIAGEN, Crawley, UK) following the manufacturer's instructions.

### **2.2.6 Quantitation of DNA**

DNA concentration was measured by PicoGreen assay [Ahn et al, 1996; Ferrari et al, 1998; Murakami and McCaman, 1999]. DNA standards were prepared using bacteriophage lambda DNA at 1-1000ng/ml (New England Biolabs, Hitchin, UK) diluted in T<sub>10</sub>E<sub>1</sub>. Triplicate 100µl aliquots of sample and standard DNA were placed into wells of a 96-well plate. PicoGreen® reagent (Invitrogen, Paisley, UK) was diluted 1:200 with T<sub>10</sub>E<sub>1</sub> and 100µl added to each well, and incubated in the dark for 2 minutes. Fluorescence was measured at 485nm excitation / 535nm emission on a Wallac Victor<sup>2</sup> 1430 Multilabel counter. DNA concentration was calculated from the standard curve.

### **2.2.7 DNA Ligations**

DNA ligation was performed using T4 DNA ligase (Roche, Welwyn Garden City, UK). Ligation reactions were set up in a volume of 20µl containing 1µl T4 DNA ligase and 2µl

of 10x enzyme buffer (supplied with ligase). A 3:1 molar ratio of insert:vector DNA was used for 'sticky end' ligations.

When required the 5' ends of the plasmid were dephosphorylated before ligation, using calf intestinal alkaline phosphatase (CIAP) (New England Biolabs, Hitchin, UK), following manufacturer's instructions. Dephosphorylation was carried out for 1 hour at 37°C.

### **2.2.8 Polymerase Chain Reaction (PCR)**

PCR was used for DNA amplification. When required KOD Hot Start DNA polymerase (Novagen, Merck, Nottingham, UK) was used to increase PCR fidelity, otherwise GoTaq<sup>®</sup> DNA polymerase (Promega, Southampton, UK) was used. PCR reactions were set up following manufacturer's instructions. A typical PCR reaction consisted of 10µl 10x reaction buffer, 10µl 2mM dNTP mixture, 0.5µM (final concentration) of forward and reverse primer, 10-50ng of template DNA, 1 unit of enzyme in a final volume of 100µl. A full list of forward and reverse primers can be found in Table 2-1.

<b>Primer</b>	<b>Description</b>	<b>Sequence (5' – 3')</b>	<b>Details or Position in Ad5 wt genome (5' - 3')</b>
MHp001	Forward eGFP primer with MfeI site	CGTCAATTGT ACTAAGCGGT GATGTTTCTGA TC <b>AGCCACCAT</b> <u>GGTGAGCAAG</u> GGCGAG	Primer used to introduce an MfeI site (bold), splice acceptor site (red), Kozak sequence (italics) with eGFP complementary region (underlined)
MHp002	Reverse eGFP primer with MfeI site	CAGCAATTGA AAAATAAAGT TTATTACTTGT <u>ACAGCTCGTC</u> <u>CATGCC</u>	Primer used to introduce a MfeI site (bold) with eGFP complementary region (underlined)
MHp003	pMH003/4 sequencing primer and eGFP screening	CGGTACACAG GAAACAGGAG A	32652 - 32672
MHp004	pMH003/4 sequencing primer and eGFP screening	TCGTGACCAC CCTGACCTAC	182 - 201 in eGFP ORF
MHp005	pMH003/4 sequencing primer	GAACTCCAGC AGGACCATGT	672 - 653 in eGFP ORF
MHp006	pMH003/4 sequencing primer and eGFP screening	GACAGGAAAC CGTGTGGAAT	33056 - 33037
MHp007	Fibre sequencing primer	GCTCTGGTATT GCAGCTTCC	30930 - 30949
MHp008	Fibre sequencing primer	GGAACCATAG CCTTGTTTGAA	32165 - 32145
MHp009	Fibre sequencing primer	CAAACCCAA GGCTCCAGTA	31777 - 31758
MHp010	Fibre sequencing primer	ACAGCACAGG TGCCATTACA	32192 - 32211
MHp017	ICOVIR-7 promoter sequencing primer	TGTCTGTCCCC ACCTAGGAC	Labelled in appendix 2.
MHp018	ICOVIR-7 promoter sequencing and reverse primer used to amplify the ICOVIR-7 promoter region	TCGTGAAGGG TAGGTGGTTC	693 - 674
MHp019	ICOVIR-7 promoter sequencing primer and forward primer used to amplify the ICOVIR-7 promoter region	TTTGGGCGTA ACCGAGTAAG	245 - 264
MHp020	ICOVIR-7 promoter sequencing primer	GGGGACAGCC TATTTTGCTA	Labelled in appendix 2.

MHp021	ICOVIR-7 promoter sequencing primer	GCAAATTTCC CGAGTAAGCA	Labelled in appendix 2.
MHp022	ICOVIR-7 promoter sequencing primer	CCCCACCTATC GTTGGTTC	Labelled in appendix 2.
MHp023	ICOVIR-7 promoter sequencing primer	GGATCACAGG ACTGGAGCTG	Labelled in appendix 2.
MHp024	ICOVIR-7 promoter sequencing primer	CGATAGGTAC CATCCGGACA	Labelled in appendix 2.
FibreFwd	Forward pMH003/4 screening primer within the fibre ORF	CCCTTACTATC ACTGCCTCAC C	31556 - 31577
GFPRvs	Reverse pMH003/4 screening primer within the eGFP ORF	TTACGTCGCC GTCCAGCTCG	70 - 51 in eGFP ORF
PS1368A	Forward primer within the $\Delta 24$ deletion	CTGCCACGAG GCTGGC	928 - 943
PS1368B	Forward primer across the $\Delta 24$ deletion	<u>AGGTGATCGA</u> <u>TC CACCCAG</u>	912 - 923 (underlined), 948 - 954 (plain text)
PS1368C	Reverse primer in the E1A ORF	CCACACACGC AATCACAGG	1572 - 1554
PS1300A	Forward NTR primer with MfeI site	<u>CGTCAATTGT</u> <u>ACTAAGCGGT</u> <u>GATGTTTCTGA</u> <u>TCAGCCACCAT</u> <u>GGATATCATT</u> <u>CTGTCGCCT</u>	Same as MHp001 but replacing eGFP complementary sequence with NTR (underlined).
PS1300B	Reverse NTR primer with MfeI site	<u>CAGCAATTGA</u> <u>AAAATAAAGT</u> <u>TTATTACACTT</u> <u>CGGTAAAGT</u> <u>GATGT</u>	Same as MHp002 but replacing eGFP complementary sequence with NTR (underlined).

**Table 2-1. PCR primers used for cloning, screening and sequencing**

Reactions were cycled in a Perkin Elmer Gene Amp 2400 thermocycler (PE Applied Biosystems, Waltham, MA, USA) following the manufacturer's instructions. Thermal cycling conditions were:

Initial denaturation: 94°C for 5 minutes

30-40 cycles: 94°C for 45 seconds, 55°C for 40 seconds, 72°C for 1-3 minutes (depending on target length)

Final extension: 72°C for 5 minutes.

Amplified products were analysed by agarose gel electrophoresis.

### **2.2.9 DNA Sequencing**

PCR based sequencing reactions were carried out on purified DNA samples using the ABI Prism Big Dye Terminator cycle sequencing ready reaction kit (Applied Biosystems, Warrington, UK), according to manufacturer's instructions. Sequencing reactions consisted of 4µl of 2.5x reaction buffer, 0.5-1µg of template DNA, 5pmoles primer, 4µl terminator mix in a final volume of 20µl. Reactions were run in a thermal cycler as follows:

25 cycles: 96°C for 30 seconds, 50°C for 15 seconds.

Then: 60°C for 4 minutes.

The extension products were transferred to a 1.5ml microcentrifuge tube and precipitated by addition of 50µl of absolute ethanol and 2µl of 3M sodium acetate. The samples were incubated at room temperature for 15 minutes before being centrifuged at 16,000g for 20 minutes in a microcentrifuge. The pellets were washed with 250µl of 70% ethanol and samples centrifuged at 16,000g for 5 minutes in a microcentrifuge. Finally the DNA pellets were left to air dry for 15 minutes and stored at -20°C.

Immediately prior to loading into the sequencing 96-well plate, pellets were resuspended in 12µl of loading dye (5:1 mixture of de-ionised formamide:50mg/ml dextran blue in 25mM EDTA pH 8), vortexed and briefly centrifuged. Samples were heated at 90°C for 2 minutes in a heating block and kept on ice while loading. 7µl of each sample was loaded into individual wells of a 96-well plate and analysed on a Prism<sup>®</sup> 377 DNA sequencer (Applied Biosystems, Warrington, UK) according to manufacturer's instructions.

### 2.2.10 Preparation of Chemically Competent Cells

Transformation competent *E. coli* cells were prepared using the calcium chloride method. 1ml of overnight culture was used to inoculate 100ml of LB medium (bacterial growth medium, Table 2-2) and incubated at 37°C until the O.D.<sub>600</sub> was 0.45-0.55 but for no longer than 4 hours. The culture was equally divided into two 50ml tubes and cooled on ice for 15 to 20 minutes. Cells were pelleted by centrifugation at 4°C (500g for 10 minutes in a Beckman GS-6R benchtop centrifuge), pellets resuspended in 10ml of ice-cold 0.1M calcium chloride and incubated on ice for 30 minutes. Cells were repelleted, resuspended in 2ml of ice-cold 0.1M calcium chloride, incubated on ice for 2-3 hours, repelleted and finally resuspended in 2ml of 0.1M calcium chloride / 15% glycerol. 200µl aliquots were transferred into 1.5ml microcentrifuge tubes, frozen in liquid nitrogen and stored at -80°C until required.

<b>Culture Medium</b>	<b>Ingredients</b>
LB medium	6g LB broth base (Invitrogen) in 300ml ddH <sub>2</sub> O
SOB medium	8.4g SOB mixture (Difco) in 300ml ddH <sub>2</sub> O
LB agar	6g LB broth base (Invitrogen), 4.5g Bactoagar (Difco) in 300ml ddH <sub>2</sub> O
SOC medium	SOB medium supplemented with 20mM filter sterilised glucose

**Table 2-2. Bacterial growth medium**

### 2.2.11 Bacterial Transformation

*E. coli* XL2 cells were used for transformation with plasmid DNA. 50ng of ligated plasmid DNA (section 2.2.7) was mixed gently with 100µl of competent cells, previously defrosted on ice, and the DNA/cell mixture incubated on ice for 30-45 minutes. The mixture was heat-shocked at 42°C for 90-120 seconds and immediately placed on ice for a further 2

minutes. 900µl of SOC, prewarmed to 37°C, was added to the DNA/cell mixture and incubated at 37°C for 1 hour in a shaking incubator. 100µl and 20µl of the cell suspension was spread on to LB agar plates, containing appropriate antibiotic (100µg/ml ampicillin or 30µg/ml kanamycin). Plates were allowed to dry for 20-30 minutes before incubation at 37°C overnight.

*E.coli* BJ5183 cells were used for homologous recombination to introduce novel sequences into the Ad genome. The insert sequences were digested away and gel purified from the plasmid backbone. The vector was cleaved at the site of recombination, phenol/chloroform extracted, ethanol precipitated and re-dissolved in an appropriate volume of T<sub>10</sub>E<sub>1</sub> (a full description of insert/vector can be found in CHAPTER 3 ). Cut vector and purified insert were mixed at a 1:1 molar ratio and transformed into *E.coli* BJ5183 cells following the above transformation protocol. 100µl and 20µl of each transformation was plated onto LB agar plate containing the appropriate antibiotic. Plates were incubated overnight at 32°C.

### **2.2.12 Small Scale Preparation of Plasmid DNA**

Well-defined colonies were picked into 3ml SOB containing appropriate antibiotic and grown for 16 hours. 2ml of the culture was pelleted by centrifugation (5 minutes, 3,100g, in SM24 rotor) at 4°C, and the pellets resuspended in 100µl of ice-cold solution 1 (50mM glucose, 25mM Tris pH8, 10mM EDTA). 50µl of lysozyme solution (10mg/ml lysozyme freshly dissolved in solution 1) was added and incubated on ice for 10 minutes. 300µl of solution 2 (0.2M NaOH, 1% (w/v) SDS) was added, mixed gently and incubated on ice for a further 10 minutes to denature proteins and chromosomal DNA. 225µl of solution 3 (147g potassium acetate and 57.5ml glacial acetic acid in 500ml ddH<sub>2</sub>O) was added, carefully mixed and incubated for 10 minutes on ice to precipitate protein and single stranded DNA. Samples were centrifuged (7,900g, 10 minutes, 4°C in a SM24 rotor) and the supernatant

decanted into a 1.5ml microcentrifuge tube. Nucleic acids were precipitated by addition of 675µl of isopropanol and incubated at -20°C for 20 minutes. Nucleic acids were pelleted by centrifugation (9,500g for 10 minutes in a microcentrifuge), and redissolved in 200µl of T<sub>100</sub>E<sub>5</sub>N<sub>100</sub> containing 10µg/ml RNase A (previously heated for 1 hour at 100°C to inactivate contaminating DNase). Samples were incubated for 1 hour at 37°C, to digest RNA. DNA was phenol/chloroform extracted, ethanol precipitated and redissolved in T<sub>10</sub>E<sub>1</sub>.

### **2.2.13 Large Scale Preparation of Plasmid DNA**

Transformed XL2 clones were picked into 5ml of LB medium (containing appropriate antibiotic) and grown for 3-4 hours in a shaking incubator at 37°C. These cultures were used to inoculate 200ml of LB medium (containing appropriate antibiotic) and grown at 37°C for 16 hours in a shaking incubator. Cultures were centrifuged (3,100g in a Sorvall SLA-1500 rotor for 5 minutes at 4°C) to pellet the bacteria, and the pellet resuspended in 4ml of ice-cold solution 1. Bacterial cell walls were digested by addition of 1ml lysozyme solution (10mg/ml freshly dissolved in solution 1) and incubation on ice for 10 minutes. 10ml of solution 2 was added, mixed gently and incubated on ice for 10 minutes before addition of 7.5ml of solution 3 and further incubation for 10 minutes on ice. Samples were centrifuged (7,900g for 15 minutes at 4°C in a Sorvall SLA-1500 rotor), supernatant transferred to a fresh 225ml centrifuge tube. 22.5ml of isopropanol was added and samples incubated at -20°C for 30 minutes, to precipitate nucleic acids. Nucleic acids were pelleted by centrifugation (7,900g for 20 minutes at 4°C in a Sorvall SMA-1500 rotor) and pellets air dried. Pellets were re-dissolved for 16 hours in 2.5ml of T<sub>50</sub>E<sub>10</sub> prior to caesium chloride purification.

To redissolved nucleic acid pellets, 3.29g of caesium chloride and 290µl of 10mg/ml ethidium bromide were added and total weight made up to 5.29g with T<sub>50</sub>E<sub>10</sub>. The solution

was incubated on ice for 10 minutes and RNA pelleted by centrifugation (10,000g for 10 minutes in a SM24 rotor at 4°C). Supernatant containing plasmid DNA was transferred into 3.9ml Beckman Quick-Seal™ (Beckman Coulter) tubes, filled with isopycnic caesium chloride solution (1g of CsCl in 1ml of T<sub>50</sub>E<sub>10</sub>), heat sealed and ultra-centrifuged at 100,000 rpm (353,288g) for 4 hours, followed by 95,000 rpm (318,842g) for 2 hour and finally 65,000 rpm for 30 minutes (106,870g) (Beckman Optima™ TLX bench top ultra-centrifuge with a TLN-100 near vertical rotor). The lower plasmid band was carefully removed using a 21 gauge needle and 2ml syringe and diluted with 3 volumes of ddH<sub>2</sub>O. Ethidium bromide was removed by two rounds of phenol/chloroform extraction, DNA precipitated with 1 volume of isopropanol and pelleted by centrifugation (7,900g for 10 minutes in a Sorvall SM24 rotor at 4°C). Plasmid DNA was re-suspended in 500µl of T<sub>100</sub>E<sub>1</sub>N<sub>100</sub>, precipitated with 2 volumes of absolute ethanol, pelleted and plasmid DNA pellet dissolved in T<sub>10</sub>E<sub>1</sub>.

## **2.3 Tissue Culture**

All cells were kept in a Galaxy R 37°C humidified incubator with 5% CO<sub>2</sub> (RS Biotech, Irvine, UK). All tissue culture reagents were sourced from Sigma-Aldrich (Poole, UK) or Invitrogen (Paisley, UK). All culture flasks and plates were from Iwaki (Japan).

### **2.3.1 Maintenance of Cell Lines**

Details of the cells used in this study are listed in Table 2-3. Cells were routinely cultured as monolayers in 25cm<sup>2</sup>, 75cm<sup>2</sup> or 150cm<sup>2</sup> tissue culture flasks in DME medium supplemented with 10% foetal calf serum (FCS), 2mM glutamine, 100U/ml penicillin and 100µg/ml streptomycin (referred to as full culture medium).

Cells were passaged at approximately 80% confluence by removing the medium, washing once with phosphate buffered saline (PBS) and incubating with PBS containing 0.05% (v/v)

trypsin until the cells detached. Fresh medium was added up to a final volume of 10ml and cells seeded into fresh flasks for routine growth.

Cell Line	Origin	Source	ATCC Number	Reference
HEK293	Human embryonic kidney transformed with left end of Ad5 DNA	Donated by Dr V. Mautner	CRL-1573	[Graham et al, 1977]
A549	Human lung adenocarcinoma	Donated by Dr V. Mautner	CCL-185	[Giard et al, 1973]
DU145	Human brain metastases from prostate adenocarcinoma	Donated by Prof. E. Lalani	HTB-81	[Stone et al, 1978]
PC3	Human bone metastases from prostate adenocarcinoma	Donated by Prof. E. Lalani	CRL-1435	[Kaighn et al, 1978]
22RV1	Human prostate adenocarcinoma	Purchased from ATCC	CRL-2505	[Sramkoski et al, 1999]
SKOV3	Human ovarian carcinoma	Donated by Dr R. Hoeben	HTB-77	[Fogh et al, 1977]
MZ2-MEL3.0	Human melanoma	Donated by Dr R. Hoeben	n/a	[Herin et al, 1987]
MRC5	Primary human foetal lung fibroblasts	Donated by Sue Rookes	CCL-171	[Jacobs et al, 1970]
KS Fibroblasts	Primary human skin fibroblasts	Donated by Prof. M. Taylor	n/a	Isolated at University of Birmingham
A549-RA	A549 cells from Dr R. Alemany	Donated by Dr R. Alemany	CCL-185	[Giard et al, 1973]

**Table 2-3. Cell lines and culture media**

### 2.3.2 Cell Counting

Cells were counted using FAST-READ 102<sup>®</sup> disposable counting slides (ISL, Paignton, UK) according to manufacturer's instructions. 20µl of cell suspension was pipetted into a

single counting chamber and cell number counted from 3 individual large grid squares.

Total cell concentration = average number of cells in one large grid square x  $10^4$ .

### **2.3.3 Cryogenic Preservation of Cell Lines**

Frozen stocks of cell lines were kept in the vapour phase of liquid nitrogen storage tanks. Cells to be stored in nitrogen were trypsinised, full culture medium added and cells pelleted by centrifugation (177g for 10 minutes in a Heraus Megafuge 2.0R). The cell pellet was resuspended in ice cold FCS supplemented with 10% (v/v) diethyl sulphoxide (DMSO) at 1ml per 80% confluent 75cm<sup>2</sup> flask, transferred to a 1ml CryoTube™ (Nunc, Roskilde, Denmark) and slowly frozen to -80°C in a Cryo 1C freezing container (NALGENE™, Hereford UK) filled with isopropanol. 24 hours later cells were transferred for long-term storage in liquid nitrogen storage tanks.

Recovery of frozen cells was performed by rapidly defrosting in a 37°C water bath, before transferring the cell suspension into 10ml of culture medium prewarmed to 37°C. Cells were pelleted by centrifugation, supernatant discarded and cell pellet was resuspended in pre-warmed culture medium.

## **2.4 Adenovirus Methods**

All virus work was performed in class 2 biological safety cabinets in a designated tissue culture room at ACGM containment level 2. All work with RGD-retargeted vectors was performed in a safety cabinet dedicated to retargeted vectors with dedicated pipettes and incubators.

#### **2.4.1 Adenovirus Rescue by Calcium Phosphate Co-Precipitation**

Adenovirus rescue was performed by co-transfection of relevant left and right end plasmids into HEK293 cells using the calcium phosphate co-precipitation method [Graham and van der Eb, 1973]. Left and right end plasmids (see CHAPTER 3 for plasmid structures) were digested with the appropriate enzyme to separate Ad sequences from the plasmid backbone, phenol/chloroform extracted and ethanol precipitated. DNA was pelleted (9,500g for 10 minutes in a microcentrifuge) and dissolved in an appropriate volume of sterile 10mM Tris-HCl pH 7.5. HEK293 cells were plated in 60mm tissue culture dishes for transfection. When approximately 75% confluent (approximately  $1.5 \times 10^6$  cells/dish), a 1:1 molar ratio of left and right end adenovirus fragments were used at a total of 5-20 $\mu$ g per dish. The appropriate volumes of left and right end fragments were mixed in a 5ml tube and made up to 175 $\mu$ l of 10mM Tris-HCl pH 7.5. 25 $\mu$ l of 2M CaCl<sub>2</sub> was added to the DNA solution and gently mixed. The DNA/CaCl<sub>2</sub> solution was added dropwise to 200 $\mu$ l of 2xHEBS (50 mM HEPES pH 7.05, 0.25M NaCl and 1.5mM Na<sub>3</sub>PO<sub>4</sub>, adjusted to pH 7.05 with NaOH), while gently mixing, and incubated for 20-30 minutes at room temperature, during which time a fine white precipitate formed. Chloroquin was added directly to the culture medium to a final concentration of 100 $\mu$ M, just before the DNA/CaCl<sub>2</sub>/HEBS suspension was added dropwise. Cells were incubated with the DNA for 4-5 hours, before the medium was removed and replaced with fresh culture medium. Cells were incubated for up to 14 days post transfection at 37°C 5% CO<sub>2</sub> in a humidified incubator until signs of significant cytopathic effect (CPE), when they were harvested as primary virus seed stocks.

#### **2.4.2 Harvesting of Adenovirus Seed Stocks**

Upon significant CPE, cells were harvested into the culture medium, pelleted by centrifugation (840g, 10 minutes, 4°C in a Heraeus Megafuge 2.0R) and resuspended in full

culture medium (normally 0.5ml per 150cm<sup>2</sup> per flask of infected cells) Virus was released from the cells by 3 cycles of freezing in liquid nitrogen and thawing at 37°C. Cell debris was pelleted by centrifugation (840g, 10 minutes, 4°C in a Heraeus Megafuge 2.0R) and supernatant containing virus stored at -80°C until required.

### **2.4.3 Infecting Tissue Culture Cells with Adenovirus Seed Stock**

Unless otherwise stated virus seed stock was prepared in A549 cells (for replication competent viruses) or HEK293 cells (for replication deficient viruses). 80% confluent monolayers were infected with adenovirus seed stock (typically at a 1:1,000 dilution) in a minimal volume of full culture medium (4ml for a 150cm<sup>2</sup> flask). Cells were incubated with the virus for 90 minutes at 37°C before the virus containing medium was removed and replaced with infection medium (DME + HEPES supplemented with 2% FCS, 2mM glutamine, 100U/ml penicillin and 100µg/ml streptomycin).

Flasks were maintained at 37°C 5%CO<sub>2</sub> in a humidified incubator until extensive CPE was observed, when virus was harvested as in section 2.4.2.

### **2.4.4 Plaque Purification of Adenovirus**

All viruses constructed were subjected to double plaque purification. DU145 cells were grown to 80% confluency on 60mm tissue culture treated dishes. Medium was removed to leave 400µl per dish, to which 100µl of unpurified virus seed stock was added, that had previously been serially diluted in infection medium (typically 10<sup>-2</sup> to 10<sup>-6</sup>). Dishes were incubated for 90 minutes at 37°C, 5% CO<sub>2</sub> before the medium was removed and monolayers covered with 4ml of overlay mixture (0.7% w/v Noble agar (Invitrogen, Paisley, UK) in DME + HEPES, 2% v/v FCS, 100U/ml penicillin, 100µg/ml streptomycin, 491µM MgCl<sub>2</sub>, 898µM CaCl<sub>2</sub>, 6mM NaHCO<sub>3</sub>). An additional 3ml of overlay mixture was

added every 3-4 days. When distinct plaques were observed (typically 7-14 days), 6 well isolated plaques were picked into 500µl of infection medium (termed primary plaques A-F). Picked plaques were freeze/thawed three times and three (A, B, C) used in a second round of plaque purification (primary plaques were stored at -80°C). From each primary plaque 6 secondary plaques were picked into 500µl of infection medium (A1-6, B1-6 and C1-6), freeze/thawed 3 times and stored at -80°C.

#### **2.4.5 Caesium Chloride Purification of Adenovirus**

Virus seed stocks were used to prepare caesium chloride banded virus stocks. To virus seed stocks water saturated n-butanol was added (to 1% v/v) and incubated on ice for 1 hour. Cell debris was pelleted by centrifugation (840g for 10 minutes at 4°C in a Heraeus Megafuge 2.0R) and the supernatant layered onto glycerol/CsCl gradients (2ml lower layer of  $\rho=1.45$  CsCl (in 10mM Tris, pH7.9), a 3ml middle layer of  $\rho=1.32$  CsCl (in 10mM Tris, pH7.9), a 2ml top layer of 40% glycerol (in 10mM Tris, pH7.9)). Gradients were centrifuged using a SW40Ti rotor (Beckman Coulter, High Wycombe, UK) at 25,000 rpm (160,000g) for 90 minutes at 4°C. The lower opalescent band corresponding to intact virus particles was removed using a 21 gauge needle and 5ml syringe. Virus particles were dialysed in a Slide-A-Lyzer dialysis cassette with a 10,000 molecular weight cut off (Thermo Scientific, Waltham, MA, USA) against 400ml of PBSg (PBS, 10% (v/v) glycerol, 491µM MgCl<sub>2</sub> and 898µM CaCl<sub>2</sub>) at 4°C overnight, changing the dialysis buffer 3 times. Dialysed, banded virus was aliquoted and stored at -80°C.

#### **2.4.6 Plaque Assay for Quantitation of Infectious Viral Particles**

DU145 (for replication competent viruses) or HEK293 (for replication deficient viruses) cells were grown until 80% confluency (approximately  $1.5 \times 10^6$  cells/dish) on 60mm tissue

culture treated dishes. Plaque assays were set up as for plaque purification, described in section 2.4.4. Cells were fed by the addition of 3ml of overlay mixture every 3-4 days. Plaques were identified by macroscopic inspection of monolayers and counted 14 days post infection when appearance of plaques was stable. The mean value from triplicate plates was used to calculate the concentration of infectious virus particles in the undiluted virus stock, expressed as plaque forming units (PFU/ml).

#### **2.4.7 Quantitation of Virus Particle Number by PicoGreen Assay**

Virus particle concentration was calculated by PicoGreen assay [Murakami and McCaman 1999]. 10 $\mu$ l of banded virus was mixed with 10 $\mu$ l of 0.1% (w/v) SDS before heat-inactivation at 56°C for 30 minutes. DNA concentration was quantified by PicoGreen assay using a standard curve of bacteriophage lambda DNA, as described in section 2.2.6. Virus particle number was calculated on the basis 1 $\mu$ g of DNA = 2.54x10<sup>10</sup> virus particles.

#### **2.4.8 Infecting Monolayers with Banded Virus Stocks**

Banded virus stocks were routinely used for infection of monolayer cultures in 96-well and 24-well tissue culture plates. For infections in 24-well plates: cells were plated at 1x10<sup>5</sup> or 3x10<sup>4</sup> cells/well for tumour cell lines and fibroblasts, respectively. Cells were allowed to adhere for 16 hours before infection with the appropriate dilution of banded virus, (to give the required multiplicity of infection (MOI)), diluted in 250 $\mu$ l of infection medium per well. Cells were incubated with virus for 90 minutes at 37°C, before the medium was removed, cells washed once, and replaced by 2ml of fresh infection medium per well. For infections in 96-well plates: cells were plated at 3x10<sup>4</sup> or 1x10<sup>4</sup> cells/well for tumour cell lines and fibroblasts, respectively. Cells were allowed to adhere for 16 hours before infection with the appropriate dilution of banded virus, (to give the required MOI), diluted in 100 $\mu$ l of

infection medium per well. Cells were incubated with virus for 90 minutes at 37°C, before the medium was removed, cells washed once, and replaced by 200µl of fresh infection medium per well.

Infected cells were incubated at 37°C 5% CO<sub>2</sub> in a humidified incubator until required.

## **2.5 Measurement of Cell Viability**

### **2.5.1 Acid Phosphatase Cell Viability Assay**

The intracellular acid phosphatase (AP) assay was used routinely to measure cell viability in monolayer cultures [Yang et al, 1996a]. The intracellular acid phosphatase in viable cells hydrolyzes *p*-nitrophenyl phosphate to *p*-nitrophenol, which can be measured by absorption at 405nm. For cells grown as monolayers in 96-well plates, the cell culture medium was aspirated using a Vacusafe Comfort (INTEGRA Bioscience, Zizers, Switzerland), wells washed once with 200µl of PBS and to each well 100µl of AP assay solution (5mM *p*-nitrophenyl phosphate in 0.1M sodium acetate pH5, 0.1% (v/v) Triton X-100) added.

Cells in suspension were pelleted (500g for 10 minutes in a Heraeus Megafuge 2.0R), washed once with 200µl of PBS and resuspended in 100µl of assay solution.

Cells were incubated with assay solution for 30 minutes at 37°C. The reaction was stopped by addition of 10µl 1M NaOH and absorbance read immediately at 405nm using a Wallac Victor<sup>2</sup> 1420 Multilabel counter

### **2.5.2 MTS Cell Viability Assay**

When stated cell survival was measured by Cell Titer 96<sup>®</sup> AQueous One Solution Cell Proliferation Assay (Promega, Southampton, UK), following manufacturer's instructions. For monolayer cultures in 96-well plates the culture medium was aspirated using a Vacusafe Comfort (INTERGRA Biosciences, Zizers, Switzerland) and cells washed once

with PBS. 100µl of full culture medium and 20µl of Aqueous One Solution was added before cells were incubated for 30 minutes (unless otherwise stated) at 37°C.

For suspension cultures the cells were first pelleted by centrifugation (500g for 10 minutes in a Heraeus Megafuge 2.0R), the supernatant gently aspirated and the cells resuspended in 100µl of fresh culture medium per well. To each well 20µl of Aqueous Once Solution was added and cell incubated for 30 minutes (unless otherwise stated) at 37°C.

Following incubation the wells were read immediately for absorbance at 490nm using a Wallac Victor<sup>2</sup> 1420 Multilabel counter.

## **2.6 Extraction of DNA and RNA**

### **2.6.1 Extraction of DNA from Virus Seed stocks**

The required volume of viral seed stock was thawed and transferred to a clean tube. 5M NaCl was added to a final concentration of 1M, mixed and incubated on ice for 16 hours. Samples were centrifuged (16,000g for 30 minutes at 4°C in a microcentrifuge) to pellet the chromatin and the supernatant transferred to a new tube. DNA was extracted using the QIAamp DNA mini kit (QIAGEN, Crawley, UK), following the manufacturer's instruction.

### **2.6.2 Extraction of DNA from CsCl Purified Virus**

Extraction of pure viral DNA was performed on CsCl purified banded virus stocks using the QIAamp DNA mini kit (QIAGEN, Crawley, UK), following the manufacturer's instructions.

### **2.6.3 Extraction of Total DNA**

DNA was extracted from infected monolayers for analysis of virus DNA replication, using the QIAamp DNA mini kit (QIAGEN, Crawley, UK). The medium was first removed from

the cells, before 200µl of lysis buffer AL was added to each well of a 24 well plate, incubated at room temperature for 5 minutes and the lysate transferred into a 1.5ml microcentrifuge tube. Each sample was mixed with 200µl of infection medium and stored at -20°C prior to DNA extraction. Once all samples had been collected DNA was extracted using the QIAamp DNA mini kit, following manufacturer's protocol. Total DNA was eluted in 200µl of elution buffer AE and stored at -20°C ready for Q-PCR.

#### **2.6.4 Extraction of Total RNA**

RNA was extracted from virus infected monolayers using the RNeasy mini kit (QIAGEN, Crawley, UK) following manufacturer's instructions. To begin, the medium was removed from monolayers and cells lysed by the addition of 200µl of buffer RTL to each well of a 24-well plate. Plates were incubated at room temperature for 2 minutes and transferred to a sterile, RNase-, DNase-free 1.5ml microcentrifuge tube. Samples were stored at -20°C prior to RNA extraction.

Once all samples were harvested, they were thawed rapidly at 37°C and RNA extracted using the RNeasy mini kit, following manufacturer's instructions. Contaminating DNA was digested using RNase-free DNase set (QIAGEN, Crawley UK) following the off-column DNase protocol. A second RNeasy mini kit column was used to clean up the RNA following the RNA Cleanup protocol. RNA was eluted in 50µl of RNase-free water.

### **2.7 DNA and RNA Detection**

#### **2.7.1 Quantitative-PCR (Q-PCR)**

Q-PCR was performed to quantify adenovirus and cellular DNA copies in virus infected cells. Total DNA was extracted from cells as described in section 2.6.3. For detection of virus genomes the 'BARTS' primers and probe set (donated by Dr D. Onion) was used,

which lie within the adenovirus hexon gene. For cell DNA control  $\beta$ -2M primers and probe set were used. Information on primers and probes, including final reaction concentration, can be found in Table 2-4 below.

<b>Primers and Probes</b>	<b>Description</b>	<b>Final Concentration</b>	<b>Sequence</b>	<b>Position in Ad5 Genome or Reference</b>
BARTS forward primer	Forward hexon primer for detection of Ad genomes	300nM	CCACCCTTCT TTATGTTTTG TTGA	21579-21602
BARTS reverse primer	Reverse hexon primer for detection of Ad genomes	300nM	GCAGGTACA CGGTCTCGA TGA	21665-21645
BARTS probe	FAM labelled hexon probe	200nM	TCTTTGACGT GGTCCGTGT GCACC	21606-21629
$\beta$ -2M forward primer	Forward $\beta$ -2M primer for detection of cell copies	225nM	GGAATTGAT TTGGGAGAG CAT	[Murray et al, 2003]
$\beta$ -2M reverse primer	Reverse $\beta$ -2M primer for detection of cell copies	300nM	CAGGTCCTG GCTCTACAA TTTACTAA	[Murray et al, 2003]
$\beta$ -2M probe	VIC labelled $\beta$ -2M probe	50nM	AGTGTGACT GGGCAGATC ATCCAGCCT C	[Murray et al, 2003]

**Table 2-4. Primers and probes for Q-PCR**

Reactions were set up in UV irradiated class I PCR hoods to prevent DNA contamination, with 10 $\mu$ l of TaqMan™ Universal Master Mix (Applied Biosystems, Warrington, UK), appropriate dilution of primers and probes, 5 $\mu$ l of sample DNA in a final volume of 20 $\mu$ l. All samples were set up in triplicate along with ‘no template’ control wells and a 10-fold serial dilution of standard DNA. Standard DNA was DNA extracted from a known number of Ad5 wt virus particles mixed with a known number of DU145 cells. Reactions were set

up in MicroAmp Fast optical 96-well reaction plates (Applied Biosystems, Warrington, UK), covered tightly with EU Opti-Seal optical films (Geneflow, Fradley, UK) before centrifugation at 360g for 5 minutes in a Heraeus Megafuge 2.0R. Reactions were run in an AB7500FAST machine, using the absolute quantification protocol, (Applied Biosystems, Warrington, UK) with the following cycling conditions:

Initial cycle: 50°C for 2 minutes, 95°C for 10 minutes

40 cycles: 94°C for 15 seconds, 60°C for 1 minute.

Data were analyzed with Applied Biosystems 7500 System Software (Applied Biosystem, Warrington, UK) using the standard curve to quantify copy number. Q-PCR reactions were carried out using BARTS and  $\beta$ -2M primers/probe for each sample, and virus genome copy number normalized to cellular genome number.

### **2.7.2 Production of cDNA by Reverse Transcription**

Total RNA extracted and treated with DNase was used to make cDNA for quantification by Q-PCR. cDNA was made using the High-Capacity cDNA Reverse Transcription kit (Applied Biosystems, Warrington, UK.), following manufacturer's instructions. Briefly, total RNA was quantified using a NanoDrop ND-100 spectrophotometer for absorbance at 260nm (Labtech International, Ringmer, UK) with RNase-free water as blank measurement. 50ng of RNA was used for reverse transcription in 20 $\mu$ l reactions with 2 $\mu$ l of 10x RT buffer, 0.8 $\mu$ l of 25x dNTP mix, 2 $\mu$ l 10x RT random primers, 1 $\mu$ l of MultiScribe™ reverse transcriptase, 1 $\mu$ l of DNase inhibitor. Reactions were prepared on ice and cycled in a Perkin Elmer Gene Amp 2400 thermocycler (PE Applied Biosystems, Warrington, UK) as follows:

25°C for 10 minutes,

37°C for 120 minutes,

85°C for 5 seconds

and finally hold at 4°C.

cDNA samples were stored at -20°C ready for Q-PCR.

### 2.7.3 Relative Quantification

E1A RNA expression was measured using the  $\Delta\Delta\text{CT}$  method for relative quantification.

Standard Q-PCR reactions were set up as described in section 2.7.1 using 5 $\mu\text{l}$  of cDNA (as described above) and E1A primers/probe set shown in Table 2-5.

Primer and Probe	Description	Final Concentration	Sequence (5' – 3')	Reference
E1A 13S.SEQ-541F	Forward E1A primer	900nM	ATGTTTGTCTAC AGTCCTGTGTCT GAA	Donated by Dr A. Turnell
E1A 13S.SEQ-639R	Reverse E1A primer	900nM	GATAGCAGGCG CCATTTTAGG	Donated by Dr A. Turnell
E1A 13S.SEQ-586T	FAM labelled E1A probe	100nM	CCAGAACCGGA GCCTGCAAGAC CTAC	Donated by Dr A. Turnell

**Table 2-5. E1A primers and probe**

Separate reactions were set up for 18S rRNA as endogenous control using the TaqMan™ Gene Expression Assay Eukaryotic 18S rRNA 20x (Applied Biosystems, Warrington, UK), with 5 $\mu\text{l}$  of cDNA, 1 $\mu\text{l}$  of TaqMan™ Gene Expression Assay, 4 $\mu\text{l}$  of water and 10 $\mu\text{l}$  of TaqMan™ Universal Master Mix.

Both sets of reactions were run on the AB 7500FAST machine (Applied Biosystems, Warrington, UK) using the relative quantification plate protocol. Cycling conditions were as described previously (section 2.7.1).

Data was analysed with Applied Biosystems 7500 System Software (Applied Biosystem, Warrington, UK) using the relative quantification study protocol with E1A as the target and

18S rRNA as endogenous control. Samples were normalised to E1A expression in DU145 cells infected with 10 PFU/cell of Ad5 wt at 4 hours post infection.

## **2.8 Detection of Proteins by Western Blotting**

### **2.8.1 Preparation of Protein Samples**

The culture medium from virus infected monolayer was removed and wells washed once with PBS, 8M urea (typically 200µl per well of a 24-well tissue culture plate) was added to the well and incubated for 2 minutes at room temperature. Following incubation the entire protein suspension was carefully transferred into a 1.5ml microcentrifuge tube. The samples were stored at -20°C until required, ready for protein quantification and SDS-PAGE.

### **2.8.2 Protein Quantitation by Bradford Assay**

Protein concentration was quantified by Bradford assay. Protein standards were 0.1 to 1mg/ml bovine serum albumin in PBS. 5µl of sample and standard protein was pipetted into triplicate wells of a 96-well plate, already containing 95µl of T<sub>10</sub>E<sub>1</sub>N<sub>100</sub>. Bradford reagent (BioRad, Hemel Hempstead, UK) was diluted 1:4 with ddH<sub>2</sub>O and filtered through a 0.45µm pore size Acrodisc (Pall, Portsmouth, UK). 100µl was added to each well of the 96-well plate and incubated at room temperature for 1 minute. Plates were read for absorbance at 595nm on a Wallac Victor<sup>2</sup> 1430 Multilabel counter. Protein concentration was determined from the standard curve.

### **2.8.3 SDS-Polyacrylamide Gel Electrophoresis (SDS-PAGE)**

Proteins were separated by SDS-PAGE using a 12% resolving gel and 4% stacking gel. All gels were run using the Mini-PROTEAN® Tetra Cell apparatus (BioRad, Hemel Hempstead, UK), following the manufacturer's instructions. 1.5mm separators were used

with 8ml of resolving gel (4ml 30% acrylamide/bis (BioRad), 2.5ml 1.5M Tris-HCl pH 8.8, 100µl 10% SDS, 50µl 10% APS, 10µl TEMED and 3.35ml of ddH<sub>2</sub>O) and 4ml of stacking gel (1.33ml 30% acrylamide/bis (BioRad), 2.5ml 0.5M Tris-HCl pH 6.8, 100µl 10% w/v SDS, 50µl 10% w/v APS and 10µl TEMED). Polymerised gels were transferred into the running apparatus, place in an electrophoresis tank with sufficient SDS-PAGE running buffer (25mM Tris, 200 mM glycine and 1% SDS).

2.5µg of protein sample in 15µl of 8M urea was mixed with 5µl of 4x (U)SB (8% SDS, 40% glycerol, 320mM Tris pH 6.8, 400mM DTT, Bromo-phenol blue), incubated at 95°C for 5 minutes and loaded into preformed wells. PageRule™ prestained protein ladder plus (Fermentas, York, UK) was loaded in adjacent lanes for determination of molecular weight. Electrophoresis was carried out for 90 to 120 minutes at 100V to achieve the required degree of separation.

#### **2.8.4 Western Blotting**

Following electrophoresis the resolving gel was incubated for 5 minutes in transfer buffer (39mM glycine, 48mM Tris pH 8.3, 20% (v/v) methanol), with four pieces of Whatman 3MM blotting paper and two synthetic sponges.

Immuno-Blot PVDF membrane (BioRad, Hemel Hempstead, UK) was soaked for 5 minutes in methanol then for 5 minutes in transfer buffer, before being assembled with the gel in the transfer stacks. Proteins were transferred onto the membrane at 100V for 90 minutes using a semi-dry blotting tank. Following electrophoresis the membrane was briefly washed in PBSt (PBS with 0.1% v/v tween-20) before being blocked in PBSt with 5% skimmed milk (w/v) for one hour at room temperature.

Membranes were probed with primary antibodies diluted to the appropriate concentration in PBSt with 2% skimmed milk (w/v) for 16 hours at 4°C. The membranes were washed with

4 changes of PBSt, changing the buffer every 10-15 minutes. Species-specific IgG secondary antibodies, pre-conjugated with peroxidase, were incubated with the membrane at the required dilution in PBSt with 2% skimmed milk (w/v), for 1 hour at room temperature. Details of the antibodies used for western blotting can be found in Table 2-6.

<b>Antibody</b>	<b>Target(s) and Size(s)</b>	<b>Information</b>	<b>Dilution</b>	<b>Source</b>
anti-NTR	NTR, 24kDa	Sheep Polyclonal	1:50,000	Donated by Dr P. Searle
R2/99	Adenovirus late proteins	Rabbit polyclonal	1:1,000	Donated by Dr V. Mautner
M73 E1A	E1A, 26-32kDa	Mouse monoclonal	1:100	Donated by Dr E. Blair
Anti- $\beta$ -tubulin	$\beta$ -tubulin, 55kDa	Mouse monoclonal	1:20,000	Sigma-Aldrich, Poole, UK
Anti-mouse	n/a	Goat polyclonal, peroxidase conjugate	1:20,000	Sigma-Aldrich, Poole, UK
Anti-rabbit	n/a	Goat polyclonal, peroxidase conjugate	1:20,000	Sigma-Aldrich, Poole, UK
Anti-sheep	n/a	Donkey polyclonal, peroxidase conjugate	1:20,000	Sigma-Aldrich, Poole, UK

**Table 2-6. Antibodies used in western blotting**

Membranes were washed as before and peroxidase activity detected using an Amersham ECL™ Advance Western Blotting Detection Kit (GE Healthcare, Chalfont St Giles, UK), following the manufacturer's instructions. 1ml of component A was mixed with 1ml of component B, the membrane soaked in this for 2 minutes, and transferred to an Amersham Hypercassette (GE Healthcare, Chalfont St Giles, UK). Signal was detected using Amersham Hyperfilm™ MP autoradiography film (GE Healthcare, Chalfont St Giles, UK) with varying exposure times (dependent on signal strength), and developed using a Kodak X-O-graph developer (Kodak, Hemel Hempstead, UK).

## **2.9 Imaging Techniques**

### **2.9.1 Flow Cytometry**

Flow cytometry was used to directly measure eGFP expression, and surface antigen expression using antibodies.

#### **2.9.1.1 GFP Sample Preparation and Antibody Staining**

GFP expression from eGFP expressing viruses was analysed by flow cytometry. For analysis of eGFP expression, the medium was removed from the virus infected cells, cells washed once with PBS and detached by trypsinisation. The cell suspension was transferred into a FACS tube containing 3ml of FACS buffer. The cells were pelleted by centrifugation (840g for 5 minutes in a Heraeus Megafuge 2.0R), resuspended in 300-500µl of FACS fix, and stored at 4°C prior to analysis.

For antibody surface staining, cells were detached into the medium by scraping and the cell suspension transferred to a FACS tube. Cells were washed with FACS buffer, resuspended in 50µl of FACS buffer containing the appropriate dilution of primary antibody, incubated for 1 hour at 4°C then washed with 4ml of FACS buffer. If the primary antibody was directly conjugated to a fluorophore, cells were resuspended in 300-500µl of FACS buffer ready for analysis. If a secondary antibody was required the cell pellet was resuspended in 50µl FACS buffer containing the appropriate dilution of labelled secondary antibody. Cells were incubated for a further 1 hour at 4°C before being washed with 4ml of FACS buffer and resuspended in 300-500µl of FACS buffer ready for analysis. Details of the antibodies used for flow cytometry can be found in Table 2-7.

<b>Antibody</b>	<b>Target</b>	<b>Information</b>	<b>Dilution</b>	<b>Source</b>
RmCB	CAR	unconjugated, mouse monoclonal	neat	CRUK (ATCC # CRL-237)
anti-human $\alpha_V\beta_3$	Human integrin $\alpha_V\beta_3$	PE-conjugated, mouse monoclonal	1:5000	R and D Systems, Abingdon, UK
anti-human $\alpha_V\beta_5$	Human integrin $\alpha_V\beta_5$	PE-conjugated, mouse monoclonal	1:5000	R and D Systems, Abingdon, UK
Anti-mouse	n/a	FITC-conjugated	1:2000	Sigma-Aldrich, Poole, UK

**Table 2-7. Antibodies used for flow cytometry**

### 2.9.1.2 Analysis of Cells by Flow Cytometry

Cells were analysed using either a 4 colour Beckman Coulter XL flow cytometer (Beckman Coulter, High Wycombe, UK) with Coulter System II software for data acquisition, or a 15 colour BD LSRII flow cytometer (Becton Dickinson, Oxford, UK) with DIVA software (Becton Dickinson, Oxford, UK). Data was analysed using FlowJo7.5.3 (Tree Star Inc., Ashland, OR, USA).

Unstained or mock infected cells were the first samples to be analysed, followed by negative and isotype controls and finally test samples. The desired cell population was gated using forward scatter and side scatter properties, gating out debris and the majority of dead cells. Voltages were appropriately set for photo multiplier tubes (PMT) in all channels using the negative controls. If multicolour staining was being performed appropriate colour controls were run and compensation performed to eliminate cross talk into all other colours being analysed. Voltages, gates and compensation controls were kept constant for all samples analysed. At least  $10^4$  cell events were analysed per sample from replicate samples. Data was analysed for percentage positive cells and fold increase in mean fluorescence. Percentage positive refers to the percentage of gated cells fluorescing above the appropriate negative control, measured using a gate set to include 2% of the negative control cells.

Mean fluorescence was taken as an arithmetic mean expressed in arbitrary units of the positive population. Fold increase in mean fluorescence was calculated by dividing the fluorescence of the positive population by the fluorescence of the negative control sample.

### **2.9.2 Microscopy**

A Zeiss Axiovert 25 (Carl Zeiss, Welwyn Garden City, UK) inverted microscope was used for phase-contrast and eGFP fluorescence microscopy of monolayer cultures. Objectives used were 5x, 10x, 20x and 40x with 21x, 42x, 84x and 168x overall magnification, respectively. Images were taken using a SPOT camera with SPOT Advanced software (Diagnostic Instruments, Michigan, USA). The exposure time and gain was kept constant for all fluorescent images, throughout one experiment.

### **2.10 Graph Plotting and Statistical Analysis**

All graph plotting and statistical analysis was performed using GraphPad Prism version 5 software (GraphPad software Inc, La Jolla, CA, USA). Unless otherwise stated, sigmoid dose response curves were plotted to data normalised using empty wells (0% viability) and mock infected wells (100% viability). All EC50 values with 95% confidence intervals (C.I) were calculated by GraphPad software to 3 significant figures.

## **CHAPTER 3**

### **vMH Vector Construction**

### 3.1 Introduction

Arguably the two most successful strategies using Ad vectors for the treatment of cancer utilise oncolytic CRAAd vectors or enzyme/prodrug suicide gene therapy. Previous studies by The University of Birmingham, SCS-GT group combined these two strategies by arming two E1B-55K deleted oncolytic CRAAd vectors with the therapeutic transgene NTR for NTR/CB1954 enzyme/prodrug therapy [Chen et al, 2004; Roesen 2006]. Of these, vNR6 (pIX ORF replaced with NTR) demonstrated higher oncolytic cytotoxicity than CRAAd-NTR (NTR under CMV promoter control), particularly at low MOI (discussed in section 1.2.4.4.3). However experiments with vNR6 and an equivalent vector expressing eGFP in place of NTR (vNR3), demonstrated some cytotoxicity and transgene expression in primary human fibroblasts.

Recently Dr R. Alemany's group at the Institut Català d'Oncologia constructed an E1A CR2  $\Delta$ 24 vector, vICOVIR-5, which had the E1A promoter replaced by the E2F-1 promoter insulated by an upstream poly(A) site and DM-1 insulator element [Alonso et al, 2007a; Alonso et al, 2007b; Cascallo et al, 2007; Majem et al, 2006]. This ICOVIR-5 promoter was designed to increase replication specificity by restricting E1A expression to tumour cells with high levels of free E2F. The ICOVIR-5 promoter was further developed by inserting two additional E2F binding regions within the E2F-1 promoter to create vICOVIR7 [Rojas et al, 2009]. Within this new ICOVIR-7 promoter both E2F binding regions were positioned upstream of the existing E2F-1 binding elements. The ICOVIR-7 promoter was designed to increase tumour specificity by further restricting E1A expression to cells with the highest E2F levels. Schematics of the ICOVIR-5 and ICOVIR-7 promoters can be found in Figure 3-1.

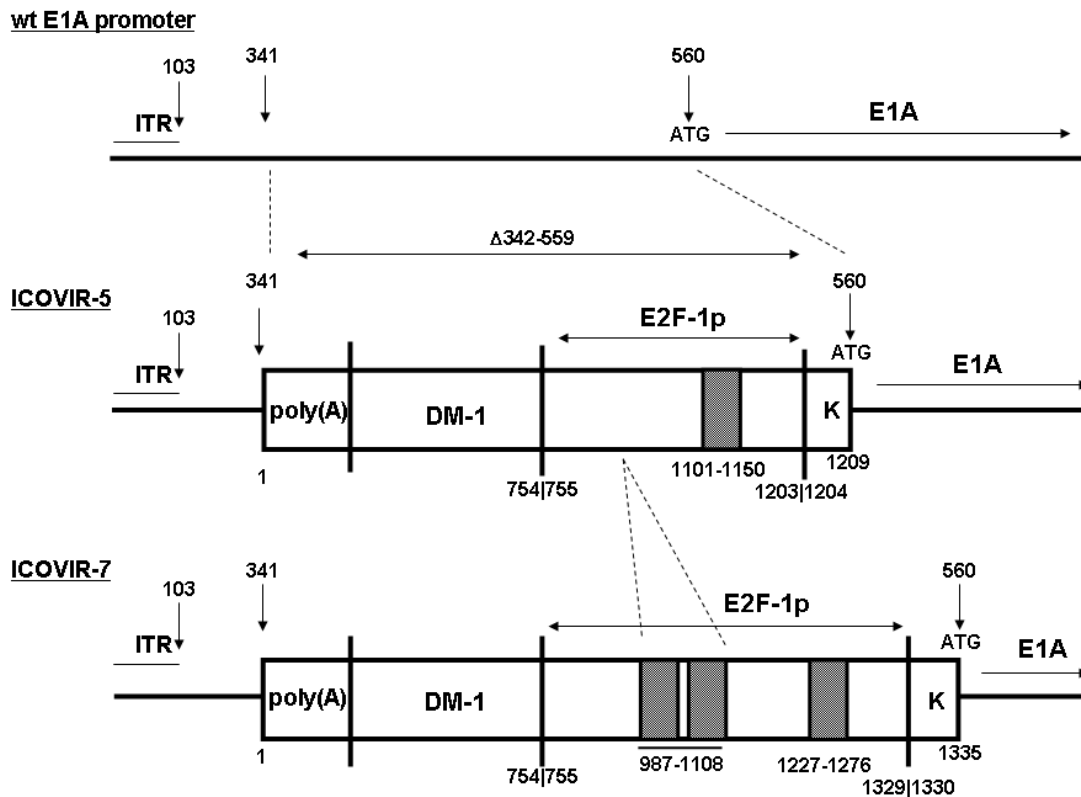


**Figure 3-1. Schematic of the ICOVIR-5 and ICOVIR-7 promoters**

The wt E1A promoter from position 342 to 559 was deleted and replaced by the ICOVIR-5 or ICOVIR-7 promoter. The ICOVIR-5 promoter consists of a poly(A) site, followed by the DM-1 insulator element, the E2F promoter and a Kozak sequence directly before the E1A translational start site. The ICOVIR-7 promoter has two additional E2F binding regions inserted upstream of the existing E2F binding region.

ITR = inverted terminal repeat, poly(A) = poly(A) sequence, DM-1 = DM-1 insulator element, E2F-1p = E2F-1 promoter sequence, K = Kozak sequence, ATG = E1A ATG site. Grey boxes indicate the E2F binding regions. Numbers above the sequence refer to the position in the Ad5 wt genome, numbers below the sequence refer to position within the ICOVIR-5 or ICOVIR-7 promoter (diagrams not to scale).

Both of these vectors would provide appropriate oncolytic Ad backbones for the introduction of the therapeutic transgene NTR: at the beginning of this study there was no published data on either vector, therefore, to identify which might be the best candidate for the introduction of NTR, both vectors were first modified to express the marker transgene

eGFP (enhanced green fluorescent protein) from the MLP. Marker transgene was used to assess the background oncolytic activity of the vector while taking into account any effect transgene insertion might have, and to assess the level and timing of transgene expression before insertion of NTR. The MLP was chosen to achieve high transgene expression and elicit a good therapeutic effect, but late in Ad infection to have a minimal negative effect on Ad progeny production.

Alongside, similar constructs were made with the wildtype (wt) E1A promoter and E1A CR2  $\Delta$ 24 deletion, to investigate the effect of E1A promoter replacement.

### **3.2 Aim of Chapter**

The aim of this chapter was to construct new adenovirus vectors expressing eGFP, based on the E2F-1 responsive vectors from Dr R. Alemany's laboratory. The vectors generated in this chapter were characterised in subsequent chapters to identify the optimal vector, in terms of tumour selectivity, cytotoxicity and transgene expression, for insertion of the therapeutic transgene NTR.

### **3.3 Overview of Vector Design**

Figure 3-2 shows a schematic of the eGFP expressing vector vNR3 [Roesen 2006], alongside the 5 new vMH vectors. The vNR vector contains an E1B-55K gene deletion rendering it conditionally replicating. In comparison, all vMH vectors contain the E1A CR2  $\Delta$ 24 deletion which takes advantage of the mutated E2F/pRB pathway (discussed in section 1.2.4.2.1). The first of these vectors, vMH2, contains the wt E1A promoter. Vectors vMH4 and vMH5 have the E1A promoter replaced by the ICOVIR-5 promoter (described above) for increased tumour specificity. vMH5 contains the RGD-4C sequence introduced into the

fibre knob HI-loop. This insert confers the ability to use  $\alpha_v\beta_{3/5}$  integrins as the primary cell surface receptor in order to enhance virus uptake in CAR negative cells.

Vectors vMH6 and vMH7 incorporate two additional E2F binding regions within the E2F-1 promoter region of the ICOVIR-5 promoter. This larger ICOVIR-7 promoter (described above) is designed to further restrict E1A expression to tumour cells which have high levels of free E2F, thus increasing tumour specificity. vMH7 also contains the RGD-4C sequence introduced into the fibre knob HI-loop.

All vMH vectors express the eGFP transgene from a splice acceptor site, inserted directly downstream of the fibre gene, for expression from the Ad MLP. Furthermore, a Kozak sequence has been inserted directly upstream of the eGFP translational start site for enhanced translation. In vNR3 the pIX ORF has been directly substituted with the eGFP ORF, retaining the pIX promoter, ATG site and E1B/pIX poly(A) signal, for expression at intermediate times of infection.

All vMH vectors retained the wt E3 region whereas vNR3 had a partial E3 deletion between the XbaI restriction sites at position 28593 and 30470 of the Ad5 genome.

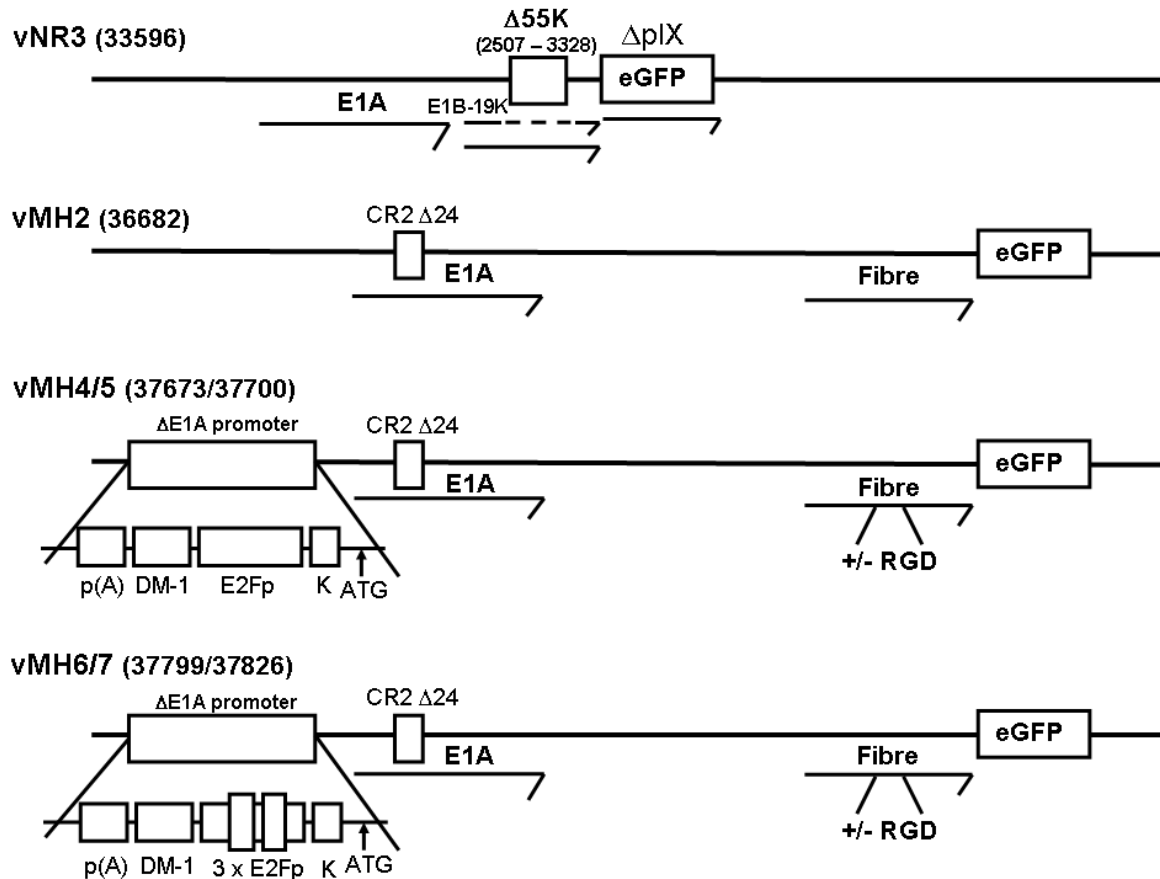


**Figure 3-2. Schematic of vMH viruses**

Schematic layout of vNR3 and the vMH vectors. vNR3 has an E1B-55K from 2507-3328bp, an E3 deletion from 28593 - 30470 and the pIX ORF is replaced by the eGFP ORF. All vMH vectors contain the E1A CR2 Δ24 deletion (Δ922-947). vMH4 and vMH5 have the wt E1A promoter replaced by the ICOVIR-5 promoter. vMH6 and vMH7 have the wt E1A promoter replaced by the ICOVIR-7 promoter. Both vMH5 and vMH7 have the RGD-4C motif inserted into the fibre knob HI loop. All vMH vectors have a wt E3 region and express the eGFP transgene from a splice acceptor site, inserted directly downstream of the fibre gene.

p(A) = poly(A) sequence, DM-1 = DM-1 insulator element, E2Fp = E2F-1 promoter, K = Kozak sequence, ATG = E1A translation initiation site, RGD = RGD-4C motif (diagrams not to scale)

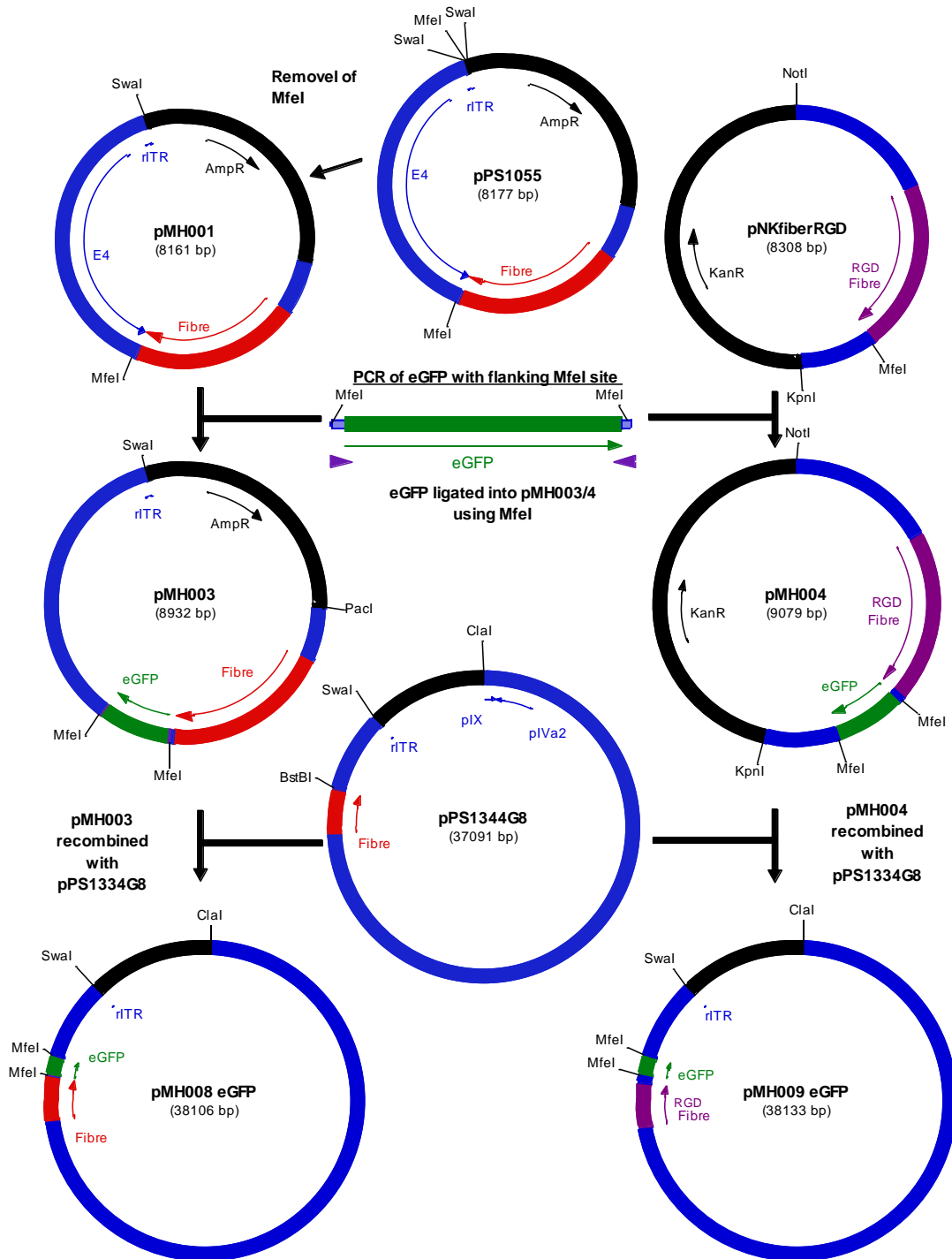
### 3.4 Virus Cloning Strategy

All viruses were constructed using plasmids previously made in Dr P. Searle's lab or by our collaborator, Dr R. Alemany's group at the Institut Català d'Oncologia in Barcelona (see Table 3-1). A detailed 'road map' of virus construction can be found in Figure 3-3.

<b>Plasmid</b>	<b>Source</b>	<b>Reference</b>
pPS1055	Dr P. Searle	Shown in Figure 3-3 (A)
pPS1344G8	Dr P. Searle	Shown in Figure 3-3 (A)
pPS1335M	Dr P. Searle	Shown in Figure 3-3 (B)
pNKfibreRGD	Dr R. Alemany	[Majem et al, 2006], Shown in Figure 3-3 (A)
pICOVIR-5 (also known as pShuttleDME2FKE1Δ24)	Dr R. Alemany	[Cascallo et al, 2007], Shown in Figure 3-3 (B)
pICOVIR-7 ( also known as pShDME2FKE1ad24E2F2)	Dr R. Alemany	[Rojas et al, 2009], Shown in Figure 3-3(B)

**Table 3-1. Starting plasmids used in the study**

(A)



(B)

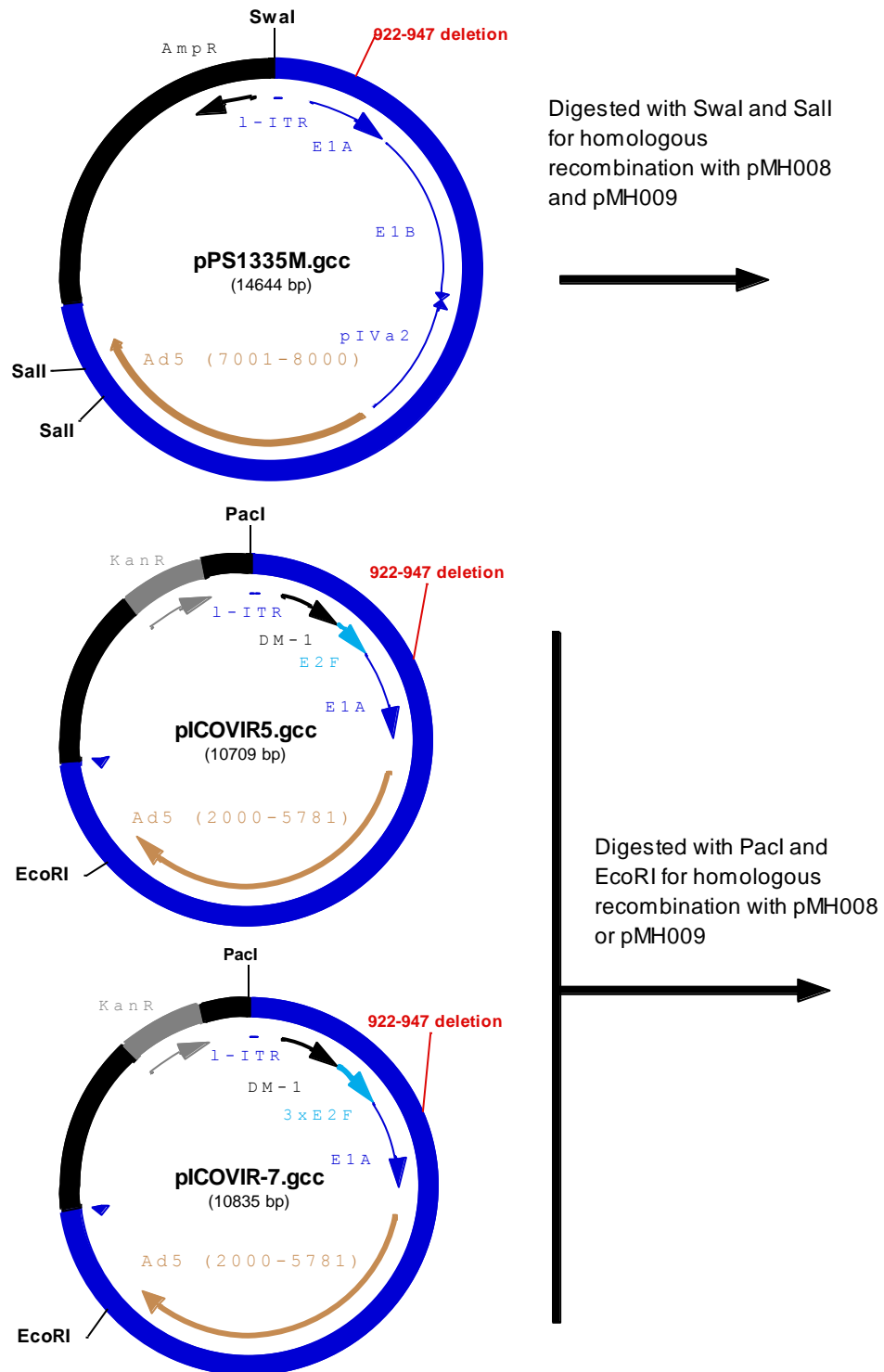


**Figure 3-3. vMH Virus construction ‘road map’**

‘Road map’ of vMH virus contraction. See text for details of the cloning pathway.

Nucleotide markers are for Ad5 wt. Blue = Ad sequence, black = plasmid backbone, green = eGFP, red = wt fibre and purple = RGD-retargeted fibre.

Initially plasmid pPS1055, containing the right end of Ad5 from position 30475, was fully digested with *Swa*I, gel purified and religated to remove the *Mfe*I site between the two *Swa*I sites. The resultant plasmid, pMH001, retains a unique *Mfe*I site, 38bp downstream of the fibre ORF, suitable for downstream cloning.

Plasmid pNKfibreRGD contains the Ad5 sequence from position 29511 to 33598 of the Ad5 wt genome. This plasmid includes the 32bp RGD-4C motif introduced into the fibre ORF replacing nucleotides 32680-32684 (of the Ad5 wt genome) and also retains the unique *Mfe*I site 38bp downstream of the fibre ORF.

The entire eGFP ORF was amplified and purified from vector pxLNCX-GFP [Vass, 2007], using primers MHP001 and MHP002 to introduce flanking *Mfe*I sites (described in Table 2-1). Primer MHP001 introduces a splice acceptor site, for subsequent splicing from the MLP, located between the *Mfe*I site and complementary eGFP sequence with a Kozak sequence directly before the eGFP translation initiation codon. The purified eGFP PCR fragment was cloned into pMH001 and into pNKfibreRGD using *Mfe*I to give pMH003 and pMH004, respectively. Following cloning the entire insert and 100bp of flanking region were sequenced by PCR using primers MHP003, p004, p005 and p006 to verify the insert sequence was correct (data not shown).

Plasmids pMH008 eGFP and pMH009 eGFP were created via homologous recombination in *E.coli* BJ5183, between pPS1344G8 and pMH003 or pMH004, respectively. Plasmid pPS1344G8 contains the Ad5 sequence from position 3525 near the start of pIX up to the right end and has a unique *Bst*BI site introduced 42bp downstream of the fibre ORF. For recombination pPS1344G8 was linearised by digestion at the unique *Bst*BI site. Plasmid pMH003 was digested with *Swa*I and *Pac*I, pMH004 was digested with *Not*I and *Kpn*I, and the Ad sequence fragment gel purified. Recombination was performed using chemically

competent *E.coli* BJ5183 cells grown at 32°C with a total of 50ng of DNA (see section 2.2.11). Single recombinant colonies were picked, DNA extracted and screened by digestion with HindIII and SacII. The HindIII digestion identifies a successful insert/vector recombination and SacII differentiates between wildtype and RGD-retargeted fibre.

The resultant plasmids pMH008 eGFP and pMH009 eGFP contain the Ad5 sequence from position 3525 near the start of pIX up to the right end, with the eGFP ORF downstream of fibre. Plasmid pMH008 eGFP contains a wildtype fibre, whereas pMH009 eGFP contains the RGD-4C retargeted fibre.

Virus rescue was performed using plasmids pMH008 eGFP and pMH009 eGFP in combination with left end plasmids; pPS1335M, pICOVIR-5 and pICOVIR-7 (shown in Figure 3-3 (B)).

Plasmid pPS1335M has the left end of the Ad5 genome up to the XbaI site at position 10589 and the E1A CR2  $\Delta$ 24 at position 922-947 of the Ad5 genome [this deletion has been previously reported by Heise et al, 2000].

Plasmids pICOVIR-5 and pICOVIR-7 were constructed by our collaborators and have been described recently [Cascallo et al, 2007; Majem et al, 2006; Rojas et al, 2009]. Both pICOVIR-5 and pICOVIR-7 contain the Ad5 sequence from the left end to position 5781 of the Ad5 genome beyond the pIX gene. pICOVIR-5 has the SV40 late poly(A) signal from pGL3-plasmid, (Promega, Southampton, UK) followed by the DM-1 insulator element from nucleotides 13006 to 13474 of the DM-1 locus, containing the CTCF-binding sites and CTG repeats required for insulation. Located downstream of this is the E2F-1 promoter sequence (taken from the -218 to +51 region of the E2F-1 gene); this contains the E2F-1 binding region, which includes four E2F binding sites organised into two imperfect

palindromes. Finally a GCCACC Kozak consensus sequence was inserted directly before the E1A ATG site.

To obtain pICOVIR-7, site directed mutagenesis was used to introduce a unique BsiWI site into pICOVIR-5, 222bp upstream of the E1A ATG site. Into this unique site, complementary oligonucleotides containing the E2F binding region (consisting of the two imperfect palindromes) were used to introduce two additional E2F binding regions, thus increasing the total number of E2F binding regions to three (and the number of actual E2F binding sites to 12).

### **3.5 Virus Recovery and Verification**

Virus recovery was performed by homologous recombination in HEK293 cells with appropriate combinations of left end plasmids; pPS1335M, pICOVIR-5 and pICOVIR-7 with the right end plasmids pMH008 eGFP and pMH009 eGFP, to make 5 novel vectors. To remove plasmid backbones both right end plasmids were first digested with ClaI and SmaI. pPS1335M was digested with SmaI and Sall while pICOVIR-5 and pICOVIR-7 were digested with EcoRI and PacI. HEK293 cells (used for the high transfection efficiency) were co-transfected with appropriate left and right ends using the calcium phosphate transfection protocol (described in section 2.4.1) with a 1:1 molar ratio of left: right ends, to rescue viruses as outlined in Table 3-2 (see also Figure 3-3)

		<b>Right End</b>	
		<b>pMH008</b>	<b>pMH009</b>
<b>Left End</b>	<b>pPS1335M</b>	vMH2	Not rescued
	<b>pICOVIR-5</b>	vMH4	vMH5
	<b>pICOVIR-7</b>	vMH6	vMH7

**Table 3-2. Virus recovery combinations**

See Figure 3-3 for plasmid constructs

When significant CPE and eGFP expression was observed, indicating virus production, cells were harvested and 1<sup>o</sup> seed stocks generated (see section 2.4.2 for generation of seed stocks). All subsequent virus passages were performed in A549 cells. 1<sup>o</sup> virus seed stocks were passaged once (at a 1/10 dilution) into 25cm<sup>2</sup> flasks to generate 2<sup>o</sup> seed stocks, which were then used for double plaque purification (as described in section 2.4.4). Nine plaques were picked, after screening by fluorescent microscopy to confirm eGFP expression, and used to infect 25cm<sup>2</sup> flasks (using half of the plaque for infection) to obtain a p1 seed stock. DNA was extracted from half of each p1 seed stock and screened by PCR for the presence of contaminating wt E1A sequences using primers PS1368A, PS1368B and PS1368C (see Table 2-1).

Primers PS1368A and B are designed to distinguish between contaminating wt E1A sequences and the E1A CR2  $\Delta$ 24 deletion. Primer PS1368A is located within the E1A CR2  $\Delta$ 24 deletion and should only detect wt E1A and not the CR2  $\Delta$ 24 deletion. Primer PS1368B is complementary to the sequences flanking the CR2  $\Delta$ 24 deletion and thus should only detect CR2  $\Delta$ 24 E1A and not wt E1A. Both were used with reverse primer PS1368C located 636bp downstream.

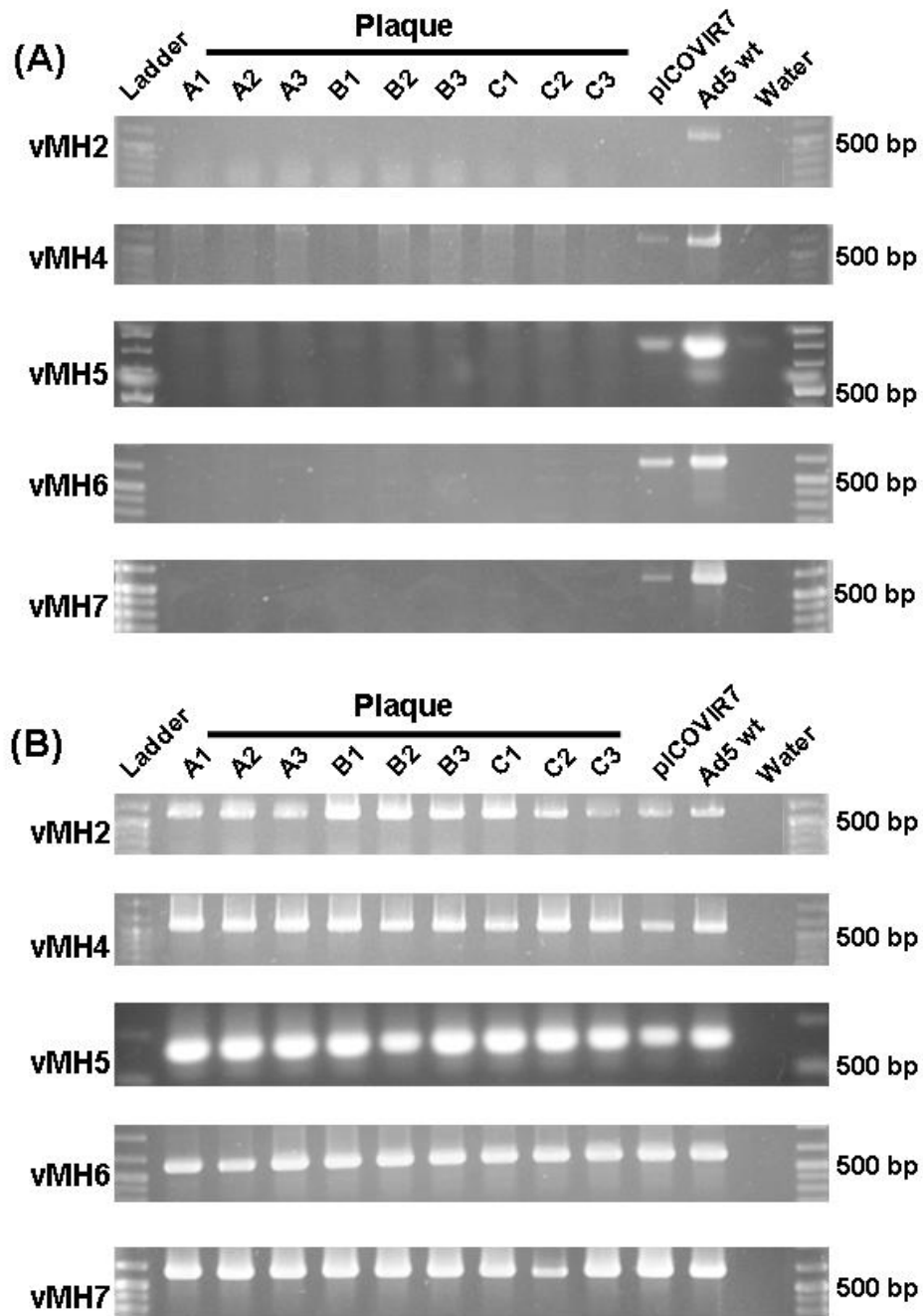


**Figure 3-4. PCR screening vMH vectors for E1A CR2  $\Delta$ 24 deletion**

DNA was extracted from the plaque purified p1 seed stocks and screened for contaminating wt E1A sequences. Reactions were set up with forward primer PS1368A (A) within the CR2 deletion or PS1368 (B) spanning the CR2 deletion, with reverse primer PS1368C. Reactions were setup using GoTaq polymerase in a final volume of 50 $\mu$ l and run for 40 cycles in a thermal cycler (as described in section 2.2.8 ). 10 $\mu$ l of each reaction were analysed by agarose gel electrophoresis.

Figure 3-4 shows the results of the E1A screening. All plaques screened were free of contaminating wt E1A sequences shown by the lack of band with primer PS1368A. As would be expected, no band was observed in the PCR grade water control and a clear band of correct size can be seen in the Ad5 wt positive control. However in three of the screens (vMH4, vMH6 and vMH7) a band can be observed with the pICOVIR-7 control samples. Since this plasmid contains the E1A CR2  $\Delta$ 24 deletion this contamination is probably due to water contamination since the plasmid prep used was not sterile. If this experiment was to be repeated a sterile prep of pICOVIR-7 dissolved in PCR grade water should be used to avoid the Ad contamination.

With primer PS1368B clear bands of the expected size were seen with all the picked plaques and pICOVIR-7 control. Again no band was observed with the PCR grade water as would be expected. A band was also observed with Ad5 wt control, probably due to PS1368B mispriming.

Following E1A screening the DNA samples were screened by PCR for the presence of eGFP insert and for contaminating transgene-deleted virus, using primer MHP003, MHP004 and MHP006 (described in Table 2-1). Primer MHP003 is located upstream of the transgene insertion site and detects both virus with insert and insert-deleted virus. Primer MHP004 is located within the eGFP insertion and thus only detects virus with the eGFP insertion. Both primers were used with MHP006 designed downstream of the insertion site. This primer produces an 1175bp band with MHP003 in the presence of transgene, a 404bp band with MHP003 and Ad5 wt, and a 784bp band with primer MHP004 and full length transgene.

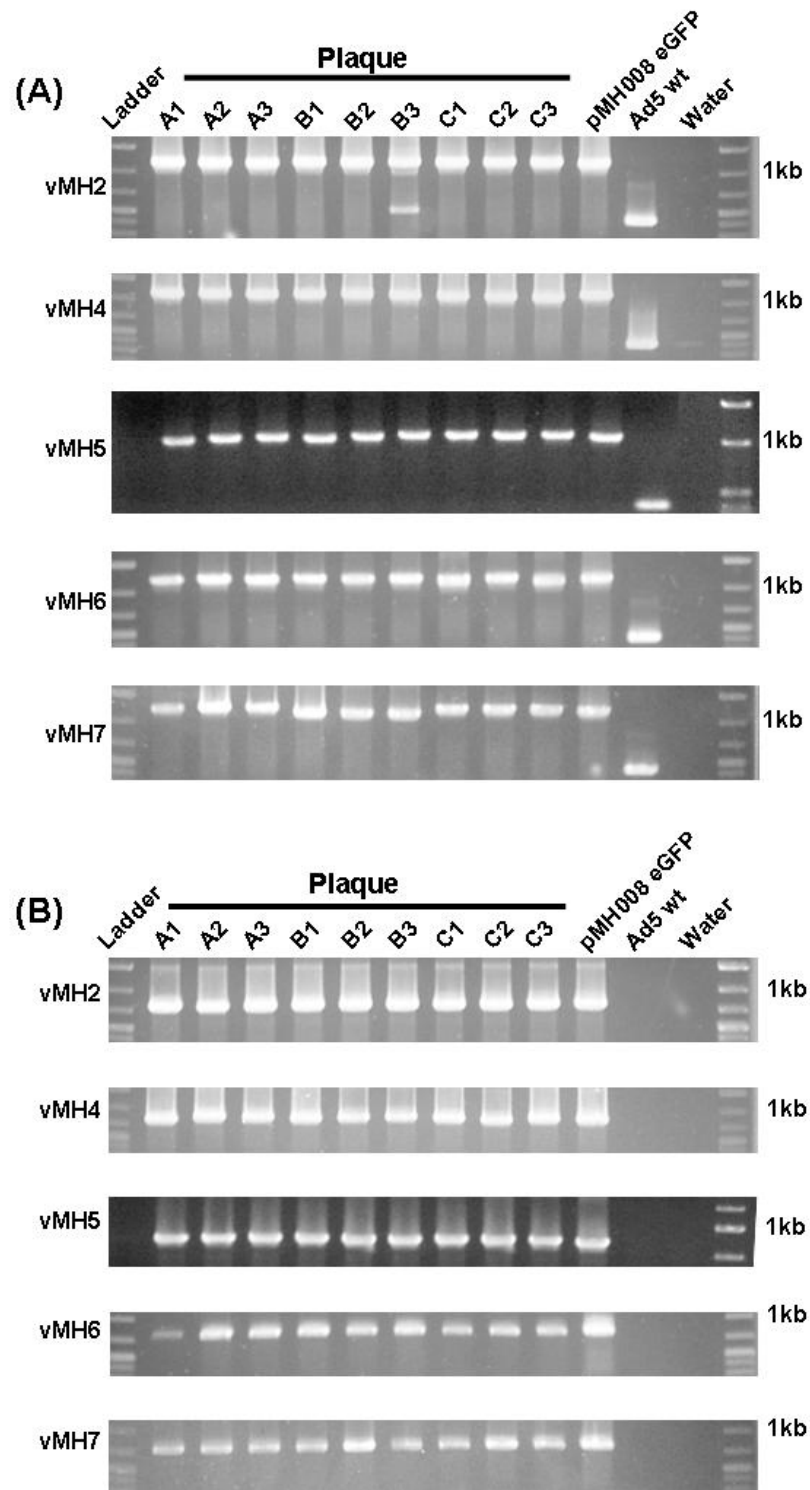


**Figure 3-5. PCR screening vMH vectors for eGFP insertion**

DNA was extracted from the plaque purified p1 seed stocks and screened for the presence of the eGFP transgene. Reactions were set up with forward primer MHP003 (A) located upstream of the insertion or MHP004 (B) located within the eGFP insertion, with reverse primer MHP006. Reaction were setup using GoTaq polymerase in a final volume of 50 $\mu$ l and run for 40 cycles in a thermal cycler (as described in section 2.2.8 ). 10 $\mu$ l of each reaction were analysed by agarose gel electrophoresis.

Figure 3-5 shows the results of eGFP insert screening. As predicted, no band was observed for PCR grade water with primer MHP003 or MHP004. Primer MHP003 produced a band of approximately 1200bp with all plaques, demonstrating the presence of eGFP insert. However one plaque, vMH2 plaque B3, also produced a band of approximately 500bp, demonstrating contamination with a virus which had undergone rearrangement to delete part of the insertion.

No band was observed for Ad5 wt with MHP004, and as expected a clear band of approximately 800bp could be seen with all plaques screened.

For each virus three p1 seed stocks (A1, B1 and C3), which were free of contaminating viruses, were chosen and each passaged into three 150cm<sup>2</sup> flasks, to generate p2 seed stocks. For each virus the p2 seed stock which showed the most CPE was chosen and passaged into 20x150cm<sup>2</sup> flasks. When good CPE was observed the flasks were harvested and virus purified by CsCl centrifugation to give a p3 banded virus stock.

DNA was extracted from each p3 banded stock and restriction enzyme profile confirmed with HindIII, BglII, and KpnI (detailed in appendix 1). Restriction profiles for all vectors were as predicted, confirming they had not undergone any major re-arrangements.

Following restriction enzyme profiling, the p3 banded stocks were quantitated by PicoGreen assay for virus particles and plaques counted on DU145 cells for infectious particles (as described in 2.4.6). The results of virus particles count, plaque count and the particle to infectivity (P:I) ratios are shown in Table 3-3, along with vector size and percentage size relative to the Ad5 wt genome. Table 3-3 also shows the data for banded Ad5 wt, vNR3 and Ad-GFP (replication deficient  $\Delta$ E1,  $\Delta$ E3 Ad vector expressing eGFP

from the CMV immediate early promoter) used in this thesis, all of which were generated from p2 or p3 seed stocks (kind gifts from Dr V. Mautner).

All banded viruses possessed a P:I ratio in the acceptable range of 10-110. With increasing genome size there is a clear increase in P:I ratio. Spearman rank analysis showed a statistically significant correlation between virus genome size and P:I ratio (spearman rank = 0.9429 and P value = 0.0167). All vectors have similar virus particle counts and the increase in P:I ratio comes from a decrease in infectious virus particle count, with vMH6 and vMH7 having the lowest values. Because of the low infectious virus count with vMH6 and vMH7, a second batch of p3 banded virus was made using the appropriate seed stocks. The second batches of these viruses showed similar properties to the first batches, with high P:I ratios and low infectious virus counts.

Virus	Particle count (VP/ml)	Plaque count (PFU/ml)	P:I ratio	Size (bp)	Percentage of Ad5 wt	
vMH2	$2.12 \times 10^{12}$	$4.00 \times 10^{10}$	28.0	36682	102.07	
vMH4	$3.13 \times 10^{11}$	$1.00 \times 10^{10}$	31.6	37673	104.83	
vMH5	$3.41 \times 10^{11}$	$6.67 \times 10^9$	51.2	37700	104.90	
vMH6	Batch 1	$1.58 \times 10^{11}$	$1.40 \times 10^9$	112.6	37799	105.18
	Batch 2	$1.22 \times 10^{11}$	$1.20 \times 10^9$	101.0		
vMH7	Batch 1	$2.07 \times 10^{11}$	$2.00 \times 10^9$	104.0	37826	105.25
	Batch 2	$9.68 \times 10^{10}$	$1.00 \times 10^9$	97.0		
vNR3	$4.65 \times 10^{11}$	$2.20 \times 10^{10}$	21.0	33596	93.48	
Ad5 wt	$3.26 \times 10^{12}$	$3.00 \times 10^{11}$	11.0	35938	100.00	
Ad-GFP	$9.30 \times 10^{11}$	$9.30 \times 10^{10}$	10.0	33871	94.25	

**Table 3-3. Virus particle count, plaque count and P:I ratios.**

## **3.6 Discussion**

### **3.6.1 Virus Construction and Screening**

Standard molecular cloning techniques were used to construct 5 CRAAd vectors for oncolytic virotherapy. Virus p1 seed stocks were screened by PCR for the presence of contaminating virus which could have acquired the wt E1A region from recombination with DNA sequences in HEK293 cells or could have deleted the eGFP transgene. All p1 seed stocks screened showed no E1A or eGFP recombination with one exception where an eGFP rearrangement had taken place.

The restriction profile of each banded p3 stock was also confirmed by digestion with HindIII, BglIII and KpnI.

No problems were encountered while culturing any vMH vectors and good eGFP expression was observed throughout. However, in culturing vMH vectors differences were observed in the time taken to achieve good CPE, plaque size and rate of plaque appearance. vMH2 reached complete CPE in 3-4 days and also formed the largest plaques. Both vMH6 and vMH7 were slower growing, taking 5-6 days to reach good CPE and also having smaller plaques.

### **3.6.2 Virus Titres and Particle to Infectivity Ratios**

All vMH vectors had reasonable virus particle counts comparable to the E1B-55K deleted virus vNR3, but not as high as Ad5 wt. All vMH vectors have P:I ratios of 10 to 100, which are acceptable for *in vitro* studies. However it is notable that with increase in genome size there is a decrease in infectious virus particles, which gives an increase in the P:I ratio. Bett *et al* identified the adenovirus packaging limit as approximately 105% of the wildtype Ad5

genome [Bett et al, 1993]: by passage 9, virus constructs at 106.2, 106.1 and 105.4% of the Ad5 genome underwent rearrangements to decrease vector size. In comparison vectors of 104.6 and 103.1% were stable up to 20 passages. Taken together these results show Ad has a relatively tight constraint on the packaging limit and whereas vectors below 105% are stable a packaging limit exists between 104.6 and approximately 105.4%. Unfortunately, there have been no more recent reports investigating the upper Ad packaging limit which might have narrowed down this range. Both vMH6 and vMH7 have genomes over 105% of the Ad5 wt genome (105.18 and 105.25%, respectively) and it is worth noting this may have an effect on packaging efficiency and P:I ratio.

Whereas the low infectious virus titre and higher P:I ratios do not pose a direct problem for this study, there are some possible implications for any future clinical work with these vectors. All batches of adenovirus for clinical use have to be made to GMP (good manufacturing practice) standards, which includes production and quality control specifications. Part of the UK GMP guidelines state “clinical grade adenovirus requires a P:I ratio less than 100”. Both batches of vMH6 and vMH7 have P:I ratios close to or higher than 100 and therefore could potentially pose a fundamental problem in the manufacture of clinical virus. It may also be worth noting that whereas no regulations are set out as to minimum virus titre, the low virus particle yield from vMH6 and vMH7 may have significant cost implication for the production of clinical grade virus stocks.

### **3.7 Summary**

I have cloned and constructed 5 new adenovirus vectors expressing eGFP for prostate oncolytic virotherapy. These vectors have been screened by PCR and profiled by restricting enzyme digestion. These vectors will be characterised in subsequent chapters to select the optimal vector for introduction of the therapeutic transgene NTR.

## **CHAPTER 4**

### **Characterisation of vMH Viruses**

## 4.1 Introduction

The 5 new vMH vectors (vMH2, 4, 5, 6 and 7) incorporate E1A modifications for improved tumour specificity, RGD-retargeted fibre for increased tumour transduction and all are designed to express eGFP at late times of infection. These vectors were characterised alongside the  $\Delta$ E1B-55K vector vNR3, to identify the optimal vector in terms of tumour selectivity, cytotoxicity and transgene expression, for the introduction of the therapeutic transgene NTR. Initial experiments were conducted to investigate the tumour specificity of these vectors, by measuring the cytotoxicity in prostate tumour cell lines and non-transformed human fibroblasts. Further characterisation was performed to see the effects of each modification on virus replication, gene expression and spread. Finally, the vMH vectors were compared with similar vectors which lacked any transgene, to investigate the effects of transgene insertion.

Chen *et al* demonstrated over-expression of NTR from the CMV immediate early promoter had a detrimental effect virus recovery when combined with high concentration of the prodrug CB1954 [Chen et al, 2004]. Dr Roesen expressed NTR at intermediate times of replication from the pIX virus promoter [Roesen 2006]. This alleviated the CB1954 associated toxicity on virus replication and spread; however NTR expression from the pIX promoter was significantly lower than from the CMV promoter, resulting in a lower therapeutic potential. All vMH vectors were designed to express transgene from the Ad MLP to achieve late and high transgene expression. It was therefore anticipated that subsequent replacement of the eGFP transgene with NTR should not affect virus replication, but would give high NTR expression late in virus infection (post DNA replication), resulting in a high therapeutic potential.

## **4.2 Aims of Chapter**

The aim for this chapter was to characterise 5 eGFP expressing vMH vectors in term of virus replication, gene expression, spread and tumour specificity. These vectors were compared with vNR3 (the  $\Delta$ E1B-55K virus constructed by Dr Roesen), which expressed eGFP from the pIX promoter.

## **4.3 Results**

### **4.3.1 CAR and Integrin Expression**

To begin, the CAR and  $\alpha_v\beta_{3/5}$  integrin status of the cell lines; A549, DU145, 22RV1, PC3, MRC5, KS fibroblasts, SKOV3 and MZ2-MEL3.0 was assessed by flow cytometry. Cells were plated at three concentrations to see if confluence affected cell surface expression. The percentage of cells CAR or integrin positive cells was calculated relative to the appropriate isotype control; see Figure 4-1.

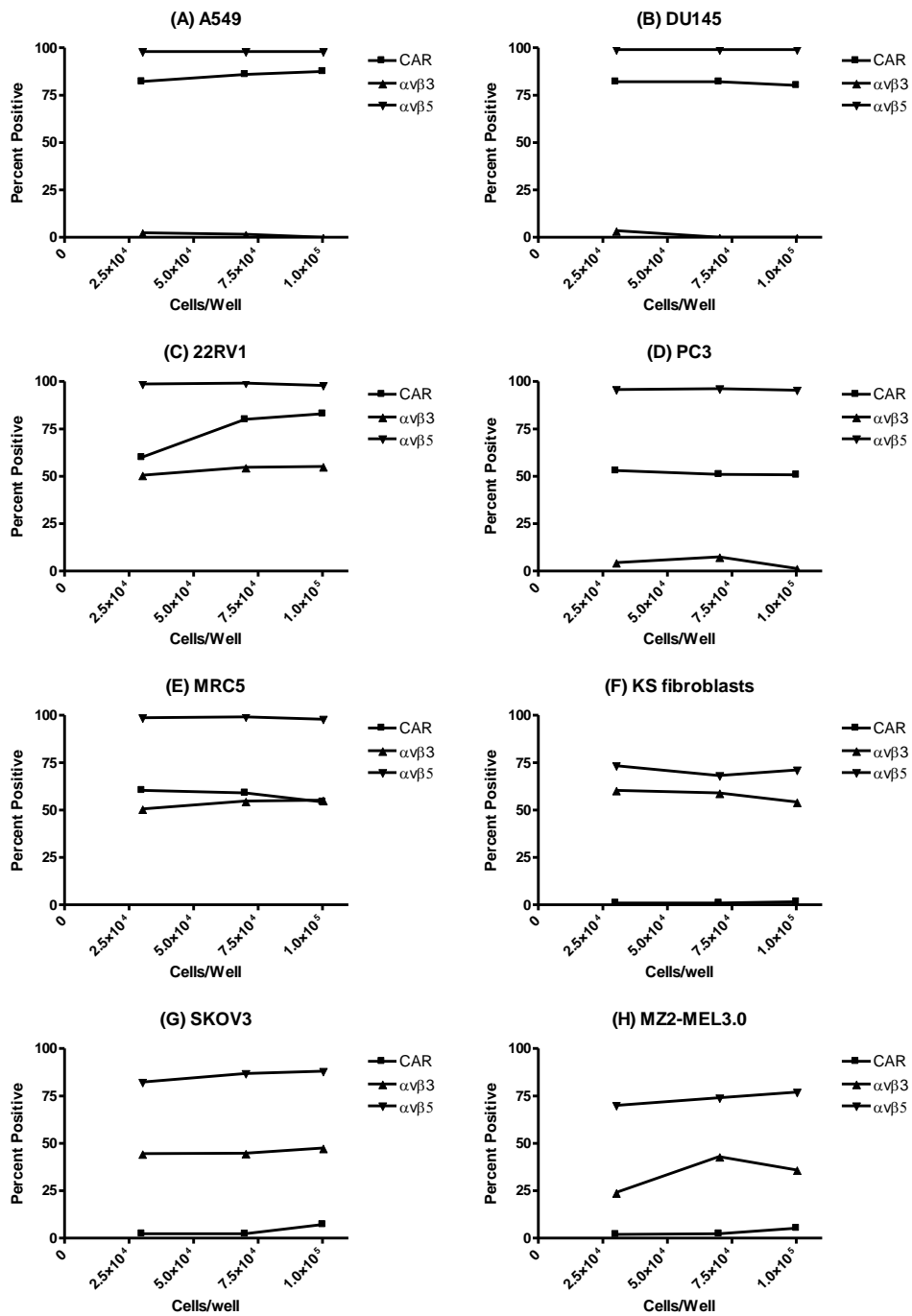


**Figure 4-1. Surface CAR and integrin expression of the cells used in this study**  
 A549 (A), DU145 (B), 22RV1 (C), PC3 (D), MRC5 (E), KS fibroblast (F), SKOV3 (G) and MZ2-MEL3.0 (H) cells were seeded in 24-well plates at 3x10<sup>4</sup>, 7x10<sup>4</sup> and 1x10<sup>5</sup> cells per well in 2ml of medium per well. Cells were allowed to adhere for 48 hours before being harvested and stained with anti-CAR, anti-αvβ<sub>3</sub> or anti-αvβ<sub>5</sub> for 1 hour at 4°C (as described in section 2.9.1), and analysed by flow cytometry. Graphs show the percent positive relative to the isotype control.

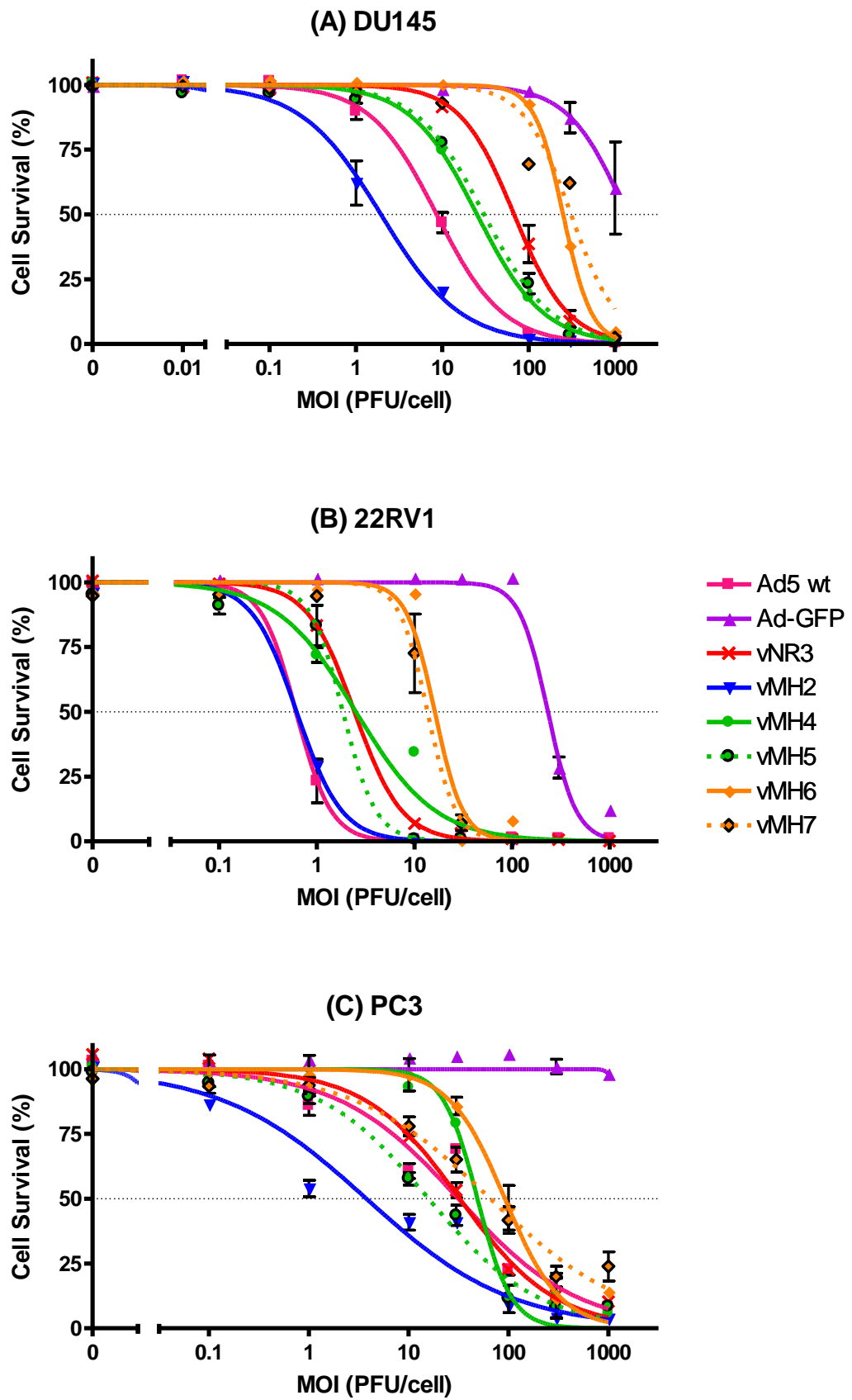
A549 and DU145 cells expressed similar levels of CAR and integrins; both showing high CAR expression (>80% positive), high  $\alpha_v\beta_5$  expression (>98% positive) and no detectable  $\alpha_v\beta_3$  expression. 22RV1 cells also expressed a high level of  $\alpha_v\beta_5$  (>95% positive) and good CAR expression (66-75% positive), but also had moderate  $\alpha_v\beta_3$  expression (approximately 50% positive). PC3 cells showed little  $\alpha_v\beta_3$  expression (<10% positive), a moderate level of CAR expression (approximately 50% positive) and also a high level of  $\alpha_v\beta_5$ . A high level of  $\alpha_v\beta_5$  expression (>98% positive) was observed with MRC5 fibroblasts, with moderate levels of CAR and  $\alpha_v\beta_3$  (both approximately 50% positive). In contrast, KS fibroblasts showed no CAR expression and moderate levels of  $\alpha_v\beta_3$  and  $\alpha_v\beta_5$  expression, both approximately 50-60% positive. Both SKOV3 and MZ2-MEL3.0 showed little CAR expression (>5% positive), some  $\alpha_v\beta_3$  expression (25-40% positive) and good levels of  $\alpha_v\beta_5$  expression (approximately 75% positive). For all cell lines, no major change in CAR or integrin expression was observed with varying cell density. The levels of mean fluorescent intensity corroborated these observations (data not shown).

#### **4.3.2 Cytotoxicity of vMH Vectors**

All vMH vectors were designed to replicate conditionally within tumour cells and to spare normal cells. Previous studies have demonstrated that E1A CR2  $\Delta$ 24 vectors show good cytotoxicity to cancer cells, but high levels of cytotoxicity are also observed with non-transformed primary cells which have not been growth arrested [Bazan-Peregrino et al, 2008]. The further modifications within vMH4, 5, 6 and 7 are designed to enhance the tumour cell selectivity by restricting E1A expression to cells with high E2F levels. Furthermore vMH5 and vMH7 contain a retargeted fibre which should aid in transduction of cells expressing low amounts of CAR.

To investigate the comparative selectivity of these vectors, cytotoxicity was measured in three prostate cancer cells lines; DU145, 22RV1 and PC3, and two non-transformed human fibroblasts lines; MRC5 and KS fibroblasts.

Cells in 96-well plates were infected in triplicate with 10-fold serial dilutions of vMH vectors, Ad5 wt, Ad-GFP and vNR3 from  $1 \times 10^{-2}$  to  $3 \times 10^3$  PFU/cell (as described in section 2.4.8). Cell survival was measured 5 days post infection by acid phosphatase (AP) assay (described in section 2.5.1), dose response curves fitted (Figure 4-2) and EC50 values calculated (Table 4-1), as described in section 2.10.



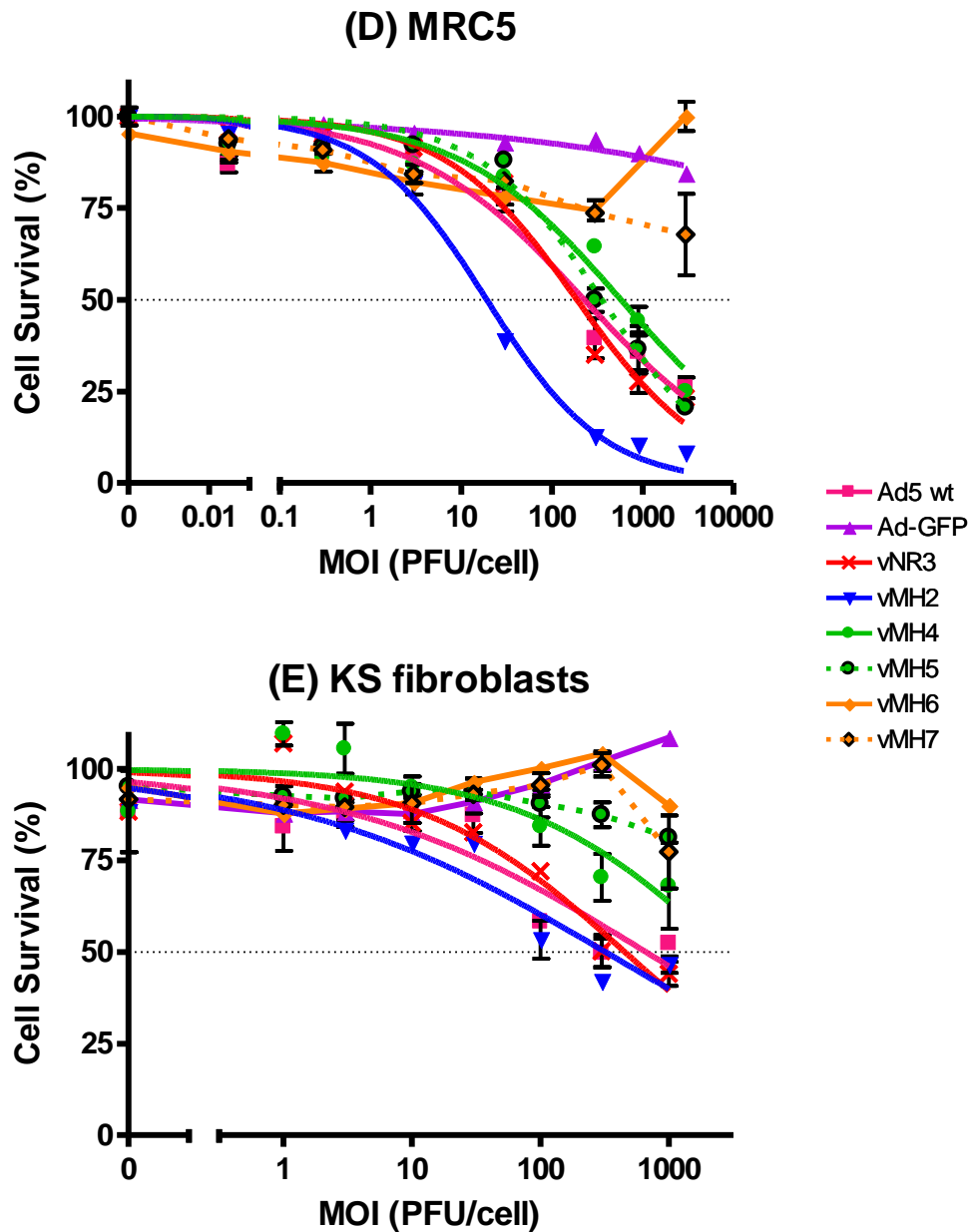


**Figure 4-2. Dose response curves for vMH cytotoxicity**

DU145 (A), 22RV1 (B), PC3 (C) were seeded in 96-well plates at  $3 \times 10^4$  cells per well, while MRC5 (D) and KS (E) fibroblasts were seeded in 96-well plates at  $1 \times 10^4$  cells per well. Triplicate wells were infected with a serial dilution of Ad5 wt, Ad-GFP, vNR3 and vMH vectors as described in section 2.4.8. Cell survival was measured 5 days post infection by AP assay and normalised to mock infected cells (100% survival) and empty wells (0% cell survival). Plots show mean cell survival,  $\pm$  S.D. (where no error bars are visible S.D. was  $<5\%$ ), where  $n=3$  for each data point and fitted sigmoid dose response curves. Dose response curves were used to calculate EC50 values. GraphPad software was used to calculate error bars, dose response curves and EC50 values. A schematic of each CRAAd can be found in Figure 3-2.

<b>Virus</b>	<b>DU145</b>	<b>22RV1</b>	<b>PC3</b>	<b>MRC5</b>	<b>KS fibro</b>
<b>Ad5 wt</b>	8.61 (7.85 - 9.43)	0.613 (0.479 - 0.784)	31.4 (22.1 - 44.7)	720 (571 - 909)	661 (260 - 1680)
<b>vNR3</b>	67.9 (60.2 - 76.7)	2.44 (2.15 - 2.76)	32.5 (28.2 - 37.4)	191 (138 - 264)	453 (282 - 729)
<b>vMH2</b>	1.95 (1.64 - 2.32)	0.622 (0.568 - 0.681)	2.83 (1.67 - 4.79)	78.1 (66.7 - 91.5)	319 (165 - 616)
<b>vMH4</b>	25.3 (22.8 - 28.1)	2.52 (1.82 - 3.51)	48.8 (42.2 - 56.4)	791 (386 - 1620)	>1000
<b>vMH5</b>	30.6 (26.8 - 34.9)	1.86 (1.22 - 2.82)	15.8 (13.1 - 19.1)	392 (314 - 489)	>1000
<b>vMH6</b>	251 (243 - 260)	15.0 (9.93 - 22.7)	91.9 (76.8 - 110)	>3000	>1000
<b>vMH7</b>	311 (251 - 384)	13.5 (12.0 - 15.2)	65.9 (51.2 - 84.7)	>3000	>1000

**Table 4-1. EC50 values with 95% C.I. (PFU/cell) for vMH cytotoxicity**

vMH2 (wt E1A promoter, CR2  $\Delta$ 24) demonstrated cytotoxicity equal to or up to 10-fold greater than Ad5 wt, in all prostate cancer cells lines and non-transformed fibroblasts. vMH4 (ICOVIR-5 promoter, CR2  $\Delta$ 24) demonstrated a 3- to 5-fold reduction in cytotoxicity relative to Ad5 wt in prostate cancer cells, with cytotoxicity equal to Ad5 wt in MRC5 cells and very little cytotoxicity in KS fibroblasts, with an EC50 value greater than 1000 PFU/cell. In comparison, the equivalent RGD-retargeted vector vMH5, demonstrated a range of cytotoxicities in prostate cancer cell lines, with a 2-fold increase in cytotoxicity over Ad5 wt in PC3 cells, but a 3-fold decrease in cytotoxicity in DU145 and 22RV1 cells. Little cytotoxicity was observed with vMH5 in KS fibroblasts; however a 2-fold increase in cytotoxicity over Ad5 wt was seen in MRC5 fibroblasts. No significant difference was observed in the cytotoxicity of vMH6 (ICOVIR-7 promoter, CR2  $\Delta$ 24) and the equivalent RGD-retargeted vector vMH7, both of which showed a 3- to 30-fold decrease in cytotoxicity relative to Ad5 wt in prostate cancer cell lines, and very little cytotoxicity in MRC5 or KS fibroblasts, with over 50% cell survival at the highest MOI.

Very little difference in cytotoxicity was observed between matched wt fibre and RGD-retargeted fibre vectors (i.e. vMH4 vs vMH5 and vMH6 vs vMH7). In both 22RV1 and PC3 cells the RGD-retargeted vectors showed a small reduction in the EC50 values compared to the wt equivalent vector. vMH5 also showed a slight increase in cytotoxicity over vMH4 in MRC5 cells, however no difference was observed in these cells between vMH6 and vMH7. In contrast the opposite was observed in DU145 cells, with the RGD-retargeted fibre vectors demonstrating a slightly higher EC50 value than the wt equivalents. However it must be noted that, with one exception, the 95% confidence intervals of EC50 values between wt and RGD-retargeted vectors were overlapping. The one exception was vMH5, which showed a 3-fold increase in cytotoxicity over vMH4 in PC3 cells.

Flow cytometry for CAR expression demonstrated CAR expression on all the prostate cancer cell lines used here, and on MRC5 cells. However, PC3 and MRC5 cells expressed lower levels of CAR compared DU145 and 22RV1 cells (see Figure 4-1), therefore if any cytotoxic advantage were to be observed with the RGD-retargeted fibre it would possibly be expected in these cells. Since CAR expression was high in 22RV1 and DU145 cells, the CAR receptor is unlikely to be saturated by the MOI used in this study ( $3 \times 10^4$  PFU/cell), therefore it was not unexpected that the RGD-retargeted vectors did not show an oncolytic advantage in these cells.

To give an indication of the tumour cell selectivity, the therapeutic index (TI) was calculated for each virus, by dividing the non-transformed cell EC50 values by the target tumour cell EC50 values; the higher the index the more selective the vector (see Figure 4-3). As no EC50 value was observed with vMH4-7 in KS fibroblasts, MRC5 cells were used as the non-transformed cell references. Since even in MRC5 fibroblasts, no EC50

value was obtained for vMH6 and vMH7 the indices of these viruses were calculated using the top dose used (3000 PFU/cell), and is therefore is an underestimation of the actual tumour selectivity.

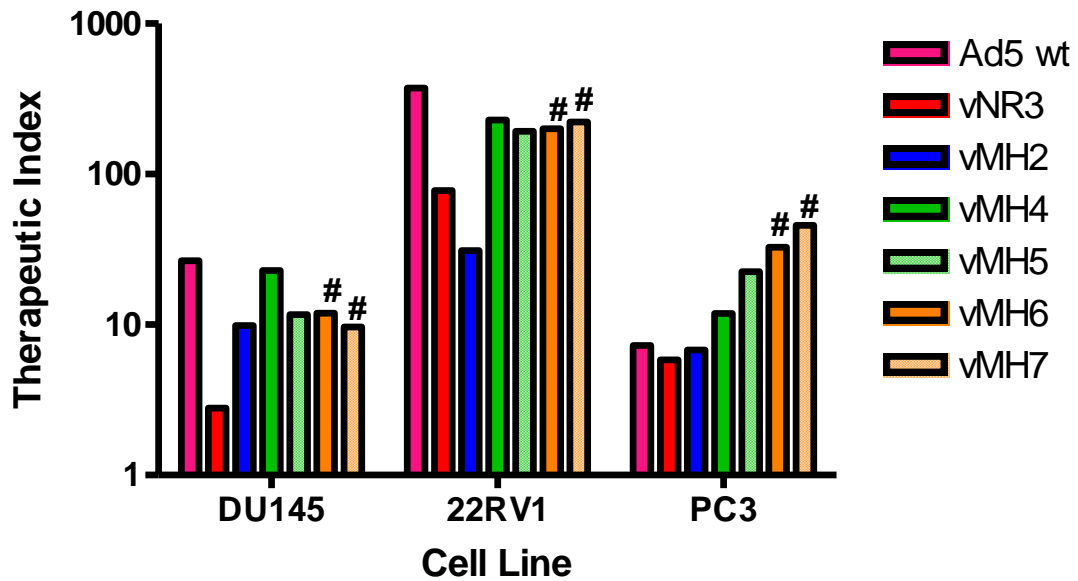


**Figure 4-3. Therapeutic indices for vMH vectors**

The therapeutic index for each virus was calculated in DU145, 22RV1 and PC3 cells by dividing the MRC5 EC50 value by the target prostate cell line EC50 value. No definitive EC50 value was ascertained for vMH6 and vMH7 in MRC5 cells therefore the value of 3000 PFU/cell was used; however the actual therapeutic index for these vectors is higher than shown (indicated by #).

A range of therapeutic indices was observed for the vectors, with no single virus having the highest therapeutic index throughout all cell lines, this is probably a result of the varying p53 status, pRb status and CAR expression, discussed further in section 4.4.1. Furthermore, Ad5 wt showed the highest therapeutic index in both DU145 and 22RV1 cells, also discussed in section 4.4.1. However, all ICOVIR-5 (vMH4 and vMH5) and ICOVIR-7 (vMH6 and vMH7) based vectors were more selective than the CR2 Δ24 vector with the wt

E1A promoter (vMH2) and the  $\Delta$ E1B-55K virus (vNR3). In both DU145 and 22RV1 cells vMH4 showed the highest therapeutic index of all CRAd vectors, followed by vMH5 and vMH6. In PC3 cells vMH6 and vMH7 showed the highest therapeutic index, followed by vMH6 and then vMH5. However, it must be noted the actual ranking of vMH6 and vMH7 is not known, and the 'true' TI of both vMH6 and vMH7 could be greater than Ad5 wt in DU145 and 22RV1 cells.

### **4.3.3 eGFP Transgene Expression with vMH Vectors**

All vMH vectors were designed to express the eGFP transgene from the Ad MPL, to achieve high but late transgene expression. In comparison, vNR3 expresses eGFP from the intermediate pIX viral promoter. To investigate eGFP transgene expression level and timing, eGFP expression was measured by flow cytometry. 24-well plates of DU145 and 22RV1 were infected with 100 VP/cell of Ad-GFP or vMH vectors and MRC5 cells were infected at 1000 VP/cell. For practical reasons 2 individual experiments were carried out with two groups of viruses; vMH2, vMH7 and vNR3 or vMH4, vMH5 and vMH6 with Ad-GFP included in both experiments as an internal reference. At timepoints between 0 and 60 hours post infection duplicate infected wells were analysed by flow cytometry (as described in section 2.9.1).

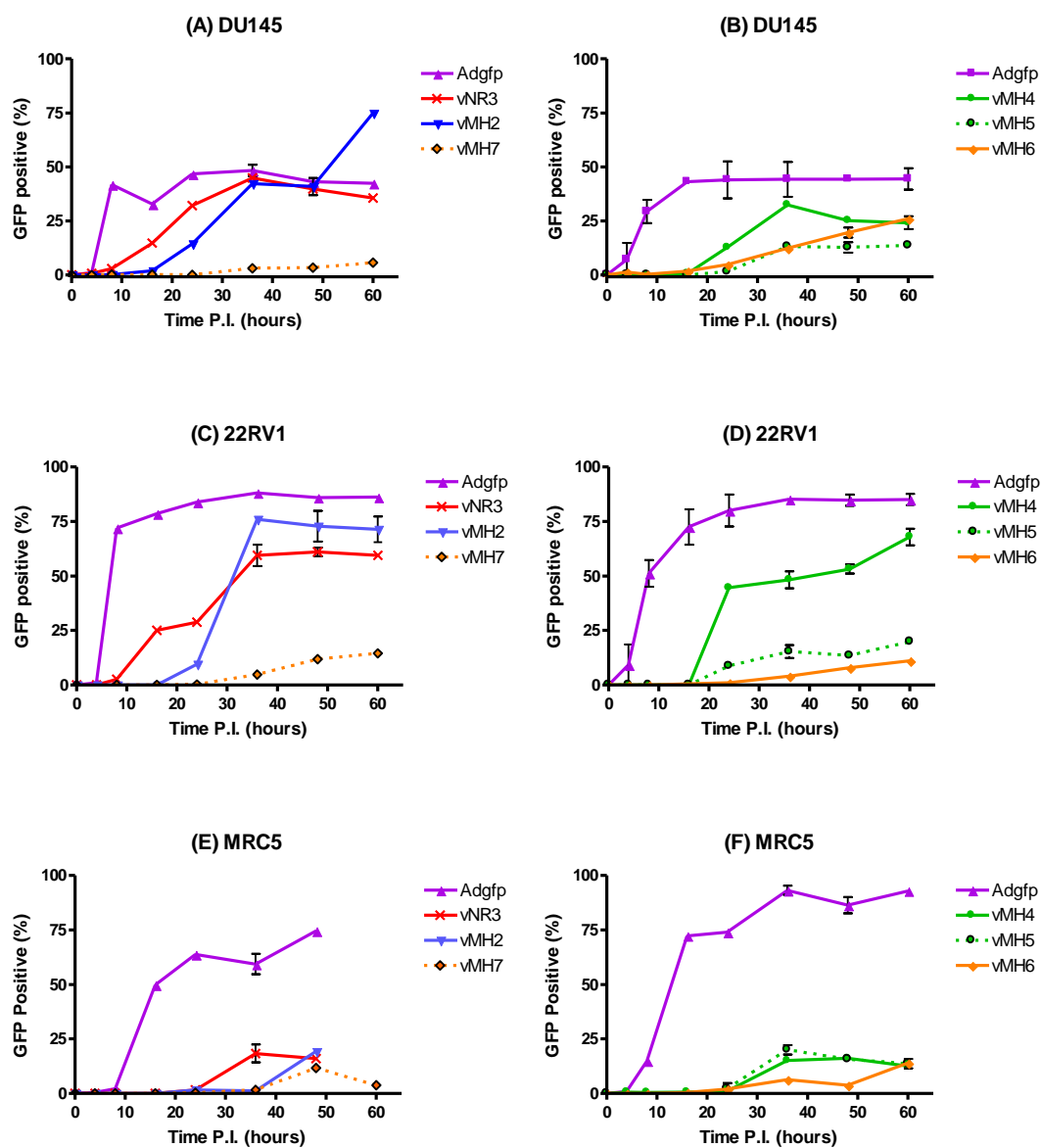


**Figure 4-4. eGFP percentage positive with vMH vectors**

DU145 cells (A and B) and 22RV1 cells (C and D) in 24-well plates were infected with Ad-GFP, vNR3, vMH2 and vMH7 (A, C and E) or Ad-GFP, vMH4, vMH5 and vMH6 (B, D and F) at 100 VP/cell for DU145 and 22RV1 cells or 1000 VP/cell for MRC5 cells (as described in 2.4.8). Duplicate wells were harvested at timepoints from 4 to 60 hours post infection, washed, fixed and eGFP expression analysed by flow cytometry. Graphs show the mean percentage eGFP positive (n=2),  $\pm$  S.D. (where no error bars are visible S.D. was <5%).

Figure 4-4 shows the percentage eGFP positive cells for all three cell lines. Ad-GFP clearly expressed detectable levels of GFP at 8 hours post infection in all cell lines tested. vNR3 expressed detectable levels of eGFP in both prostate cell lines from 8 hours post infection, which rose steadily until plateauing at approximately 36 hours. In contrast, eGFP expression with the vMH viruses, with the exception of vMH7, was not observed until 24 hours post infection, as would be expected for late gene expression. With vMH7 no eGFP expression was detected until 36 hours post infection, approximately 8 hours after all other vMH vectors. The maximum number of cells transduced with each vMH vector reflected the variation in P:I ratio (e.g. vMH7 achieved a maximum transduction 4-fold lower than vMH2, but vMH7 had a 4-fold higher P:I ratio).

Within the normal cell line MRC5, the vMH vectors and vNR3 did not express detectable levels of eGFP until 24-36 hours post infection. Furthermore, the maximum number of positive cells remained under 20% up to 60 hours post infection, despite using 10-fold more virus than with prostate carcinoma cell lines. In comparison, Ad-GFP transduced 75% of cells by 60 hours post infection, demonstrating selective transgene expression with vMH vectors and vNR3.

The fold increase in mean fluorescence intensity (MFI) relative to mock infected cells was calculated for the eGFP positive population, shown in Figure 4-5. vNR3 had detectable levels of eGFP from 24 hours post infection, after which the intensity increased steadily reaching maximal expression at 36 hours post infection. With all vMH vectors except vMH7, eGFP expression began at 16-24 hours post infection, after which the level of expression rose rapidly, reaching maximum intensity at 36 hours post infection. vMH7 clearly demonstrated an 8-10 hour delay in eGFP compared to the other vMH vectors, with

eGFP expression not detectable until 24-36 hours post infection. Despite this delay the intensity of eGFP expression with vMH7 reached a level similar to that of all other vMH vectors. The maximum level eGFP expression with all vMH vectors was 10-fold and 3-fold higher than vNR3, in DU145 and 22RV1 cells, respectively.

At the final timepoint (60 hours post infection) CPE could clearly be observed with vNR3 and vMH2. In comparison little CPE was observed with all the E2F-1 controlled vMH vectors at 60 hours post infection.

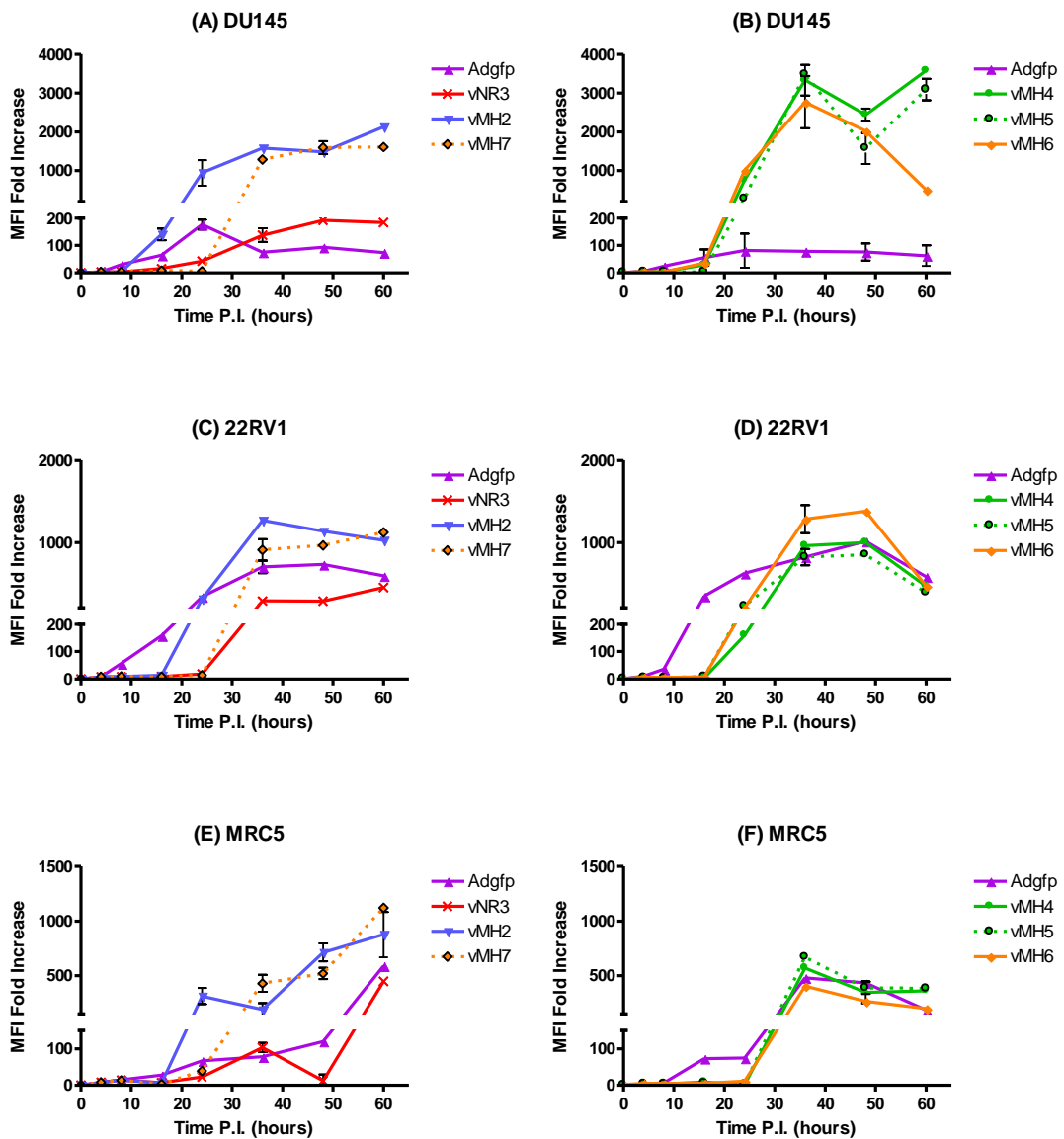


### Figure 4-5. eGFP MFI with vMH vectors

The same experiment as in Figure 4-4; showing calculated fold increase in MFI over mock infection was calculated. Graphs show the mean of the duplicate infection ( $n=2$ ),  $\pm$  S.D. (where no error bars are visible S.D. was  $<5\%$ ).

#### 4.3.4 DNA Replication with vMH Vectors

Full length MLP transcription first requires the initiation of DNA replication. With vMH2, 4, 5 and 6 eGFP expression began 24 hours post infection and accelerated rapidly over the next 12 hours. One vector, vMH7, had an 8-10 hour delay in the onset of eGFP expression.

To investigate whether this was a consequence of delayed virus DNA replication, Q-PCR was used to measure the timecourse of virus DNA replication for the MH vectors. DU145 cells in 24-well plates were infected with 100 VP/cell of Ad5 wt, vNR3 or vMH vectors (as described in section 2.4.8). Two individual experiments were carried out with two groups of viruses; vMH2, vMH7 and vNR3 or vMH4, vMH5 and vMH6. Ad5 wt was included in both experiments as an internal control. At timepoints between 0 to 60 hours post infection duplicate wells. Q-PCR was carried out for virus DNA and cellular DNA as described in section 2.7.1.

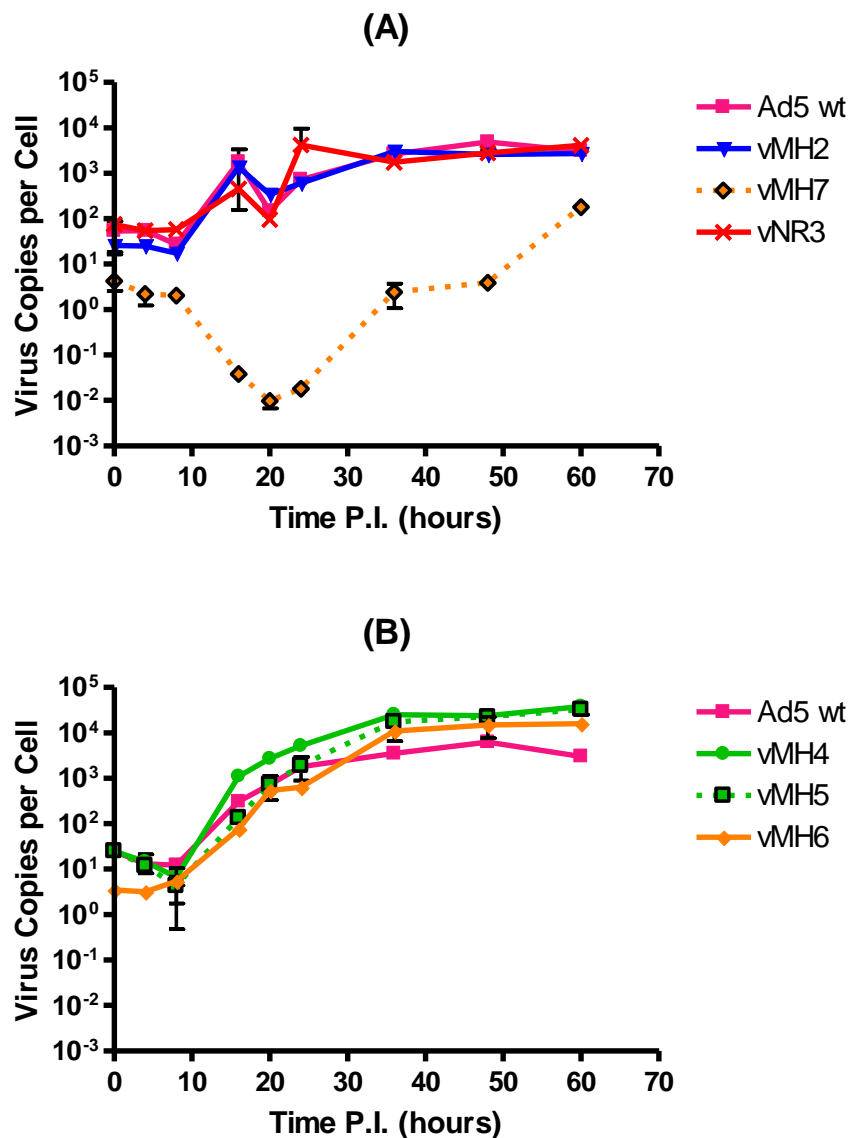


**Figure 4-6. DNA replication of vMH vectors**

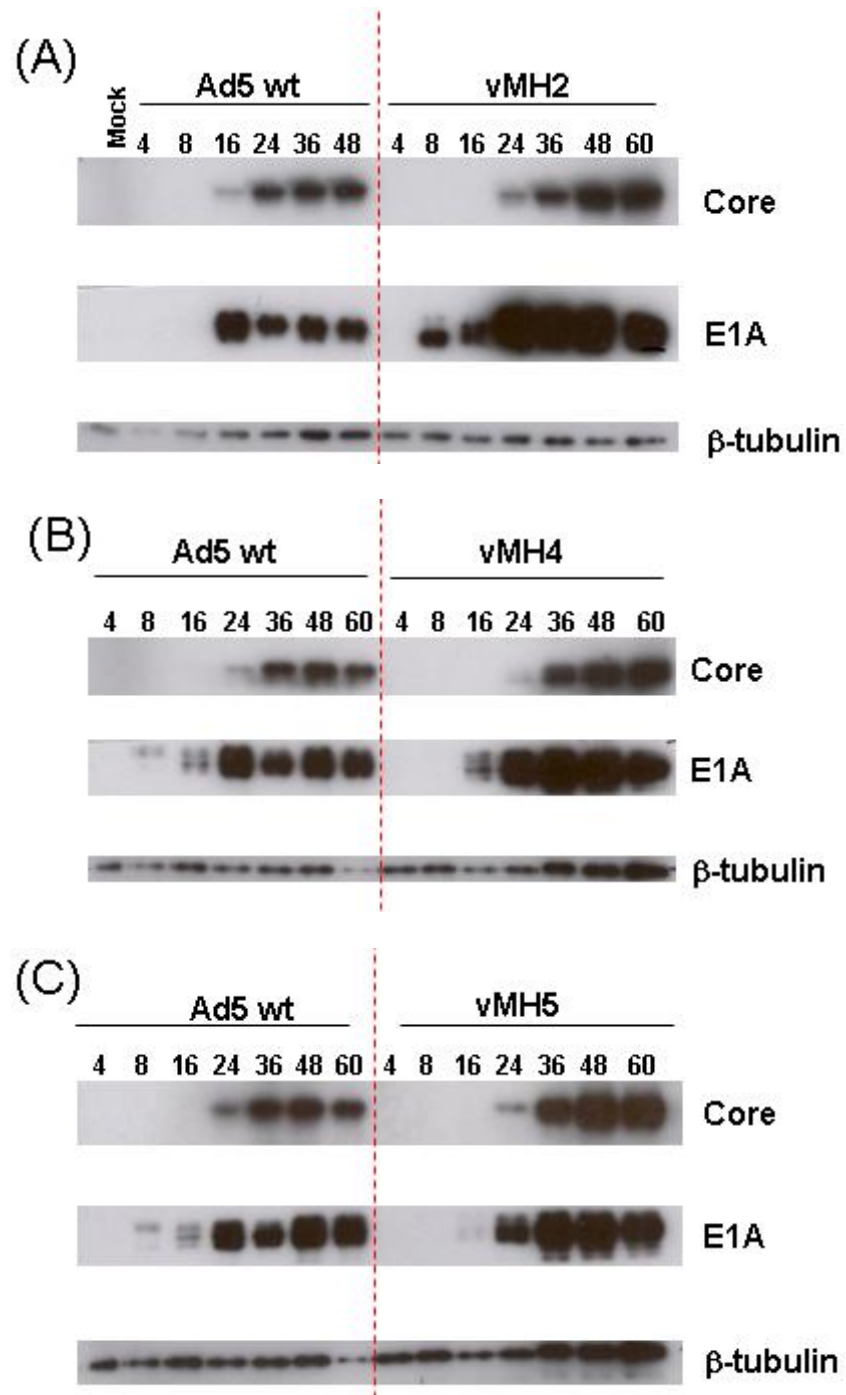
DU145 cells were seeded at  $1 \times 10^5$  cells per well in 24-well plates before being infected with 100 VP/cell of vMH2, vMH7, vNR3 and Ad5 wt (A), or vMH4, vMH5, vMH6 and Ad5 wt (B) as described in section 2.4.8. Duplicate wells were harvested at timepoints from 4 to 60 hours post infection, DNA extracted, and Q-PCR performed for viral genomes and cellular DNA. Virus genome copies were normalised to cellular DNA copies. Graphs show the mean of duplicate wells ( $n=1$ ),  $\pm$  S.D. (where no error bars are visible S.D. was  $<5\%$ ).

Figure 4-6 shows the timecourse of viral DNA replication profile normalised to copies of cellular DNA. Ad5 wt virus DNA replication began 8-16 hours post infection and started to plateau 24-36 hours post infection. All vMH vectors, except vMH7, had DNA replication profiles very similar to Ad5 wt. As would be expected, the end of virus DNA replication coincides with the onset of eGFP expression, at approximately 24 hours post infection. vMH7 virus DNA replication did not begin until 20-24 hours post infection, approximately 8-10 hours later than all other vMH vectors. It therefore seems the 8-10 hour delay observed with vMH7 eGFP expression reflects an 8-10 hour delay in the onset of virus DNA replication. vMH7 also showed a 100-fold decrease in virus genomes/cell before the onset of DNA replication, which was due to a decrease in virus copy number, not an increase in cellular DNA.

#### **4.3.5 E1A Expression**

All E2F responsive vectors have a 10-100 fold reduction in oncolytic activity compared to vMH2, which has the wt E1A promoter. Replacing the E1A promoter could result in lower or delayed E1A expression, which in turn could result in reduced oncolytic activity. It was therefore decided to investigate the E1A expression from vMH vectors by western blot. 24-well plates of DU145 cells were infected with 10 PFU/cell of Ad5 wt or vMH vectors, as described in section 2.4.8. At timepoints between 4 and 60 hours post infection, total protein was harvested and prepared for western blot, as described in section 2.8. For each vMH vector separate western blots were performed, alongside Ad5 wt to act as an internal control. Blots were probed for E1A and  $\beta$ -tubulin (loading control) using unconjugated primary antibodies, with anti-mouse HRP conjugate secondary antibody and an ECL detection kit. Westerns were subsequently reprobed for late protein production using rabbit

serum to whole heat inactivated virus, with anti-rabbit HRP secondary antibody and ECL detection. All antibodies for western blotting are listed in Table 2-6.



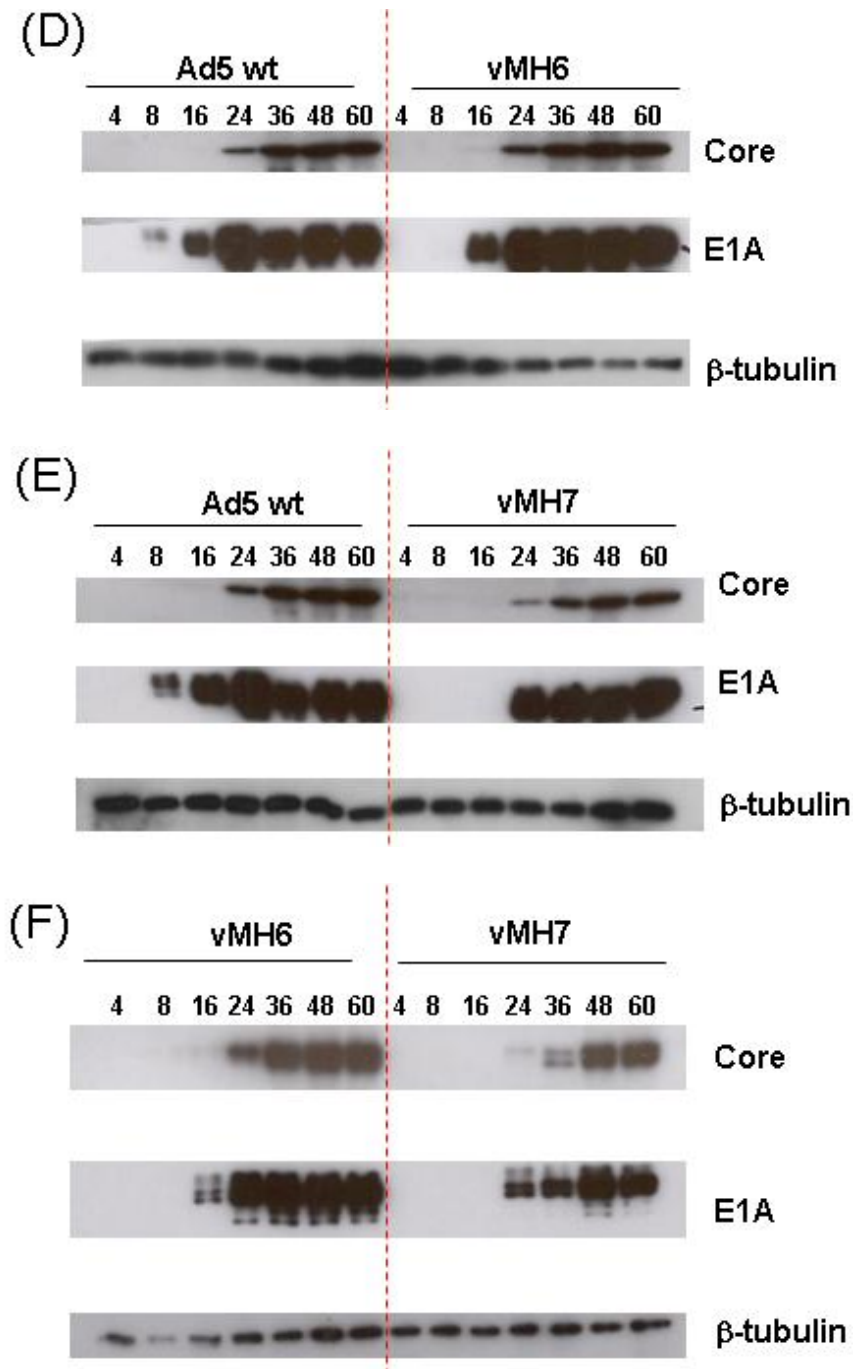


**Figure 4-7. Western blots for E1A expression with vMH vectors**

DU145 cells were seeded at  $1 \times 10^5$  cells per well in 24-well plates were infected with 10 PFU/cell of Ad5 wt or vMH vectors as described in section 2.4.8. Total protein was harvested from wells at 4 to 60 hours post infection and  $2.5 \mu\text{g}$  of each sample separated by SDS-PAGE and western blotted. Separate blots were performed for each vMH vector, each ran alongside Ad5 wt as an internal control. Blots were probed for E1A, Ad core and  $\beta$ -tubulin expression (loading control). An additional western was performed directly comparing vMH6 and vMH7 to verify the differential E1A expression observed.

Figure 4-7 shows compiled western blots for all vMH viruses alongside Ad5 wt. Ad5 wt E1A expression was just detectable 8 hours post infection and clearly detectable at 16 hours post infection. In comparison, with vMH2 E1A expression can clearly be observed at 8 hours post infection and ultimately rises to produce more E1A than Ad5 wt.

Both ICOVIR-5 based vectors vMH4 and vMH5, and the ICOVIR-7 based vector vMH6, show similar E1A expression profiles, with no E1A detectable until 16 hours post infection. However, all three vectors produced E1A levels equivalent to Ad5 wt by 24 hours post infection. In comparison, vMH7 did not produce a detectable level of E1A until 24 hours post infection, significantly later than observed with the other vMH vectors.

Core protein (protein V, part of the MLTU) was first detected with Ad5 wt at 24 hours post infection. With vMH2, 4, 5 and 6 it was first detectable at 24 hours post infection, and showed a similar level of expression to Ad5 wt. vMH7 also produced detectable core protein by 24 hours post infection, however it was markedly reduced compared to Ad5 wt.

The reduced E1A expression observed with vMH4, 5 and 6 compared to Ad5 wt is consistent with the reduced oncolytic activity observed with these vectors. Furthermore, the onset of protein V expression observed with vMH2, 4, 5 and 6 coincided with the start of eGFP expression with these vectors.

The ICOVIR-7 based vectors vMH6 and vMH7 have the E1A promoter replaced by the same ICOVIR-7 promoter and were therefore expected to produce very similar levels of E1A. The data in Figure 4-7(D) and (E) would suggest vMH7 produces lower amounts of E1A compared to vMH6. To confirm these results the experiment was repeated, directly comparing vMH6 and vMH7, as shown in Figure 4-7(F).

To further investigate whether the delayed and lower E1A expression observed was a result of reduced promoter activity, E1A RNA levels were investigated using rtQ-PCR. 24-well plates of DU145 cells were infected with 10 PFU/cell of Ad5 wt or vMH vectors. At 4, 8 and 16 hours post infection wells were harvested, total RNA extracted, and used to synthesise complete cDNA with random primers (as described in section 2.6.4 and 2.7.2, respectively). Q-PCR was performed on samples for the E1A RNA target and for 18S rRNA endogenous control, using the  $\Delta\Delta\text{CT}$  method as described in section 2.7.3, referenced to Ad5 wt 4 hours post infection.

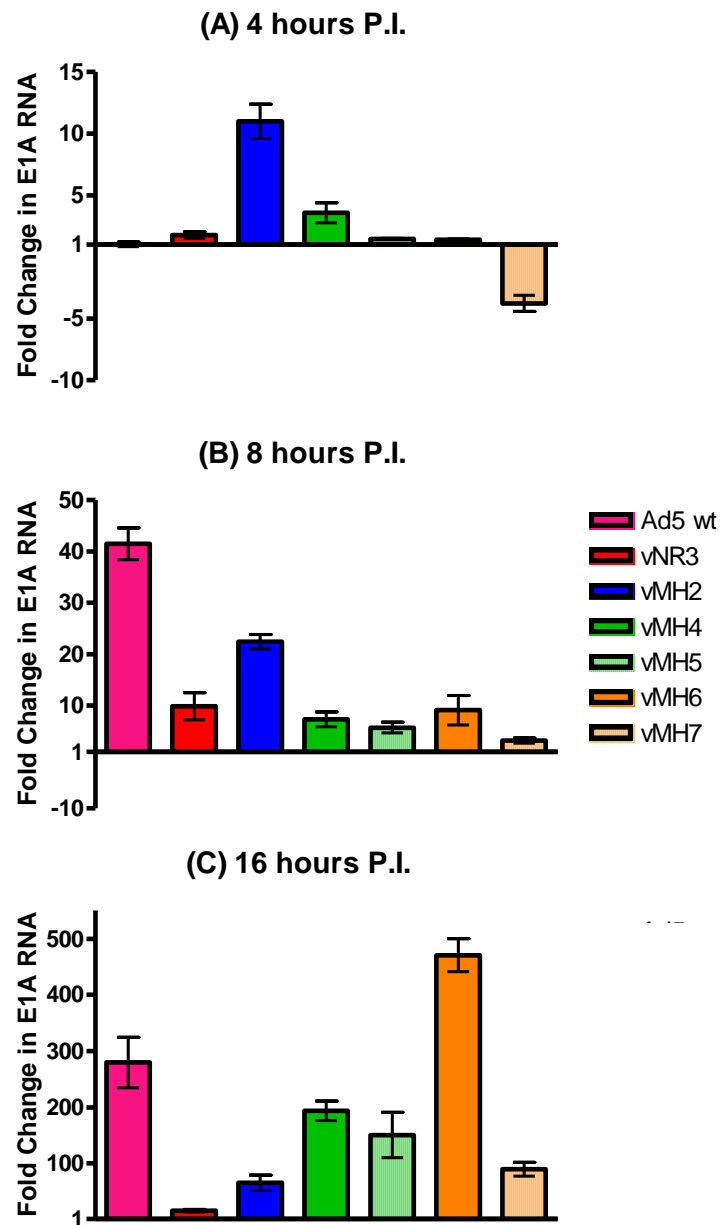


**Figure 4-8. rtQ-PCR for E1A expression with vMH vectors**

DU145 cells were seeded at  $1 \times 10^5$  cells per well in 24-well plates before being infected with 10 PFU/cell of Ad5 wt, vNR3 or vMH vectors as described in section 2.4.8. Samples were harvested at 4 (A), 8 (B) and 16 (C) hours post infection and total RNA extracted. 50ng of total RNA was used to synthesis cDNA using random primers. Q-PCR was performed in on cDNA for E1A RNA (target sample) and 18S rRNA (endogenous control) using the  $\Delta\Delta CT$  method for relative quantification. Bar graphs show E1A expression relative to Ad5 wt 4 hour post infection,  $\pm$  S.E.M. from triplicate Q-PCR reactions experiment (n=1).

Figure 4-8 shows that at 4 hours post infection vMH2 produced approximately 10-fold more E1A RNA than Ad5 wt, vMH4 expressed 3-fold more E1A RNA compared to Ad5 wt, and vMH5 and vMH6 expressed the same level as Ad5 wt. In contrast, vMH7 E1A RNA expression was approximately 4-fold lower than Ad5 wt.

At 8 hours post infection vMH5 and vMH6 E1A RNA expression were equivalent to vMH4, however vMH7 E1A RNA expression was still markedly lower. Finally at 16 hours post infection E1A RNA expression was high for all vMH viruses, with vMH6 showing the highest expression level.

#### **4.3.6 DNA Replication and Transgene Expression in HEK293 Cells**

Although vMH6 and vMH7 have E1A under control of the same E2F-1 promoter, vMH7 produces less E1A RNA and protein, which could explain the delay in virus DNA replication of approximately 8-10 hours, and the resultant delay in eGFP expression.

HEK293 cells express a high level of Ad5 E1A (greater than A549 cells with 10 PFU/cell of Ad5 wt at 24 hour post infection, Dr D. Onion, personal communication) and they should overcome any variation in E1A expression between vMH6 and vMH7. Therefore if the lower E1A expression observed with vMH7 is directly responsible for the delay in DNA replication and eGFP expression, the delay should not be observed in HEK293 cells. Therefore, vMH6 and vMH7 DNA replication was measured in HEK293 cells by Q-PCR. 24-well plates of HEK293 cells were infected with 100 VP/cell of vMH6, vMH7 or Ad5 wt (as described in section 2.4.8). At timepoints between 4 and 48 hours post infection duplicate wells were harvested and analysed as in section 4.3.4.

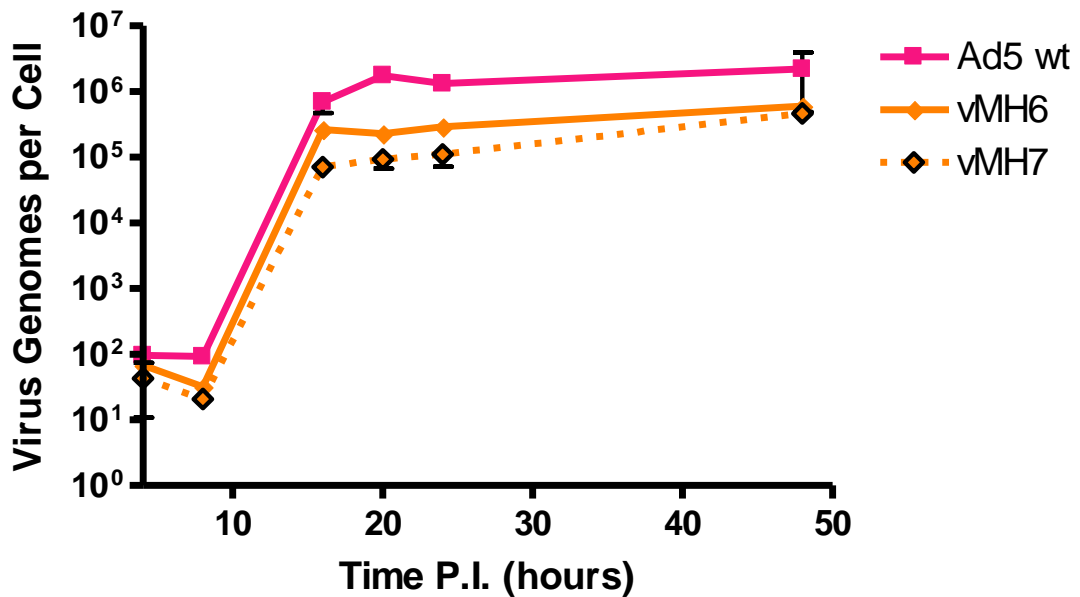


**Figure 4-9. DNA replication of vMH vectors in HEK293 cells**

HEK293 cells were seeded at  $1 \times 10^5$  cells per well in 24-well plates and duplicate wells were infected with Ad5 wt, vMH6 or vMH7 at 100 VP/cell as described in section 2.4.8. Duplicate wells were harvested at timepoints from 4 to 60 hours post infection, DNA extracted, and Q-PCR performed for viral genomes and cellular DNA. Virus genome copies were normalised to cellular DNA copies. Graph shows the mean of duplicate wells ( $n=1$ ),  $\pm$  S.D. (where no error bars are visible S.D. was  $<5\%$ ).

Figure 4-9 shows the virus DNA replication profile, normalised to cell DNA copies. The profiles of vMH6, vMH7 and Ad5 wt were all very similar, with essentially no difference between vMH6 and vMH7. vMH6 and vMH7 showed a  $1 \times 10^4$ -fold increase in genome copy number. In comparison Ad5 wt showed a  $2.5 \times 10^4$ -fold increase in genome copy number: this small difference may have been due to the 10-fold lower P:I ratio of Ad5 wt or the smaller genome size, or a possibly a minor detrimental effect of the eGFP insert.

To investigate eGFP expression HEK293 cells in 24-well plates were infected with 100 VP/cell of vMH2, vMH6, vMH7 or Ad-GFP, as described in section 2.4.8. At timepoints

between 0 and 48 hours post infection duplicate wells were harvested, fixed and analysed by flow cytometry for percentage eGFP positive cells (Figure 4-10 (A)). For the eGFP positive population the fold increase in MFI over uninfected cells was calculated (Figure 4-10 (B)).

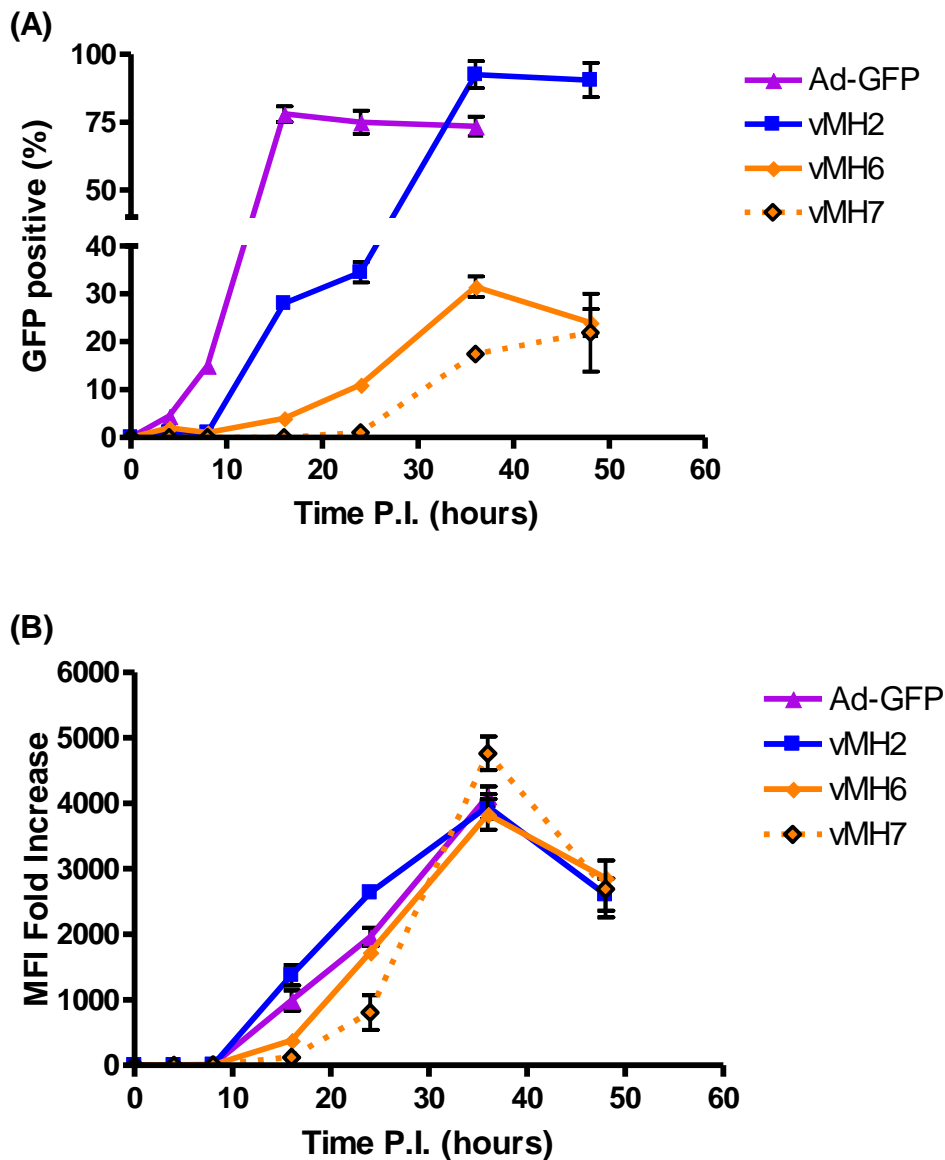


**Figure 4-10. vMH eGFP expression in HEK293 cells**

HEK293 cells were seeded at  $1 \times 10^5$  cells per well in 24-well plates before being infected with 100 VP/cell of Ad-GFP, vMH2, vMH6 or vMH7 as described in 2.4.8. Duplicate wells were harvested at timepoints from 4 to 60 hours post infection, washed, fixed and eGFP expression analysed by flow cytometry. The mean percentage eGFP positive from duplicate wells was calculated (A) and of the fold increase in MFI of the eGFP positive population calculated over mock infected (B). Graphs show average from duplicate wells ( $n=2$ ),  $\pm$  S.D. (where no error bars are visible S.D. was  $<5\%$ ).

For Ad-GFP, expression was first detected 4 hours post infection and showed a maximal transduction of 75% by 12 hours post infection. With vMH2, vMH6 and vMH7 no eGFP expression was detected until 16 hours post infection. All vMH vectors showed maximal transduction by approximately 36 hours post infection; with the maximum number of cells transduced reflecting the variation in P:I ratio (i.e. in comparison to vMH6 and vMH7, vMH2 had a 4-fold higher maximal transduction and a 4-fold lower P:I ratio). vMH7 also had a slightly slower rate of increase in percentage positive compared to vMH6, which itself was slightly slower than vMH2. However all vMH vectors reached a similar level of fluorescent intensity, peaking at 36 hours post infection.

#### **4.3.7 Cytotoxicity of vMH Vectors in HEK293 Cells**

Results in section 4.3.5 demonstrated that replacement of the E1A promoter with the insulated E2F-1 promoter from ICOVIR-5 or ICOVIR-7 results in lower E1A RNA and protein expression. Reduced E1A expression could in turn lead to the reduced lytic activity observed with these vectors in prostate cancer cell lines. However replacement of the natural E1A promoter also results in an increase in viral genome size: vMH2 is 102.07% of the Ad5 wt genome, vMH4 with the ICOVIR-5 promoter is 104.83% and vMH6, with the ICOVIR-7 promoter is 105.18%. This could also have a detrimental effect on virus packaging, resulting in reduced infectious virus yields and subsequently reduced lytic activity. It was therefore decided to investigate virus induced cytotoxicity in HEK293 cells. HEK293 cells express a high level of E1A, compensating for the range of E1A expression observed with vMH vectors, allowing assessment of vector genome size on cytotoxicity. 96-well plates of HEK293 cells were infected with a serial dilution of Ad5 wt, vNR3 or vMH vectors from  $1 \times 10^{-4}$  to  $1 \times 10^2$  PFU/cell (as described in section 2.4.8). Cell survival

was measured 5 days post infection by AP assay, data normalised, dose response curves fitted (Figure 4-11) and EC50 values calculated (Table 4-2).

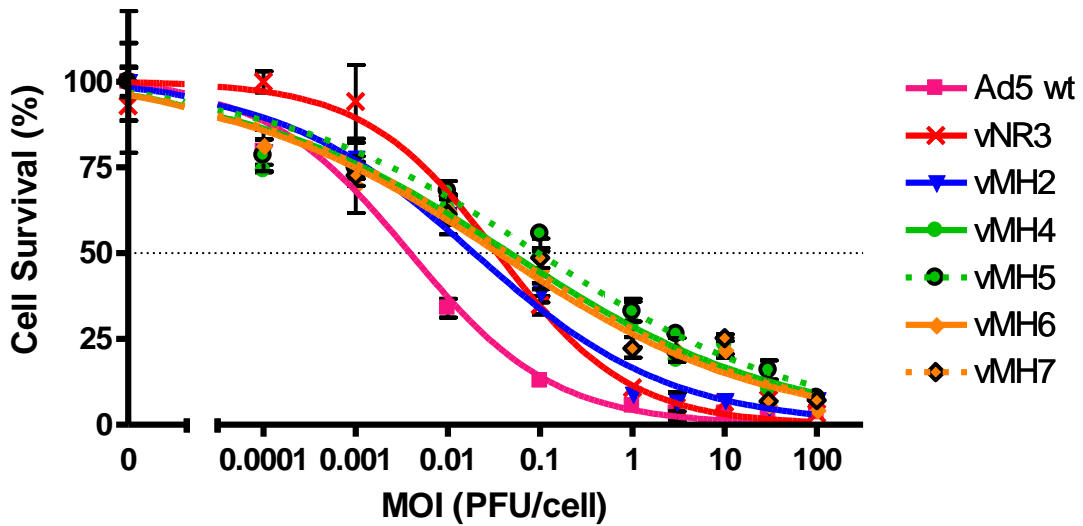


**Figure 4-11. Dose response curves for vMH cytotoxicity in HEK293 cells**

HEK293 were seeded in 96-well plates at  $3 \times 10^4$  cells per well. Triplicate wells were infected with a serial dilution of Ad5 wt, vNR3 or vMH vectors as described in section 2.4.8. Cell survival was measured 5 days post infection by AP assay and normalised to mock infected cells (100% survival) and empty wells (0% cell survival). Plots show mean cell survival from triplicate wells ( $n=1$ ),  $\pm$  S.D. (where no error bars are visible S.D. was  $<5\%$ ), and fitted sigmoid dose response curves. Dose response curves were used to calculate EC50 values.

Virus	HEK293 EC50 (95% C.I.) PFU/cell
Ad5 wt	0.00404 (0.00713 - 0.0110)
vNR3	0.0343 (0.0254 - 0.0462)
vMH2	0.0193 (0.0130 - 0.0289)
vMH4	0.0433 (0.0271 - 0.0692)
vMH5	0.0917 (0.0531 - 0.159)
vMH6	0.0354 (0.0225 - 0.0556)
vMH7	0.0449 (0.0227 - 0.0737)

**Table 4-2. EC50 values with 95% C.I. (PFU/cell) in HEK293 cells**

No significant difference was observed in the cytotoxicity for all vMH vectors in HEK293 cells, all of which had similar EC50 values with overlapping 95% confidence intervals. However, it is worth noting that vMH2, which has the smallest genome of all vMH vectors, did show the lowest EC50 value. Ad5 wt was significantly more cytotoxic than all vMH vectors, with 3- to 10-fold lower EC50 values. This would suggest the additional genome size resulting from replacement of the wt E1A promoter with the ICOVIR-5 or ICOVIR-7 promoter may cause a minor reduction in cytotoxicity. However, in comparison to Ad5 wt, all vMH vectors demonstrated lower EC50 values, potentially indicating the introduction of transgene may have had a detrimental effect on cytotoxicity. However, the difference was only small, and it was not clear whether this is specifically due to the position at which the transgene was inserted, or due to the increase in genome size conferred by transgene insertion.

#### **4.3.8 Sequencing the ICOVIR-7 Promoter in vMH6 and vMH7**

vMH6 and vMH7 were created by homologous recombination in HEK293 with the same left end plasmid, pICOVIR-7, and pMH008 or pMH009, respectively (as described in section 3.5). Both viruses were shown to be free of contaminating wt E1A sequences by PCR, and had no evidence of the wt E1A promoter by restriction enzyme profiling. However vMH7 produced significantly lower levels of E1A RNA compared to vMH6. It was possible a mutation had occurred in the ICOVIR-7 promoter sequence in either vMH6 or vMH7, which would result in differential RNA expression. It was therefore decided to sequence the E1A promoters from vMH6 and vMH7 banded virus stocks, plus the pICOVIR-7 plasmid stock used for virus recovery.

The entire E1A promoter region was amplified by PCR using KOD Taq (for increased fidelity) with primers MHp018 and MHp019 (see Table 2-1 for description of primers). The

amplified 1.5kb promoter region was gel purified and sequenced as described in section 2.2.9, with primers MHP017-024.

vMH6 and vMH7 possess an ICOVIR-7 promoter with identical sequence (see appendix 2.) and also identical to the sequence found in pICOVIR-7. Sequencing results do however show that both viruses and the original plasmid contain base differences at 5 positions in comparison to the expected plasmid sequence (provided by Dr R. Alemany) (differences are annotated in appendix 2). These changes were at the cloning junctions between the promoter components, and it was therefore likely they were accidentally introduced during the original cloning of pICOVIR-7 by our collaborators. It is possible but unlikely that these mutations would have an effect on promoter activity. Furthermore, there was no difference in the ICOVIR-7 promoter region of vMH6 and vMH7 and this deviation from the expected sequence did not explain the differential E1A RNA expression observed between the two vectors.

#### **4.3.9 Lytic Timecourse in DU145**

Figure 4-2 indicated that there was no significant difference in the cytotoxicity between vMH6 and vMH7 at 5 days post infection. However, this data was a single timepoint (5 days post infection), and it is possible vMH6 and vMH7 have different timecourses of cell lysis. To investigate this possibility, timecourse experiments were undertaken to measure the cell survival, up to 7 days post infection. DU145 cells in 96-well plates were infected with vMH2, vMH6, vMH7 and Ad5 wt at 30 and 100 PFU/cell, as described in section 2.4.8. On days 1-7 post infection cell survival was measured from triplicate wells by AP assay. The data was normalised, and used to plot survival timecourses, shown in Figure 4-12.

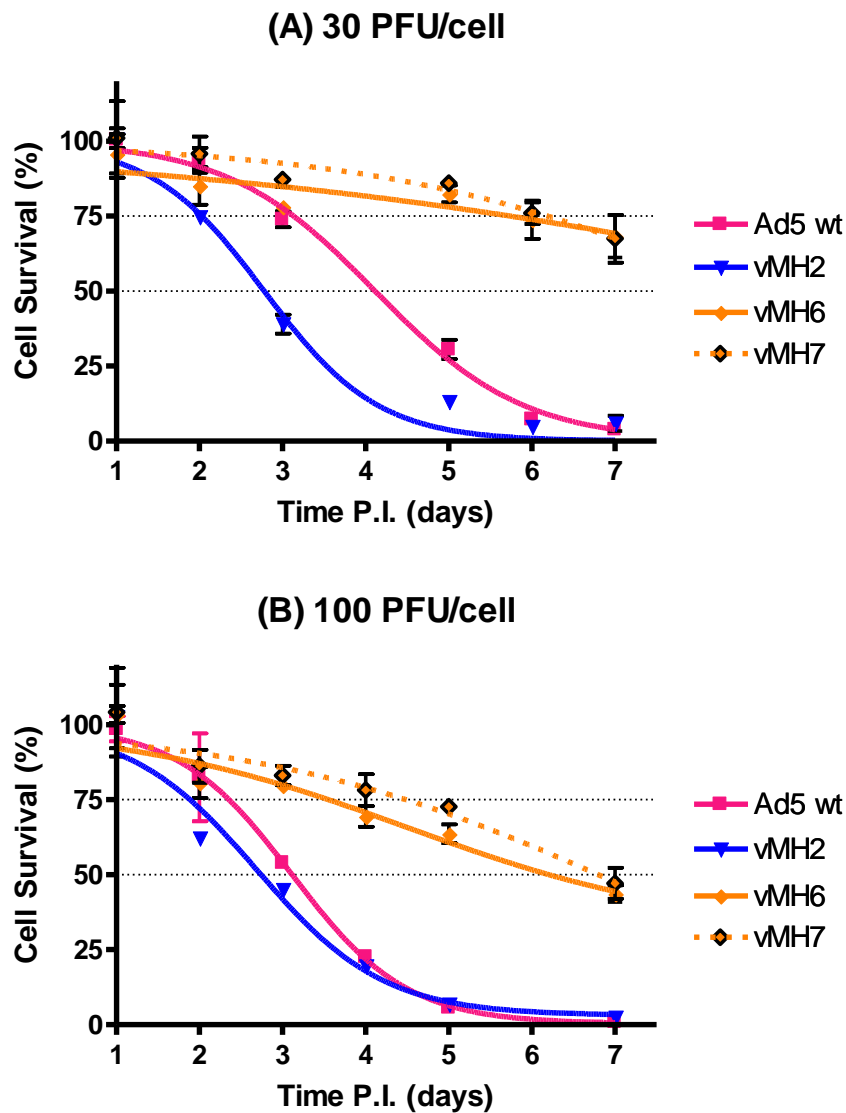


**Figure 4-12. Lytic timecourse for vMH vectors**

DU145 cells were seeded in 96-well plates at  $3 \times 10^4$  cells per well before being infected with 30 (A) and 100 (B) PFU/cell of Ad5 wt, vMH2, vMH6 or vMH7 as described in section 2.4.8. Cell survival was measured daily up to 7 days post infection by AP assay and the data normalised on each day to mock infected cells (100% survival) and empty wells (0% survival). Plots show mean cell survival from triplicate wells ( $n=1$ ),  $\pm$  S.D. (where no error bars are visible S.D. was  $<5\%$ ), with fitted cell survival curves.

At both MOI, vMH2 showed the most rapid and complete cytotoxicity, reaching 50% cell death approximately one day earlier than Ad5 wt at 30 PFU/cell, and 12 hours earlier than

Ad5 wt at 100 PFU/cell. Both vMH6 and vMH7 showed little cytotoxicity at 30 PFU/cell, reaching approximately 25% cell death by 6 days post infection. At 100 PFU/cell both vMH6 and vMH7 showed 50% cell death by 7 days post infection, however there was a very slight difference in the rate of cell death, with vMH7 taking approximately one day longer to reach 25% cell death. This suggests vMH6 may have a slightly greater rate of cell lysis compared to vMH7, however the difference at these MOIs was only minor. There was no difference in the P:I ratios of vMH6 and vMH7, both of which were approximately 100.

#### **4.3.10 Effect of Transgene Insertion**

##### **4.3.10.1 Comparison of vMH6 and vMH7 with vICOVIR-7**

The vMH vectors incorporate the eGFP transgene downstream of fibre, for expression from the adenovirus MLP. Whereas this was not predicted to have a direct detrimental effect on virus cytotoxicity, it does increase the virus genome size, which could result in reduced packaging efficiency, lower infectious virus yields and reduced cytotoxicity. While this work was in progress Dr R. Alemany constructed vICOVIR-7, an ICOVIR-7 based oncolytic Ad vector (i.e. E1A promoter replaced with the ICOVIR-7 promoter and the E1A CR2  $\Delta$ 24 deletion) with an RGD-retargeted fibre, but lacking a transgene insertion. This gave the opportunity to compare vMH6 and vMH7 with vICOVIR-7, which should have the same oncolytic 'backbone' but lacking the eGFP insertion.

##### **4.3.10.1.1 Cytotoxicity of vICOVIR-7 vs vMH6 and vMH7**

Approximately 100 $\mu$ l of CsCl banded vICOVIR-7 was kindly donated by Dr R. Alemany (2.4x10<sup>11</sup> VP/ml, 1.1x10<sup>10</sup> PFU/ml, P:I ratio = 21.8). This was initially used to investigate oncolytic activity in two cell lines; DU145 and A549-RA. DU145 cells were used for comparison with previous results with vMH vectors and A549-RA cells are A549 cells

from Dr. R. Alemany and were used for comparison with Dr R. Alemany's observations. 96-well plates of DU145 and A549-RA cells were infected with serial dilutions of vMH6, vMH7, vICOVIR-7, Ad5 wt or Ad-GFP from  $1 \times 10^{-1}$  to  $1 \times 10^3$  PFU/cell (as described in section 2.4.8). Cell survival was measured 5 days post infection by AP assay, dose response curves plotted (Figure 4-13) and EC50 values calculated (Table 4-3).

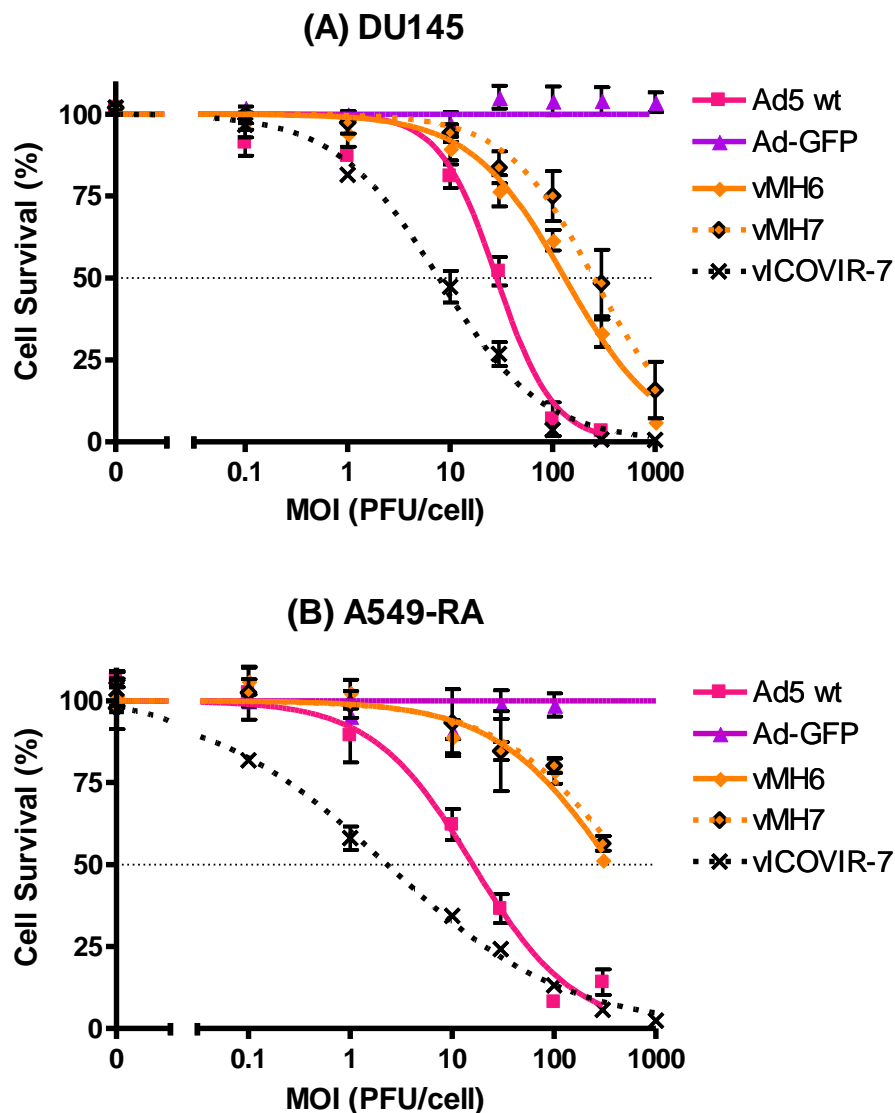


**Figure 4-13. Dose response curves for vMH6 and vMH7 vs vICOVIR-7 cytotoxicity**  
 DU145 (A) and A549-RA (B) cells seeded in 96-well plates at  $3 \times 10^4$  cells per well were infected with a serial dilution of Ad5 wt, Ad-GFP, vMH2, vMH6, vMH7 or vICOVIR-7 as described in section 2.4.8. Cell survival was measured 5 days post infection by AP assay and the data normalised to mock infected cells (100% survival) and empty wells (0% survival). Plots show mean cell survival from triplicate wells ( $n=3$ ),  $\pm$  S.D. (where no error bars are visible S.D. was  $<5\%$ ), with fitted sigmoid dose response curves. Dose response curves were used to calculate EC<sub>50</sub> values.

<b>Virus</b>	<b>DU145 EC50 (95% C.I.) PFU/cell</b>	<b>A549-RA EC50 (95% C.I.) PFU/cell</b>
<b>Ad5 wt</b>	28.6 (11.2 - 73.1)	16.0 (12.21 - 20.94)
<b>vMH6</b>	132 (42.5 - 412)	369 (256 - 534)
<b>vMH7</b>	253 (82.5 - 779)	507 (253 - 1010)
<b>vICOVIR-7</b>	7.78 (1.79 - 33.9)	2.23 (1.87 - 2.83)

**Table 4-3. EC50 values with 95% C.I. for vMH6 and vMH7 vs vICOVIR-7**

vICOVIR-7 was the most cytotoxic vector in both cell lines, with a 4- to 5-fold increase in lytic activity of Ad5 wt. vMH6 and vMH7 demonstrated a 10-fold reduction in cytotoxicity over Ad5 wt in DU145 cells (as was previously observed in section 4.3.2), and a 20- to 30-fold reduction in cytotoxicity in A549-RA cells. However, vICOVIR-7 is approximately 20- to 30-fold more lytic than vMH6 and vMH7 in DU145 cells, and over 100-fold more cytotoxic in A549-RA cells. No difference in the pattern of cytotoxicity between all the vectors was observed in DU145 cell and A549-RA cells, demonstrating the reduction in cytotoxicity observed with vMH6 and vMH7 was not prostate cancer cell specific.

#### **4.3.10.1.2 Restriction Profiling and PCR Screening of vICOVIR-7**

The banded vICOVIR-7 virus was passaged once into 20x150cm<sup>2</sup> flasks of A549 cells and CsCl banded to be used for restriction profiling. DNA was extracted from 200µl of the new banded vICOVIR-7 virus stock, termed vICOVIR-7MHB1, and 200µl of Ad5 wt for direct comparison (as described in 2.6.2) and digested with HindIII, BglII and KpnI, which distinguishes between the wt E1A promoter and the ICOVIR-7 promoter. The restriction enzyme profile of each virus is shown in Figure 4-14 (A), and the predicted restriction enzyme profile is shown in Figure 4-14 (B).

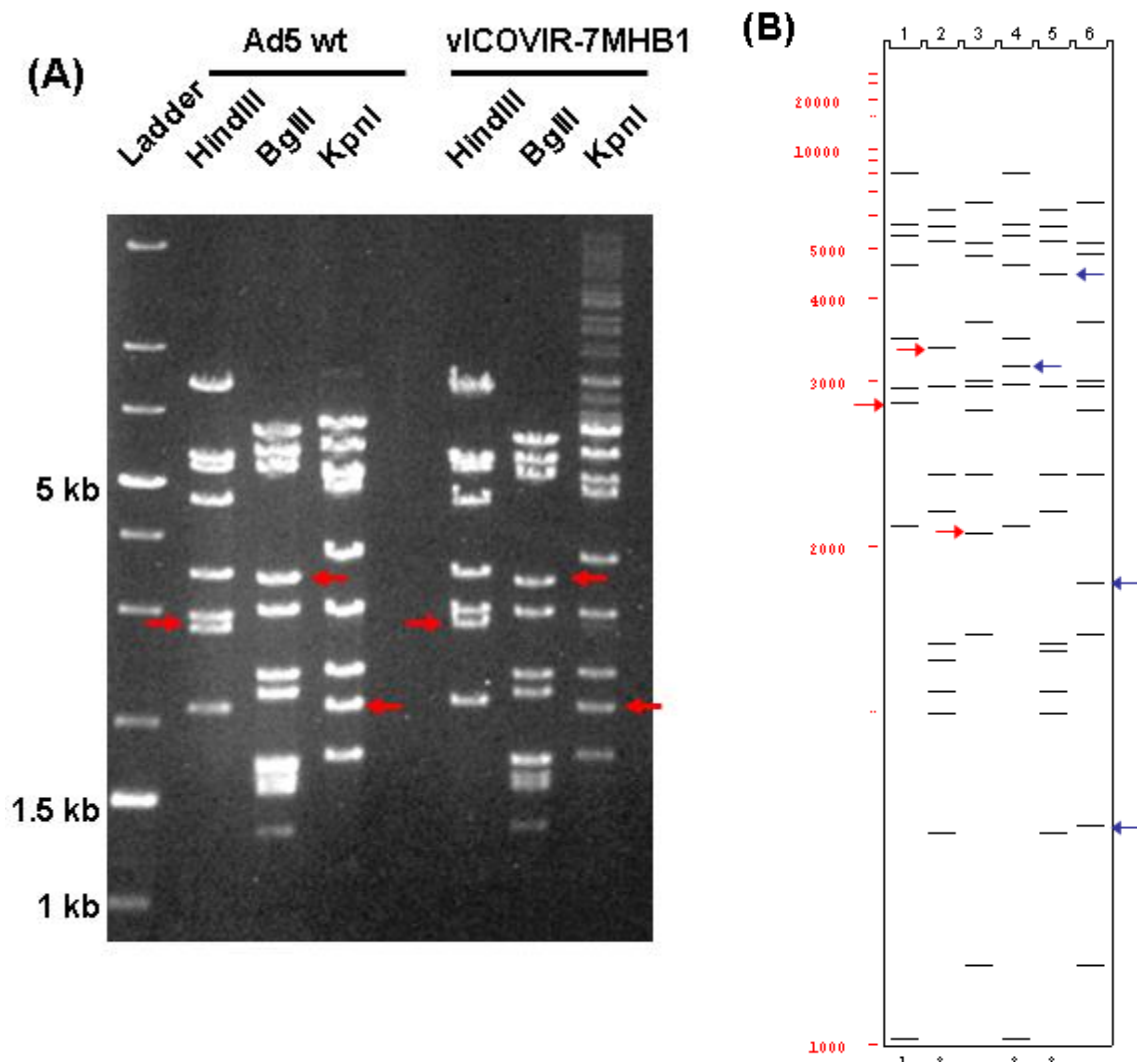


**Figure 4-14. Restriction enzyme profile of Ad5 wt and vICOVIR-7**

DNA was extracted from 200µl of banded Ad5 wt and vICOVIR-7MHB1 as described in section 2.6.2 and digested with HindIII, BglIII and KpnI using excess enzyme for 16 hours. Digested samples were analysed by gel electrophoresis (A) and compared to the predicted restriction enzyme profile (B). Red arrows mark the bands diagnostic of Ad5 wt left end and the blue arrows mark the bands diagnostic of vICOVIR-7 left end.

For vICOVIR-7MHB1 we predict; loss of the Ad5 wt HindIII 2.8kb band and appearance of 750bp and 3.1kb bands; increase of the Ad5 wt BglIII 3.3kb band to 4.4kb; loss of the Ad5 wt KpnI 2kb band and appearance of 1.3kb and 1.8kb bands. Figure 4-14 shows that the passaged and banded vICOVIR-7MHB1 virus had a restriction enzyme profile almost

indistinguishable from Ad5 wt. However there was slight differences between the HindIII digest at approximately 3kb, with vICOVIR-7MHB1 possibly showing slightly larger bands than Ad5 wt. Additional large bands (>5kb) could be observed with the KpnI digested vICOVIR-7MHB1, possibly due to an incomplete digestion, despite use of excess enzyme at optimal conditions for 36 hours.

The restriction pattern in Figure 4-14 suggested vICOVIR-7MHB1 was predominately a virus which was almost indistinguishable from Ad5 wt. To investigate this further the banded vICOVIR-7MHB1 and the original vICOVIR-7 stock were subject to PCR analysis using primers designed within the E1A CR2  $\Delta$ 24 deletion (primer PS1368A), spanning the E1A CR2  $\Delta$ 24 deletion (primer PS1368B), within the DM-1 insulator element found only in the ICOVIR-7 promoter (primer MHp022) or just downstream of the left ITR (MHp019). The same reverse primer located just downstream of the E1A ORF (primer PS1368C) was used with each forward primer. These PCR reactions allow discrimination between the E1A CR2  $\Delta$ 24 deletion and wt E1A, and between the ICOVIR-7 promoter and the wt E1A promoter. A schematic of primer layout can be found in Figure 4-15 below, along with a table of predicted band sizes in Table 4-4.

Banded vMH7 and pICOVIR-7 were also analysed as control samples. PCR was carried out as described in section 2.2.8, with  $10^8$  VP/reaction for 35 cycles and products analysed by gel electrophoresis, shown in Figure 4-16.

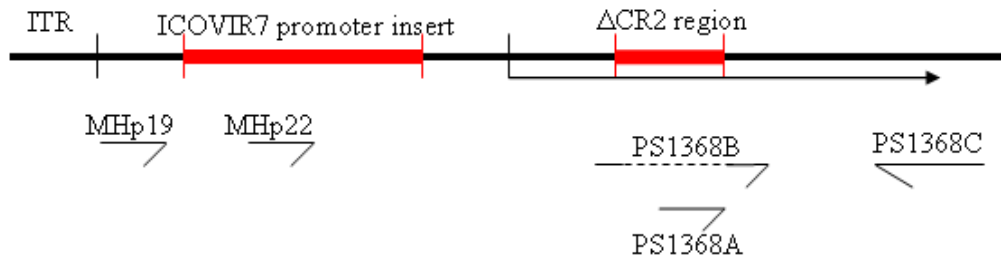


**Figure 4-15. Schematic of PCR primers covering E1A and its promoter region**

Schematic layout of the PCR primers used to screen for the E1A CR2  $\Delta$ 24 deletion and the ICOVIR-7 promoter. See text for description of the primers. Details of the primers can be found in Table 2-1.

Forward Primer	Reverse Primer	Band with vICOVIR-7	Band with Ad5 wt
PS1368A	PS1368C	No Band	636bp
PS1368B	PS1368C	636bp	636bp (misprime)
MHP19	PS1368C	2.4kb	1.3kb
MHP22	PS1368C	2kb	No Band

**Table 4-4. Predicted PCR bands with E1A screening primes**

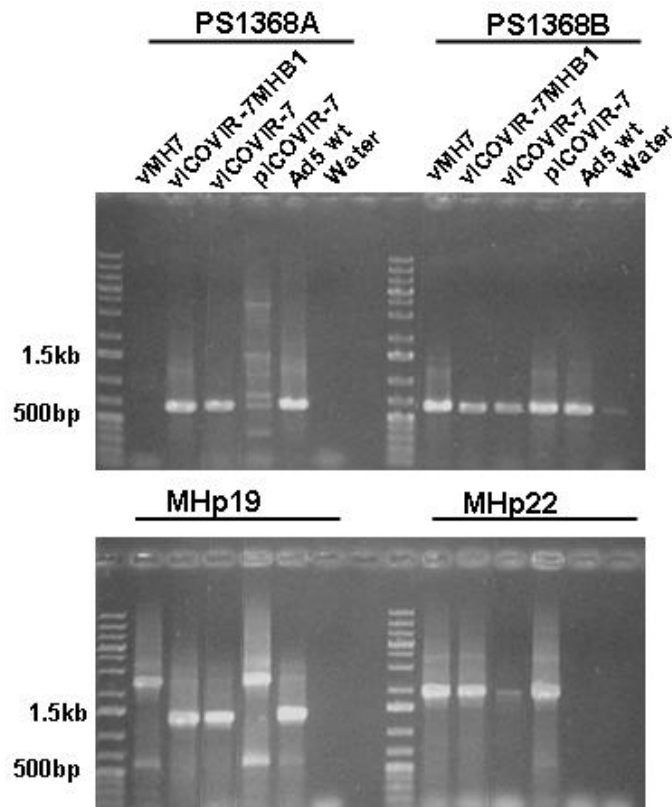


**Figure 4-16. E1A PCR screening of vICOVIR-7**

DNA was extracted from banded vMH7, vICOVIR-7MHB1, vICOVIR-7 and Ad5 wt and screened for contaminating wt E1A sequences, along with pICOVIR-7 and water for

controls. Four reactions were setup using forward primers PS1369A, vPS1368B, MHp19 and MHp22 all with reverse primer PS1368C. A schematic of primer locations can be found in Figure 4-15 and predicted bands in Table 4-4. Reactions were setup using GoTaq polymerase in a final volume of 50 $\mu$ l and run for 40 cycles in a thermal cycler (as described in section 2.2.8 ). 10 $\mu$ l of each reaction were analysed by agarose gel electrophoresis.

With primer PS1368A we only predict to see a band with wt E1A, as this primer is located within the CR2  $\Delta$ 24 deletion. As expected no band was observed with vMH7. Clear bands consistent with the 636bp expected from wt E1A can be observed in both vICOVIR-7 and vICOVIR-7MHB1 indicating both of these virus stocks are contaminated with wt E1A sequences. No band was expected with the pICOVIR-7 template, however at least 4 faint bands between 300 and 4000bp were observed. These bands could not be matched with any predicted bands, and are possibility due to mispriming and because the template used was supercoiled, resulting in aberrant PCR products A clear band of correct size was observed with Ad5 wt positive control.

Primer PS1368B spans the E1A CR2  $\Delta$ 24 deletion and therefore is predicted to detect E1A CR2  $\Delta$ 24 but not wt E1A. As predicted, clear bands can be observed with vMH7, vICOVIR-7, vICOVIR-7MHB1 and the pICOVIR-7 positive control, demonstrating these virus stocks contain the E1A CR2  $\Delta$ 24 deletion. A band was also observed with Ad5 wt and PS1368B. Although this primer was intended not to prime from the wt E1A sequence, previous observations have also shown that this can detect wt E1A, due to the short region of homology with the wt E1A sequence either side of the  $\Delta$ 24 deletion (see section 3.5). This band was not observed in subsequent experiments using PS1368B with Ad5 wt for touchdown PCR, further suggesting this band product is due to mispriming.

Primer MHP19 is located downstream of the left ITR and detects both the wt E1A promoter and the ICOVIR-7 promoter to produce bands of 1.3kb and 2.4kb, respectively. As expected, bands of approximately 2.4kb were observed with vMH7 and the pICOVIR-7 positive control, demonstrating that vMH7 contains the ICOVIR-7 promoter. vICOVIR-7 and vICOVIR-7MHB1 had a predominant band of approximately 1.3kb, demonstrating that both of these virus stocks are heavily contaminated with a virus lacking the full ICOVIR-7 promoter sequence. However, this band appeared slightly smaller than the Ad5 wt band, suggesting this promoter region is not identical to the wt E1A promoter region. The minor band at approximately 500bp with vMH7 and pICOVIR-7 cannot be attributed to any predicted product.

Primer MHP22 is located within the DM-1 insulator element and therefore should only detect the ICOVIR-7 promoter to produce a 2kb band. A band of 2kb was observed with vMH7, demonstrating the presence of the ICOVIR-7 promoter sequence. Bands of identical size were also observed with vICOVIR-7 and vICOVIR-7MHB1, suggesting both of these stocks also contains a virus with the ICOVIR-7 promoter sequence. As expected a clear 2kb band was observed with the pICOVIR-7 positive control, and no band was observed with Ad5 wt negative control.

Together these results indicate that both vICOVIR-7 and vICOVIR-7MHB1 predominately contained genomes which do not have the E1A CR2  $\Delta$ 24 deletion, and also predominately contained a promoter region much shorter than the ICOVIR-7 promoter. However, the ICOVIR-7 promoter was still detected within these stocks. This data, in addition to the restriction enzyme profile, suggested that both the vICOVIR-7MHB1 and the original vICOVIR-7 stock from Dr R. Alemany were heavily contaminated with a virus similar to

Ad5 wt, but still contain some ICOVIR-7 promoter-containing virus. However, from this data it was not possible to identify the source or identity of the contaminating virus.

The vICOVIR-7 vectors from Dr R. Alemany incorporate the RGD-4C insertion into the fibre HI loop, which introduces an extra SacII restriction site. Introduction of this site cleaves a 6.6kb SacII band from the Ad5 wt sequence into two 3.3kb bands. Furthermore, replacement of the wt E1A promoter with the ICOVIR-7 promoter increases a 3.2kb SacII band up to approximately 4.5kb. vICOVIR-7MHB1 was therefore digested with SacII to investigate both the presence of the wt E1A region, and the presence of the RGD-4C fibre. For an ICOVIR-7 left end and a wt fibre we predict a 4.5kb band and a 6.6kb band, for ICOVIR-7 left end and RGD-retargeted fibre we predict a 4.5kb band and a 3.3kb doublet, for a wt left end and a wt fibre we predict a 3.2kb band and a 6.6kb band and finally for a wt left end and RGD-retargeted fibre we predict a triplet at approximately 3.3kb.

As shown in Figure 4-17, the last of these potential band combinations was observed.

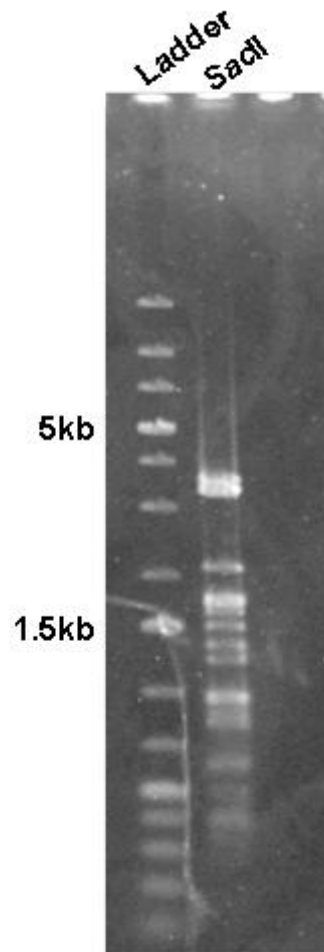


**Figure 4-17. SacII restriction enzyme profile of vICOVIR-7MHB1**

DNA was extracted from 100µl of banded Ad5 wt and vICOVIR-7MHB1 as described in section 2.6.2 and digested with SacII for 16 hours. Digested samples were analysed by gel electrophoresis.

Together with the previous evidence, this suggests vICOVIR-7 and vICOVIR-7MHB1 are highly contaminated with an adenovirus with a wildtype left end and an RGD-retargeted fibre. No virus of this composition had previously been handled in our laboratory.

**4.3.10.2 Cytotoxicity of vPS1393 vs vMH Vectors**

Towards the end of this work The University of Birmingham SCS-GT group constructed vPS1393, an oncolytic Ad vector with the ICOVIR-7 promoter (poly(A) site, DM-1

insulator and triple E2F promoter), E1A CR2  $\Delta$ 24 deletion but with a wt fibre protein, and no transgene. Thus vPS1393 was similar to vMH6, but without the eGFP transgene insertion. This vector was used to further investigate the effect of eGFP transgene insertion on virus induced cytotoxicity.

The virus vPS1393 has been rescued in A549 cells, double plaque purified on DU145 cells, screened by PCR and confirmed free of contaminating wt E1A sequences (Dr P. Searle, personal communication). Following confirmation of the E1A status and restriction profile, I passaged a p2 seed stock once in 20x150cm<sup>2</sup> flasks of A549 cells to produce a p3 seed stock, which was used to make a vPS1393 banded virus stock. Virus particle concentration was determined by PicoGreen assay and infectious virus counted by plaque assay on DU145 cells ( $5.92 \times 10^{11}$  VP/ml,  $2.15 \times 10^{10}$  PFU/ml, P:I ratio= 27.5, Size= 103.04% of Ad5).

Experiments were undertaken to examine the lytic activity of vPS1393 compared to vMH vectors in cancer cell lines. 96-well plates of DU145 and 22RV1 cells were infected with serial dilutions of vMH vectors, Ad5 wt, vPS1393 or Ad-GFP from  $1 \times 10^{-1}$  to  $1 \times 10^3$  PFU/cell. Cell survival was measured 5 days post infection by AP assay, dose response curves plotted and EC50 values calculated. Figure 4-18 shows the dose response curves for Ad5 wt, vMH6, vMH7 and vPS1393, and the EC50 values for all viruses can be found in Table 4-5.

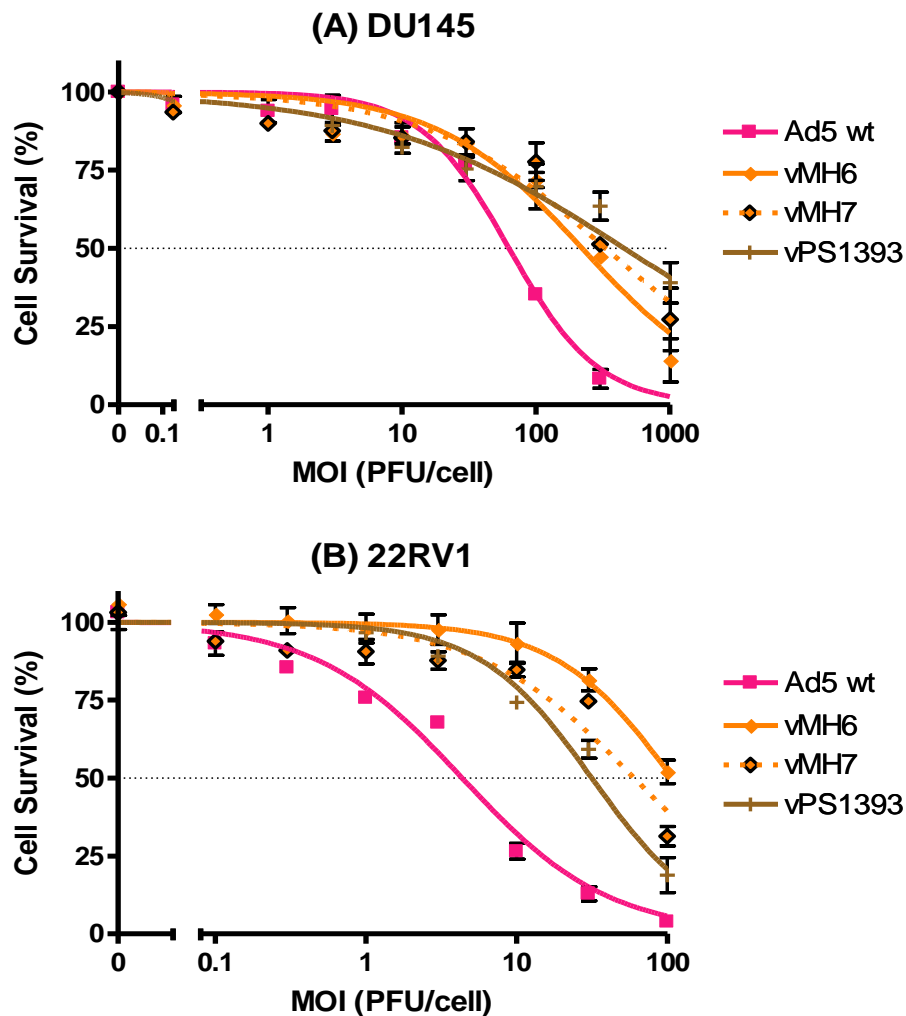


**Figure 4-18. Dose response curves for vPS1393 cytotoxicity**

DU145 (A) and 22RV1 (B) cells were seeded in 96-well plates at  $3 \times 10^4$  cells per well before triplicate wells were infected with a serial dilution of Ad5 wt, vMH vectors, or vPS1393 as described in section 2.4.8. Cell survival was measured 5 days post infection by AP assay and the data normalised to mock infected cells (100% survival) and empty wells (0% survival). Plots show mean cell survival from triplicate wells ( $n=1$ ),  $\pm$  S.D. (where no error bars are visible S.D. was  $<5\%$ ), with fitted sigmoid dose response curves. Dose response curves were used to calculate EC50 values.

<b>Virus</b>	<b>DU145 EC50 (95% C.I.) PFU/cell</b>	<b>22RV1 EC50 (95% C.I.) PFU/cell</b>
<b>Ad5 wt</b>	62.9 (55.0 - 71.9)	4.42 (3.68 - 5.30)
<b>vMH2</b>	15.7 (14.2 - 17.3)	1.42 (1.28 - 1.57)
<b>vMH4</b>	62.8 (53.5 - 73.6)	23.1 (20.1 - 26.6)
<b>vMH5</b>	34.8 (28.2 - 42.9)	30.8 (25.6 - 37.1)
<b>vMH6</b>	250 (190 - 320)	109 (86.4 - 138)
<b>vMH7</b>	331 (231 - 475)	60.2 (42.2 - 90.0)
<b>vPS1393</b>	356 (274 - 463)	31.5 (26.7 - 37.3)

**Table 4-5. EC50 values with 95% C.I. (PFU/cell) for vMH vectors and vPS1393**

There was no notable difference in the cytotoxicity of vMH6, vMH7 and vPS1393 in DU145 cells, all of which showed a 5- to 8-fold higher EC50 compared to Ad5 wt and have overlapping 95% confidence intervals. In 22RV1 cells both vMH6 and vMH7 showed similar cytotoxicities, with EC50 values 15- to 20-fold higher than Ad5 wt. In comparison, vPS1393 had a 5- to 10-fold lower cytotoxicity compared to Ad5 wt and showed a 2- to 3-fold increase in cytotoxicity compared to vMH6 and vMH7.

To further analyse the effect of eGFP introduction, the lytic activity of these vectors was assessed in HEK293 cells, where any variation in E1A expression between vectors will be eliminated, allowing a more direct comparison of the effect of transgene insertion. HEK293 cells in 96-well plates were infected with a serial dilution for vMH vectors, Ad5wt and vPS1393 from  $1 \times 10^{-5}$  to  $1 \times 10^1$  PFU/cell (this range of MOI was used based on previous observations in Figure 4-11). Cell survival was measured 5 days post infection, data normalised, dose response curves plotted (Figure 4-19) and EC50 values calculated (Table 4-6).

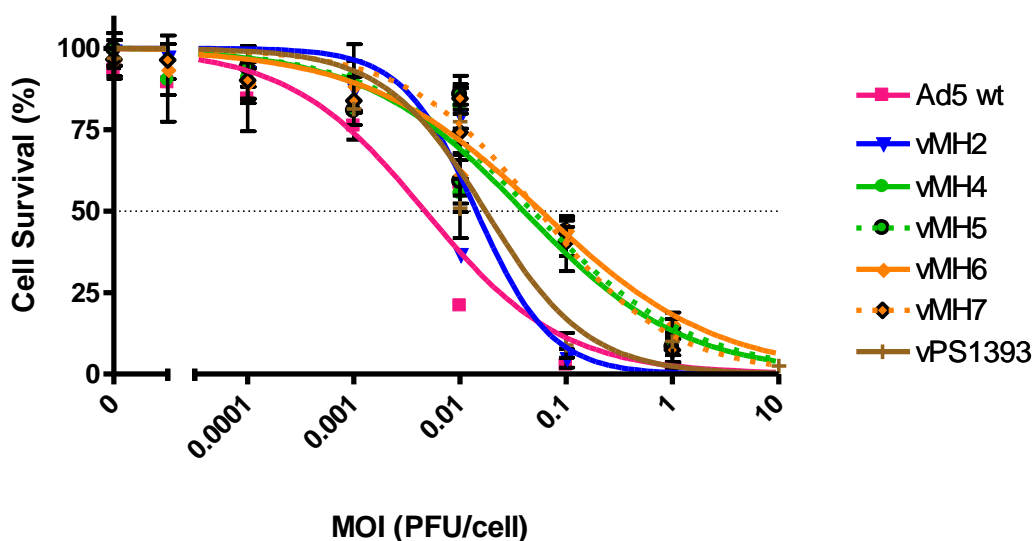


**Figure 4-19. Dose response curves for vPS1393 cytotoxicity in HEK293 cells**

HEK293 cells were seeded in 96-well plates at  $3 \times 10^4$  cells per well before triplicate wells were infected with a serial dilution of Ad5 wt, vMH vectors, or vPS1393 as described in section 2.4.8. Cell survival was measured 5 days post infection by AP assay and the data normalised to mock infected cells (100% survival) and empty wells (0% survival). Plots show mean cell survival from triplicate wells ( $n=3$ ),  $\pm$  S.D. (where no error bars are visible S.D. was  $<5\%$ ), with fitted sigmoid dose response curves. Dose response curves were used to calculate EC50 values.

Virus	HEK293 EC50 (95% C.I.) PFU/cell
Ad5 wt	0.00470 (0.00262 - 0.00842)
vMH2	0.0143 (0.00954 - 0.0216)
vMH4	0.0399 (0.0240 - 0.0667)
vMH5	0.0484 (0.0290 - 0.0808)
vMH6	0.0584 (0.0341 - 0.0998)
vMH7	0.0555 (0.0358 - 0.0859)
vPS1393	0.0175 (0.0118 - 0.0259)

**Table 4-6. EC50 values with 95% C.I. (PFU/cell) for cytotoxicity in HEK293**

No significant difference was observed in the cytotoxicity of vMH4, 5, 6 and 7, which had similar EC50 values with overlapping 95% confidence intervals. vMH2 was slightly more cytotoxic than the other vMH vectors, with a 2- to 4- fold lower EC50 values compared to

the other vMH vectors. vPS1393 showed cytotoxicity equivalent to that of vMH2, and was approximately 3-fold more cytotoxic than the equivalent eGFP expressing vector vMH6. Ad5 wt was significantly more cytotoxic than all vMH vectors or vPS1393, with 3- to 13-fold lower EC50 values. This data suggests insertion of the ICOVIR-5 or ICOVIR-7 promoter or insertion of eGFP transgene results in a minor reduction of vector cytotoxicity.

#### **4.3.11 Transduction of Carcinoma Cell Lines**

In 1998 Dmitriev *et al* characterised the use of an RGD-retargeted adenovirus vector which was able to use  $\alpha\beta_{3/5}$  integrin as the primary cell surface receptor, and showed increased uptake into CAR negative cells [Dmitriev et al, 1998]. Since then the RGD-retargeted fibre has been extensively and successfully used to increase transduction into CAR negative and low CAR cells. Two vMH vectors, vMH5 and vMH7, contain the RGD-retargeted fibre and were expected to display increased viral uptake compared to their wt fibre equivalents, vMH4 and vMH6, respectively. It was therefore necessary to demonstrate the RGD-retargeted fibres in vMH5 and vMH7 were functional and could increase viral uptake in cell lines expressing low levels of CAR.

Virus mediated transduction was assayed by eGFP expression in two CAR negative cell lines; SKOV3 and MZ2-MEL3.0, plus DU145 cells which expresses high levels of CAR (see section 4.3.1 for CAR and integrin staining). Cells in 24-well plates were infected with Ad-GFP, vMH4, vMH5, vMH6 and vMH7 at 10, 30 and 100 PFU/cell (as described in section 2.4.8). 48 hours post infection (when eGFP expression was maximal, as shown in Figure 4-4), wells were harvested and analysed for eGFP expression by flow cytometry. The experiment was repeated twice and the mean percent eGFP positive calculated, shown in Figure 4-20.

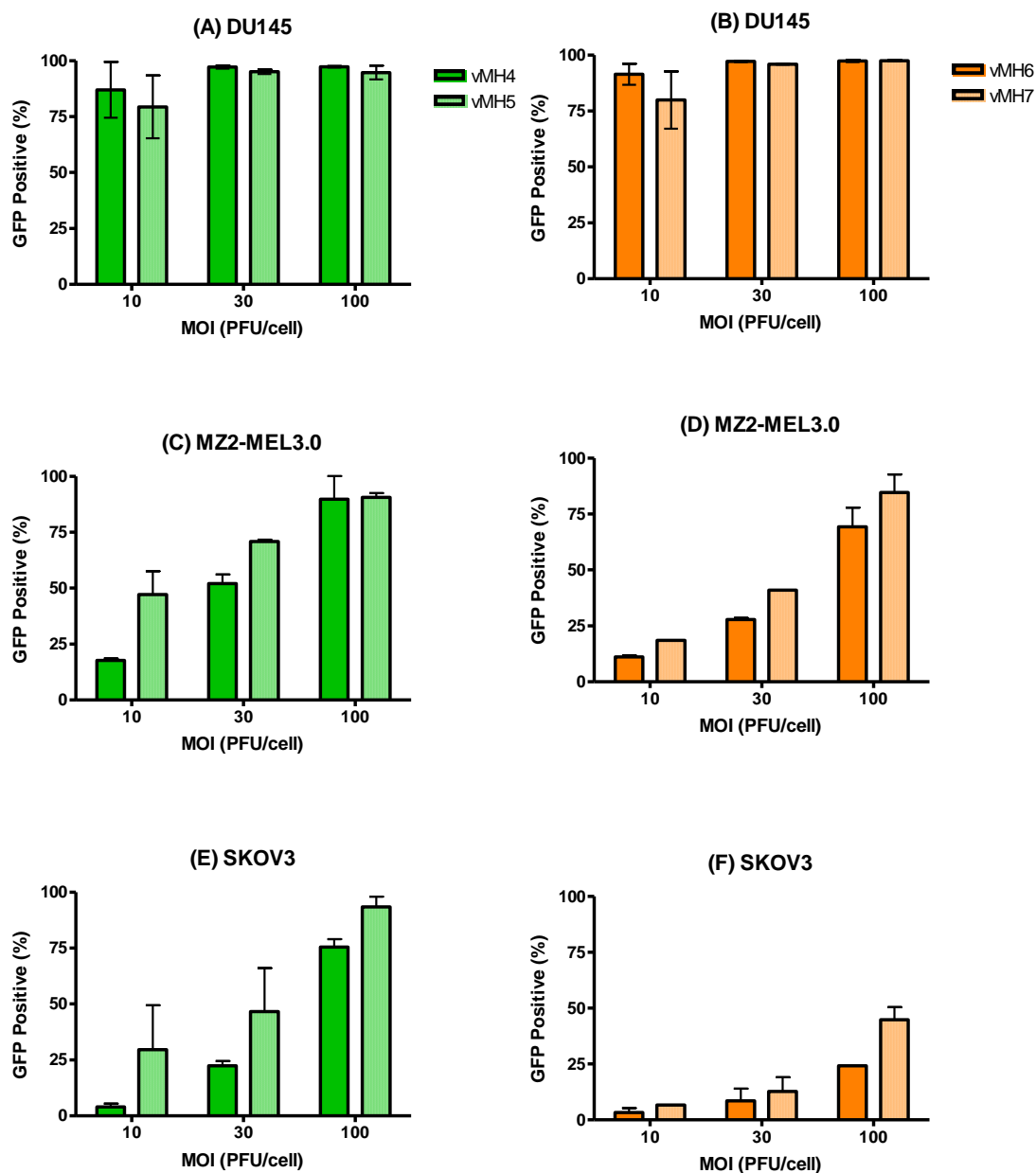


**Figure 4-20. Transduction of CAR negative cells by vMH vectors**

DU145 (A and B), MZ2-MEL3.0 (C and D) and SKOV3 (E and F) cells were seeded into 24-well plates at  $1 \times 10^5$  cells per well and infected with 10, 30 or 100 PFU/cell of vMH4 or vMH5 (A, C and E) and vMH6 or vMH7 (B, D and F), as described in section 2.4.8. 48 hours post infection cells were harvested, fixed and analysed by flow cytometry. The experiment was repeated twice, results collated and percent eGFP positive population calculated. Graphs show the mean of the two experiments ( $n=2$ )  $\pm$  S.D. (where no error bars are seen the S.D. was  $< 1\%$ ).

In DU145 cells the same level of transduction was achieved at all 3 MOI, with approximately 80% of the cells eGFP positive at 10 PFU/cell and >95% of cells positive at 30 and 100 PFU/cell.

In both MZ2-MEL3.0 and SKOV3 cells, vMH5 showed increased transduction at all MOI compared to the wt fibre equivalent vector vMH4 (except MZ2-MEL3.0 cells at 100 PFU/cell, where no significant difference was observed). In both cell lines and at all 3 MOI vMH7 showed higher transduction efficiencies compared to the equivalent wt fibre vector, vMH6.

#### **4.3.12 Virus Dissemination in Monolayers**

In plaque assaying vMH vectors some phenotypic differences were observed, with vMH2 showing the largest plaques, which appeared more rapidly than all other vMH vectors. To investigate this further, infectious centre assays were undertaken using DU145 cells to directly compare vMH vectors in terms of rate of plaque appearance and plaque size. DU145 cells were scraped into suspension and infected with 3 or 30 PFU/cell of vMH vectors for 90 minutes at 37°C. Infected cells were washed once with trypsin (to remove any virus which had not internalised) and once with infection medium. 120 infected DU145 cells was mixed with  $3 \times 10^6$  uninfected DU145 cells in a final volume of 12ml of infection medium, which was spread equally across three 60mm plates, to achieve 40 infected cells and  $1 \times 10^6$  uninfected cells per plate. Cells were allowed to adhere for 8 hours before the medium was carefully removed and replaced with 4ml of agar overlay mixture (as in section 2.4.4). Every 3 days an extra 4ml of agar overlay mixture was added, and plaque appearance was monitored from 2 days post infection.

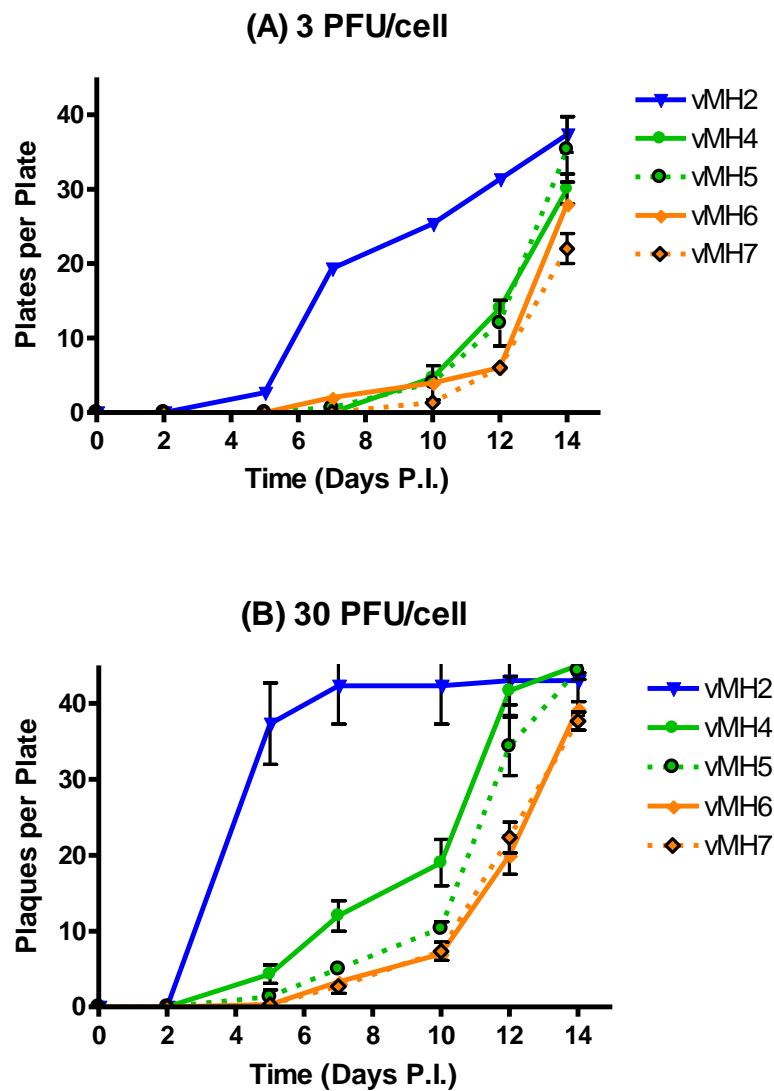


**Figure 4-21. Infectious centre assays for vMH vectors in DU145 cells**

$10^5$  DU145 cells were infected in suspension with 3 (A) or 30 (B) PFU/cell of vMH vectors for 90 minutes at  $37^\circ\text{C}$  before being washed once with trypsin and once with full culture medium. Infected DU145 cells were mixed at a ratio of  $40:10^6$  with uninfected DU145 cells and plated out in triplicate onto 60mm dishes in 4 ml of culture medium. Cells were allowed to adhere for 8 hours before the medium was removed and replaced with overlay mixture. Plaques were counted from 2 to 14 days post infection. Plots show the mean of triplicate plates ( $n=1$ ),  $\pm$  S.D.

Figure 4-21 shows the average number of plaques per plate from 2 to 14 days post infection. At both MOI, plaque appearance with vMH2 is significantly faster than other

vMH vectors. Little difference in the rate of plaque appearance was observed between vMH4, 5, 6 and 7; however both ICOVIR-7 based vectors may be very slightly slower compared to ICOVIR-5 based vectors. No difference was observed in the rate of plaque appearance between the RGD-retargeted vectors, vMH5 and vMH7, and their equivalent wt fibre vectors, vMH4 and vMH6, respectively. These observations were also reflected by assessing the plaque size at 10 days post infection via eGFP expression, imaged by fluorescence microscopy. Examples are shown in Figure 4-22, below.

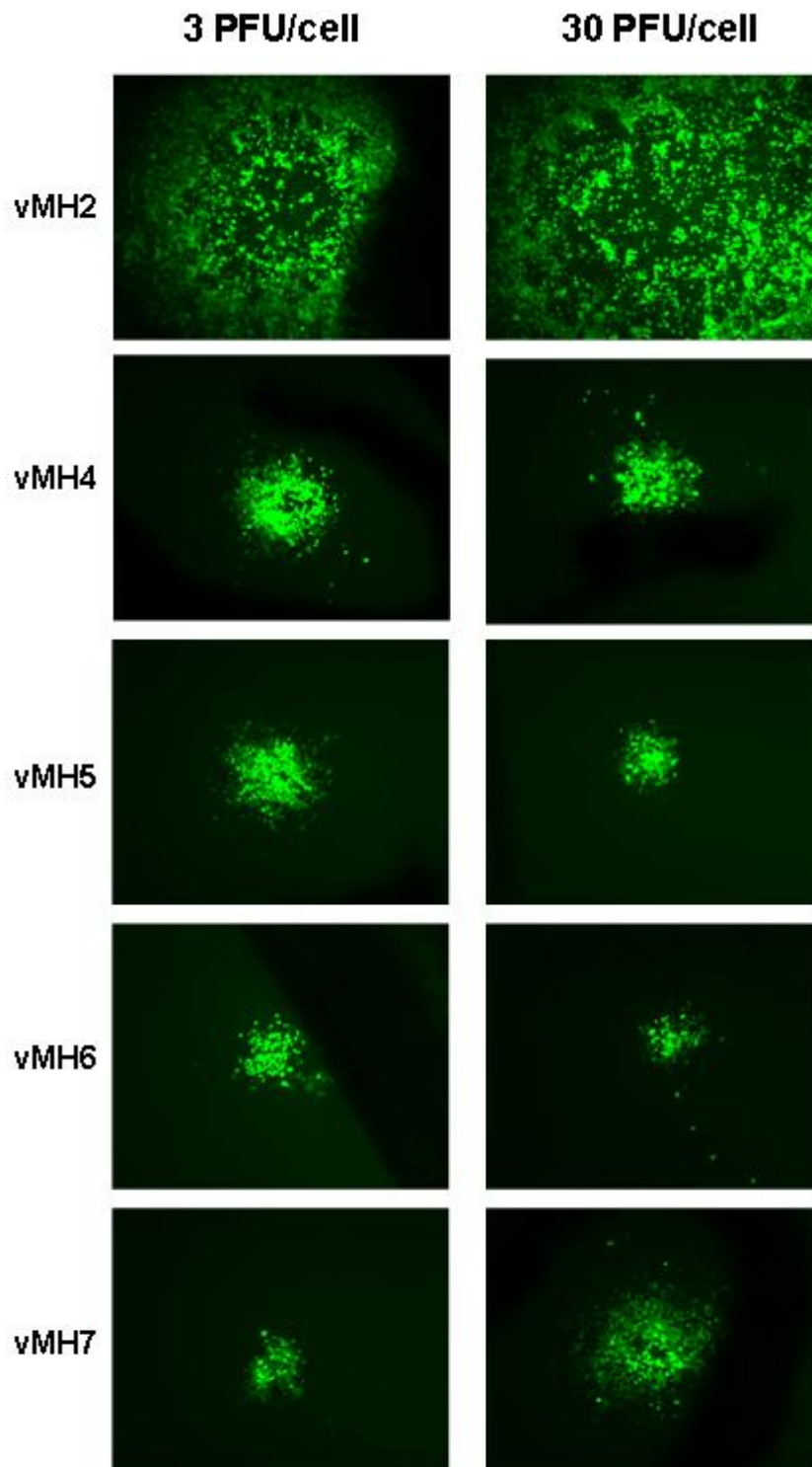


**Figure 4-22. Fluorescence microscopy images of representative vMH vector plaques**  
 Representative plaques at 10 days post infection from the infectious centre assay shown in Figure 4-21. Plaques were imaged by UV microscopy at 21x magnification.

The experiment was repeated using infected MRC5 cells mixed with uninfected DU145 cells to further study the selective nature of vMH vectors. Any productive infection within the MRC5 cells would result in release of progeny infectious virus, which would subsequently infect surrounding DU145s, resulting in plaque formation. Furthermore, plaque size gives an indication of the number of infectious virus progeny released, as release of more infectious virus would result in more rapid formation of larger plaques. MRC5 cells were scraped into suspension and infected with 30 or 300 PFU/cell of vMH vectors for 90 minutes at 37°C. Infected cells were washed once with trypsin then once with infection medium. Infected MRC5 cells were mixed with uninfected DU145 cells and treated as above to achieve triplicate plaques at 40 MRC5 cells per plate. Again plaque appearance was monitored from 2 to 14 days post infection.

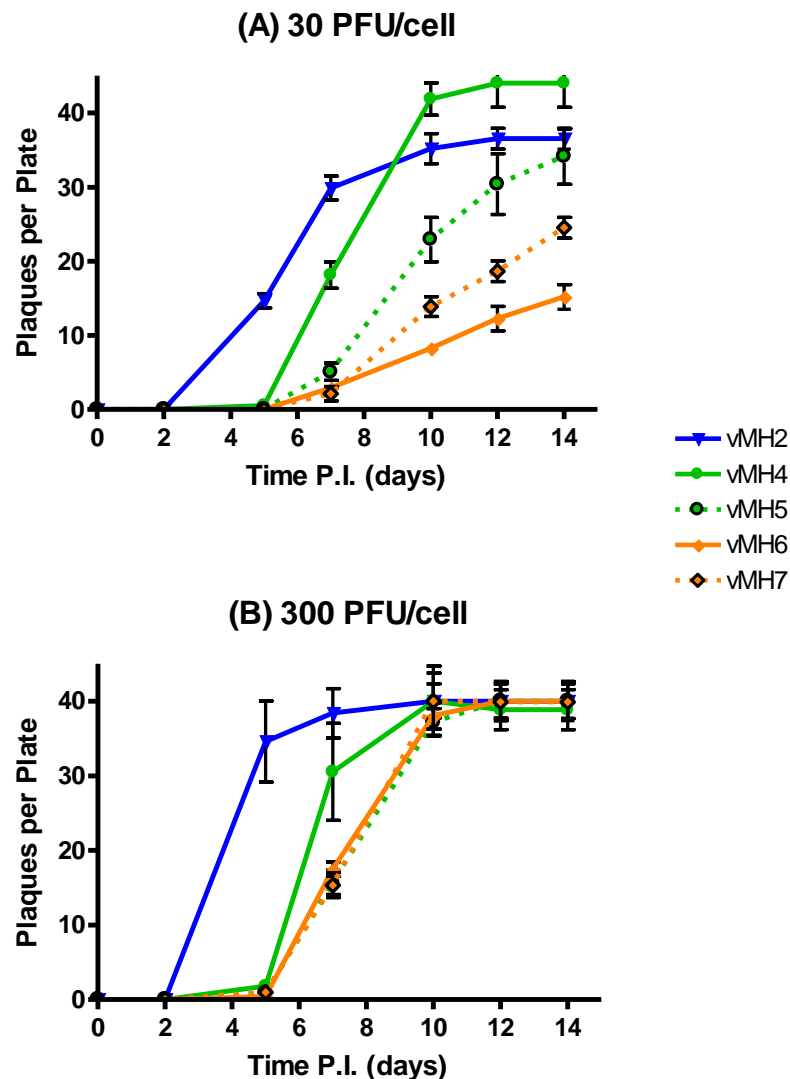


**Figure 4-23. Infectious centre assays for vMH vectors in MRC5 cells**

$10^5$  MRC5 cells were infected in suspension with 30 (A) or 300 (B) PFU/cell of vMH vectors for 90 minutes at  $37^\circ\text{C}$  before being washed once with trypsin and once with full culture medium. Infected MRC5 cells were mixed at a ratio of  $40:10^6$  with uninfected DU145 cells and plated out in triplicate onto 60mm dishes in 4 ml of culture medium. Cells were allowed to adhere for 8 hours before the medium was removed and replaced with overlay mixture. Plaques were counted from 2 to 14 days post infection. Plots show the mean of triplicate plates ( $n=1$ ),  $\pm$  S.D.

At both MOIs, vMH2 showed the fastest rate of plaque appearance with plaques first detected at 5 days post infection. With the remaining vMH vectors at 30 PFU/cell plaques

were first observed at 7 days post infection; with vMH4 and vMH5 showing more rapid plaque appearance, followed by vMH7 and finally vMH6. At 30 PFU/cell neither vMH6 nor vMH7 reached 40 plaques per plate by 14 days post infection. At 300 PFU/cell there was no noticeable difference in the rate of plaque appearance between vMH4, 5 6 and 7; all of which rapidly formed plaques from 5 days post infection. This data would suggest the ICOVIR-7 based vectors were the most attenuated vectors in MRC5 fibroblasts, showing the least number of plaques at 30 PFU/cell. However this attenuation can be overcome with a 10-fold greater MOI.

## **4.4 Discussion**

This chapter characterised the new vMH vectors and compared them to the  $\Delta$ E1B-55K vector vNR3. All vMH vectors and vNR3 express eGFP allowing assessment of transgene expression in preparation for introduction of the therapeutic transgene NTR. Experiments conducted in this chapter allow assessment of the vector lytic activities and tumour cell selectivity by calculating the therapeutic index. Western blot and rtQ-PCR demonstrated differential E1A protein and RNA expression with each vMH vector. Cytotoxicity experiments in HEK293 cells allow for the assessment of lytic activity while removing some of the effect of varying E1A expression. Finally, comparisons to vPS1393 allow for the assessment of any effect on cytotoxicity of introduction of the transgene eGFP. Each one of these points will be discussed in detail below.

### **4.4.1 Lytic Activity and Therapeutic Index**

The lytic activity of vMH vectors was assessed in three prostate cancer cell lines and two non-transformed human fibroblasts. Table 4-7 ranks the cytotoxicity, therapeutic indices and E1A expression with vMH vectors and vNR3. In all cell lines vMH2 showed the most

cytotoxicity, equal to or greater than Ad5 wt. This was followed by the ICOVIR-5 based vectors, vMH4 and vMH5, and finally both ICOVIR-7 based vectors, vMH6 and vMH7, which showed the least cytotoxicity in all cells. Both RGD-retargeted vectors (vMH5 and vMH7) showed similar levels of cytotoxicity in prostate cancer cell lines compared to their wt fibre equivalents (vMH4 and vMH6). Since vMH4 and vMH5 contained the same E1A modifications, as do vMH6 and vMH7, and all prostate cancer cell lines express moderate to high levels of CAR, no difference in cytotoxicity would be expected. However, this also shows that introduction of the RGD-retargeted fibre does not have a detrimental effect on cytotoxicity in CAR positive cell lines.

<b>Virus</b>	<b>Cytotoxicity to prostate cancer</b>	<b>TI</b>	<b>E1A protein expression</b>	<b>E1A RNA expression</b>	<b>Cytotoxicity to HEK293 cells</b>
vMH2	1	6	1	1	1
vMH4	=2	=3	=2	=2	=2
vMH5	=2	=3	=2	=2	=2
vMH6	=5	=1	4	5	=2
vMH7	=5	=1	5	6	=2
vNR3	=2	5	Not tested	=2	=2

**Table 4-7. Rank scoring from 1 - 7 (most - least) of vMH vectors**

Previous studies using E1A CR2  $\Delta$ 24 vectors, similar to vMH2 but without the transgene, have observed increased cytotoxicity in relation to Ad5 wt, in both tumour and non-growth arrested non-transformed cells [Bazan-Peregrino et al, 2008]. Currently, the exact reason for the increase in lytic activity is still not fully understood. A recent report has demonstrated E1A CR2  $\Delta$ 24 viruses induce a novel non-apoptotic non-necrotic mode of cell death, which may be responsible for the increase in cytotoxicity. Speculations have also been made that by deleting the CR2 region and preventing the ability to bind to any pRb, more E1A is free to perform other functions which increase the rate of replication.

Concerns were raised in section 1.2.4.4.2 that replacement the wt E1A promoter with an E2F responsive promoter, in the context of a virus with a wt E4 region, may replace the E1-E4 negative feedback loop with a positive feedback loop, resulting in reduced attenuation in non-transformed cells. Contrary to this idea, both ICOVIR-5 and ICOVIR-7 based vectors show reduced E1A RNA and protein expression at early timepoints (up to 24 hours post infection), compared to Ad5 wt. However, vMH4, 5 and 6 do possibly expresses more E1A protein at later timepoints (36 to 60 hours post infection), potentially suggested a positive feedback loop at late times of infection.

For all the viruses used the therapeutic index was calculated to give an indication of the relative tumour selectivity (summarised in Table 4-7). In all cell lines the ICOVIR-5 and ICOVIR-7 based vectors (vMH4, 5, 6 and 7) had higher TI than the wt E1A promoter, E1A CR2  $\Delta$ 24 virus, vMH2, and the  $\Delta$ E1B-55K virus vNR3. Thus despite reduction of lytic activity observed with these vectors, replacement of the wt E1A promoter with the ICOVIR-5 or ICOVIR-7 promoter does increase the tumour selectivity. In DU145 and 22RV1 cells vMH4 had the highest TI, followed by both ICOVIR-7 based vectors. Whereas in PC3 cells both ICOVIR-7 vectors had the highest TI, followed by both ICOVIR-5 based vectors (shown in Figure 4-3). It is essential to note the TI values used underestimate the actual selectivity of the ICOVIR-7 based vectors. A large variation of TI was observed across the three prostate cancer cell lines, probably due to the varying p53, pRb and E2F status (summarised in Table 4-8) plus the different levels of CAR and integrin expression. However there was no direct correlation p53 and pRb status and the lytic activity of the CRAd vectors and E2F expression levels are high in all three cell lines. Furthermore, in both 22RV1 and DU145 cells Ad5 wt showed higher TI than all other vectors, probably due

to the fact the MRC5 cells were not growth arrested. If the fibroblasts were growth arrested it would be anticipated the CRAAd vectors would show higher TI than Ad5 wt, in both of these cell lines.

Cell line	p53 status	pRb status	E2F levels	Surface CAR	Surface $\alpha V\beta 3$	Surface $\alpha V\beta 5$	Reference
DU145	Mutant	Mutant	High	High	No	High	[Sun et al, 2007; Supiot et al, 2008]
22RV1	wt	wt	High	High	Moderate	High	[Sun et al, 2007; Supiot et al, 2008]
PC3	Null	wt	High	Moderate	No	High	[Sun et al, 2007; Supiot et al, 2008]

**Table 4-8. p53, pRb, E2F and Ad receptor levels of prostate cancer cell lines**

Cytotoxicity experiments in HEK293 cells provide wt E1A, constitutively present, thus are expected to remove some of the E1A associated reduction in lytic activities and provide a more level ‘playing-field’. Cytotoxicities of vMH vectors in HEK293 cells show replacement of the natural E1A promoter by either the ICOVIR-5 promoter or ICOVIR-7 promoter results in a slight reduction in lytic activity. However, no significant difference was observed in lytic activities between vMH4, vMH5, vMH6 and vMH7. These results may suggest the reduction in cytotoxicities observed with ICOVIR-5 and ICOVIR-7 based vectors compared to vMH2, was a due to the increase in genome size. Concerns were also raised previously, whereby the increase in vector genome size may result in an increase in P:I ratio (discussed in section 3.6.2). However, the ICOVIR based vectors contain E1A under control of an E2F responsive promoter, not the wt E1A promoter. Normally in Ad infection E1A expression is down-regulated at late times, however this would not be the

case with either E2F responsive promoter. Therefore despite HEK293 cells supplying wt E1A, all the ICOVIR based vectors would be expected to express more E1A than vMH2 in HEK293 cells, at late times of infection. Thus the differential cytotoxicities observed in HEK293 cells may not be entirely due to the difference in vector genome size. However in my opinion it is likely the increase in vector genome size would contribute at least in part to the reduction in lytic activities observed with vMH4, 5, 6 and 7, compared to vMH2.

#### **4.4.2 E1A Expression in vMH Viruses**

Replacement of the natural E1A promoter with the ICOVIR-5 or ICOVIR-7 promoter results in reduced E1A expression at both the RNA and protein level (Figure 4-7 and Figure 4-8, respectively), which was associated with a subsequent reduction in virus cytotoxicity (Figure 4-11). Despite this, the tumour specific promoters do increase the tumour specificity of the viruses as has been discussed in section 4.4.1. Notably, vMH2 produced more E1A RNA and protein than Ad5 wt at early timepoints (4 and 8 hours post infection), which may contribute to the increased cytotoxicity observed with vMH2 over Ad5 wt.

Interestingly, the RGD-retargeted virus vMH7 produces less E1A RNA and protein than the equivalent wt fibre vector, vMH6, both of which have the E1A promoter replaced with the same ICOVIR-7 promoter. Moreover, vMH7 shows an 8-10 hour delay in the onset of DNA replication, presumably due to the reduced level of E1A expression, which subsequently delayed the start of transgene and late protein expression. This delay can be almost completely eliminated in HEK293 cells, further demonstrating the delayed DNA replication, late protein and transgene expression, was a result of reduced E1A expression. The ICOVIR-7 promoter has been fully sequenced in both vMH6 and vMH7, from 100bp upstream of the DM-1 insulator element to 100bp into the E1A ORF, and was shown to be

identical to each other, and to the sequence in pICOVIR-7 used for recovery for both vectors (see section 4.3.8). Thus the differential E1A expression observed with vMH6 and vMH7 was not due to unintentional promoter mutations. Sequence of the ICOVIR-7 promoter did reveal unexpected differences from the predicted sequence at 5 points within the ICOVIR-7 promoter sequence (see appendix 2 for sequence). Analysis of the cloning pathway used for construction of pICOVIR-7 demonstrated all of these mutations were at the cloning junction between the various promoter components (i.e. the DM-1 insulator element, E2F-1 promoter region, and the two additional E2F-1 binding regions) [Majem et al, 2006; Rojas et al, 2009], and were therefore likely to be accidentally introduced during the cloning of pICOVIR-7. It is therefore possible, but in my opinion very unlikely, these mutations would affect the promoter activity. Despite this, the promoter regions from vMH6 and vMH7 are identical, therefore these mutations would not account for the differential E1A expression. The pICOVIR-7 cloning pathway describes the ICOVIR-7 promoter as having a poly(A) site, followed by the DM-1 insulator and the E2F-1 promoter with the two additional E2F-1 binding regions. It is worth noting the ICOVIR-7 promoter sequencing results show a AATAAA poly(A) consensus sequence between the E2F-1 promoter and DM-1 insulator element, i.e. following the DM-1 insulator elements (including the CTG repeats sequences and GC rich regions) (as marked in appendix 2). Additionally, no clear poly(A) consensus sequence was apparent upstream of the DM-1 insulator.

The exact reason behind the differential expression observed between vMH6 and vMH7 is currently not known. Both vectors were screened by PCR for contaminating wt E1A sequences. However it is probably first advisable to screen banded batches of viruses for

the presence of wt E1A sequences by Q-PCR. The restriction profiles of both vectors showed they contained the correct ICOVIR-7 promoter sequence. However it is worth noting no vectors were screened by PCR for the presence of the wt E1A promoter, using a primer situated within the deleted promoter region. It is therefore also first advisable to screen batches of virus by PCR for the presence of the wt E1A promoter, which could have been acquired through recombination with the adenovirus sequences in HEK293 cells (used for virus rescue). The differential E1A protein expression observed appeared proportional to the observed differences in the E1A RNA levels, suggesting the differential is not due to post-translation effects. There are several possible explanations for the difference in E1A RNA expression observed. vMH7 could have acquired an unintentional mutation during the recovery of this virus which had a detrimental effect on E1A expression. Conversely vMH6 could have acquired an unintentional mutation which enhanced E1A expression. Such mutations could be within; gene(s) that could effect transcription from the ICOVIR-7 promoter (such as E4orf6/7), the regions surrounding the promoter region which might effect transcription (such as with the enhancer elements upstream of the DM-1 insulator element) or within regions affecting E1A mRNA stability (such as within the E1A ORF). At the end of this study the entire genomes of vMH6 and vMH7 were sent away for sequencing, to try and identify a mutation which might explain the difference in E1A expression. However, at the time of writing the results from the genome sequencing had not yet arrived. If any mutation was observed which could affect E1A expression then specific experiments would have to investigate the mutation. Assuming there are no mutations within either genome it is possible the differential E1A expression observed was due to a direct or indirect interaction between the ICOVIR-7 promoter and the RGD-retargeted fibre. No difference in E1A expression was observed between vMH4 (wt fibre) and vMH5

(RGD-retargeted fibre). Both of these vectors incorporate the ICOVIR-5 promoter, which is very similar to ICOVIR-7. Therefore, in my opinion, it seems unlikely the reduced E1A expression observed with vMH7 is due to insertion of the RGD-4C motif. Further possibilities exist such as; delayed endosomal escape, virus unpackaging or nuclear trafficking with vMH7, however these seem unlikely since the delay in DNA replication can be eliminated using HEK293 cells.

#### **4.4.3 Effect of Transgene Insertion**

At the start of this project no reports were published using either ICOVIR-5 or ICOVIR-7 based vectors. Since then several reports have been published using an ICOVIR-5 based vector [Alonso et al, 2007a; Alonso et al, 2007b; Cascallo et al, 2007] and one report using an ICOVIR-7 based vector [Rojas et al, 2009]. The ICOVIR-5 reports generally demonstrated a potent anti-glioma effect and low systemic toxicities in *in vivo* mouse models. Furthermore restoration of pRb function led to down-regulation of E1A and a dramatic reduction in adenovirus replication. The ICOVIR-7 paper reported greater anti-tumour potency compared to Ad5 wt in subcutaneous xenografts treated by intravenous injection and low liver toxicity in mouse models.

During this work it was suggested introduction of the eGFP transgene into the ICOVIR-7 background may result in reduced lytic activity. Direct comparison between vMH vectors and vICOVIR-7 were attempted; unfortunately these comparisons were invalidated by the discovery that the vICOVIR-7 stock was heavily contaminated with a virus having a restriction enzyme profile similar to Ad5 wt, but apparently with the RGD-retargeted fibre. In comparison of vMH6 with vPS1393 (an ICOVIR-7 based vector lacking eGFP transgene with wt fibre), showed a slight decrease in cytotoxicity in 22RV1 cells (2- to 3- fold), associated with transgene insertion, however no significant difference in DU145 cells.

Experiments in HEK293 cells also showed approximately a 3-fold reduction in cytotoxicity of vMH6 compared to vPS1393, associated with eGFP transgene insertion. These results suggest introduction of eGFP does result in a minor reduction of oncolytic activity. There are three possible explanations for the reduction in cytotoxicity observed by eGFP introduction; the increase in genome size is having a direct negative effect on vector cytotoxicity, a direct 'toxic' effect of the eGFP transgene or the transgene insertion results in specific problem for expression of virus proteins such as fibre and the E4 region.

Unfortunately from the data here it is not possible to identify which of these factors is responsible for the reduced cytotoxicity, thus further experiments would be required to identify how much each factor is contributing to this observation.

#### **4.4.4 RGD-Retargeted Fibre**

The RGD-retargeted fibre has been used in multiple studies for nearly 10 years and therefore is not novel in this study. This mutation has been well characterised and shown to increase binding to cells expressing low amounts of CAR, by directly using  $\alpha_v\beta_{3/5}$  integrins as the primary cell surface attachment receptor [Dmitriev et al, 2002]. I have demonstrated that both vMH5 and vMH7 show increased transduction in cells expressing low levels of CAR, in comparison to the equivalent wt fibre vectors; vMH4 and vMH6, respectively.

In all prostate cancer cell lines no growth advantage was observed with the RGD-retargeted viruses in comparison to their wildtype fibre equivalents, either in a single replication cycle, or in plaque assays which require multiple cycles of replication and cell-to-cell spread. Furthermore no transduction advantage was observed with the RGD-retargeted vectors in DU145 cells. These observations would fit in line with previous studies that have also seen little or no transduction advantage in the PC3 [Work et al, 2004] and DU145 cells [Rajecki et al, 2007]. All the prostate cell lines tested in this study express moderate to high levels of

CAR on their cell surface, which would probably not be saturated by the range of MOI used here. Of all the cell lines tested PC3 express the lowest amount of CAR and are therefore most likely to show any advantage with the RGD-retargeted fibre. Indeed with PC3 cells a very slight increase in cytotoxicity was observed with the RGD-retargeted vectors, however the decrease in EC50 values was not significant. Despite this no specific disadvantage was conferred by introduction of the RGD-retargeted fibre in CAR positive cells. Whereas previous reports have shown some CAR expression in prostate carcinoma samples, there does seem to be a general down-regulation CAR expression compared to normal tissue, especially in higher grade tumours [Rauen et al, 2002]. Therefore although the RGD-retargeted fibre may not confer an *in vitro* increase in cytotoxicity, a cytotoxic advantage may still be observed in prostate cancer patients.

#### **4.4.5 Virus Dissemination in Monolayers**

Virus spread is an important factor in the *in vivo* efficacy of gene therapy vectors. An ideal gene therapy vector should be able to spread rapidly throughout the tumour tissue but be unable to replicate in normal non-carcinoma cells. Of all vMH vectors, vMH2 is clearly the quickest at spreading through prostate cancer monolayer cultures. However significant normal cell toxicity was also observed, as demonstrate by the rapid spread from MRC5 cells in infectious centre assays. Little difference was observed in the spread of vMH4, vMH5, vMH6 and vMH7 through prostate cancer monolayers. Despite this, vMH6 and vMH7 show a reduce spread and plaque formation from MRC5 cells in infectious centre assays, at the lowest MOI tested (30 PFU/cell). These two vectors should therefore be able to spread throughout tumour tissue as efficiently as vMH4 and vMH5, but stop spreading when normal tissue is reached.

There was no difference in the speed of virus spread between RGD-retargeted vectors and matched wt fibre vectors, probably due to the high levels of CAR expressed on both DU145 and MRC5.

## **4.5 Summary**

I have characterised 6 new CRAAd vectors for oncolytic virotherapy of prostate cancer. From all vectors tested the ICOVIR-7 vectors possess the highest therapeutic index in prostate cancer cell lines. As might be expected, replacement of the wt E1A promoter does result in lower E1A expression at both the RNA and protein level. The increase in genome size caused by the replacement of the E1A promoter by either the 'ICOVIR-5 promoter' or 'ICOVIR-7 promoter' may cause a decrease in lytic activity, as does introduction of the therapeutic transgene eGFP. However no reduction in lytic activity is observed between ICOVIR-5 and ICOVIR-7 based vectors attributed to the increase in genome size. Both RGD-retargeted vectors show increased transduction of CAR negative cell lines.

Based on these data the ICOVIR-7 based vectors were selected for the introduction of the therapeutic transgene NTR and NTR variants.

## **CHAPTER 5**

# **Characterisation of NTR Expressing Vectors**

## 5.1 Introduction

As described in CHAPTER 3 novel oncolytic CRAd viruses expressing eGFP were constructed, based on the ICOVIR vectors from Dr R. Alemany's lab at the Institut Català d'Oncologia. These vectors were expected to be more tumour selective than the E1A CR2  $\Delta$ 24 vector with a wt E1A promoter, displaying cytotoxicity in cancer cell lines while avoiding toxicity to normal non-transformed cells.

These vectors were characterised in CHAPTER 4 to identify the most tumour selective vectors for the introduction of NTR. The ICOVIR-7 based vectors, vMH6 and vMH7, were the most tumour selective, showing no toxicity to primary human fibroblasts, thus the ICOVIR-7 backbone was chosen for introduction of the therapeutic transgene NTR. The new NTR vectors were constructed prior to full characterisation of vMH6 and vMH7. Therefore NTR was inserted into both RGD-retargeted and wt fibre vectors, while bearing in mind a potential difference in E1A expression.

The latest clinical trials with enzyme/prodrug systems utilise mutant enzymes which have increased catalytic activity for their specific substrate [Barton et al, 2008]. Two recent reports from The University of Birmingham SCS-GT group have identified novel *nfsB* NTR mutants which are catalytically enhanced for CB1954 reduction [Guise et al, 2007; Jaberipour et al, 2010]. The double NTR mutant T41L N71S showed a 14-fold increase in CB1954 sensitisation over wt NTR when expressed in a replication deficient Ad vector. The second variant is the triple NTR mutant T41Q N71S F124T, which showed up to 80-fold increase in CB1954 sensitisation over wt NTR when expressed in a replication deficient Ad vector. It was therefore decided to introduce both NTR mutants, as well as wt NTR, into the ICOVIR-7 backbone, in order to improve the NTR mediated cytotoxicity.

Six new NTR expressing ICOVIR-7 based vectors were constructed, combining the RGD-retargeted and wt fibre with the three NTR variants: wt NTR, double mutant NTR and triple mutant NTR.

## 5.2 Aim of Chapter

The aim of this chapter was to characterise new ICOVIR-7 based oncolytic vectors expressing NTR and NTR mutants. Vectors were compared with vNR6, an E1B-55K deleted vector expressing NTR from the pIX virus promoter, in terms of virus replication, gene expression and lytic activity, alone or in combination with the prodrug CB1954, to identify the optimal vector for the treatment of prostate cancer.

## 5.3 Construction of NTR Expressing ICOVIR-7 Vectors

Figure 5-1 shows a schematic of the 6 NTR expressing ICOVIR-7 based vectors (vPS1361-vPS1366, collectively referred to as vPS136X), along with the  $\Delta$ E1B-55K,  $\Delta$ pIX, NTR expressing vector vNR6. All vPS136X vectors contain the E1A CR2  $\Delta$ 24 deletion and have the E1A promoter replaced by the ICOVIR-7 promoter (described in section 3.3), derived from the same modified E1A plasmid pICOVIR-7. vPS1361, vPS1363 and vPS1365 encode the RGD-4C sequence introduced into the fibre knob HI-loop.

All vPS136X vectors express NTR (wt or mutant) from the MLP via an upstream splice acceptor site, inserted directly downstream of the fibre gene, and have a Kozak sequence directly before the translation start site. Thus the organisation of NTR expression in vPS136X vectors is the same as eGFP expression in vMH vectors.

vPS1361 and vPS1362 express the wt NTR gene, encoded by the *E.coli nfsB* gene [Michael et al, 1994]. vPS1363 and vPS1364 express T41L N71S double NTR mutant and vPS1365 and vPS1366 express the T41Q N71S F124T triple NTR mutant.

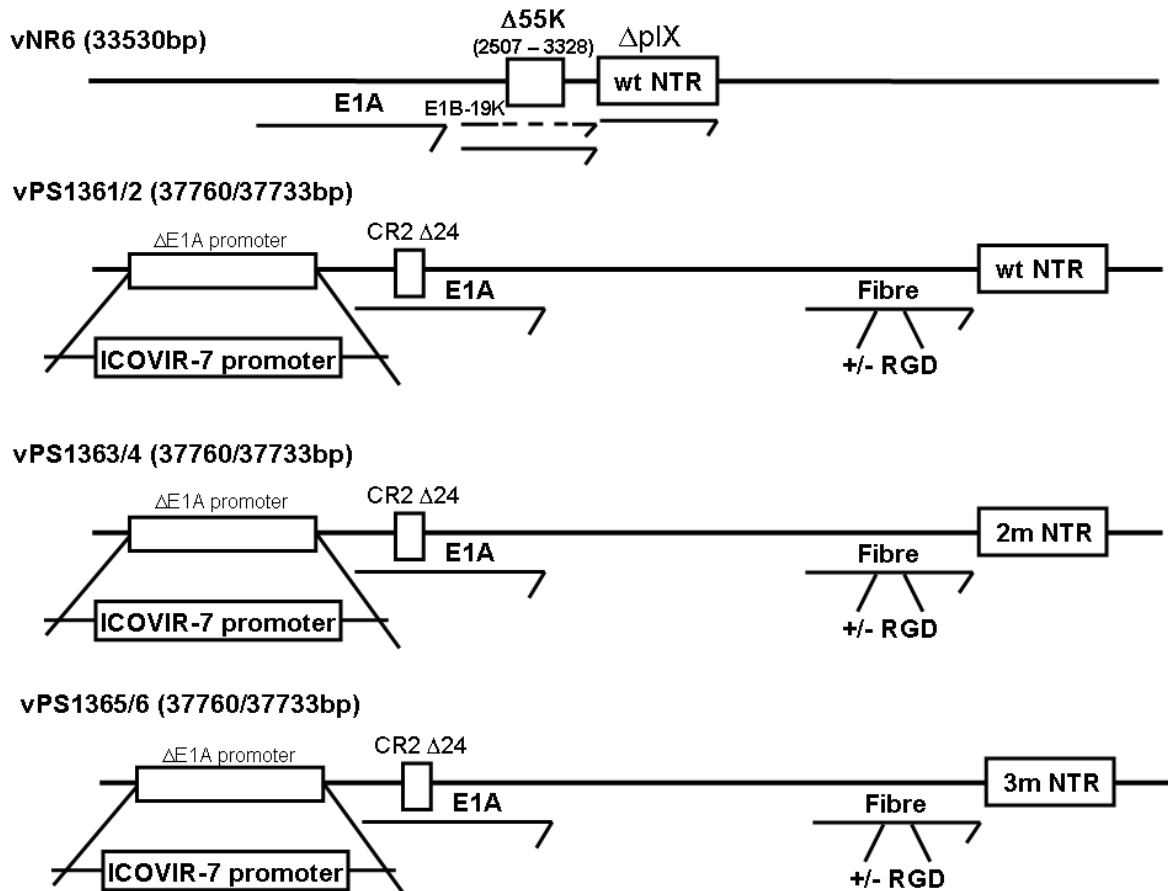


**Figure 5-1. Schematic of vPS136X Vectors**

vNR6 has the  $\Delta E1B-55K$  deletion and has the pIX ORF replaced by the wt NTR ORF. All vPS136X vectors have the E1A CR2  $\Delta 24$  deletion; the wt E1A promoter replaced by the ICOVIR-7 promoter and are designed to express an NTR variant from a splice acceptor site downstream of the fibre ORF. vPS1361 and 2 encode wt NTR, vPS1363 and 4 encode T41L N71S double mutant (2m) NTR and vPS1365 and 6 encode the T41Q N71S F124T triple mutant (3m) NTR. vPS1361, 3 and 5 also have the RGD-4C motif inserted into the HI-loop of the fibre knob.

All vPS136X vectors were constructed following the same cloning pathway used for the construction of vMH6 and vMH7 (as described in CHAPTER 3 ). Due to time limitations, the cloning and recovery of NTR expressing viruses was performed by Dr P. Searle and E. Hodgkins.

Briefly, the entire ORF from NTR (wt and mutants) was amplified by PCR using primers PS1300A and PS1300B (described in Table 2-1). Primers PS1300A and PS1300B are

similar to MHP001 and MHP002, with the eGFP complementary sequence replaced by NTR complementary sequence.

The purified NTR fragments were cloned into pNKfibreRGD to give pPS1300F, G, H before the NTR sequences confirmed by DNA sequencing and all three pPS1300 plasmids recombined with pPS1344G8. Since pPS1344G8 contains the wt fibre, whereas pPS1300F, G and H contain the RGD-retargeted fibre, the same recombination generated plasmids with either wt or RGD-retargeted fibre which were discriminated between via a SacII digest (since the RGD-4C insertion introduced an additional SacII site). The resulting plasmids with RGD fibre were pPS1300Q1, R1 and S1, while those with wt fibre were pPS1300Q20, R20 and S7 (with wt NTR, double mutant and triple mutant NTR, respectively). These plasmids were used in virus rescue with pICOVIR-7 via homologous recombination in HEK293 cells, to generate 1<sup>o</sup> seed stocks. All subsequent passages were performed in A549 cells.

All vectors were double plaque purified in DU145 cells, and all subsequent passages were performed in A549 cells. P1 seed stocks were screened for contaminating viruses which may have recovered the wt E1A region (from the HEK293 cells) or rearranged the NTR insert. Screening was performed by E. Hodgkins using the methods described in section 3.5. Following screening the p1 seed stocks were used to generate p2 seed stocks. The sequence of the NTR insert and 50bp of flanking sequence was verified by Dr P. Searle either from the p1 DNA or the final CsCl banded stock.

I used p2 seed stocks to infect 20x150cm<sup>2</sup> tissue culture flasks of A549 cells. Upon complete CPE, flasks were harvested and virus CsCl banded. DNA was extracted from each p3 banded stock and restriction enzyme profile confirmed with HindIII, BglIII, and KpnI

(performed by E. Hodgkins, data not shown). Restriction profiles for all viruses were as predicted, confirming they had not undergone any major re-arrangements.

Following restriction enzyme profiling, virus particle concentration was determined by PicoGreen assay and infectious virus particles counted by plaque assay. Table 5-1 shows the results of virus particle count, plaque count, P:I ratio and the genome size expressed as percentage of Ad5 wt.

All banded virus stocks were greater than  $1 \times 10^{11}$  particles/ml and possessed acceptable P:I ratios below 110. These batches of p3 banded viruses were used in all subsequent experiments for vPS136X characterisation.

<b>Virus</b>	<b>Mutations</b>	<b>Particle count (VP/ml)</b>	<b>Plaque count (PFU/ml)</b>	<b>P:I ratio</b>	<b>Percentage size of Ad5 wt genome</b>
<b>vNR6</b>	$\Delta$ pIX, wt NTR, wt fibre	$2.89 \times 10^{11}$	$4.50 \times 10^9$	64.2	93.30
<b>vPS1361</b>	wt NTR, RGD fibre	$3.41 \times 10^{11}$	$3.70 \times 10^9$	92.2	105.07
<b>vPS1362</b>	wt NTR, wt fibre	$5.50 \times 10^{11}$	$1.20 \times 10^{10}$	45.8	105.00
<b>vPS1363</b>	2m NTR, RGD fibre	$1.62 \times 10^{12}$	$2.60 \times 10^9$	62.3	105.07
<b>vPS1364</b>	2m NTR, wt fibre	$3.79 \times 10^{11}$	$3.50 \times 10^9$	108.2	105.00
<b>vPS1365</b>	3m NTR, RGD fibre	$1.41 \times 10^{12}$	$1.33 \times 10^{10}$	105.4	105.07
<b>vPS1366</b>	3m NTR, Wt fibre	$1.13 \times 10^{12}$	$3.00 \times 10^{10}$	34.7	105.00

**Table 5-1. Particle count, plaque count and P:I ratios of NTR expressing vectors**

## **5.4 Results**

### **5.4.1 vPS1361 and vPS1362 DNA replication**

Previous investigations with the ICOVIR-7 based eGFP expressing vectors vMH6 and vMH7 showed that the RGD-retargeted version, vMH7, has delayed E1A expression resulting in a delay in DNA replication and late gene expression. It was therefore decided to investigate the DNA replication of the RGD-retargeted vector vPS1361 and the wt fibre vector vPS1362, which contain the same wt NTR transgene, to see if the same delay occurred.

DU145 cells seeded in 24-well plates were infected with vPS1361, vPS1362 or Ad5 wt at 100 VP/cell (as described in section 2.4.8). At timepoints between 0 and 48 hours post infection duplicate wells from each infection were harvested, DNA extracted and Q-PCR performed for virus and cell DNA.

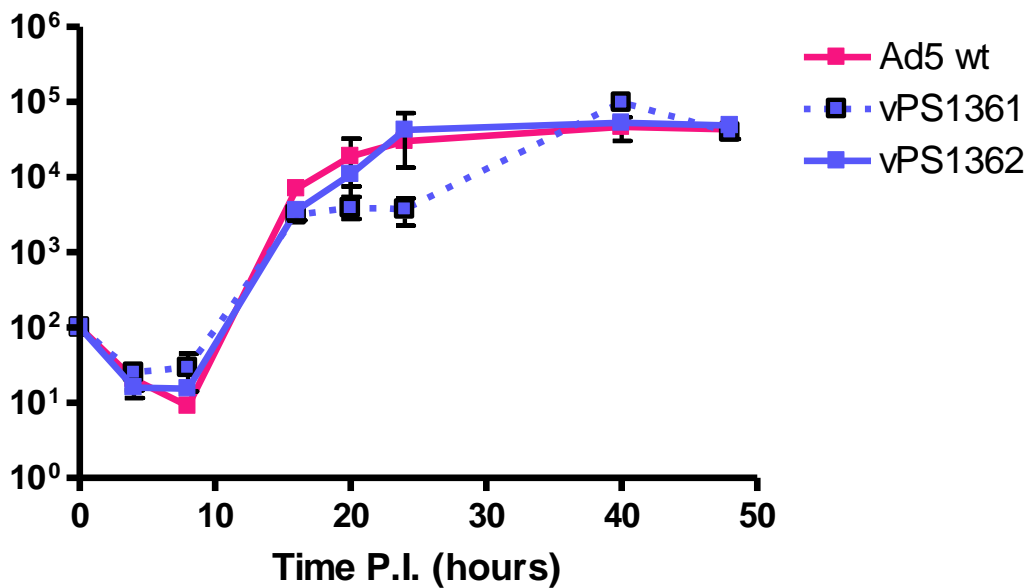


**Figure 5-2. DNA replication profile of vPS1361 and vPS1362**

DU145 cells were seeded at  $1 \times 10^5$  cells per well in 24-well plates and duplicate wells were infected with Ad5 wt, vPS1361 or vPS1362 at 100 VP/cell as described in section 2.4.8. Duplicate wells were harvested at timepoints from 4 to 48 hours post infection, DNA extracted, and Q-PCR performed for viral genomes and cellular DNA. Virus genome copies were normalised to cellular DNA copies. Graph shows the mean of duplicate wells ( $n=1$ ),  $\pm$  S.D. (where no error bars are visible S.D. was  $<5\%$ )

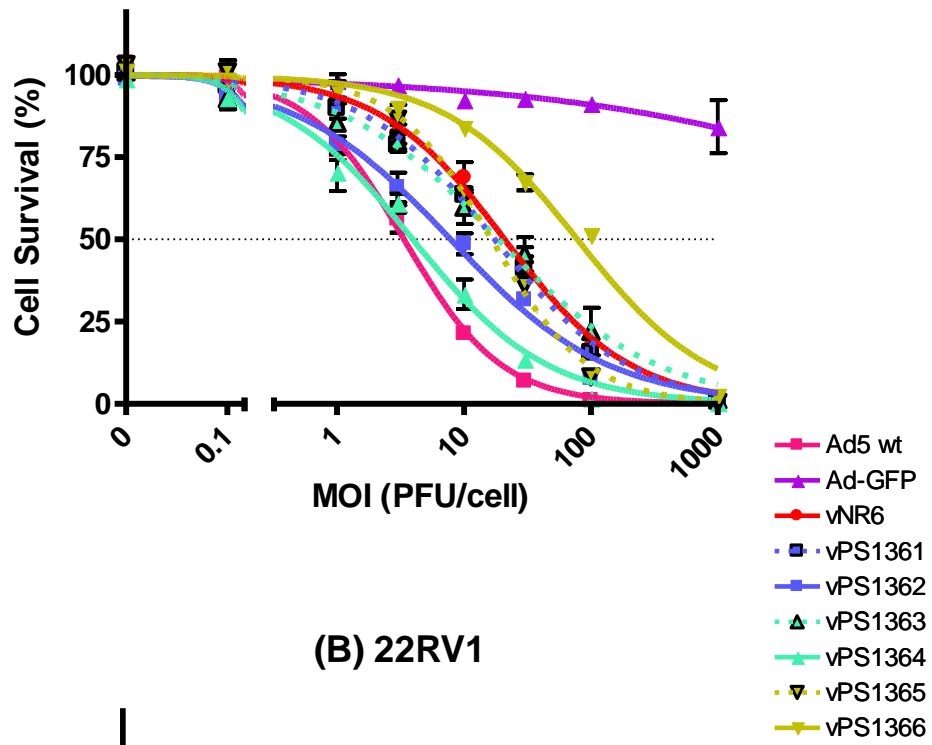
Figure 5-2 shows the virus DNA replication profile, expressed as virus copy number normalised to cell number. For both vPS1361 and vPS1362 the virus DNA replication profile closely matched that of Ad5 wt, which was similar to that seen previously (Figure 4-6). DNA replication began between 8 and 16 hours post infection, reaching maximal levels of DNA at 36 hours post infection. The delay previously observed with vMH7 is not apparent in vPS1361 which expresses RGD-retargeted fibre and wt NTR.

#### **5.4.2 Cytotoxicity of vPS136X Vectors**

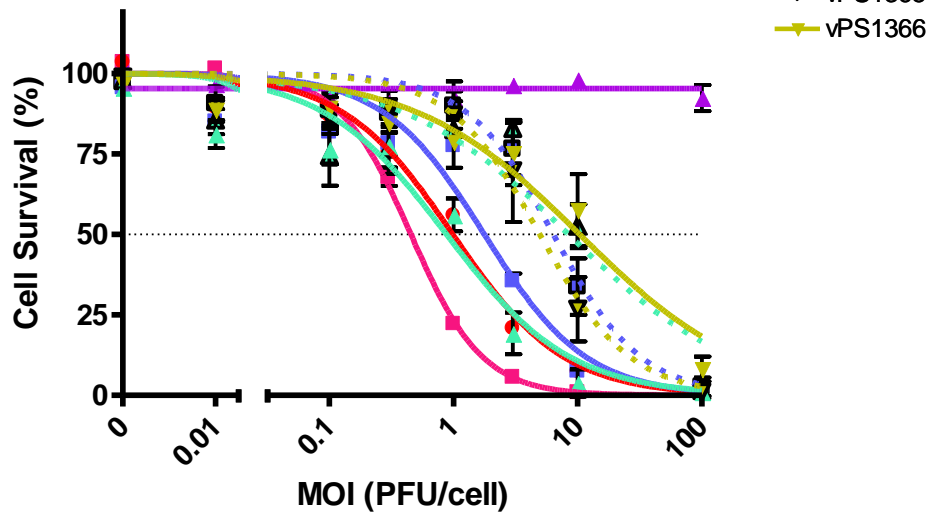
The oncolytic activity and replication selectivity of vPS136X vectors was assessed in prostate cancer cell lines and the primary human fibroblast line MRC5. Work in previous chapters has shown ICOVIR-7 based vectors to be the most selective for prostate cancer cells. Therefore it was necessary to establish that the same level of selectivity had been maintained after replacement of eGFP with the therapeutic transgene NTR. Initial experiments were conducted using a wide range of MOI. Based on this data a second round of experiments was conducted with a narrower range of MOI which were anticipated to show a clear dose response.

Prostate cancer cells lines DU145, PC3 and 22RV1 and MRC5 human lung fibroblasts plated in 96-well plates were infected with 10-fold dilutions of Ad5 wt, Ad-GFP, vNR6 or vPS136X vectors between  $1 \times 10^{-2}$  and  $3 \times 10^3$  PFU/cell (as described in section 2.4.8). Cell survival was measured 5 days post infection by AP assay and data normalised against mock infected cells (100% viability) and empty wells (0% viability). Sigmoid dose response curves are shown in Figure 5-3, with EC50 values in Table 5-2.

(A) DU145



(B) 22RV1



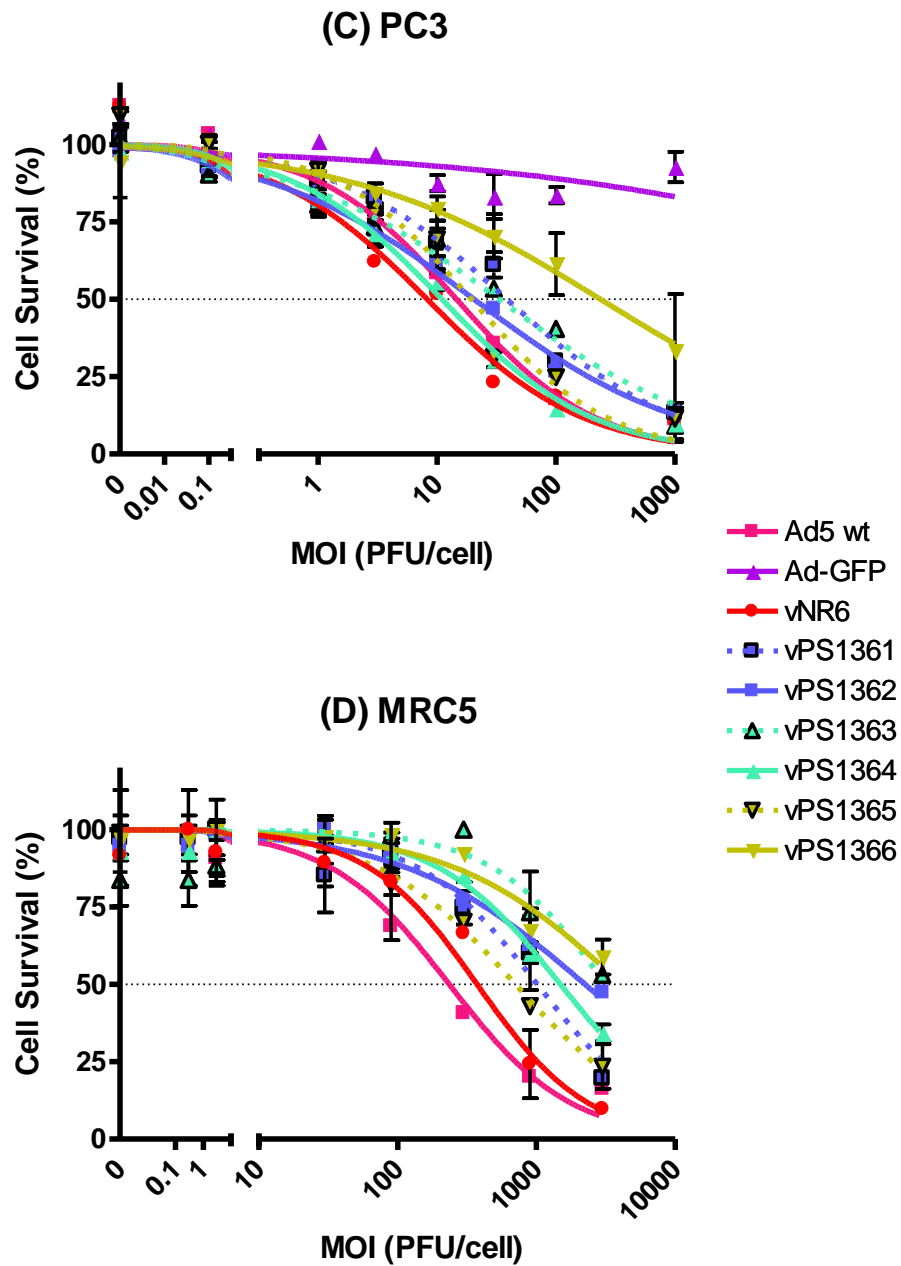


**Figure 5-3. Dose response curves for vPS136X cytotoxicity**

DU145 (A), 22RV1 (B), PC3 (C) were seeded in 96-well plates at  $3 \times 10^4$  cells per well and MRC5 (D) were seeded in 96-well plates at  $1 \times 10^4$  cells per well. Triplicate wells were infected with a serial dilution of Ad5 wt, Ad-GFP, vNR6 and vPS136X vectors as described in section 2.4.8. Cell survival was measured 5 days post infection by AP assay and normalised to mock infected cells (100% survival) and empty wells (0% cell survival). Plots show mean cell survival,  $\pm$  S.D. (where no error bars are visible S.D. was  $<5\%$ ), where  $n=3$  for each data point and fitted sigmoid dose response curves. GraphPad software was used to calculate error bars, dose response curves and EC<sub>50</sub> values. A schematic of each NTR expressing CRAAd can be seen in Figure 5-1.

<b>Virus</b>	<b>DU145</b>	<b>22RV1</b>	<b>PC3</b>	<b>MRC5</b>
<b>Ad5 wt</b>	3.37 (3.11 – 3.66)	0.453 (0.416 - 0.494)	14.6 (11.6 - 18.4)	236 (151 – 370)
<b>Ad-GFP</b>	>3000	>3000	>3000	>3000
<b>vPS1361</b>	17.5 (15.8 - 19.4)	6.38 (4.94 - 8.23)	38.7 (30.6 - 49.1)	1020 (657 - 1580)
<b>vPS1362</b>	7.85 (6.75 - 9.12)	1.77 (1.25 - 2.51)	20.5 (17.9 - 23.5)	2250 (1750 - 2910)
<b>vPS1363</b>	18.7 (15.6 - 22.4)	8.45 (4.15 - 17.2)	33.3 (23.9 - 46.5)	3180 (1530 - 6640)
<b>vPS1364</b>	3.96 (3.37 - 4.64)	0.878 (0.625 - 1.23)	11.0 (9.34 - 12.9)	1495 (1120 - 2000)
<b>vPS1365</b>	16.5 (15.1 - 18.2)	4.97 (3.74 - 6.61)	19.5 (14.2 - 26.6)	709 (591 – 851)
<b>vPS1366</b>	78.4 (65.5 - 93.9)	10.4 (6.69 - 16.2)	237 (122 - 463)	4160 (2400 - 7200)
<b>vNR6</b>	21.0 (18.3 - 24.0)	0.987 (0.831 - 1.17)	8.28 (5.74 - 11.9)	375 (262 – 538)

**Table 5-2. EC50 values with 95% C.I. (PFU/cell) for vPS136X induced cytotoxicity**

With only one exception, all vPS136X vectors were less cytotoxic than Ad5 wt in all 4 cell types, with a range of EC50 values 2- to 23-fold fold lower than Ad5 wt. This wide range of cytotoxicity is unexpected, as they all have the same oncolytic backbone (i.e. the same E1A modification). However, a pattern of cytotoxicity can be observed in all prostate cancer cell lines, whereby vPS1364 is the most oncolytic and vPS1366 is the least oncolytic vector. Lytic activity of the remaining vPS136X vectors fall in-between vPS1364 and vPS1366, however vPS1362 and vPS1365 are consistently more cytotoxic than vPS1361 and vPS1363. The cytotoxicity of vNR6 is equivalent to that of vPS1364 in 22RV1 and PC3 cells, but is almost 10-fold less lytic than vPS1364 in DU145 cells.

In MRC5 cells vPS1365 was the most lytic vector (3-fold lower than Ad5 wt), followed by vPS1361, vPS1364, vPS1362 and vPS1363 (4-, 6-, 9- and 13-fold lower than Ad5 wt, respectively); with vPS1366 is the least cytotoxic to MRC5 cells, with an EC50 value 18-

fold lower than Ad5 wt. All vPS136X vectors were significantly more cytotoxic to both prostate and MRC5 cells than would be anticipated from the equivalent data with vMH6 and vMH7 (see section 4.3.2).

The therapeutic index of each vector was calculated to assess the tumour selectivity (Figure 5-4).

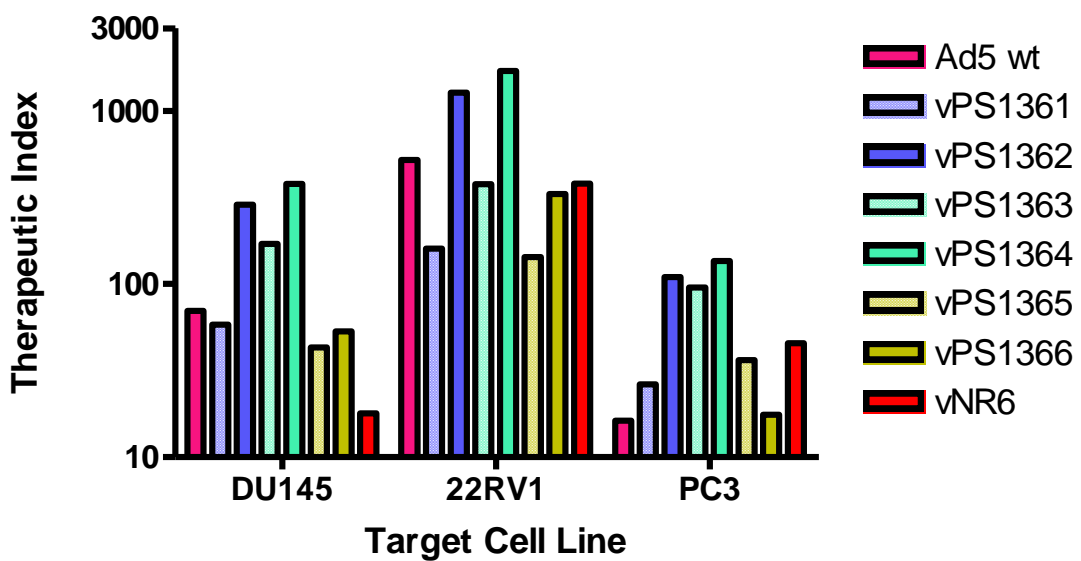


**Figure 5-4. Therapeutic index values for vPS136X vectors**

The therapeutic index for each virus was calculated in DU145, 22RV1 and PC3 cells by dividing the MRC5 EC50 value by the target prostate cell line EC50 value.

A large variation in TI can be observed across the range of vPS136X vectors. However in all three prostate cell lines vPS1364 had the highest therapeutic index, followed by vPS1362, both of which were the only vectors to have TI consistently higher than vNR6 and Ad5 wt.

Since each vector has the same oncolytic backbone, i.e. the same E1A modifications, it was anticipated that all RGD-retargeted vectors would have similar oncolytic activities and TI values, as would all wt fibre vectors. Only vPS1366 showed EC50 values similar to those previously observed with vMH6 and vMH7, while the other vPS136X vectors were significantly more cytotoxic. Furthermore, whereas no vMH vector had TI greater than Ad5 wt in DU145 and 22RV1 cells (see Figure 4-3), both vPS1362 and vPS1364 show TI higher than that of Ad5 wt.

#### **5.4.3 vMH6/7 vs vPS136X Vectors**

If cytotoxicity was entirely due the lytic activity of the virus, all vPS136X vectors would be expected to show lytic activities similar to that of vMH6 and vMH7. However all vPS136X vectors, with the exception of vPS1366, demonstrated EC50 values lower than were previously observed with vMH6 and vMH7. To directly compare the lytic activities of vPS136X vectors with vMH6 and vMH7, virus induced cytotoxicity was measured in DU145. Cells in 96-well plates were infected with  $1 \times 10^{-2}$  to  $3 \times 10^2$  PFU/cell of Ad5 wt, Ad-GFP, vMH6, vMH7 and vPS136X vectors (as described in section 2.4.8) and cell survival measured 5 days post infection by AP assay. Dose response curves are shown in Figure 5-5 and EC50 values in Table 5-3.

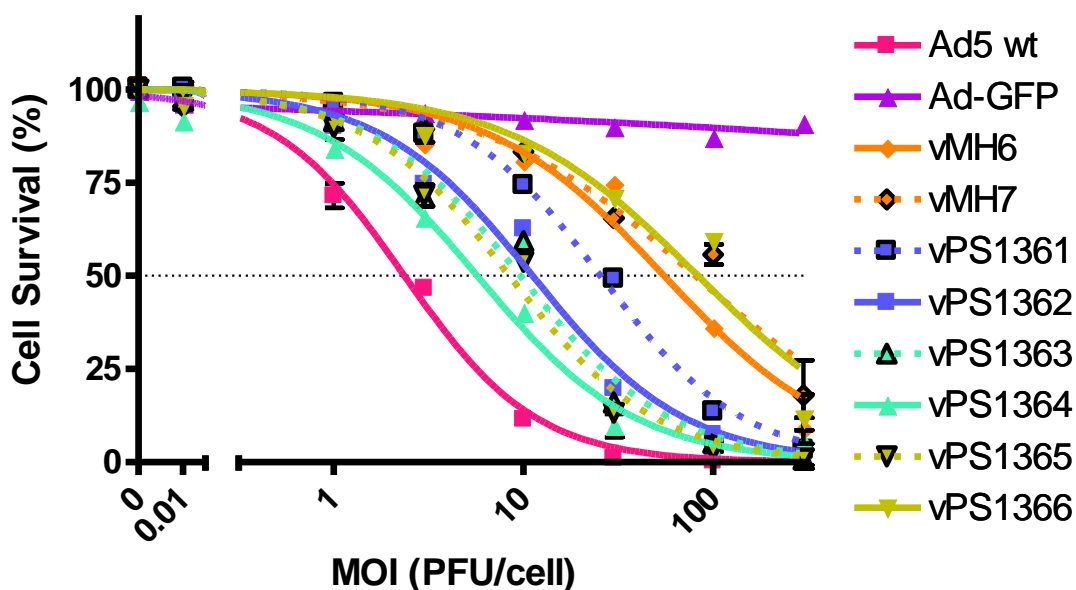


**Figure 5-5. Cytotoxicity of vPS136X vs vMH6 and vMH7 in DU145 cells.**

DU145 cells were seeded in 96-well plates at  $3 \times 10^4$  cells per well. Triplicate wells were infected with serial dilutions of Ad5 wt, Ad-GFP, vMH6, vMH7 and vPS136X vectors as described in section 2.4.8. Cell survival was measured 5 days post infection by AP assay and normalised to mock infected cells (100% survival) and empty wells (0% cell survival). Plots show mean cell survival from triplicate wells ( $n=1$ ),  $\pm$  S.D. (where no error bars are visible S.D. was  $<5\%$ ), and fitted sigmoid dose response curves. Dose response curves were used to calculate EC50 values.

Virus	EC50 values (95% C.I.)
Ad5 wt	2.37 (2.18 - 2.57)
Ad-GFP	$>3000$
vMH6	55.4 (42.6 - 71.9)
vMH7	80.8 (62.0 - 106)
vPS1361	25.6 (23.5 - 27.9)
vPS1362	11.2 (9.64 - 13.1)
vPS1363	9.67 (8.19 - 11.4)
vPS1364	5.73 (4.88 - 6.72)
vPS1365	8.46 (7.36 - 9.72)
vPS1366	83.6 (62.8 - 111)

**Table 5-3. EC50 values with 95% C.I. (PFU/cell) for vPS136X vs vMH6 and vMH7**

As was previously observed in section 4.3.2, vMH6 and vMH7 show a greater than 20-fold reduction in lytic activity compared to Ad5 wt. vPS1366 shows cytotoxicity equivalent to vMH6 and vMH7, with no significant difference in the EC50 values. All other vPS136X vectors have EC50 values between that of vMH7 and Ad5 wt, with a range of EC50 values 2-10 fold lower than vMH6 and vMH7.

#### **5.4.4 vPS136X NTR Expression**

The experiments above demonstrated the vPS136X vectors were significantly more cytotoxic than equivalent eGFP expressing vectors vMH6 and vMH7. This observation could be explained by high levels of NTR expression, resulting in additional 'background' cytotoxicity. It was therefore decided to investigate the level of NTR expression in vPS136X vectors and vNR6 by western blot. 24-well plates of DU145 cells were infected with 10 PFU/cell of vNR6 or vPS136X vectors as described in section 2.4.8. Total protein was harvested at 16, 24 and 48 hours post infection and prepared for western blotting. Blots were probed for NTR and  $\beta$ -tubulin (loading control) using unconjugated primary antibodies with appropriate species-specific HRP-labeled secondary antibodies (all described in section 2.8). Recombinant purified NTR produced in *E.coli* (kindly donated by Dr S. Vass) was analysed alongside to act as a positive control and reference sample.

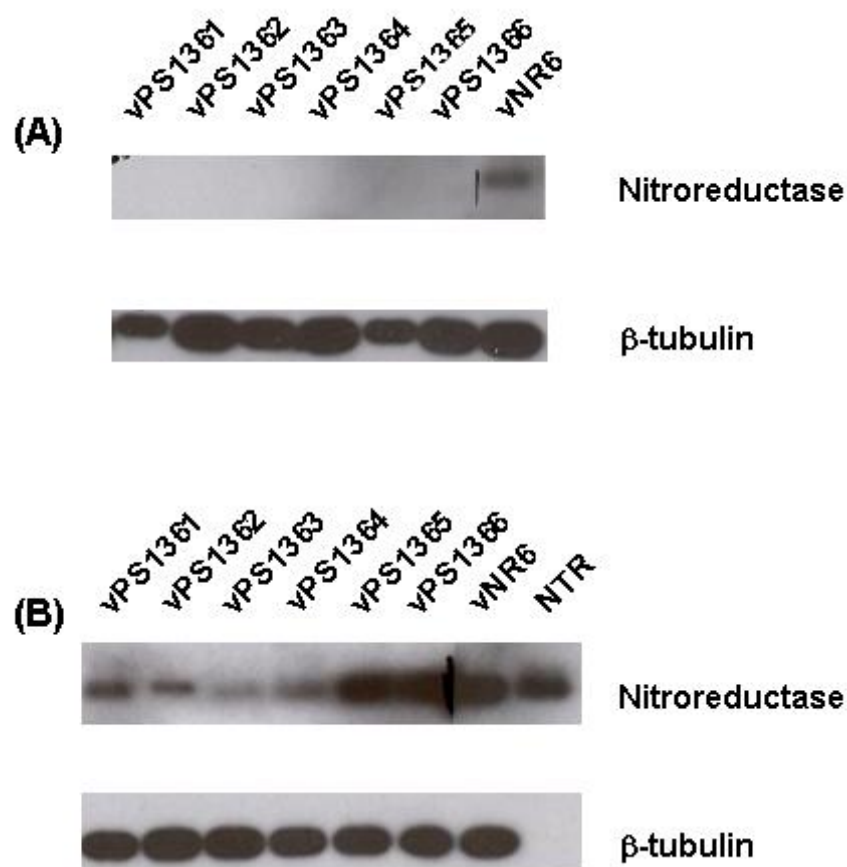


**Figure 5-6. Western blot of NTR expression in vPS136X and vNR6**

DU145 cells seeded at  $1 \times 10^5$  cells per well in 24-well plates were infected with 10 PFU/cell of vNR6 or vPS136X vectors as described in section 2.4.8. Total protein was harvested from wells at 24 (A) and 48 (B) hours post infection, 2.5ng of each sample separate by SDS-PAGE and western blotted, as described in section 2.8. Blots were probed for NTR and  $\beta$ -tubulin expression (loading control).

No NTR expression was observed with any vector at 16 hours post infection (data not shown). Figure 5-6 shows the western blots at 24 and 48 hours post infection for all vPS136X vectors and vNR6. Clear NTR expression was observed with vNR6 at 24 hours post infection, but not with the vPS136X vectors. At 48 hours post infection NTR was detected with all vectors, with a range of expression levels evident from the vPS136X vectors. Of all the vPS136X vectors, vPS1365 and vPS1366 expressed the most NTR,

followed by vPS1361, vPS1362, vPS1364, with vPS1363 expressing the least amount of NTR. Furthermore, at 48 hours post infection, NTR expression from vNR6 was greater than from vPS1361-4, and similar to that of vPS1365 and vPS1366.

All vPS136X vectors express NTR from the same splice acceptor site, the presence of which was confirmed by PCR sequencing (data not shown), and therefore were expected to express equivalent amounts of NTR. No correlation was observed between NTR expression and P:I ratios. Furthermore, there was no clear correlation between oncolytic cytotoxicity and NTR expression.

#### **5.4.5 vPS136X E1A Expression**

Each vPS136X vector demonstrated different cytotoxicities and NTR expression, despite the fact they were all derived from the same left end plasmid. Both virus lytic activity and transgene expression are related to E1A expression levels thus both of these observations could be explained by difference in E1A levels. It was therefore decided to investigate E1A protein expression of the 6 vPS136X viruses.

DU145 cells plated in 24-well plates were infected with 10 PFU/cell of vPS136X vectors or Ad5 wt as described in section 2.4.8. At 8, 16 and 24 hours post infection total protein was harvested and prepared for western blotting. Blots were probed for E1A and  $\beta$ -tubulin (loading control) using unlabelled primary antibodies with HRP-labelled species-specific secondary antibodies and detected using an ECL kit (as described in section 2.8.4).

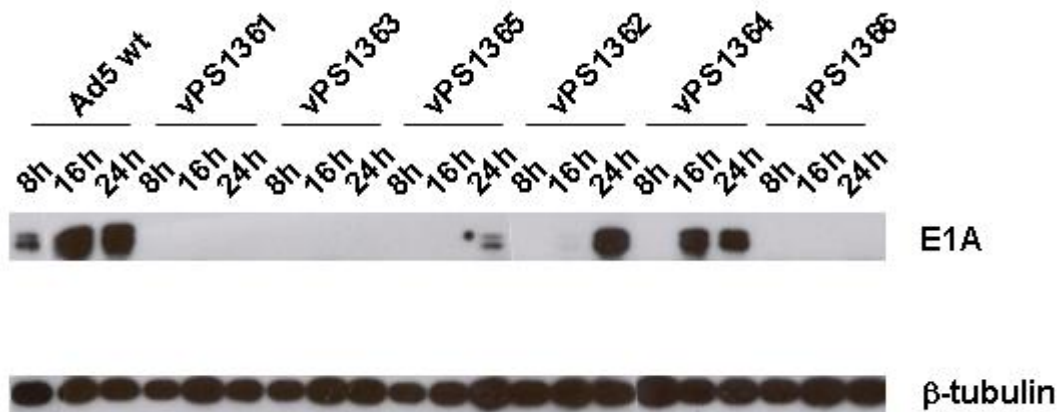


**Figure 5-7. Western blot for E1A expression in vPS136X vectors**

DU145 cells seeded at  $1 \times 10^5$  cells per well in 24-well plates were infected with 10 PFU/cell of Ad5 wt or vPS136X vectors as described in section 2.4.8. Total protein was harvested at 8, 16 and 24 hours post infection, 2.5 $\mu$ g of each sample separate by SDS-PAGE and western blotted, as described in section 2.8. Blots were probed for E1A and  $\beta$ -tubulin expression (loading control).

Figure 5-7 shows the E1A expression from each vPS136X vector and Ad5 wt at 8, 16 and 24 hours post infection. E1A expression was clearly seen with Ad5 wt at all three timepoints. No E1A expression was detected for vPS1361, 3 and 6 at any of the timepoints, even after prolonged exposure (data not shown). In contrast E1A expression was observed for vPS1362, 4 and 5. vPS1364 had a detectable level of E1A 16 hours post infection, which was maintained at 24 hours. For vPS1362 and vPS1365, E1A was only detectable at 24 hours post infection, with vPS1362 expressing significantly more than vPS1365.

The different levels of E1A expression between vPS136X vectors is somewhat unexpected, as all vectors have E1A driven by the same ICOVIR-7 promoter. There was no clear correlation between E1A expression and NTR expression or P:I ratio. However, the differential E1A expression does correlate with the oncolytic activity; the vectors expressing the most E1A have the lowest EC50 values in prostate cancer cell lines (see Table 5-2 for EC50 values).

#### **5.4.6 vPS136X ICOVIR-7 Promoter Sequencing**

All vPS136X vectors were created by homologous recombination using the same batch of the left end plasmid pICOVIR-7, which was also used for construction of vMH6 and vMH7. All vPS136X vectors were shown to be free of contaminating wt E1A sequences by PCR screening (performed by Dr P. Searle and E. Hodgkins, data not shown). Despite this, the vPS136X vectors expressed different levels of E1A protein. To investigate whether this difference was a result of unintentional mutations acquired within the region controlling E1A expression, the ICOVIR-7 promoter region in each vPS136X virus was sequenced. Sequencing was performed as described in section 4.3.8.

All vPS136X vectors were shown to have an ICOVIR-7 promoter sequence identical to that found in vMH6 and vMH7 (see section 4.3.8 and appendix 2). This sequence includes the base changes identified in vMH6, vMH7 and the plasmid pICOVIR-7, located at the cloning junctions in the construction of pICOVIR-7 (discussed in section 4.4.2). Therefore the differential E1A expression was not due to a mutation within the ICOVIR-7 promoter insertion. However the possibility of unintentional mutations elsewhere in the vectors genome still exists (discussed in section 5.5.3).

#### **5.4.7 Cytotoxicity of vPS136X Vectors with CB1954**

To investigate the NTR/CB1954 mediated cytotoxicity with the vPS136X vectors, DU145 cells plated in 96-well plates were infected with Ad-GFP, vNR6 or vPS136X at 3 or 10 PFU/cell (as described in section 2.4.8). 48 hours post infection the medium was replaced with 200µl of fresh infection medium containing 1-1000µM of CB1954. Cells were incubated with prodrug for 16 hours before the CB1954 was removed and replaced with 200µl of fresh infection medium. At 120 hours post infection (96 hours after prodrug exposure) cell survival was measured by AP assay. The data was normalised to empty wells

(0% viability) and infected cells with no CB1954 (100% viability) to assess the NTR/CB1954 mediated cytotoxicity. Dose response curves are shown in Figure 5-8 with EC50 values in Table 5-4.

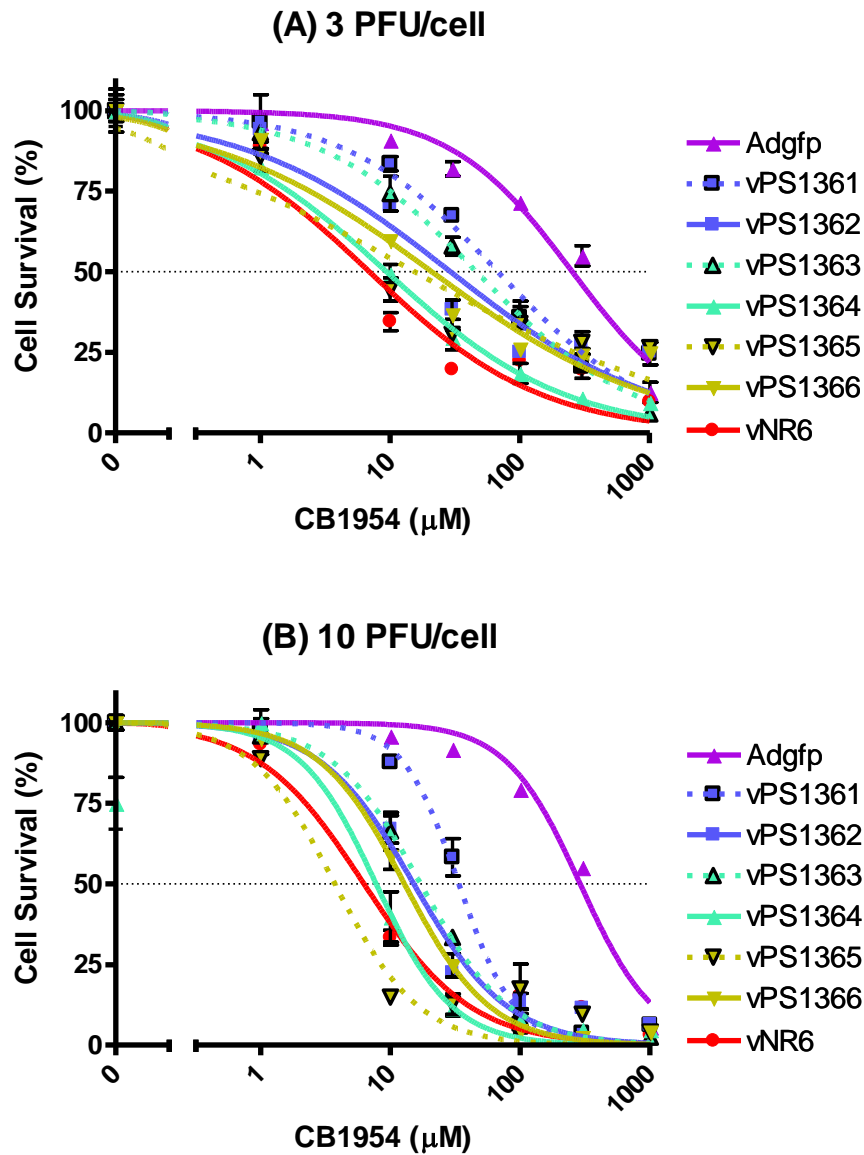


**Figure 5-8. Dose response curves for 16 hour CB1954 exposure**

DU145 seeded in 96-well plates at  $3 \times 10^4$  cells per well before infection with Ad-GFP, vPS136X vectors or vNR6 at 3 PFU/cell (A) or 10 PFU/cell (B), as described in section 2.4.8. 48 hours post infection the virus was removed and replaced with 200 $\mu\text{l}$  of infection medium containing 1-1000 $\mu\text{M}$  CB1954. Cells were incubated with prodrug for 16 hours at 37°C before the CB1954 was removed, wells washed and replaced with 200 $\mu\text{l}$  of fresh infection medium. Cell survival was measured 5 days post infection by AP assay and normalised to infected cells with no prodrug (100% survival) and empty wells (0% cell survival). Plots show mean cell survival from triplicate wells ( $n=3$ ),  $\pm$  S.D. (where no error bars are visible S.D. was  $<5\%$ ), and fitted sigmoid dose response curves. Dose response curves were used to calculate EC50 values.

<b>Virus</b>	<b>3 PFU/cell 16 hour CB1954</b>	<b>10 PFU/cell 16 hour CB1954</b>
<b>Ad-GFP</b>	254 (205 - 315)	289 (254 - 329)
<b>vPS1361</b>	67.6 (50.8 - 89.8)	33.7 (30.5 - 37.2)
<b>vPS1362</b>	29.2 (18.9 - 45.1)	15.1 (12.5 - 18.4)
<b>vPS1363</b>	46.3 (40.7 - 52.6)	17.1 (15.9 - 18.4)
<b>vPS1364</b>	9.39 (7.91 - 11.2)	7.76 (5.28 - 11.4)
<b>vPS1365</b>	15.4 (7.98 - 29.9)	3.74 (2.53 - 5.51)
<b>vPS1366</b>	21.0 (14.1 - 31.2)	12.8 (11.8 - 13.9)
<b>vNR6</b>	6.92 (4.37 - 11.0)	6.25 (4.72 - 8.29)

**Table 5-4. EC50 values with 95% C.I. (PFU/cell) after 16 hours CB1954 exposure**

Greater sensitisation to CB1954 was observed at the higher MOI of 10 PFU/cell. At 3 PFU/cell (Figure 5-8A), vNR6 showed the greatest sensitisation to CB1954, closely followed by vPS1364 (double mutant NTR, wt fibre vector). Both triple mutant viruses, vPS1365 and vPS1366, showed the third greatest sensitisation to CB1954, followed by vPS1363 and finally vPS1361.

At 10 PFU/cell (Figure 5-8B), vPS1365, vNR6 and vPS1364 showed the greatest sensitisation to CB1954, with no significant difference between the three vectors. vPS1366, vPS1362 and vPS1363 are next and showed similar levels of sensitisation. Again vPS1361 showed the least sensitisation to CB1954.

The data above is normalised to infected cells with no CB1954 and therefore only assesses the NTR/CB1954 mediated cytotoxicity, not taking into account the intrinsic oncolytic activity of the virus. To investigate the combined oncolytic activity and NTR/CB1954 mediated cytotoxicity of each vector, the same data was normalised to empty wells (0% viability) and mock infected cells (100% viability); the results are shown in Figure 5-9.

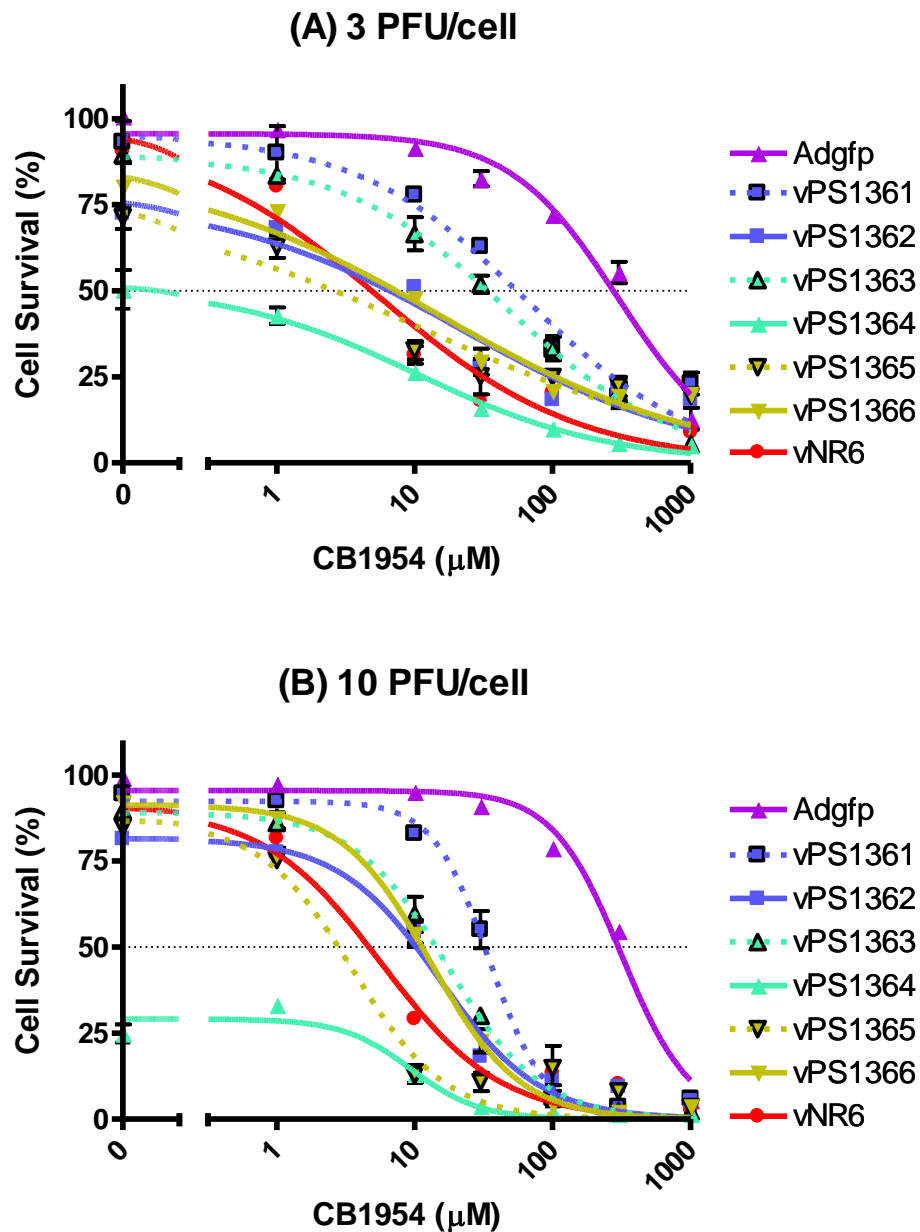


**Figure 5-9. Dose response curves for combined cytotoxicity with 16 hour CB1954 exposure**

The same data is presented as in Figure 5-8, but normalised to mock infected cells (100% survival) and empty wells (0% survival), to assess the combined oncolytic and NTR/CB1954 mediate cytotoxicity. Plots show mean cell survival from triplicate wells ( $n=1$ ),  $\pm$  S.D. (where no error bars are visible S.D. was  $<5\%$ ), and fitted sigmoid dose response curves.

At both MOIs, vPS1364 showed more cytotoxicity in the absence of prodrug compared to all the other vectors, which achieved <20% cell death in the absence of prodrug.

Looking at the combined effect, vPS1364 was the most cytotoxic vector at both MOIs, followed by vPS1365, which showed less lytic activity in the absence of prodrug, but gave a greater sensitization to prodrug. vPS1361 showed the least combined cytotoxicity at both MOIs, requiring the highest prodrug concentration of all NTR expressing vectors to reach 100% cell death.

The above experiments used a 16 hour prodrug exposure. A recent phase I/II clinical trial using the NTR/CB1954 enzyme/prodrug system in a replication deficient Ad vector, observed the concentration of CB1954 in patient plasma peaked 6 minutes post administration (mean peak concentration of 7.8 $\mu$ M, S.D. 3.1 $\mu$ M) and had completely cleared after 4-6 hours [Patel et al, 2009]. Thus, a 16 hour prodrug exposure time is far greater than the maximum prodrug exposure time observed physiologically. It was therefore decided to investigate the NTR/CB1954 mediated cytotoxicity after a shorter (4 hour) prodrug exposure. The experiment as described above was repeated infecting the cells with 10 PFU/cell of Ad-GFP, vNR6 or vPS136X vectors, with a 4 hour prodrug exposure (1-1000 $\mu$ M). Cell survival was measured 5 days post infection by AP assay. The data was normalised to empty wells (0% survival) and infected cells with no prodrug (100% survival) to analyse the NTR/CB1954 mediated cytotoxicity. Dose response curves are shown in Figure 5-10, with EC50 values in Table 5-5.

The same data was also normalised to mock infected cells (100% survival) and empty wells (0% survival) to ascertain the combined oncolytic activity and NTR/CB1954 mediated cytotoxicity (Figure 5-11).

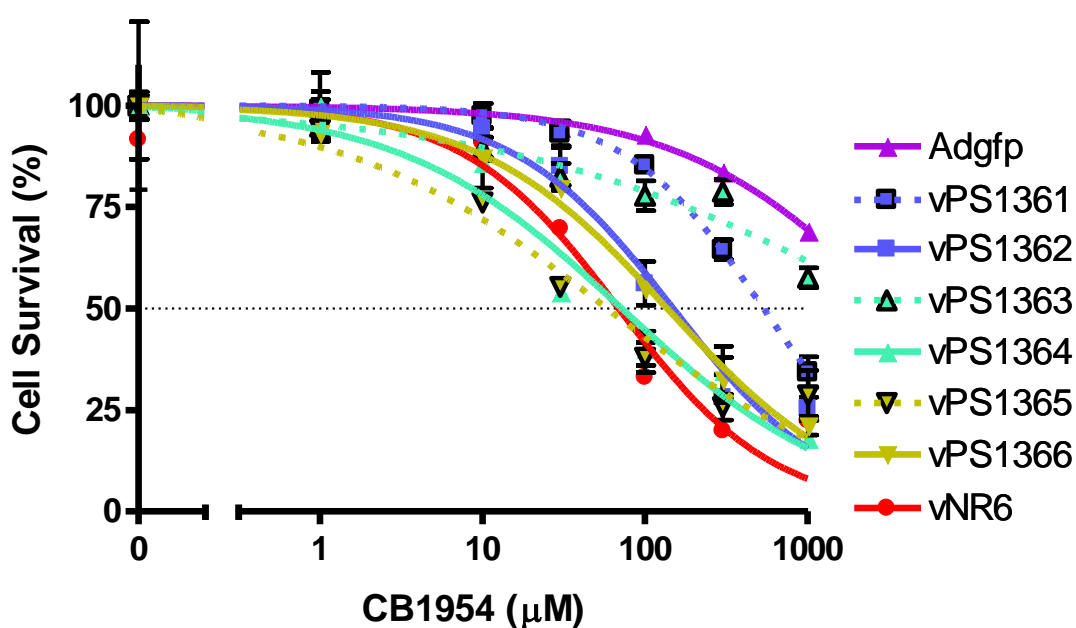


**Figure 5-10. Dose response curves for 4 hour CB1954 exposure**

DU145 were seeded in 96-well plates at  $3 \times 10^4$  cells per well before infection with Ad-GFP, vPS136X vectors or vNR6 at 10 PFU/cell, as described in section 2.4.8. 48 hours post infection the virus was removed and replaced with 200 $\mu$ l of infection medium containing 1-1000 $\mu$ M of CB1954. Cells were incubated with prodrug for 4 hours at 37°C before the CB1954 was removed, wells washed and replaced with 200 $\mu$ l of fresh infection medium. Cell survival was measured 5 days post infection by AP assay and normalised infected cells with no prodrug (100% survival) and empty wells (0% cell survival). Plots show mean cell survival from triplicate wells (n=3),  $\pm$  S.D. (where no error bars are visible S.D. was <5%), and fitted sigmoid dose response curves. Dose response curves were used to calculate EC50 values.

Virus	10 PFU/cell 4 hour CB1954
Ad-GFP	>1000
vPS1361	535 (490 - 585)
vPS1362	149 (120 - 184)
vPS1363	>1000
vPS1364	71.8 (47.1 - 110)
vPS1365	58.4 (43.4 - 78.5)
vPS1366	137 (119 - 158)
vNR6	68.8 (52.2 - 90.6)

**Table 5-5. EC50 values with 95% C.I. (PFU/cell) for 4 hour CB1954 exposure**

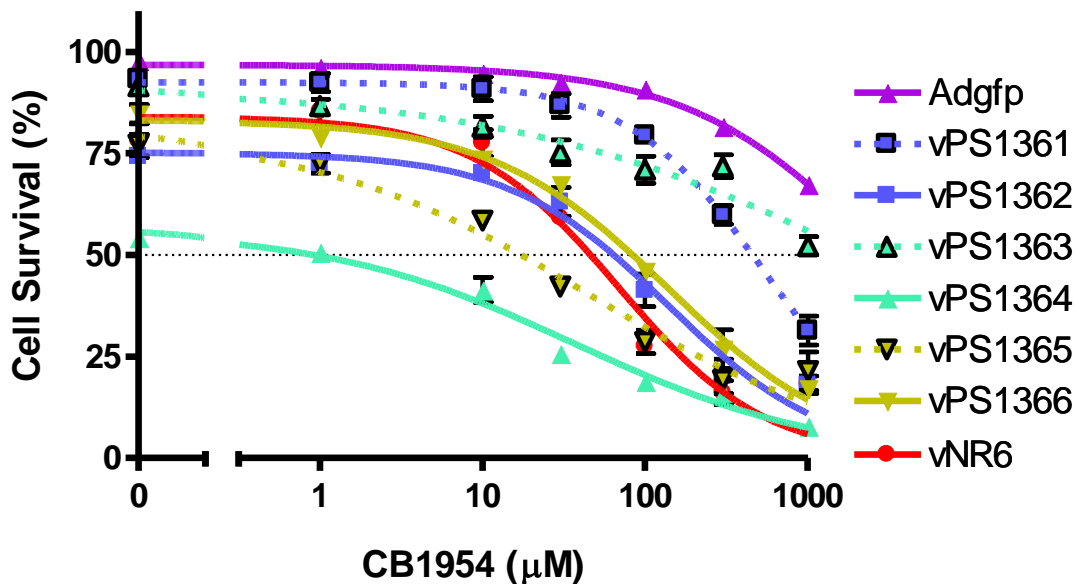


**Figure 5-11. Dose response curves for combined cytotoxicity with 4 hour CB1954 exposure**

The same data is presented as in Figure 5-10 but normalised to mock infected cells (100% survival) and empty wells (0% survival), to assess the combined oncolytic and NTR/CB1954 mediated cytotoxicity. Plots show mean cell survival from triplicate wells ( $n=1$ ),  $\pm$  S.D. (where no error bars are visible S.D. was  $<5\%$ ), and fitted sigmoid dose response curves.

Looking at the NTR/CB1954 mediated cytotoxicity (Figure 5-10), vPS1365, vPS1364 and vNR6 showed the greatest cytotoxicity, all with no significant difference between the EC50 values, ranging from 58-72 $\mu$ M (Table 5-5). These are followed by vPS1362 and vPS1366, both with EC50 values of approximately 140 $\mu$ M, and finally vPS1361 and vPS1363 with EC50 values of 500 $\mu$ M and 1000 $\mu$ M respectively.

The same pattern of virus oncolytic activity was observed, with only vPS1364 demonstrating 45% cell death and all other vectors showing  $<25\%$  cell death in the absence of prodrug (Figure 5-11). vPS1364 also showed the greatest combined effect, with 50% cell death at 1 $\mu$ M CB1954, however most of this cytotoxicity was from virus oncolytic activity.

vPS1365 was the second most cytotoxic vector, with 50% cell death achieved at approximately 18 $\mu$ M CB1954. vPS1361 and vPS1363 were the least cytotoxic vectors, requiring 450 $\mu$ M and >1000 $\mu$ M CB1954 to achieve 50% cell death, respectively.

At both MOIs and both prodrug exposure times vPS1364 showed the greatest combined cytotoxicity; followed by vPS1365 and vNR6. By looking at the NTR/CB1954 mediated cytotoxicity alone it was clear the additional cytotoxicity observed with vPS1364 over vPS1365 and vNR6 was due to a greater oncolytic activity as opposed to a greater NTR/CB1954 mediated cytotoxicity. vPS1362 and vPS1366 gave the next greatest combined cytotoxicity, with little difference between them. At both MOI and prodrug exposure times vPS1363 and vPS1361 showed the least combined cytotoxicity.

With respect to the NTR/CB1954 associated cytotoxicity, a clear pattern was observed, with vPS1365 and vPS1364 showing the greatest toxicity of all vPS136X vectors, equal to that of vNR6. This was followed by vPS1361 and vPS1366 and finally vPS1361 and vPS1363, both of which showed little sensitisation to CB1954 at the lower MOI and shorter CB1954 exposure time.

## **5.5 Discussion**

### **5.5.1 Construction of vPS136X Vectors and P:I Ratios**

Six new oncolytic Ad vectors expressing NTR or NTR mutants (vPS131-6) were constructed based on the ICOVIR-7 oncolytic backbone. All vectors possessed acceptable P:I ratios ratios in the range of 10-110, comparable to that of the E1B-55K deleted NTR expressing vector vNR6. Previous attempts to recover replication defective Ad vectors expressing some of the triple NTR mutants from the CMV promoter have been

unsuccessful, probably because high level expression of the mutant NTR affected virus growth, resulting in low yield and high P:I ratios (Dr P. Searle, personal communication). However the late transgene expression in the vPS136X vectors did not have any significant detrimental effect on virus production.

Work in CHAPTER 3 with eGFP expressing vectors found a positive correlation between increasing genome size and increasing P:I ratio with all batches of the ICOVIR-7 based vectors (vMH6 and vMH7) having the largest genomes and P:I ratios of approximately 100. One explanation is that the increase in genome size may lead to a reduction in virus packaging efficiency, resulting in lower infectious vector concentrations and higher P:I ratios (discussed in section 3.6.2). Three vP136X vectors (vPS1361, 4 and 5) have P:I ratios at the upper limit of the acceptable range, of approximately 100, whereas vPS1362, 3 and 6 have P:I ratios between 35 and 62. Figure 5-12 plots the vector P:I ratio against the vector genome size, combining the observations with all batches of vMH and vPS136X vectors plus Ad5 wt.

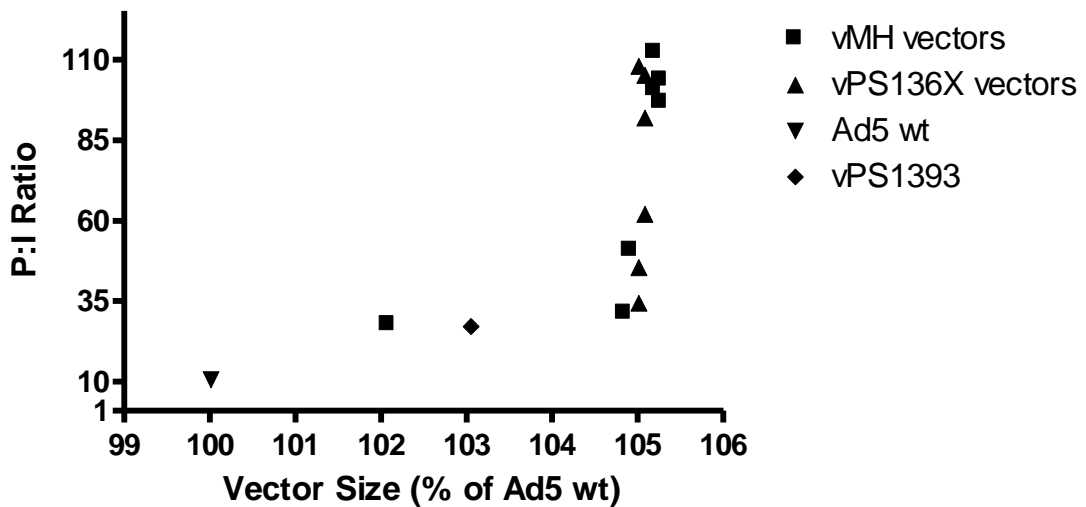


**Figure 5-12. Scatter plot of vector size vs P:I ratio**

The P:I ratio of the banded stocks of Ad5 wt, vMH vectors and vPS136X vectors was plotted against the vector genome size relative to Ad5 wt. For each data point n=1. GraphPad software was used to perform Spearman rank analysis (Spearman rank = 0.9762 and p=0.0004)

Spearman rank analysis of the combined vMH and vPS136X vector observation shows a positive correlation between increase in virus genome size and P:I ratio (Spearman rank = 0.9762, p value = 0.0004), similar to the previous observations for the vMH vectors (discussed in section 3.6.2). Bett *et al* previously suggested a relatively tight Ad packaging limit between 104.6% and 105.4% of Ad5 wt [Bett et al, 1993]. All ICOVIR-7 based vectors (vMH6, vMH7 and vPS136X vectors) have genomes between 105% and 105.25% of Ad5 wt and it is tempting to speculate the increase in P:I ratio is a result of reduced packaging efficiency, thus reducing the infectious virus yields. However there does not appear to be any hard limit as all ICOVIR-7 vectors could be easily grown and worked with. It also important to remember this study was not designed to investigate viral packaging limits and a more detailed study would be required to make a full correlation

between virus genome size and packaging efficiency. Furthermore, if virus genome packaging was a problem it would be anticipated the vectors would undergo rearrangements and deletions to reduce genome size, possibly within regions not required for *in vitro* culture, such as the E3 region. However all vectors had the predicted restriction profile, demonstrating they had not undergone any major rearrangements or deletions, however these may become apparent at higher passage number. It is therefore possible the increase in P:I ratios observed is not entirely due to vector genome size, however in my opinion it is likely the packaging limit contributes to the higher P:I ratio of the viruses with larger genomes. It is also essential to note all plaque assays were performed on DU145 cells and up to a 5-fold greater number in plaques has been observed with the vPS136X vectors on HEK293 cells (data not shown). For a more rigorous comparison of P:I ratios between vMH or vPS136X vectors and any replication deficient vector, HEK293 cells should be used, not the DU145 values presented in this study.

### **5.5.2 vPS136X Cytotoxicity and Therapeutic Index**

All vPS136X vectors are based around the same oncolytic ICOVIR-7 backbone and were therefore expected to show similar levels of cytotoxicity and tumour cell selectivity. The eGFP expressing ICOVIR-7 based vectors, vMH6 and vMH7, show similar cytotoxicities to both tumour cells and fibroblasts, with a 3-, 20- and 30- fold reduction in lytic activity relative to Ad5 wt in PC3, 22RV1 and DU145 cells respectively, and no toxicity to MRC5 cells.

In contrast to this expectation, lytic activity with vPS136X vectors ranged from equal to Ad5 wt to a 28-fold reduction in lytic activity. In addition, there was no clear correlation between RGD-retargeted and equivalent wt fibre vectors. Table 5-6 shows the vPS136X

vectors and vNR6, ranked 1-7 for oncolytic activity, tumour selectivity, relative E1A and NTR expression, NTR/CB1954 mediated cytotoxicity and combined cytotoxicity.

<b>Virus</b>	<b>P:I ratio</b>	<b>E1A</b>	<b>NTR</b>	<b>Oncolytic Activity</b>	<b>TI</b>	<b>NTR/CB1954 Cytotoxicity</b>	<b>Combined Cytotoxicity</b>
vNR6	64.2	n/d	= 1	4	= 4	= 1	3
vPS1361	92.2	Neg	4	= 5	= 6	6	7
vPS1362	45.8	2	5	= 2	2	= 4	= 4
vPS1363	62.3	Neg	7	= 5	3	6	6
vPS1364	108.2	1	6	1	1	= 1	1
vPS1265	105.4	3	= 1	= 2	= 6	= 1	2
vPS1366	34.7	Neg	= 1	7	= 4	= 4	= 4

**Table 5-6. Rank scoring from 1 - 7 (most - least) of vPS136X vectors**

A clear pattern of lytic activity can be observed with the vPS136X vectors, with vPS1364 being most lytic in all prostate cancer cell lines, followed by vPS1362 and vPS1365. This pattern is slightly different in MRC5 cells, with vPS1365 being most lytic, followed by vPS1364 and then vPS1362. Both vPS1361 and vPS1363 show similar lytic activities in all cell lines, and vPS1366 is consistently the least lytic vector.

The TI was used to give an indication of vector tumour selectivity. Once again it was anticipated the three RGD-retargeted vectors would show a similar therapeutic index, as would the three wt fibre vectors. However a wide range of TI was observed across the panel of vPS136X vectors. vPS1364 (wt fibre, double mutant NTR) was shown to be the most selective vector in all the prostate cancer cell lines tested. This was followed by vPS1362 (wt fibre, wt NTR) and vPS1363 (RGD-retargeted fibre, double mutant NTR). In addition these are the only three vectors which had TIs greater than vNR6 in all prostate tumour cell lines. Furthermore, vPS1364 and vPS1362 showed TIs greater than Ad5 wt in all prostate cell lines, whereas no vMH vector showed TI greater than Ad5 wt in DU145 and 22RV1

cells (discussed in section 4.4.1). No consistent pattern could be observed with the remaining vectors; vPS1361, 5 and 6.

It is not clear why a range of lytic activities was observed with the vPS136X vectors, nor why they showed cytotoxicity greater than vMH6 or vMH7. As has been previously discussed, both vector genome size and the replacement of eGFP with NTR may result in the additional cytotoxicity observed with vPS136X vectors, compared with vMH6 and vMH7. However, there was a direct correlation between vPS136X oncolytic activity and E1A expression, whereby vPS1364 was the most oncolytic and expressed the most E1A, followed by vPS1362 which expressed the second highest amount of E1A and was the second most oncolytic, and finally vPS1365 being the third most oncolytic and the only other vPS136X vector to have detectable levels of E1A. No E1A was detected with vPS1361, 3 and 6 which were the least cytotoxic. The differential E1A expression is discussed fully in section 5.5.3 below.

From the data presented in this thesis it is not possible to ascertain to what extent these factors contribute to the range of oncolytic activities observed with the vPS136X vectors or the additional cytotoxicity over vMH6 and vMH7. Cytotoxicity experiments with HEK293 cells may help to eliminate some variation in the E1A expression between vPS136X vectors, thus elucidating more information regarding the NTR associated cytotoxicity.

Ideally for a direct comparison with vMH6 and vMH7 to assess the NTR associated increase in cytotoxicity, each vPS136X virus would have been constructed by reverse engineering, directly replacing the eGFP ORF in the vMH vectors with that of NTR or NTR mutants. This would allow assessment of any additional cytotoxicity directly from the NTR, as any base changes in vMH vectors would be transferred into all the vPS136X vectors.

However this method is substantially more time consuming and the vectors would still have to be cultured and plaque purified, allowing opportunity for additional mutations to be accumulated.

### **5.5.3 E1A Expression and Promoter Sequencing**

All vPS136X vectors are based on the ICOVIR-7 left end backbone, and thus have the wt E1A promoter replaced by the tumour-specific ICOVIR-7 promoter. Furthermore, all vPS136X vectors were recovered using the same stock of left end plasmid, pICOVIR-7, as were vMH6 and vMH7. It was therefore expected that all vPS136X would express similar levels of E1A protein. As shown in Figure 5-7, a range of E1A protein expression levels was detected in the panel of vPS136X vectors, summarised in Table 5-6, with vPS1364 showing the highest level of E1A expression, followed by vPS1362 and vPS1365. No E1A was detected with vPS1361, 3 and 6. All vPS136X vectors were screened by PCR to confirm the absence of contaminating wt E1A sequences. In addition the restriction profiles have been confirmed with HindIII, BglII and KpnI, demonstrating that all the banded stocks consisted predominantly of a virus with the correct ICOVIR-7 left end.

A clear positive correlation was observed between vPS136X oncolytic activity and E1A expression (discussed in section 5.5.2 above). However, the reason behind the differential E1A expression observed with vPS136X vectors is unknown. The promoter region controlling E1A expression (including the first 50bp of the E1A ORF) were sequenced and shown to be identical in all vPS136X vectors and identical to vMH6 and vMH7.

In CHAPTER 4 vMH7 was shown to produce less E1A RNA and protein than vMH6, resulting in delays in DNA replication and late gene expression. Several reasons were suggested for this difference including minor contamination with wt E1A sequences not detectable by standard PCR, an unintentional mutation introduced with vMH6 increasing

E1A expression, an unintentional mutation in vMH7 reducing E1A expression, or a direct interaction between the RGD-retargeted fibre and the ICOVIR-7 promoter (for a full discussion see section 4.4.2). All vectors were shown to be free of contaminating wt E1A CR2 region by PCR, but they were not PCR screened for the presence of the wt E1A promoter. Restriction enzyme profiling demonstrated the majority of the banded stocks contained the ICOVIR-7 left end; however this method is not as sensitive as PCR. It is therefore possible that low level contamination with virus containing the wt E1A promoter was responsible for the differential E1A expression. It would therefore in my opinion be informative to screen all vMH and vPS136X vectors for the presence of the wt E1A promoter by PCR. Since no delay in E1A RNA expression was observed with the other RGD-retargeted vector vMH5, it seems unlikely this delay was the result of an interaction between the RGD-retargeted fibre and the ICOVIR-7 promoter (for example, the RGD-fibre may activate an intracellular signalling pathway which is detrimental to ICOVIR-7 promoter activation). If the delay observed with vMH7 was due to an interaction between the RGD-retargeted fibre and ICOVIR-7 promoter it would be predicted that the same delay would be observed with other RGD-retargeted ICOVIR-7 based vectors. However no significant difference was observed in the DNA replication profiles of the RGD-retargeted vector vPS1361 and wt fibre vector vPS1362, both of which contain the same wt NTR transgene. This would suggest the delay in E1A expression and thus DNA replication observed with vMH7 is not common for all RGD-retargeted ICOVIR-7 vectors, and is probably not due to an interaction between the ICOVIR-7 promoter and the RGD-retargeted fibre. It is possible mutations have also arisen in vPS1361, 3 and 6 resulting in aberrant E1A expression, or in vPS1362, 4 and 5 resulting in increased E1A expression. If the results of vMH6 and vMH7 genome sequencing clearly indicate a mutation which would

explain the difference in E1A expression, it would perhaps be worth investigating vPS136X vectors for further mutations.

#### **5.5.4 NTR Expression and NTR/CB1954 Mediated Cytotoxicity**

As would be expected increasing the virus MOI (from 3 to 10 PFU/cell) and increasing the prodrug exposure time (from 4 to 16 hours) reduced cell survival. At both prodrug exposures, vPS1364 was the most cytotoxic combined therapy, followed by vPS1365 and vNR6 (see Table 5-6 for ranking). vPS1362 and vPS1366 showed combined cytotoxicity slightly lower than vNR6. vPS1363 and vPS1361 demonstrated the lowest cytotoxicity with combined therapy, which was most evident at lower MOI (3 PFU/cell with 16 hour prodrug exposure) and shorter prodrug exposure (10 PFU/cell with 4 hour prodrug exposure).

Normalisation of cell survival to virus infected cells in the absence of prodrug allows assessment of the NTR/CB1954 mediated toxicity alone, disregarding the virus oncolytic activity. By this criterion, vNR6, vPS1364 and vPS1365 gave the greatest sensitisation, as indicated by the lowest EC50 value (see Table 5-4 and Table 5-5) with no significant differences between them. vPS1363 and vPS1361 gave the least sensitisation to CB1954, which was barely above the negative control (Ad-GFP) at 10 PFU/cell and a 4 hour prodrug exposure or 3 PFU/cell and a 16 hour prodrug exposure. Taking into account these observations it can be concluded that the additional combined cytotoxicity observed with vPS1364 over vPS1365 and vNR6 originates from increased oncolytic activity. In contrast, vNR6 and vPS1365 show less oncolytic activity but possibly a slightly greater NTR/CB1954 mediated cytotoxicity. A recent phase I/II clinical trial using intravenous delivery of CB1954 showed a mean peak concentration of 7.8 $\mu$ M (S.D. 3.1 $\mu$ M) in patient serum, suggesting the local tumour concentration can not be greater than approximately 7.8 $\mu$ M [Patel et al, 2009]. With this in mind, the NTR/CB1954 mediated EC50 values for

vPS1364, vPS1365 and vNR6, which showed the greatest sensitisation to CB1954 following a 4 hour CB1954 incubation, were approximately 10-fold greater than the peak concentration observed in patients. Furthermore, at the CB1954 concentrations observed in patient serum these vectors only show about a 20% increase in cell death. It is therefore worth considering whether any of these CRAd vectors would provide any additional therapeutic benefit at clinically relevant prodrug concentrations compared to the oncolytic virus alone.

When looking specifically at the NTR/CB1954 mediated cytotoxicity it is also possible to assess the increase in sensitisation to CB1954 conferred by the NTR mutants relative to wt NTR. Previous *in vitro* studies by The University of Birmingham SCS-GT group, using the double and triple NTR mutants have demonstrated a 14- and 80-fold increase in sensitivity to CB1954 over wt NTR using replication defective vectors for gene delivery [Guise et al, 2007; Jaberipour et al, 2010]. With all vPS136X vectors the maximum increase in CB1954 sensitivity observed was approximately 10-fold, when comparing the EC50 values of vPS1361 (RGD-fibre, wt NTR) to vPS1365 (RGD-fibre, triple mutant NTR) at 10 PFU/cell. Furthermore, no vPS136X vector demonstrated significantly greater sensitisation to CB1954 than vNR6. Work in section 4.3.3 with the equivalent eGFP expressing vectors demonstrated, at 48 hours post infection, vMH6 and vMH7 expressed >10-fold more eGFP than vNR3, an E1B-55K deleted vector expressing eGFP from the pIX promoter. All vPS136X vectors were therefore expected to express more NTR than vNR6 at 48 hours post infection and consequently show greater sensitisation to CB1954 than vNR6. Contrary to this prediction, western blot analysis demonstrated no vPS136X vectors express more NTR than vNR6 at 48 hours post infection (see Table 5-6 for ranking of NTR expression), thus helping to explain the reduced efficacy in comparison to vNR6. It is also likely the range of

NTR expression observed contributes to the lower than expected increase in sensitisation to CB1954 observed with NTR mutant vectors, compared to their wt NTR expressing equivalents. However, there was no direct correlation between increased NTR expression and increased CB1954 sensitisation, (for example, vPS1362 expresses less NTR than vPS1366, but vPS1362 shows a >10-fold sensitisation to CB1954 compared to vPS1366, despite the fact vPS1366 contains the catalytically enhanced triple mutant NTR). It is important to note that the western blot and CB1954 sensitisation assays were performed at a single timepoint (48 hours post infection) and it is therefore possible that the level of NTR expression differs between the vPS136X viruses with time.

Two major questions remain; why did each vPS136X virus express a different level of NTR and why was the level of NTR expression lower than vNR6 at 48 hours post infection? There is no clear correlation between NTR expression and either vector P:I ratio or E1A expression (see Table 5-6). There was no significant difference between the DNA replication profiles of vPS1361 and vPS1362, suggesting the difference was not related to DNA replication. However it would be worth investigating the DNA replication profiles of the other vPS136X vectors. Jaberipour *et al* have previously observed lower expression levels with some NTR mutants compared to wt NTR, despite expression from an identical Ad vector [Jaberipour et al, 2010]. It was suggested that the mutations may affect mRNA stability or translation, and or reduced protein stability of the mutants as possibly contributing to the lower level of mutant NTR expression. It is possible that such factors play a role in the lower level expression observed with the double mutant NTR compared to wt NTR. However in contradiction, the triple NTR mutant shows the highest NTR

expression, thus other factors must be playing a role in the differential NTR expression observed between the vPS136X vectors.

There is no clear reason why vPS136X vectors express less NTR than vNR6. However, taking into account the above suggestions by Jaberipour *et al* a comparison can only be made between vPS1361/2 and vNR6, which express wt NTR: vPS1361 and vPS1362 expressed significantly less NTR than vNR6, at 48 hours post infection. The sequence of the NTR insert in all of these vectors has been confirmed by PCR sequencing, ruling out unintentional mutations in the insertion.

Gene expression from the Ad MLP is a complicated multi-factorial process, which is regulated by several host and viral proteins via promoter activation, RNA splicing, mRNA export and translation (discussed in section 1.2.2.1.4 and 1.2.2.3). Thus there are several levels at which NTR expression in vPS136X vectors could be controlled. Over-expression of NTR (and particularly NTR mutants) in Ad vectors is known to be somewhat toxic to the virus, causing low infectious virus titres and high P:I ratios (Dr P. Searle, personal communication). It is therefore possible, and in my opinion likely, that the culture and plaque purification of vPS136X vectors selected viruses with lower NTR expression, without affecting overall late protein expression. It would be interesting to screen plaques from the original 1<sup>o</sup> seed stocks for NTR protein expression and compare the level of NTR expression to other late viral proteins such as hexon or fibre. However, to prove this theory and find at which level NTR expression is controlled, detailed investigations into late RNA expression and protein production would be required. It is also worth noting that NTR expression in vPS136X vectors (or eGFP expression with vMH vectors) has not been directly demonstrated to be under MLP control or exactly how these transgenes are spliced from the MLTU. Since transgenes are inserted downstream of fibre it is possible for

splicing to include x, y and z leader sequences as well as the compulsory 1, 2 and 3 sequences, introducing the possibility of multiple splice variants and alternative pathways for mRNA maturation. However there were no indications from any experiments conducted with vPS136X or vMH vectors that transgene expression is not controlled by the MLP, and the timing of eGFP transgene expression with vMH vectors was similar to that of other Ad proteins expressed from the MLP, such as protein V (see Figure 4-4 and Figure 4-7 for eGFP and protein V expression, respectively).

## **5.6 Summary**

Six new oncolytic CRAAd vectors were constructed, based on the ICOVIR-7 backbone, which expressed either wt NTR, double mutant NTR or triple mutant NTR. These vectors have been characterised in terms of tumour selectivity, NTR/CB1954 mediated cytotoxicity, combined cytotoxicity, transgene and E1A expression. Of all these vectors vPS1364, expressing double mutant T41L N71S NTR with a wt fibre, demonstrated the highest tumour selectivity and greatest cytotoxicity, alone and in combination with the prodrug CB1954. Furthermore, this vector was more selective than vNR6, an  $\Delta$ E1B-55K vector expressing wt NTR, and demonstrated greater cytotoxicity in combination with the prodrug CB1954.

## **CHAPTER 6**

### **Summary and Future Work**

The work presented in this study has investigated oncolytic adenoviruses, in particular the ICOVIR based vectors from Dr R. Alemany's lab, armed with nitroreductase and in combination with the prodrug CB1954, for the treatment of prostate cancer.

The use of oncolytic adenoviruses carrying NTR has been explored over the past several years primarily by The University of Birmingham SCS-GT group. Drs Chen and Roesen previously constructed two E1B-55K deleted oncolytic vectors carrying NTR, CRAd-NTR and vNR6; the latter was shown to have greater cytotoxicity at low MOI and no NTR-associated toxicity to virus replication [Chen et al, 2004; Roesen 2006]. Unfortunately vNR6 also demonstrated significant cytotoxicity to non-transformed human fibroblasts. Dr R. Alemany's lab at the Institut Català d'Oncologia designed a series of oncolytic adenoviruses vectors, the latest two of these, ICOVIR-5 and ICOVIR-7, contain the E1A CR2  $\Delta$ 24 deletion and have the wt E1A promoter replaced by one of two insulated tumour specific E2F-1 promoter. These vectors were potential oncolytic backbones for the introduction of the therapeutic transgene NTR; however at the beginning of this study no data was published on either vector. In order to assess which vector provided the most suitable backbone for introduction of therapeutic transgenes it was decided to construct and characterise ICOVIR-5 and ICOVIR-7 based vectors expressing the marker transgene eGFP. The transgene was inserted downstream of fibre and utilised a splice acceptor site for expression from the MLP. Equivalent vectors were constructed containing the wt fibre or the RGD-retargeted fibre, to investigate whether the RGD-retargeted fibre conferred any cytotoxic advantage in prostate cancer cell lines. An equivalent E1A CR2  $\Delta$ 24 vector was also constructed which retained the wt E1A promoter and wt fibre to investigate the effect of insertion of the insulated E2F-1 promoter.

The E1A CR2  $\Delta$ 24 vector vMH2 with the wt E1A promoter and wt fibre, consistently showed the greatest cytotoxicity in all prostate cancer cell lines but also showed the greatest cytotoxicity to non-transformed human fibroblasts and as a result showed the lowest tumour selectivity (as measured by the therapeutic index) of all vMH vectors. No significant toxicity was observed with either ICOVIR-7 based vector, vMH6 and vMH7, in non-transformed human fibroblasts and it was therefore deemed these vectors were the most tumours selective. However they also demonstrated the lowest cytotoxicity to prostate cancer cell lines, compared to all other vMH vectors. Transgene expression was generally observed from approximately 24 hours post infection, which coincided with the end of virus DNA replication and the start of late virus protein expression. No significant increase in cytotoxicity was observed with RGD-retargeted viruses compared to the wt fibre equivalents, probably because all prostate tumour cells used expressed moderate to high levels of CAR. However the presence of the RGD-retargeted fibre was shown to increase transduction of SKOV3 and MZ2-MEL3.0 cells which expressed no detectable levels of CAR.

Unexpectedly, the RGD-retargeted ICOVIR-7 based vector vMH7 demonstrated a delay in E1A RNA and protein expression compared to the equivalent wt fibre vector vMH6, which subsequently delayed DNA replication, late virus protein and eGFP expression. The ICOVIR-7 promoter from both vectors and the original pICOVIR-7 promoter were sequenced and shown to be identical.

In comparison to vNR3, ICOVIR-5 and ICOVIR-7 based vectors showed greater tumour selectivity in all prostate cancer cell lines and demonstrated up to a 10-fold greater transgene expression.

There is much scope for further work to be done on the ICOVIR-5 and ICOVIR-7 based vectors. More investigation is required to identify why vMH7 expresses less E1A than vMH6. Based on the observations with other RGD-retargeted viruses (vMH4 vs. vMH5 and vPS1361 vs. vPS1362) it would in my opinion seem unlikely this difference was due to a specific effect of inserting the RGD-4C motif. The genomes of both vMH6 and vMH7 are currently being sequenced, which may identify a sequence difference explaining the difference in E1A expression. Neither ICOVIR-5 or ICOVIR-7 vectors were shown to be directly pRb dependent in these experiments. Furthermore, in PC3 and 22RV1 cells that express wt pRb lower EC50 values were observed with ICOVIR-5 and ICOVIR-7 based vectors, in comparison to the mutant pRb cell line DU145. This does not rule out mutations at other points within the pRb pathway and the observations are further complicated by other factors such as varying cell surface receptor expression. However vICOVIR-5 was shown to be pRb/E2F responsive by our collaborators [Alonso et al, 2007a]. Additionally eGFP has not been directly shown to be expressed from the MLP, or whether insertion of transgenes affects viral gene expression (such as fibre or E4). It would therefore be interesting to investigate in further detail the mechanism of transgene expression and any effect of transgene insertion, before such insertions were used in future vectors. Finally, it is worth considering whether the ICOVIR-7 vectors provide sufficient oncolytic cytotoxicity to tumour cell lines to confer a significant anti-tumour effect in prostate cancer patients, thus *in vivo* animal experiments would be required to investigate oncolytic activity.

Based on the fact the ICOVIR-7 based vectors were shown to be most tumour selective, with no significant cytotoxicity to non-transformed human fibroblasts, the ICOVIR-7 backbone was chosen for the introduction of NTR. One of three NTR variants was inserted;

wildtype, double mutant or triple mutant NTR, each with either the wt fibre or RGD-retargeted fibre, thus creating a panel of 6 vectors (vPS1361-6). Each vPS136X vector was subsequently characterised in terms of cytotoxicity, tumour selectivity, E1A and NTR expression, NTR/CB1954 mediated cytotoxicity and combined cytotoxicity. Contrary to expectations each vPS136X vector showed differential virus-induced cytotoxicity and all vectors except vPS1366 were significantly more cytotoxic than the equivalent eGFP expressing vectors vMH6 and vMH7. This differential cytotoxicity resulted in a wide range of tumour selectivity with both vPS1362 and vPS1364 consistently showed the highest therapeutic indices, even greater than vNR6 and Ad5 wt. Whereas the differential cytotoxicity was not fully explained there was some correlation with E1A expression, whereby the higher the E1A expression the more cytotoxic the vector. However, the differential E1A expression was also unexpected, as all vPS136X vectors have E1A under control of the same ICOVIR-7 based promoter, which was shown by DNA sequencing to be identical in all vPS136X vectors. Each vPS136X showed a different level of NTR expression, which did not correlate with either the vector P:I ratio or E1A expression. Furthermore, the wt NTR expressing vPS136X vectors, vPS1361 and vPS1362, were shown to produce less NTR than vNR6 at 48 hour post infection. This observation was contradictory to that using equivalent eGFP expressing vectors, where vMH6 and vMH7 showed 10-fold higher transgene expression compared to vNR3. vPS1364 demonstrated the greatest combined cytotoxicity, both at 3 PFU/cell and 10 PFU/cell, and a 16 or 4 hour prodrug exposure. Looking at just the NTR/CB1954 mediated cytotoxicity vPS1364, vPS1365 and vNR6 all demonstrated equivalent sensitisation to CB1954, thus it would appear the additional combined cytotoxicity observed with vPS1364 was the result of

greater virus induced cytotoxicity. It is however clear vPS1364 shows both greater cytotoxicity and selectivity than the best previous vector vNR6.

With vPS136X vectors two essential questions remain; what is the cause of the differential E1A expression and what is the cause of the differential and lower than anticipated NTR expression. A reduction in E1A expression was previously observed with the RGD-retargeted fibre vector vMH7 compared to the wt equivalent vMH6, however there was no correlation between RGD fibre and E1A expression with vPS136X vectors. Further investigations with vMH6 and vMH7 may elicit some explanation to the difference in E1A expression observed with these vectors and it would be interesting to see if the same difference was found in any vPS136X vector. There are many possible explanations for the differential NTR expression observed, which was also lower than anticipated, such as variations in mRNA and protein stability. Additionally, MLP expression is controlled at multiple points including RNA splicing, mRNA export and translation, and it is not unconceivable transgene expression is downregulated by the MLP at one of these points. Investigations into exactly how eGFP expression is controlled in vMH vectors may be used to identify how NTR expression is controlled and potentially downregulated in vPS136X vectors. Furthermore, it may be beneficial to understand exactly how transgene expression is controlled in vMH and vPS136X vectors, before using the same splice acceptor sites for the expression of potentially toxic transgenes. Alternatively, other mechanisms to achieve late transgene expression could be investigated, such as the use of IRES (internal ribosome entry sites) sequences [Cody and Douglas 2009] or 2A sequences (which use a process called ‘ribosome skipping’) from picornaviruses [Funston et al, 2008] which could be used to directly link expression of transgenes to virus genes such as fibre.

Many various ways have been investigated to express transgenes in CRAd vectors, and it is debatable as to which mechanism is preferable, particularly where potentially toxic transgenes are required and a balance needs to be found between virus spread and enzyme/prodrug efficacy [reviewed by Cody and Douglas 2009]. Furthermore, the packaging limit of the virus must be considered, especially when designing CRAds with multiple inserts and exogenous promoters. Transgene expression from constitutive promoters such as the CMV immediate early promoter yield high levels transgene expression, conferring a good therapeutic affect. However this way can result in reduced virus yields in combination with the prodrug [Roesen 2006]. The key concern with using constitutively active promoters, such as the CMV promoter, is that transgene expression could be allowed in non-tumour tissue causing additional unwanted toxicity. However, by using tumour-specific or endogenous virus promoters reduces this risk. Exogenous tissue-specific promoters have been investigated extensively to drive transgene expression [Cody and Douglas 2009]. Such promoters are advantageous as they can give good levels of transgene expression and transgene expression is tissue targeted reducing the risk to non-target tissue types. However these promoters can again be expressed at early times post infection making them no ideal for CRAd vectors. Typically, insertion of exogenous promoters requires deletion of some viral genes to allow enough space in the genome to accommodate both the promoter and transgene. Generally these deletions were made within the E3, which removes gene involved in immune evasion and the ADP, neither of which may be required. However the E3B has been retained to keep some immune evasion functions and more importantly ADP.

Various strategies have been investigated for expression of transgenes from endogenous viral promoters. Such strategies can reduce the transgene mediated toxicity to the virus as

the timing of expression within the virus lifecycle can be controlled, for example expression of NTR from the pIX ORF showed no toxicity to the virus in combination with prodrug [Roesen 2006]. However expression from the pIX promoter is significantly lower than other virus promoters, which resulted in low level transgene expression and a poor therapeutic potential, demonstrating that the virus promoter used for transgene expression needs to be carefully chosen. Ideally therapeutic transgene expression should be higher but only activate at late times of infection, to give a good therapeutic potential but no toxicity to virus DNA replication, and it would seem expression from the E3 region or Ad MLP would be ideally suited for this. Multiple studies have inserted transgenes in the E3 region as well as replacing the interval E3 proteins and in doing so mimicking transgene expression to that of the replaced viral gene in terms of timing and levels. Several E3 genes are expressed at low level early in infection, however greatly upregulated in late Ad infection (post DNA replication). Therefore insertion of NTR into the E3 region deserves consideration as this may demonstrate both low toxicity to the virus and a good therapeutic potential.

In this study transgene expression is from a splice acceptor site inserted downstream of the fibre gene. Previous studies have used a similar system for expression of transgene from the Ad MLP both downstream of fibre and within the L3 region [Carette et al, 2005; Guedan et al, 2008; Robinson et al, 2008]. These studies identify high and late transgene expression as would be expected and a more strict dependence on initiation of DNA replication, which would be ideally suited for expression of potentially toxic transgene. None of these studies identify any unintentional toxicity or reduced expression due to transgene insertion. However an older study by Fuerer and Iggo expressing the yCD gene downstream of fibre from the Ad41 long fibre demonstrated lower than anticipated transgene expression, which was inferior to that of an IRES behind the fibre gene [Fuerer and Iggo, 2004]. These

observations coincide with those made in this study, where toxic transgene expression from the MLP is downregulated, and may also suggests further investigations are required into the control of transgenes expression using this system.

An interesting study by Jin *et al*, used a transposon-based system to scan the Ad genome for insertion sites that did no compromise the viral life cycle. In this study a reporter gene (eGFP or luciferase) was linked via a splice acceptor site so that expression was dependent on endogenous promoters [Jin et al, 2005]. Using this method a variety of insertion sites were discovered, primarily between the E3 and L5 regions and around the E4 region, and in every case the transcripts originated from the MLP. This study would suggest a fair amount of flexibility in the locations of transgene insertion, but also demonstrate there are some regions where the virus will not accept any transgene insertion. Thus, the transgene insertion site still needs to be well considered as to not unintentionally disrupt expression of viral gene. This includes both well characterised virus transcription units and potentially new or novel transcription units such as the U exon. Currently the exact promoter region driving UXP expression has not been identified and deletion of UXP was shown to cause a mild growth defect [Tollefson et al, 2007]. Thus for transgene insertion downstream of fibre conversations need to be made to fibre, E4 and UXP expression, as not to disrupt expression and virus production.

It is difficult to accurately compare the cytotoxicities of vPS136X vectors with similar Ad vectors expressing transgenes reported previously. Singleton *et al* have reported on a similar study in which they inserted wt NTR into the E3B region of ONYX-411, an E1A CR2  $\Delta$ 24 deleted virus with E1 and E4 expression controlled by the E2F-1 promoter[Singleton et al, 2007]. The resultant vector, termed ONYX-411<sup>NTR</sup>, showed no

reduction in lytic activity compared to the parental vector and typically resulting in EC50 values of 1-10 PFU/cell in PC3 and DU145 cells. It is impossible to compare EC50 values between studies due to the variation in experimental procedure and the authors did not include Ad5 wt as an internal reference which would have enabled some of a comparison. The study goes on to show high level NTR expression occurs post initiation of DNA replication and ONYX-411<sup>NTR</sup> shows a moderate increase in sensitisation to CB1954 but a greater increase in sensitisation using an alternative prodrug SN27686. It would therefore be interesting to investigate the use of alternative prodrug, such as SN27686, with the vPS136X vectors as well as perform direct comparisons between vPS136X vectors and similar oncolytic Ad vectors, such as ONYX-411<sup>NTR</sup>. The results of such investigations may help to identify the optimal vector and prodrug combination for prostate cancer gene therapy.

The work presented in this study has developed novel oncolytic adenovirus vectors for combined oncolytic virotherapy and NTR/CB1954 mediated suicide gene therapy. One vector, vPS1364 expressing double mutant NTR and wt fibre, was identified which demonstrates both greater tumour cell selectivity and combined cytotoxicity than the E1B-55K deleted NTR expressing vector vNR6. Therefore vPS1364 may warrant further investigation in *in vivo* animal models to assess any potential anti-tumour activity.

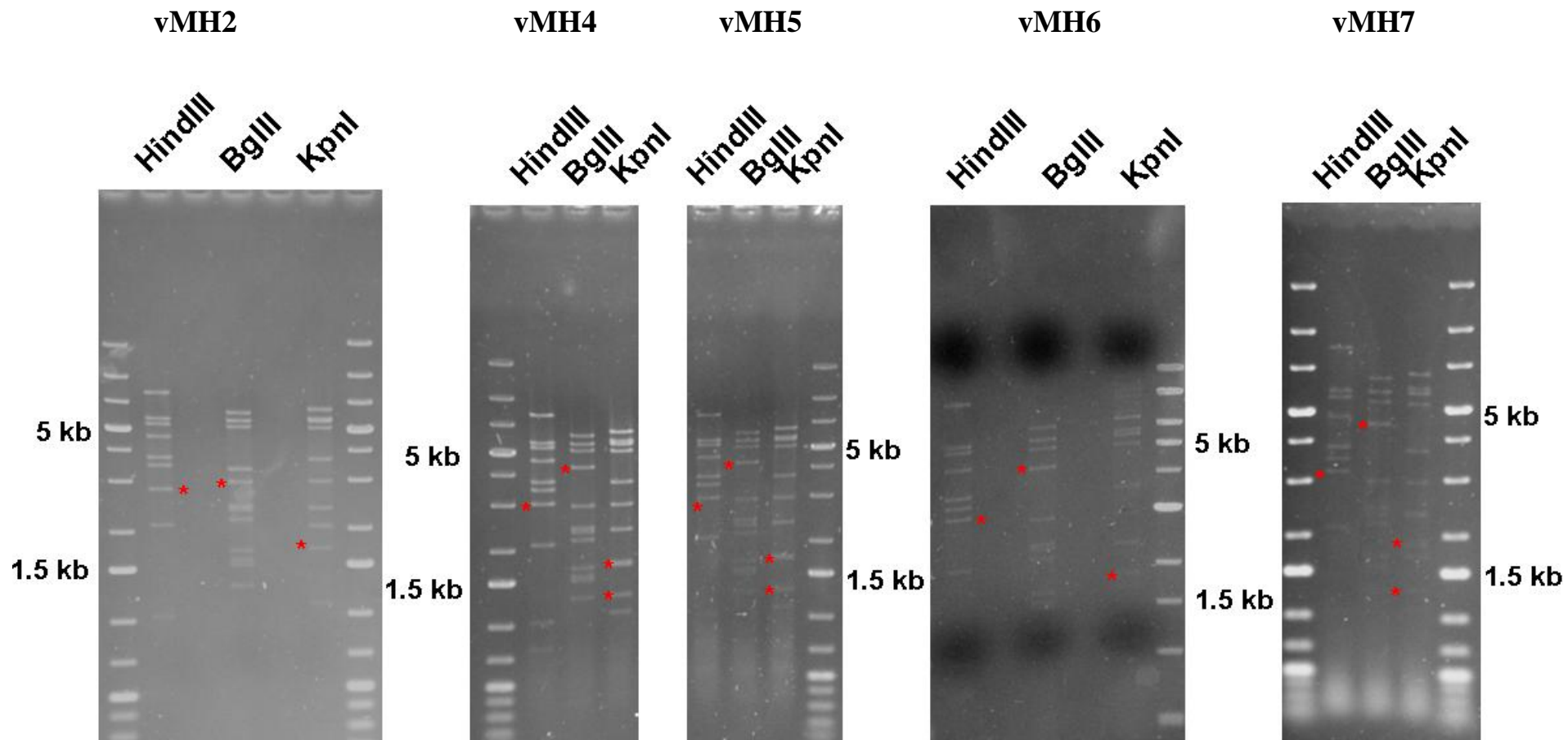
## Appendix 1

The tables below show the predicted HindIII, BglII and KpnI restriction enzyme profiles for each vMH vector. Distinctive bands are highlighted in bold text. Gels showing the restriction enzyme digests for each vMH vector are shown on the next page. Separate gels were run for each vMH vector, alongside Fermentas 1kb+ DNA ladder (300bp, 400bp, **500bp**, 650bp, 1kb, **1.5kb**, 2kb, 3kb, 4kb, **5kb**, 7kb, 10kb, 20kb) for size determination with 1.5kb and 5kb bands labelled. Distinct bands marked by an \*.

HindIII				
vMH2	vMH4	vMH5	vMH6	vMH7
8010	8010	8010	8010	8010
5665	5665	5665	5665	5665
5324	5324	5324	5324	5324
4597	4597	4597	4597	4597
		<b>3735</b>		<b>3735</b>
<b>3708</b>	<b>3708</b>		<b>3708</b>	
3437	3437	3437	3437	3437
			<b>3142</b>	<b>3142</b>
	<b>3016</b>	<b>3016</b>		
<b>2780</b>				
2081	2081	2081	2081	2081
1005	1005	1005	1005	1005

BglII				
vMH2	vMH4	vMH5	vMH6	vMH7
6182	6182	6182	6182	6182
5586	5586	5586	5586	5586
5178	5178	5178	5178	5178
			<b>4421</b>	<b>4421</b>
	<b>4295</b>	<b>4295</b>		
<b>3304</b>				
2943	2943	2943	2943	2943
		<b>2423</b>		<b>2423</b>
<b>2396</b>	<b>2396</b>		<b>2396</b>	
2334	2334	2334	2334	2334
2151	2151	2151	2151	2151
1672	1672	1672	1672	1672
1548	1548	1548	1548	1548
1497	1497	1497	1497	1497
1268	1268	1268	1268	1268
351	351	351	351	351
272	272	272	272	272

KpnI				
vMH2	vMH4	vMH5	vMH6	vMH7
6485	6485	6485	6485	6485
5753	5753	5753	5753	5753
		<b>5609</b>		<b>5609</b>
<b>5582</b>	<b>5582</b>		<b>5582</b>	
5120	5120	5120	5120	5120
3646	3646	3646	3646	3646
2949	2949	2949	2949	2949
2337	2337	2337	2337	2337
<b>2028</b>				
			<b>1864</b>	<b>1864</b>
	<b>1738</b>	<b>1738</b>		
1696	1696	1696	1696	1696
	<b>1281</b>	<b>1281</b>	<b>1281</b>	<b>1281</b>
1086	1086	1086	1086	1086



## Appendix 2

The following page shows the results from the ICOVIR-7 promoter DNA sequencing. All numbers refer to the positions within the vMH6/vMH7/vPS136X genomes. Mutations are shown in red with the nucleotides inserted or deleted in capitals. The DM-1 insulator element is underlined in black and the E2F-1 promoter region is underlined in blue. The region containing the two additional E2F binding regions is underlined in pink. Nucleotides in blue represent the E2F binding sites, each consisting of two imperfect palindromes. The E1A ATG is shown in capitals and underlined in green and the primers used for sequencing are shown in grey. A list of the primers used for sequencing can be found in table Table 2-1.

245 tttgggogta accgagtaag atttggccat tttcogggga aaactgaata agaggaagtg aaatctgaat aattttgtgt tactcatagc gcgtaatctc  
 Clal **aGgga** MHp19  
 345 tagcatogat gtog**aggatc** cctcagagacc ctgaaactgt ctctogactcc ggggccccgt tggaagactg agtgccccgg gcaocggcaca gaagccccgc  
 445 ccacocgctg ccagttcaca accogctcoga gogtgggtct ccgcccagct ccagtctgt gatccgggoc cccccctag cggccccgga gggaggggoc  
 MHp23  
 545 gggctccgcg coggcogaac gggctcgaag ggctcctgta gccgggaatg ctgctgctgc tctgggggg atcacagacc atttctttct ttoggccagg  
 645 ctgaggccct gacgtggatg ggcaaaactgc aggcctggga aggcagcaag ccgggcccgc cgtgttccat cctccacgca cccccaccta tegtgggttc  
 MHp22  
 745 gcaaagtgca aagctttctt gtgcatgaag cctgctctg gggagcgtct ggccgatct ctgctgctt actcgggaaa ttgcttttg ccaaaccocg  
 HindIII  
 845 tttttcgggg atccccgcgc cccctctca cttgcctgc totcggagcc ccagccgct ccgcccgtt cggcggtttg gatatttatt gaocctgtcc  
 MHp21  
 945 tccgactcgc tgacaggcta caggaccccc aacaaccccc atccacgttt tggatgcact gagacccoga cattcctcgg tatttattgt ctgtccccc  
 1045 ctaggacccc cccccocgac cctcoggaat aaaaggccct ccactctgcc **DELETED** Ctcgagtcta gagatggccg caataaata tctttatttt cattacatct  
 MHp17  
 1145 gtgtgttgg tttttgtgt Clal aatcogatag actaacatac gctctccatc aaaacaaaac gaaacaaaac aaactagcaa aataggctgt cccagtgca  
 MHp20  
 1245 agtcaggtg ccagaacatt totctatoga taggtaccat ccggacaaag cctgcgcgog ccccgcccc ccattggccg tacgtcggcg gctcgtggct  
 Clal MHp24  
 1345 ctttcogggc aaaaaggatt tggcogttaa agt**G**gttgc **DELETED DEL** a**AGtAC**tgg ccgctcgtgg ctctttcogc gcaaaaagga tttggcgcgt aaaagtgtt  
 BstBI  
 1445 cgaagtac**gc** **gc** gccccgcgc gccgccccat ctgccccctc gccgccccgt ccggcgcgtt aaagccaata ggaaccgcgc ccgttgttc cgtcacggcc  
 1545 ggggcagcca attgtggcgg cgtcggcgg ctcgtggctc tttcogggca aaaaggattt ggccgtaaa agtggccggg actttgcagg cagccggcgc  
 1645 cggggcgga ggggatoga gccctcgcca cc**AT**Gagaca tattatctgc cacggaggtg ttattacoga agaaatggcc gccagtctt tggaccagct  
 1745 gatogaagag gtactggctg ataactctcc acctcctagc catttgaac cacctacct tcaoga  
 MHp18

## Reference List

- Ahn, S. J., J. Costa, and J. R. Emanuel. (1996). PicoGreen quantitation of DNA: effective evaluation of samples pre- or post-PCR. *Nucleic Acids Res.* **24**, 2623-2625.
- Alba, R., A. Bosch, and M. Chillon. (2005). Gutless adenovirus: last-generation adenovirus for gene therapy. *Gene Ther.* **12 Suppl 1**, S18-S27.
- Alba, R., A. C. Bradshaw, A. L. Parker et al. (2009). Identification of coagulation factor (F)X binding sites on the adenovirus serotype 5 hexon: effect of mutagenesis on FX interactions and gene transfer. *Blood* **114**, 965-971.
- Ali, H., G. LeRoy, G. Bridge et al. (2007). The adenovirus L4 33-kilodalton protein binds to intragenic sequences of the major late promoter required for late phase-specific stimulation of transcription. *J. Virol.* **81**, 1327-1338.
- Alonso, M. M., M. Cascallo, C. Gomez-Manzano et al. (2007a). ICOVIR-5 shows E2F1 addiction and potent anti-glioma effect in vivo. *Cancer Res.* **67**, 8255-8263.
- Alonso, M. M., C. Gomez-Manzano, H. Jiang et al. (2007b). Combination of the oncolytic adenovirus ICOVIR-5 with chemotherapy provides enhanced anti-glioma effect in vivo. *Cancer Gene Ther.* **14**, 756-761.
- Anlezark, G. M., R. G. Melton, R. F. Sherwood et al. (1992). The bioactivation of 5-(aziridin-1-yl)-2,4-dinitrobenzamide (CB1954)--I. Purification and properties of a nitroreductase enzyme from *Escherichia coli*--a potential enzyme for antibody-directed enzyme prodrug therapy (ADEPT). *Biochem. Pharmacol.* **44**, 2289-2295.
- Araujo, F. D., T. H. Stracker, C. T. Carson et al. (2005). Adenovirus type 5 E4orf3 protein targets the Mre11 complex to cytoplasmic aggresomes. *J. Virol.* **79**, 11382-11391.
- Arnberg, N. (2009). Adenovirus receptors: implications for tropism, treatment and targeting. *Rev. Med. Virol.* **19**, 165-178.
- Arnberg, N., K. Edlund, A. H. Kidd et al. (2000a). Adenovirus type 37 uses sialic acid as a cellular receptor. *J. Virol.* **74**, 42-48.
- Arnberg, N., A. H. Kidd, K. Edlund et al. (2000b). Initial interactions of subgenus D adenoviruses with A549 cellular receptors: sialic acid versus alpha(v) integrins. *J. Virol.* **74**, 7691-7693.
- Atchison, R. W., B. C. Casto, and W. M. Hammon. (1965). ADENOVIRUS-ASSOCIATED DEFECTIVE VIRUS PARTICLES. *Science* **149**, 754-756.
- Bagchi, S., P. Raychaudhuri, and J. R. Nevins. (1990). Adenovirus E1A proteins can dissociate heteromeric complexes involving the E2F transcription factor: a novel mechanism for E1A trans-activation. *Cell* **62**, 659-669.

- Bagchi, S., R. Weinmann, and P. Raychaudhuri. (1991). The retinoblastoma protein copurifies with E2F-I, an E1A-regulated inhibitor of the transcription factor E2F. *Cell* **65**, 1063-1072.
- Barker, D. D. and A. J. Berk. (1987). Adenovirus proteins from both E1B reading frames are required for transformation of rodent cells by viral infection and DNA transfection. *Virology* **156**, 107-121.
- Barker, S. E., C. A. Broderick, S. J. Robbie et al. (2009). Subretinal delivery of adeno-associated virus serotype 2 results in minimal immune responses that allow repeat vector administration in immunocompetent mice. *J. Gene Med.* **11**, 486-497.
- Barton, K. N., H. Stricker, S. L. Brown et al. (2008). Phase I study of noninvasive imaging of adenovirus-mediated gene expression in the human prostate. *Mol. Ther.* **16**, 1761-1769.
- Bastian, P. J., J. Ellinger, A. Wellmann et al. (2005). Diagnostic and prognostic information in prostate cancer with the help of a small set of hypermethylated gene loci. *Clin. Cancer Res.* **11**, 4097-4106.
- Bauerschmitz, G. J., K. Guse, A. Kanerva et al. (2006). Triple-targeted oncolytic adenoviruses featuring the cox2 promoter, E1A transcomplementation, and serotype chimerism for enhanced selectivity for ovarian cancer cells. *Mol. Ther.* **14**, 164-174.
- Bazan-Peregrino, M., R. C. Carlisle, R. Hernandez-Alcoceba et al. (2008). Comparison of molecular strategies for breast cancer virotherapy using oncolytic adenovirus. *Hum. Gene Ther.* **19**, 873-886.
- Bear, C. E., C. H. Li, N. Kartner et al. (1992). Purification and functional reconstitution of the cystic fibrosis transmembrane conductance regulator (CFTR). *Cell* **68**, 809-818.
- Belousova, N., V. Krendelchtchikova, D. T. Curiel et al. (2002). Modulation of adenovirus vector tropism via incorporation of polypeptide ligands into the fiber protein. *J. Virol.* **76**, 8621-8631.
- Benedict, C. A., P. S. Norris, T. I. Prigozy et al. (2001). Three adenovirus E3 proteins cooperate to evade apoptosis by tumor necrosis factor-related apoptosis-inducing ligand receptor-1 and -2. *J. Biol. Chem.* **276**, 3270-3278.
- Berk, A. J. (2005). Recent lessons in gene expression, cell cycle control, and cell biology from adenovirus. *Oncogene* **24**, 7673-7685.
- Bett, A. J., L. Prevec, and F. L. Graham. (1993). Packaging capacity and stability of human adenovirus type 5 vectors. *J. Virol.* **67**, 5911-5921.
- Bewley, M. C., K. Springer, Y. B. Zhang et al. (1999). Structural analysis of the mechanism of adenovirus binding to its human cellular receptor, CAR. *Science* **286**, 1579-1583.
- Blackford, A. N. and R. J. Grand. (2009). Adenovirus E1B 55-kilodalton protein: multiple roles in viral infection and cell transformation. *J. Virol.* **83**, 4000-4012.

- Bobadilla, J. L., M. Macek, Jr., J. P. Fine et al. (2002). Cystic fibrosis: a worldwide analysis of CFTR mutations--correlation with incidence data and application to screening. *Hum. Mutat.* **19**, 575-606.
- Bolla, M., P. Maingon, P. Fourneret et al. (2005a). [Indications of the association of radiotherapy and hormonal treatment in prostate cancer]. *Cancer Radiother.* **9**, 394-398.
- Bolla, M., P. H. van, L. Collette et al. (2005b). Postoperative radiotherapy after radical prostatectomy: a randomised controlled trial (EORTC trial 22911). *Lancet* **366**, 572-578.
- Bondesson, M., K. Ohman, M. Manervik et al. (1996). Adenovirus E4 open reading frame 4 protein autoregulates E4 transcription by inhibiting E1A transactivation of the E4 promoter. *J. Virol.* **70**, 3844-3851.
- Bondesson, M., C. Svensson, S. Linder et al. (1992). The carboxy-terminal exon of the adenovirus E1A protein is required for E4F-dependent transcription activation. *EMBO J.* **11**, 3347-3354.
- Boudin, M. L., J. C. D'Halluin, C. Cousin et al. (1980). Human adenovirus type 2 protein IIIa. II. Maturation and encapsidation. *Virology* **101**, 144-156.
- Boudin, M. L., M. Moncany, J. C. D'Halluin et al. (1979). Isolation and characterization of adenovirus type 2 vertex capsomer (penton base). *Virology* **92**, 125-138.
- Branton, P. E. and D. E. Roopchand. (2001). The role of adenovirus E4orf4 protein in viral replication and cell killing. *Oncogene* **20**, 7855-7865.
- Bridgewater, J. A., R. J. Knox, J. D. Pitts et al. (1997). The bystander effect of the nitroreductase/CB1954 enzyme/prodrug system is due to a cell-permeable metabolite. *Hum. Gene Ther.* **8**, 709-717.
- Burgert, H. G. and S. Kvist. (1987). The E3/19K protein of adenovirus type 2 binds to the domains of histocompatibility antigens required for CTL recognition. *EMBO J.* **6**, 2019-2026.
- Burgert, H. G., J. L. Maryanski, and S. Kvist. (1987). "E3/19K" protein of adenovirus type 2 inhibits lysis of cytolytic T lymphocytes by blocking cell-surface expression of histocompatibility class I antigens. *Proc. Natl Acad. Sci U. S. A* **84**, 1356-1360.
- Burton, E. A., J. B. Wechuck, S. K. Wendell et al. (2001). Multiple applications for replication-defective herpes simplex virus vectors. *Stem Cells* **19**, 358-377.
- Cafferata, E. G., D. R. Maccio, M. V. Lopez et al. (2009). A novel A33 promoter-based conditionally replicative adenovirus suppresses tumor growth and eradicates hepatic metastases in human colon cancer models. *Clin. Cancer Res.* **15**, 3037-3049.
- Carette, J. E., H. C. Graat, F. H. Schagen et al. (2005). Replication-dependent transgene expression from a conditionally replicating adenovirus via alternative splicing to a heterologous splice-acceptor site. *J. Gene Med.* **7**, 1053-1062.

Carmody, R. J., K. Maguschak, and Y. H. Chen. (2006). A novel mechanism of nuclear factor-kappaB regulation by adenoviral protein 14.7K. *Immunology* **117**, 188-195.

Carvalho, T., J. S. Seeler, K. Ohman et al. (1995). Targeting of adenovirus E1A and E4-ORF3 proteins to nuclear matrix-associated PML bodies. *J. Cell Biol.* **131**, 45-56.

Cascallo, M., M. M. Alonso, J. J. Rojas et al. (2007). Systemic toxicity-efficacy profile of ICOVIR-5, a potent and selective oncolytic adenovirus based on the pRB pathway. *Mol. Ther.* **15**, 1607-1615.

Cascallo, M., G. Capella, A. Mazo et al. (2003). Ras-dependent oncolysis with an adenovirus VAI mutant. *Cancer Res.* **63**, 5544-5550.

Cashman, S. M., D. J. Morris, and R. Kumar-Singh. (2004). Adenovirus type 5 pseudotyped with adenovirus type 37 fiber uses sialic acid as a cellular receptor. *Virology* **324**, 129-139.

Cavazzana-Calvo, M. and A. Fischer. (2007). Gene therapy for severe combined immunodeficiency: are we there yet? *J. Clin. Invest* **117**, 1456-1465.

Cepko, C. L. and P. A. Sharp. (1982). Assembly of adenovirus major capsid protein is mediated by a nonvirion protein. *Cell* **31**, 407-415.

Chatterjee, P. K., M. E. Vayda, and S. J. Flint. (1986). Identification of proteins and protein domains that contact DNA within adenovirus nucleoprotein cores by ultraviolet light crosslinking of oligonucleotides 32P-labelled in vivo. *J. Mol. Biol.* **188**, 23-37.

Chen, J., N. Morral, and D. A. Engel. (2007). Transcription releases protein VII from adenovirus chromatin. *Virology* **369**, 411-422.

Chen, M. J., N. K. Green, G. M. Reynolds et al. (2004). Enhanced efficacy of Escherichia coli nitroreductase/CB1954 prodrug activation gene therapy using an E1B-55K-deleted oncolytic adenovirus vector. *Gene Ther.* **11**, 1126-1136.

Chen, P., J. Tian, I. Kovesdi et al. (1998). Interaction of the adenovirus 14.7-kDa protein with FLICE inhibits Fas ligand-induced apoptosis. *J. Biol. Chem.* **273**, 5815-5820.

Chen, P. H., D. A. Ornelles, and T. Shenk. (1993). The adenovirus L3 23-kilodalton proteinase cleaves the amino-terminal head domain from cytokeratin 18 and disrupts the cytokeratin network of HeLa cells. *J. Virol.* **67**, 3507-3514.

Chen, Y., T. DeWeese, J. Dilley et al. (2001). CV706, a prostate cancer-specific adenovirus variant, in combination with radiotherapy produces synergistic antitumor efficacy without increasing toxicity. *Cancer Res.* **61**, 5453-5460.

Cheng, Y. C., S. P. Grill, G. E. Dutschman et al. (1983a). Metabolism of 9-(1,3-dihydroxy-2-propoxymethyl)guanine, a new anti-herpes virus compound, in herpes simplex virus-infected cells. *J. Biol. Chem.* **258**, 12460-12464.

- Cheng, Y. C., E. S. Huang, J. C. Lin et al. (1983b). Unique spectrum of activity of 9-[(1,3-dihydroxy-2-propoxy)methyl]-guanine against herpesviruses in vitro and its mode of action against herpes simplex virus type 1. *Proc. Natl Acad. Sci U. S. A* **80**, 2767-2770.
- Chiocca, E. A., K. M. Abbeduto, S. Tatter et al. (2004). A phase I open-label, dose-escalation, multi-institutional trial of injection with an E1B-Attenuated adenovirus, ONYX-015, into the peritumoral region of recurrent malignant gliomas, in the adjuvant setting. *Mol. Ther.* **10**, 958-966.
- Chiou, S. K., L. Rao, and E. White. (1994a). Bcl-2 blocks p53-dependent apoptosis. *Mol. Cell Biol.* **14**, 2556-2563.
- Chiou, S. K., C. C. Tseng, L. Rao et al. (1994b). Functional complementation of the adenovirus E1B 19-kilodalton protein with Bcl-2 in the inhibition of apoptosis in infected cells. *J. Virol.* **68**, 6553-6566.
- Choi, V. W., D. M. McCarty, and R. J. Samulski. (2005). AAV hybrid serotypes: improved vectors for gene delivery. *Curr. Gene Ther.* **5**, 299-310.
- Chow, L. T., T. R. Broker, and J. B. Lewis. (1979). Complex splicing patterns of RNAs from the early regions of adenovirus-2. *J. Mol. Biol.* **134**, 265-303.
- Chung-Faye, G., D. Palmer, D. Anderson et al. (2001). Virus-directed, enzyme prodrug therapy with nitroimidazole reductase: a phase I and pharmacokinetic study of its prodrug, CB1954. *Clin. Cancer Res.* **7**, 2662-2668.
- Ciuffi, A., M. Llano, E. Poeschla et al. (2005). A role for LEDGF/p75 in targeting HIV DNA integration. *Nat. Med.* **11**, 1287-1289.
- Ciuffi, A., R. S. Mitchell, C. Hoffmann et al. (2006). Integration site selection by HIV-based vectors in dividing and growth-arrested IMR-90 lung fibroblasts. *Mol. Ther.* **13**, 366-373.
- Cobb, L. M., T. A. Connors, L. A. Elson et al. (1969). 2,4-dinitro-5-ethyleneiminobenzamide (CB 1954): a potent and selective inhibitor of the growth of the Walker carcinoma 256. *Biochem. Pharmacol.* **18**, 1519-1527.
- Cody, J. J. and J. T. Douglas. (2009). Armed replicating adenoviruses for cancer virotherapy. *Cancer Gene Ther.* **16**, 473-488.
- Colby, W. W. and T. Shenk. (1981). Adenovirus Type 5 Virions Can Be Assembled in Vivo in the Absence of Detectable Polypeptide IX. *Journal of Virology* **39**, 977-980.
- Coura, R. S. and N. B. Nardi. (2007). The state of the art of adeno-associated virus-based vectors in gene therapy. *Virol. J.* **4**, 99.
- Cronin, J., X. Y. Zhang, and J. Reiser. (2005). Altering the tropism of lentiviral vectors through pseudotyping. *Curr. Gene Ther.* **5**, 387-398.

- Cuconati, A., K. Degenhardt, R. Sundararajan et al. (2002). Bak and Bax function to limit adenovirus replication through apoptosis induction. *J. Virol.* **76**, 4547-4558.
- Dalba, C., B. Bellier, N. Kasahara et al. (2007). Replication-competent vectors and empty virus-like particles: new retroviral vector designs for cancer gene therapy or vaccines. *Mol. Ther.* **15**, 457-466.
- Danielsson, A., H. Dzojic, B. Nilsson et al. (2008). Increased therapeutic efficacy of the prostate-specific oncolytic adenovirus Ad[I/PPT-E1A] by reduction of the insulator size and introduction of the full-length E3 region. *Cancer Gene Ther.* **15**, 203-213.
- Danthinne, X. and M. J. Imperiale. (2000). Production of first generation adenovirus vectors: a review. *Gene Ther.* **7**, 1707-1714.
- Davison, A. J., M. Benko, and B. Harrach. (2003). Genetic content and evolution of adenoviruses. *J. Gen. Virol.* **84**, 2895-2908.
- Dehecchi, M. C., P. Melotti, A. Bonizzato et al. (2001). Heparan sulfate glycosaminoglycans are receptors sufficient to mediate the initial binding of adenovirus types 2 and 5. *J. Virol.* **75**, 8772-8780.
- Dehecchi, M. C., A. Tamanini, A. Bonizzato et al. (2000). Heparan sulfate glycosaminoglycans are involved in adenovirus type 5 and 2-host cell interactions. *Virology* **268**, 382-390.
- Delenda, C. (2004). Lentiviral vectors: optimization of packaging, transduction and gene expression. *J. Gene Med.* **6 Suppl 1**, S125-S138.
- Denby, L., L. M. Work, D. Graham et al. (2004). Adenoviral serotype 5 vectors pseudotyped with fibers from subgroup D show modified tropism in vitro and in vivo. *Hum. Gene Ther.* **15**, 1054-1064.
- DeWeese, T. L., P. H. van der, S. Li et al. (2001). A phase I trial of CV706, a replication-competent, PSA selective oncolytic adenovirus, for the treatment of locally recurrent prostate cancer following radiation therapy. *Cancer Res.* **61**, 7464-7472.
- Dilley, J., S. Reddy, D. Ko et al. (2005). Oncolytic adenovirus CG7870 in combination with radiation demonstrates synergistic enhancements of antitumor efficacy without loss of specificity. *Cancer Gene Ther.* **12**, 715-722.
- Dix, I. and K. N. Leppard. (1995). Expression of adenovirus type 5 E4 Orf2 protein during lytic infection. *J. Gen. Virol.* **76 ( Pt 4)**, 1051-1055.
- Djeha, A. H., T. A. Thomson, H. Leung et al. (2001). Combined adenovirus-mediated nitroreductase gene delivery and CB1954 treatment: a well-tolerated therapy for established solid tumors. *Mol. Ther.* **3**, 233-240.
- Dmitriev, I., V. Krasnykh, C. R. Miller et al. (1998). An adenovirus vector with genetically modified fibers demonstrates expanded tropism via utilization of a coxsackievirus and adenovirus receptor-independent cell entry mechanism. *J. Virol.* **72**, 9706-9713.

- Dmitriev, I. P., E. A. Kashentseva, and D. T. Curiel. (2002). Engineering of adenovirus vectors containing heterologous peptide sequences in the C terminus of capsid protein IX. *J. Virol.* **76**, 6893-6899.
- Dobbelstein, M. (2004). Replicating adenoviruses in cancer therapy. *Curr. Top. Microbiol. Immunol.* **273**, 291-334.
- Dobner, T., N. Horikoshi, S. Rubenwolf et al. (1996). Blockage by adenovirus E4orf6 of transcriptional activation by the p53 tumor suppressor. *Science* **272**, 1470-1473.
- Dobson, A. T., T. P. Margolis, F. Sedarati et al. (1990). A latent, nonpathogenic HSV-1-derived vector stably expresses beta-galactosidase in mouse neurons. *Neuron* **5**, 353-360.
- Donovan, J. L., S. J. Frankel, A. Faulkner et al. (1999). Dilemmas in treating early prostate cancer: the evidence and a questionnaire survey of consultant urologists in the United Kingdom. *BMJ* **318**, 299-300.
- Doronin, K., K. Toth, M. Kuppuswamy et al. (2003). Overexpression of the ADP (E3-11.6K) protein increases cell lysis and spread of adenovirus. *Virology* **305**, 378-387.
- Dyson, N., P. Guida, C. McCall et al. (1992). Adenovirus E1A makes two distinct contacts with the retinoblastoma protein. *J. Virol.* **66**, 4606-4611.
- Edelstein, M. L., M. R. Abedi, J. Wixon et al. (2004). Gene therapy clinical trials worldwide 1989-2004-an overview. *J. Gene Med.* **6**, 597-602.
- Elsing, A. and H. G. Burgert. (1998). The adenovirus E3/10.4K-14.5K proteins down-modulate the apoptosis receptor Fas/Apo-1 by inducing its internalization. *Proc. Natl Acad. Sci U. S. A* **95**, 10072-10077.
- Enders, J. F., J. A. Bell, J. H. Dingle et al. (1956). Adenoviruses: group name proposed for new respiratory-tract viruses. *Science* **124**, 119-120.
- Epstein, A. L. (2005). HSV-1-based amplicon vectors: design and applications. *Gene Ther.* **12 Suppl 1**, S154-S158.
- Estmer, N. C., S. Petersen-Mahrt, C. Durot et al. (2001). The adenovirus E4-ORF4 splicing enhancer protein interacts with a subset of phosphorylated SR proteins. *EMBO J.* **20**, 864-871.
- Evans, J. D. and P. Hearing. (2005). Relocalization of the Mre11-Rad50-Nbs1 complex by the adenovirus E4 ORF3 protein is required for viral replication. *J. Virol.* **79**, 6207-6215.
- Everitt, E., L. Lutter, and L. Philipson. (1975). Structural proteins of adenoviruses. XII. Location and neighbor relationship among proteins of adenovirion type 2 as revealed by enzymatic iodination, immunoprecipitation and chemical cross-linking. *Virology* **67**, 197-208.
- Everts, B. and H. G. van der Poel. (2005). Replication-selective oncolytic viruses in the treatment of cancer. *Cancer Gene Ther.* **12**, 141-161.

- Ewing, S. G., S. A. Byrd, J. B. Christensen et al. (2007). Ternary complex formation on the adenovirus packaging sequence by the IVa2 and L4 22-kilodalton proteins. *J. Virol.* **81**, 12450-12457.
- Fabry, C. M., M. Rosa-Calatrava, J. F. Conway et al. (2005). A quasi-atomic model of human adenovirus type 5 capsid. *EMBO J.* **24**, 1645-1654.
- Fabry, C. M., M. Rosa-Calatrava, C. Moriscot et al. (2009). The C-terminal domains of adenovirus serotype 5 protein IX assemble into an antiparallel structure on the facets of the capsid. *J. Virol.* **83**, 1135-1139.
- Fallaux, F. J., A. Bout, d. V. van, I et al. (1998). New helper cells and matched early region 1-deleted adenovirus vectors prevent generation of replication-competent adenoviruses. *Hum. Gene Ther.* **9**, 1909-1917.
- Fallaux, F. J., O. Kranenburg, S. J. Cramer et al. (1996). Characterization of 911: a new helper cell line for the titration and propagation of early region 1-deleted adenoviral vectors. *Hum. Gene Ther.* **7**, 215-222.
- Farley, D. C., J. L. Brown, and K. N. Leppard. (2004). Activation of the early-late switch in adenovirus type 5 major late transcription unit expression by L4 gene products. *J. Virol.* **78**, 1782-1791.
- Ferrari, M. E., C. M. Nguyen, O. Zelphati et al. (1998). Analytical methods for the characterization of cationic lipid-nucleic acid complexes. *Hum. Gene Ther.* **9**, 341-351.
- Fessler, S. P. and C. S. Young. (1998). Control of adenovirus early gene expression during the late phase of infection. *J. Virol.* **72**, 4049-4056.
- Fields, B. 2007. Virology 5th Edition.
- Fischer, A. (2000). Severe combined immunodeficiencies (SCID). *Clin. Exp. Immunol.* **122**, 143-149.
- Fisher, K. J., K. Jooss, J. Alston et al. (1997). Recombinant adeno-associated virus for muscle directed gene therapy. *Nat. Med.* **3**, 306-312.
- FitzSimmons, S. C. (1993). The changing epidemiology of cystic fibrosis. *J. Pediatr.* **122**, 1-9.
- Flotte, T. R. (2000). Size does matter: overcoming the adeno-associated virus packaging limit. *Respir. Res.* **1**, 16-18.
- Fogh, J., J. M. Fogh, and T. Orfeo. (1977). One hundred and twenty-seven cultured human tumor cell lines producing tumors in nude mice. *J. Natl. Cancer Inst.* **59**, 221-226.
- Fowlkes, D. M. and T. Shenk. (1980). Transcriptional control regions of the adenovirus VAI RNA gene. *Cell* **22**, 405-413.

- Fraefel, C., S. Song, F. Lim et al. (1996). Helper virus-free transfer of herpes simplex virus type 1 plasmid vectors into neural cells. *J. Virol.* **70**, 7190-7197.
- Fredman, J. N. and J. A. Engler. (1993). Adenovirus precursor to terminal protein interacts with the nuclear matrix in vivo and in vitro. *J. Virol.* **67**, 3384-3395.
- Frese, K. K., S. S. Lee, D. L. Thomas et al. (2003). Selective PDZ protein-dependent stimulation of phosphatidylinositol 3-kinase by the adenovirus E4-ORF1 oncoprotein. *Oncogene* **22**, 710-721.
- Freytag, S. O., M. Khil, H. Stricker et al. (2002). Phase I study of replication-competent adenovirus-mediated double suicide gene therapy for the treatment of locally recurrent prostate cancer. *Cancer Res.* **62**, 4968-4976.
- Freytag, S. O., B. Movsas, I. Aref et al. (2007a). Phase I trial of replication-competent adenovirus-mediated suicide gene therapy combined with IMRT for prostate cancer. *Mol. Ther.* **15**, 1016-1023.
- Freytag, S. O., H. Stricker, J. Peabody et al. (2007b). Five-year Follow-up of Trial of Replication-competent Adenovirus-mediated Suicide Gene Therapy for Treatment of Prostate Cancer. *Mol. Ther.* **15**, 636-642.
- Freytag, S. O., H. Stricker, J. Pegg et al. (2003). Phase I study of replication-competent adenovirus-mediated double-suicide gene therapy in combination with conventional-dose three-dimensional conformal radiation therapy for the treatment of newly diagnosed, intermediate- to high-risk prostate cancer. *Cancer Res.* **63**, 7497-7506.
- Fuerer, C. and R. Iggo. (2002). Adenoviruses with Tcf binding sites in multiple early promoters show enhanced selectivity for tumour cells with constitutive activation of the wnt signalling pathway. *Gene Ther.* **9**, 270-281.
- Fuerer, C. and R. Iggo. (2004). 5-Fluorocytosine increases the toxicity of Wnt-targeting replicating adenoviruses that express cytosine deaminase as a late gene. *Gene Ther.* **11**, 142-151.
- Fueyo, J., C. Gomez-Manzano, R. Alemany et al. (2000). A mutant oncolytic adenovirus targeting the Rb pathway produces anti-glioma effect in vivo. *Oncogene* **19**, 2-12.
- Funston, G. M., S. E. Kallioinen, P. de Felipe et al. (2008). Expression of heterologous genes in oncolytic adenoviruses using picornaviral 2A sequences that trigger ribosome skipping. *J. Gen. Virol.* **89**, 389-396.
- Galanis, E., S. H. Okuno, A. G. Nascimento et al. (2005). Phase I-II trial of ONYX-015 in combination with MAP chemotherapy in patients with advanced sarcomas. *Gene Ther.* **12**, 437-445.
- Gall, J., A. Kass-Eisler, L. Leinwand et al. (1996). Adenovirus type 5 and 7 capsid chimera: fiber replacement alters receptor tropism without affecting primary immune neutralization epitopes. *J. Virol.* **70**, 2116-2123.

Gallimore, P. H. and A. S. Turnell. (2001). Adenovirus E1A: remodelling the host cell, a life or death experience. *Oncogene* **20**, 7824-7835.

Gao, X., K. S. Kim, and D. Liu. (2007). Nonviral gene delivery: what we know and what is next. *AAPS. J.* **9**, E92-104.

Gao, X., A. T. Porter, D. J. Grignon et al. (1997). Diagnostic and prognostic markers for human prostate cancer. *Prostate* **31**, 264-281.

Garcia, J., F. Wu, and R. Gaynor. (1987). Upstream regulatory regions required to stabilize binding to the TATA sequence in an adenovirus early promoter. *Nucleic Acids Res.* **15**, 8367-8385.

Gaspar, H. B., A. Aiuti, F. Porta et al. (2009). How I treat ADA deficiency. *Blood* **114**, 3524-3532.

Germano, I. M., J. Fable, S. H. Gultekin et al. (2003). Adenovirus/herpes simplex-thymidine kinase/ganciclovir complex: preliminary results of a phase I trial in patients with recurrent malignant gliomas. *J. Neurooncol.* **65**, 279-289.

Giard, D. J., S. A. Aaronson, G. J. Todaro et al. (1973). In vitro cultivation of human tumors: establishment of cell lines derived from a series of solid tumors. *J. Natl. Cancer Inst.* **51**, 1417-1423.

Ginsberg, H. S., H. G. Pereira, R. C. Valentine et al. (1966). A proposed terminology for the adenovirus antigens and virion morphological subunits. *Virology* **28**, 782-783.

Goding, C. R., S. M. Temperley, and F. Fisher. (1987). Multiple transcription factors interact with the adenovirus-2 EII-late promoter: evidence for a novel CCAAT recognition factor. *Nucleic Acids Res.* **15**, 7761-7780.

Goncalves, M. A. (2005). Adeno-associated virus: from defective virus to effective vector. *Virol. J.* **2**, 43.

Gonzalez, R. A. and S. J. Flint. (2002). Effects of mutations in the adenoviral E1B 55-kilodalton protein coding sequence on viral late mRNA metabolism. *J. Virol.* **76**, 4507-4519.

Goodbourn, S., L. Didcock, and R. E. Randall. (2000). Interferons: cell signalling, immune modulation, antiviral response and virus countermeasures. *J. Gen. Virol.* **81**, 2341-2364.

Goodrum, F. D. and D. A. Ornelles. (1998). p53 status does not determine outcome of E1B 55-kilodalton mutant adenovirus lytic infection. *J. Virol.* **72**, 9479-9490.

Goossens, P. H., M. J. Havenga, E. Pieterman et al. (2001). Infection efficiency of type 5 adenoviral vectors in synovial tissue can be enhanced with a type 16 fiber. *Arthritis Rheum.* **44**, 570-577.

Graham, F. L., J. Smiley, W. C. Russell et al. (1977). Characteristics of a human cell line transformed by DNA from human adenovirus type 5. *J. Gen. Virol.* **36**, 59-74.

Graham, F. L. and A. J. van der Eb. (1973). A new technique for the assay of infectivity of human adenovirus 5 DNA. *Virology* **52**, 456-467.

Greber, U. F. (2002). Signalling in viral entry. *Cell Mol. Life Sci.* **59**, 608-626.

Greig, J. A., S. M. Buckley, S. N. Waddington et al. (2009). Influence of coagulation factor x on in vitro and in vivo gene delivery by adenovirus (Ad) 5, Ad35, and chimeric Ad5/Ad35 vectors. *Mol. Ther.* **17**, 1683-1691.

Grignon, D. J., R. Caplan, F. H. Sarkar et al. (1997). p53 status and prognosis of locally advanced prostatic adenocarcinoma: a study based on RTOG 8610. *J. Natl. Cancer Inst.* **89**, 158-165.

Grove, J. I., A. L. Lovering, C. Guise et al. (2003). Generation of Escherichia coli nitroreductase mutants conferring improved cell sensitization to the prodrug CB1954. *Cancer Res.* **63**, 5532-5537.

GTAC 14th Annual Report. (2008). Gene Therapy Advisory Committee 14th Annual Report.

Guedan, S., A. Gros, M. Cascallo et al. (2008). Syncytia formation affects the yield and cytotoxicity of an adenovirus expressing a fusogenic glycoprotein at a late stage of replication. *Gene Ther.* **15**, 1240-1245.

Guilfoyle, R. and R. Weinmann. (1981). Control region for adenovirus VA RNA transcription. *Proc. Natl. Acad. Sci. U. S. A* **78**, 3378-3382.

Guise, C. P., J. I. Grove, E. I. Hyde et al. (2007). Direct positive selection for improved nitroreductase variants using SOS triggering of bacteriophage lambda lytic cycle. *Gene Ther.* **14**, 690-698.

Guo, J. and H. Xin. (2006). Chinese gene therapy. Splicing out the West? *Science* **314**, 1232-1235.

Gupta, S., W. F. Mangel, W. J. McGrath et al. (2004). DNA binding provides a molecular strap activating the adenovirus proteinase. *Mol. Cell Proteomics.* **3**, 950-959.

Gustin, K. E. and M. J. Imperiale. (1998). Encapsidation of viral DNA requires the adenovirus L1 52/55-kilodalton protein. *J. Virol.* **72**, 7860-7870.

Gustin, K. E., P. Lutz, and M. J. Imperiale. (1996). Interaction of the adenovirus L1 52/55-kilodalton protein with the IVa2 gene product during infection. *J. Virol.* **70**, 6463-6467.

Gyurcsik, B., H. Haruki, T. Takahashi et al. (2006). Binding modes of the precursor of adenovirus major core protein VII to DNA and template activating factor I: implication for the mechanism of remodeling of the adenovirus chromatin. *Biochemistry* **45**, 303-313.

Hacein-Bey-Abina, S., A. Fischer, and M. Cavazzana-Calvo. (2002). Gene therapy of X-linked severe combined immunodeficiency. *Int. J. Hematol.* **76**, 295-298.

- Hacein-Bey-Abina, S., C. von Kalle, M. Schmidt et al. (2003). LMO2-associated clonal T cell proliferation in two patients after gene therapy for SCID-X1. *Science* **302**, 415-419.
- Hamid, O., M. L. Varterasian, S. Wadler et al. (2003). Phase II trial of intravenous CI-1042 in patients with metastatic colorectal cancer. *J. Clin. Oncol.* **21**, 1498-1504.
- Harui, A., S. Suzuki, S. Kochanek et al. (1999). Frequency and stability of chromosomal integration of adenovirus vectors. *J. Virol.* **73**, 6141-6146.
- Haruki, H., M. Okuwaki, M. Miyagishi et al. (2006). Involvement of template-activating factor I/SET in transcription of adenovirus early genes as a positive-acting factor. *J. Virol.* **80**, 794-801.
- Hasenburg, A., X. W. Tong, D. C. Fischer et al. (2001). Adenovirus-mediated thymidine kinase gene therapy in combination with topotecan for patients with recurrent ovarian cancer: 2.5-year follow-up. *Gynecol. Oncol.* **83**, 549-554.
- Hasson, T. B., D. A. Ornelles, and T. Shenk. (1992). Adenovirus L1 52- and 55-kilodalton proteins are present within assembling virions and colocalize with nuclear structures distinct from replication centers. *J. Virol.* **66**, 6133-6142.
- Haviv, Y. S., J. L. Blackwell, A. Kanerva et al. (2002). Adenoviral gene therapy for renal cancer requires retargeting to alternative cellular receptors. *Cancer Res.* **62**, 4273-4281.
- Hearing, P., R. J. Samulski, W. L. Wishart et al. (1987). Identification of a repeated sequence element required for efficient encapsidation of the adenovirus type 5 chromosome. *J. Virol.* **61**, 2555-2558.
- Hecht, J. R., R. Bedford, J. L. Abbruzzese et al. (2003). A phase I/II trial of intratumoral endoscopic ultrasound injection of ONYX-015 with intravenous gemcitabine in unresectable pancreatic carcinoma. *Clin. Cancer Res.* **9**, 555-561.
- Heise, C., T. Hermiston, L. Johnson et al. (2000). An adenovirus E1A mutant that demonstrates potent and selective systemic anti-tumoral efficacy. *Nat. Med.* **6**, 1134-1139.
- Heise, C., A. Sampson-Johannes, A. Williams et al. (1997). ONYX-015, an E1B gene-attenuated adenovirus, causes tumor-specific cytolysis and antitumoral efficacy that can be augmented by standard chemotherapeutic agents. *Nat. Med.* **3**, 639-645.
- Henning, P., K. M. Andersson, K. Frykholm et al. (2005). Tumor cell targeted gene delivery by adenovirus 5 vectors carrying knobless fibers with antibody-binding domains. *Gene Ther.* **12**, 211-224.
- Henning, P., M. K. Magnusson, E. Gunneriusson et al. (2002). Genetic modification of adenovirus 5 tropism by a novel class of ligands based on a three-helix bundle scaffold derived from staphylococcal protein A. *Hum. Gene Ther.* **13**, 1427-1439.
- Herin, M., C. Lemoine, P. Weynants et al. (1987). Production of stable cytolytic T-cell clones directed against autologous human melanoma. *Int. J. Cancer* **39**, 390-396.

Hernandez-Alcoceba, R., M. Pihalja, M. S. Wicha et al. (2000). A novel, conditionally replicative adenovirus for the treatment of breast cancer that allows controlled replication of E1a-deleted adenoviral vectors. *Hum. Gene Ther.* **11**, 2009-2024.

Hilleman, M. R. and J. H. Werner. (1954). Recovery of new agent from patients with acute respiratory illness. *Proc. Soc. Exp. Biol. Med.* **85**, 183-188.

Hindley, C. E., F. J. Lawrence, and D. A. Matthews. (2007). A role for transportin in the nuclear import of adenovirus core proteins and DNA. *Traffic.* **8**, 1313-1322.

Hoffmann, D. and O. Wildner. (2006). Restriction of adenoviral replication to the transcriptional intersection of two different promoters for colorectal and pancreatic cancer treatment. *Mol. Cancer Ther.* **5**, 374-381.

Holm, P. S., S. Bergmann, K. Jurchott et al. (2002). YB-1 relocates to the nucleus in adenovirus-infected cells and facilitates viral replication by inducing E2 gene expression through the E2 late promoter. *J. Biol. Chem.* **277**, 10427-10434.

Hong, J. S. and J. A. Engler. (1996). Domains required for assembly of adenovirus type 2 fiber trimers. *J. Virol.* **70**, 7071-7078.

Honkavuori, K. S., B. D. Pollard, M. S. Rodriguez et al. (2004). Dual role of the adenovirus pVI C terminus as a nuclear localization signal and activator of the viral protease. *J. Gen. Virol.* **85**, 3367-3376.

Horikoshi, N., A. Usheva, J. Chen et al. (1995). Two domains of p53 interact with the TATA-binding protein, and the adenovirus 13S E1A protein disrupts the association, relieving p53-mediated transcriptional repression. *Mol. Cell Biol.* **15**, 227-234.

Horton, T. M., T. S. Ranheim, L. Aquino et al. (1991). Adenovirus E3 14.7K protein functions in the absence of other adenovirus proteins to protect transfected cells from tumor necrosis factor cytolysis. *J. Virol.* **65**, 2629-2639.

Horwitz, M. S. (2004). Function of adenovirus E3 proteins and their interactions with immunoregulatory cell proteins. *J. Gene Med.* **6 Suppl 1**, S172-S183.

Howe, J. A. and S. T. Bayley. (1992). Effects of Ad5 E1A mutant viruses on the cell cycle in relation to the binding of cellular proteins including the retinoblastoma protein and cyclin A. *Virology* **186**, 15-24.

Hu, W. S. and V. K. Pathak. (2000). Design of retroviral vectors and helper cells for gene therapy. *Pharmacol. Rev.* **52**, 493-511.

Huang, M. M. and P. Hearing. (1989). The adenovirus early region 4 open reading frame 6/7 protein regulates the DNA binding activity of the cellular transcription factor, E2F, through a direct complex. *Genes Dev.* **3**, 1699-1710.

Huang, T. G., M. J. Savontaus, K. Shinozaki et al. (2003a). Telomerase-dependent oncolytic adenovirus for cancer treatment. *Gene Ther.* **10**, 1241-1247.

- Huang, W., J. Kiefer, D. Whalen et al. (2003b). DNA synthesis-dependent relief of repression of transcription from the adenovirus type 2 IVa(2) promoter by a cellular protein. *Virology* **314**, 394-402.
- Hurst, H. C. and N. C. Jones. (1987). Identification of factors that interact with the E1A-inducible adenovirus E3 promoter. *Genes Dev.* **1**, 1132-1146.
- Iftode, C. and S. J. Flint. (2004). Viral DNA synthesis-dependent titration of a cellular repressor activates transcription of the human adenovirus type 2 IVa2 gene. *Proc. Natl. Acad. Sci. U. S. A* **101**, 17831-17836.
- Invitrogen. (2007). INGN 201: Ad-p53, Ad5CMV-p53, adenoviral p53, p53 gene therapy--introgen, RPR/INGN 201. *Drugs R. D.* **8**, 176-187.
- Jaberipour, M., S. O. Vass, C. P. Guise et al. (2010). Testing double mutants of the enzyme nitroreductase for enhanced cell sensitisation to prodrugs: effects of combining beneficial single mutations. *Biochem. Pharmacol.* **79**, 102-111.
- Jacobs, J. P., C. M. Jones, and J. P. Baille. (1970). Characteristics of a human diploid cell designated MRC-5. *Nature* **227**, 168-170.
- Jakubczak, J. L., P. Ryan, M. Gorziglia et al. (2003). An oncolytic adenovirus selective for retinoblastoma tumor suppressor protein pathway-defective tumors: dependence on E1A, the E2F-1 promoter, and viral replication for selectivity and efficacy. *Cancer Res.* **63**, 1490-1499.
- Javier, R. T. (1994). Adenovirus type 9 E4 open reading frame 1 encodes a transforming protein required for the production of mammary tumors in rats. *J. Virol.* **68**, 3917-3924.
- Jin, F., P. J. Kretschmer, and T. W. Hermiston. (2005). Identification of novel insertion sites in the Ad5 genome that utilize the Ad splicing machinery for therapeutic gene expression. *Mol. Ther.* **12**, 1052-1063.
- Johnson, D. G., K. Ohtani, and J. R. Nevins. (1994). Autoregulatory control of E2F1 expression in response to positive and negative regulators of cell cycle progression. *Genes Dev.* **8**, 1514-1525.
- Johnson, J. S., Y. N. Osheim, Y. Xue et al. (2004). Adenovirus protein VII condenses DNA, represses transcription, and associates with transcriptional activator E1A. *J. Virol.* **78**, 6459-6468.
- Johnson, L., A. Shen, L. Boyle et al. (2002). Selectively replicating adenoviruses targeting deregulated E2F activity are potent, systemic antitumor agents. *Cancer Cell* **1**, 325-337.
- Jones, C. and K. A. Lee. (1991). E1A-mediated activation of the adenovirus E4 promoter can occur independently of the cellular transcription factor E4F. *Mol. Cell Biol.* **11**, 4297-4305.
- Kafri, T. (2004). Gene delivery by lentivirus vectors an overview. *Methods Mol. Biol.* **246**, 367-390.

Kaighn, M. E., J. F. Lechner, K. S. Narayan et al. (1978). Prostate carcinoma: tissue culture cell lines. *Natl. Cancer Inst. Monogr* **17**-21.

Kalyuzhniy, O., N. C. Di Paolo, M. Silvestry et al. (2008a). Adenovirus serotype 5 hexon is critical for virus infection of hepatocytes in vivo. *Proc. Natl. Acad. Sci. U. S. A* **105**, 5483-5488.

Kalyuzhniy, O., N. C. Di Paolo, M. Silvestry et al. (2008b). Adenovirus serotype 5 hexon is critical for virus infection of hepatocytes in vivo. *Proc. Natl. Acad. Sci. U. S. A* **105**, 5483-5488.

Kanerva, A., G. V. Mikheeva, V. Krasnykh et al. (2002). Targeting adenovirus to the serotype 3 receptor increases gene transfer efficiency to ovarian cancer cells. *Clin. Cancer Res.* **8**, 275-280.

Kanopka, A., O. Muhlemann, S. Petersen-Mahrt et al. (1998). Regulation of adenovirus alternative RNA splicing by dephosphorylation of SR proteins. *Nature* **393**, 185-187.

Kerem, B., J. M. Rommens, J. A. Buchanan et al. (1989). Identification of the cystic fibrosis gene: genetic analysis. *Science* **245**, 1073-1080.

Kidd, A. H., J. Chroboczek, S. Cusack et al. (1993). Adenovirus type 40 virions contain two distinct fibers. *Virology* **192**, 73-84.

King, A. J. and P. C. van der Vliet. (1994). A precursor terminal protein-trinucleotide intermediate during initiation of adenovirus DNA replication: regeneration of molecular ends in vitro by a jumping back mechanism. *EMBO J.* **13**, 5786-5792.

Kirn, D. (2001a). Clinical research results with dl1520 (Onyx-015), a replication-selective adenovirus for the treatment of cancer: what have we learned? *Gene Ther.* **8**, 89-98.

Kirn, D. (2001b). Oncolytic virotherapy for cancer with the adenovirus dl1520 (Onyx-015): results of phase I and II trials. *Expert. Opin. Biol. Ther.* **1**, 525-538.

Kleinberger, T. and T. Shenk. (1993). Adenovirus E4orf4 protein binds to protein phosphatase 2A, and the complex down regulates E1A-enhanced junB transcription. *J. Virol.* **67**, 7556-7560.

Knipe, D. M. and A. Cliffe. (2008). Chromatin control of herpes simplex virus lytic and latent infection. *Nat. Rev. Microbiol.* **6**, 211-221.

Knowlton, R. G., O. Cohen-Haguenaer, N. Van Cong et al. (1985). A polymorphic DNA marker linked to cystic fibrosis is located on chromosome 7. *Nature* **318**, 380-382.

Knox, R. J., F. Friedlos, R. F. Sherwood et al. (1992). The bioactivation of 5-(aziridin-1-yl)-2,4-dinitrobenzamide (CB1954)--II. A comparison of an Escherichia coli nitroreductase and Walker DT diaphorase. *Biochem. Pharmacol.* **44**, 2297-2301.

- Kornuc, M., S. Kliwer, J. Garcia et al. (1990). Adenovirus early region 3 promoter regulation by E1A/E1B is independent of alterations in DNA binding and gene activation of CREB/ATF and AP1. *J. Virol.* **64**, 2004-2013.
- Kotin, R. M., M. Siniscalco, R. J. Samulski et al. (1990). Site-specific integration by adeno-associated virus. *Proc. Natl Acad. Sci U. S. A* **87**, 2211-2215.
- Kovesdi, I., R. Reichel, and J. R. Nevins. (1987). Role of an adenovirus E2 promoter binding factor in E1A-mediated coordinate gene control. *Proc. Natl. Acad. Sci. U. S. A* **84**, 2180-2184.
- Kreppel, F. and S. Kochanek. (2008). Modification of adenovirus gene transfer vectors with synthetic polymers: a scientific review and technical guide. *Mol. Ther.* **16**, 16-29.
- Krougliak, V. and F. L. Graham. (1995). Development of cell lines capable of complementing E1, E4, and protein IX defective adenovirus type 5 mutants. *Hum. Gene Ther.* **6**, 1575-1586.
- Kubo, H., T. A. Gardner, Y. Wada et al. (2003). Phase I dose escalation clinical trial of adenovirus vector carrying osteocalcin promoter-driven herpes simplex virus thymidine kinase in localized and metastatic hormone-refractory prostate cancer. *Hum. Gene Ther.* **14**, 227-241.
- Kyo, S., M. Takakura, T. Fujiwara et al. (2008). Understanding and exploiting hTERT promoter regulation for diagnosis and treatment of human cancers. *Cancer Sci.* **99**, 1528-1538.
- Lang, F. F., J. M. Bruner, G. N. Fuller et al. (2003). Phase I trial of adenovirus-mediated p53 gene therapy for recurrent glioma: biological and clinical results. *J. Clin. Oncol.* **21**, 2508-2518.
- Lavoie, J. N., C. Champagne, M. C. Gingras et al. (2000). Adenovirus E4 open reading frame 4-induced apoptosis involves dysregulation of Src family kinases. *J. Cell Biol.* **150**, 1037-1056.
- Lavoie, J. N., M. Nguyen, R. C. Marcellus et al. (1998). E4orf4, a novel adenovirus death factor that induces p53-independent apoptosis by a pathway that is not inhibited by zVAD-fmk. *J. Cell Biol.* **140**, 637-645.
- Lawrence, T. S., A. W. Blackstock, and C. McGinn. (2003). The mechanism of action of radiosensitization of conventional chemotherapeutic agents. *Semin. Radiat. Oncol.* **13**, 13-21.
- Lawrence, T. S., A. Rehemtulla, E. Y. Ng et al. (1998). Preferential cytotoxicity of cells transduced with cytosine deaminase compared to bystander cells after treatment with 5-fluorocytosine. *Cancer Res.* **58**, 2588-2593.
- Lawson, R. K. (1997). Role of growth factors in benign prostatic hyperplasia. *Eur. Urol.* **32 Suppl 1**, 22-27.

- Lee, T. W., F. J. Lawrence, V. Dauksaite et al. (2004). Precursor of human adenovirus core polypeptide Mu targets the nucleolus and modulates the expression of E2 proteins. *J. Gen. Virol.* **85**, 185-196.
- Lee, T. W., D. A. Matthews, and G. E. Blair. (2005). Novel molecular approaches to cystic fibrosis gene therapy. *Biochem. J.* **387**, 1-15.
- Lee, W. S., C. C. Kao, G. O. Bryant et al. (1991). Adenovirus E1A activation domain binds the basic repeat in the TATA box transcription factor. *Cell* **67**, 365-376.
- Leppard, K. N. (1997). E4 gene function in adenovirus, adenovirus vector and adeno-associated virus infections. *J. Gen. Virol.* **78** ( Pt 9), 2131-2138.
- Li, C., D. E. Bowles, T. van Dyke et al. (2005). Adeno-associated virus vectors: potential applications for cancer gene therapy. *Cancer Gene Ther.* **12**, 913-925.
- Li, S., C. Brignole, R. Marcellus et al. (2009a). The adenovirus E4orf4 protein induces G2/M arrest and cell death by blocking protein phosphatase 2A activity regulated by the B55 subunit. *J. Virol.* **83**, 8340-8352.
- Li, S., A. Szyzborski, M. J. Miron et al. (2009b). The adenovirus E4orf4 protein induces growth arrest and mitotic catastrophe in H1299 human lung carcinoma cells. *Oncogene* **28**, 390-400.
- Lichtenstein, D. L., K. Doronin, K. Toth et al. (2004a). Adenovirus E3-6.7K protein is required in conjunction with the E3-RID protein complex for the internalization and degradation of TRAIL receptor 2. *J. Virol.* **78**, 12297-12307.
- Lichtenstein, D. L., P. Krajcsi, D. J. Esteban et al. (2002). Adenovirus RIDbeta subunit contains a tyrosine residue that is critical for RID-mediated receptor internalization and inhibition of Fas- and TRAIL-induced apoptosis. *J. Virol.* **76**, 11329-11342.
- Lichtenstein, D. L., K. Toth, K. Doronin et al. (2004b). Functions and mechanisms of action of the adenovirus E3 proteins. *Int. Rev. Immunol.* **23**, 75-111.
- Lindert, S., M. Silvestry, T. M. Mullen et al. (2009). Cryo-electron microscopy structure of an adenovirus-integrin complex indicates conformational changes in both penton base and integrin. *J. Virol.* **83**, 11491-11501.
- Liu, F. and M. R. Green. (1990). A specific member of the ATF transcription factor family can mediate transcription activation by the adenovirus E1a protein. *Cell* **61**, 1217-1224.
- Liu, G. Q., L. E. Babiss, F. C. Volkert et al. (1985). A thermolabile mutant of adenovirus 5 resulting from a substitution mutation in the protein VIII gene. *J. Virol.* **53**, 920-925.
- Liu, T. J., A. K. el Naggar, T. J. McDonnell et al. (1995). Apoptosis induction mediated by wild-type p53 adenoviral gene transfer in squamous cell carcinoma of the head and neck. *Cancer Res.* **55**, 3117-3122.

- Liu, Y. and A. Deisseroth. (2006). Tumor vascular targeting therapy with viral vectors. *Blood* **107**, 3027-3033.
- Lodygin, D., A. Epanchintsev, A. Menssen et al. (2005). Functional epigenomics identifies genes frequently silenced in prostate cancer. *Cancer Res.* **65**, 4218-4227.
- Logan, J. and T. Shenk. (1984). Adenovirus tripartite leader sequence enhances translation of mRNAs late after infection. *Proc. Natl. Acad. Sci. U. S. A* **81**, 3655-3659.
- Look, D. C., W. T. Roswit, A. G. Frick et al. (1998). Direct suppression of Stat1 function during adenoviral infection. *Immunity.* **9**, 871-880.
- Lutz, P. and C. Kedinger. (1996). Properties of the adenovirus IVa2 gene product, an effector of late-phase-dependent activation of the major late promoter. *J. Virol.* **70**, 1396-1405.
- Magi-Galluzzi, C., J. Luo, W. B. Isaacs et al. (2003). Alpha-methylacyl-CoA racemase: a variably sensitive immunohistochemical marker for the diagnosis of small prostate cancer foci on needle biopsy. *Am. J. Surg. Pathol.* **27**, 1128-1133.
- Magnusson, M. K., P. Henning, S. Myhre et al. (2007). Adenovirus 5 vector genetically re-targeted by an Affibody molecule with specificity for tumor antigen HER2/neu. *Cancer Gene Ther.* **14**, 468-479.
- Majem, M., M. Cascallo, N. Bayo-Puxan et al. (2006). Control of E1A under an E2F-1 promoter insulated with the myotonic dystrophy locus insulator reduces the toxicity of oncolytic adenovirus Ad-Delta24RGD. *Cancer Gene Ther.* **13**, 696-705.
- Makower, D., A. Rozenblit, H. Kaufman et al. (2003). Phase II clinical trial of intralesional administration of the oncolytic adenovirus ONYX-015 in patients with hepatobiliary tumors with correlative p53 studies. *Clin. Cancer Res.* **9**, 693-702.
- Mangel, W. F., M. L. Baniecki, and W. J. McGrath. (2003). Specific interactions of the adenovirus proteinase with the viral DNA, an 11-amino-acid viral peptide, and the cellular protein actin. *Cell Mol. Life Sci.* **60**, 2347-2355.
- Mannervik, M., S. Fan, A. C. Strom et al. (1999). Adenovirus E4 open reading frame 4-induced dephosphorylation inhibits E1A activation of the E2 promoter and E2F-1-mediated transactivation independently of the retinoblastoma tumor suppressor protein. *Virology* **256**, 313-321.
- Marcellus, R. C., H. Chan, D. Paquette et al. (2000). Induction of p53-independent apoptosis by the adenovirus E4orf4 protein requires binding to the Balpha subunit of protein phosphatase 2A. *J. Virol.* **74**, 7869-7877.
- Marcellus, R. C., J. G. Teodoro, T. Wu et al. (1996). Adenovirus type 5 early region 4 is responsible for E1A-induced p53-independent apoptosis. *J. Virol.* **70**, 6207-6215.

- Marienfeld, U., A. Haack, P. Thalheimer et al. (1999). 'Autoreplication' of the vector genome in recombinant adenoviral vectors with different E1 region deletions and transgenes. *Gene Ther.* **6**, 1101-1113.
- Marsh, M. P., S. K. Campos, M. L. Baker et al. (2006). Cryoelectron microscopy of protein IX-modified adenoviruses suggests a new position for the C terminus of protein IX. *J. Virol.* **80**, 11881-11886.
- Marttila, M., D. Persson, D. Gustafsson et al. (2005). CD46 is a cellular receptor for all species B adenoviruses except types 3 and 7. *J. Virol.* **79**, 14429-14436.
- Martuza, R. L., A. Malick, J. M. Markert et al. (1991). Experimental therapy of human glioma by means of a genetically engineered virus mutant. *Science* **252**, 854-856.
- Mathews, M. B. and T. Shenk. (1991). Adenovirus virus-associated RNA and translation control. *J. Virol.* **65**, 5657-5662.
- Mathias, P., T. Wickham, M. Moore et al. (1994). Multiple adenovirus serotypes use alpha v integrins for infection. *J. Virol.* **68**, 6811-6814.
- Mathis, J. M., M. A. Stoff-Khalili, and D. T. Curiel. (2005). Oncolytic adenoviruses - selective retargeting to tumor cells. *Oncogene* **24**, 7775-7791.
- Matthews, D. A. and W. C. Russell. (1998). Adenovirus core protein V is delivered by the invading virus to the nucleus of the infected cell and later in infection is associated with nucleoli. *J. Gen. Virol.* **79** ( Pt 7), 1671-1675.
- Matthews, K., P. E. Noker, B. Tian et al. (2009). Identifying the safety profile of Ad5.SSTR/TK.RGD, a novel infectivity-enhanced bicistronic adenovirus, in anticipation of a phase I clinical trial in patients with recurrent ovarian cancer. *Clin. Cancer Res.* **15**, 4131-4137.
- McCarty, D. M., P. E. Monahan, and R. J. Samulski. (2001). Self-complementary recombinant adeno-associated virus (scAAV) vectors promote efficient transduction independently of DNA synthesis. *Gene Ther.* **8**, 1248-1254.
- McNeish, I. A., N. K. Green, M. G. Gilligan et al. (1998). Virus directed enzyme prodrug therapy for ovarian and pancreatic cancer using retrovirally delivered E. coli nitroreductase and CB1954. *Gene Ther.* **5**, 1061-1069.
- Mellits, K. H., M. Kostura, and M. B. Mathews. (1990). Interaction of adenovirus VA RNA1 with the protein kinase DAI: nonequivalence of binding and function. *Cell* **61**, 843-852.
- Mellits, K. H., T. Pe'ery, and M. B. Mathews. (1992). Role of the apical stem in maintaining the structure and function of adenovirus virus-associated RNA. *J. Virol.* **66**, 2369-2377.

- Mesnil, M. and H. Yamasaki. (2000). Bystander effect in herpes simplex virus-thymidine kinase/ganciclovir cancer gene therapy: role of gap-junctional intercellular communication. *Cancer Res.* **60**, 3989-3999.
- Michael, N. P., J. K. Brehm, G. M. Anlezark et al. (1994). Physical characterisation of the Escherichia coli B gene encoding nitroreductase and its over-expression in Escherichia coli K12. *FEMS Microbiol. Lett.* **124**, 195-202.
- Miron, M. J., P. Blanchette, P. Groitl et al. (2009). Localization and importance of the adenovirus E4orf4 protein during lytic infection. *J. Virol.* **83**, 1689-1699.
- Miron, M. J., I. E. Gallouzi, J. N. Lavoie et al. (2004). Nuclear localization of the adenovirus E4orf4 protein is mediated through an arginine-rich motif and correlates with cell death. *Oncogene* **23**, 7458-7468.
- Moise, A. R., J. R. Grant, T. Z. Vitalis et al. (2002). Adenovirus E3-6.7K maintains calcium homeostasis and prevents apoptosis and arachidonic acid release. *J. Virol.* **76**, 1578-1587.
- Molin, M., L. Bouakaz, S. Berenjian et al. (2002). Unscheduled expression of capsid protein IIIa results in defects in adenovirus major late mRNA and protein expression. *Virus Res.* **83**, 197-206.
- Mondesert, G. and C. Kedinger. (1991). Cooperation between upstream and downstream elements of the adenovirus major late promoter for maximal late phase-specific transcription. *Nucleic Acids Res.* **19**, 3221-3228.
- Mondesert, G., C. Tribouley, and C. Kedinger. (1992). Identification of a novel downstream binding protein implicated in late-phase-specific activation of the adenovirus major late promoter. *Nucleic Acids Res.* **20**, 3881-3889.
- Monroe, K. R., M. C. Yu, L. N. Kolonel et al. (1995). Evidence of an X-linked or recessive genetic component to prostate cancer risk. *Nat. Med.* **1**, 827-829.
- Morin, N. and P. Boulanger. (1986). Hexon trimerization occurring in an assembly-defective, 100K temperature-sensitive mutant of adenovirus 2. *Virology* **152**, 11-31.
- Morris, D. S., S. A. Tomlins, J. E. Montie et al. (2008). The discovery and application of gene fusions in prostate cancer. *BJU. Int.* **102**, 276-282.
- Morris, S. J. and K. N. Leppard. (2009). Adenovirus serotype 5 L4-22K and L4-33K proteins have distinct functions in regulating late gene expression. *J. Virol.* **83**, 3049-3058.
- Mueller, C. and T. R. Flotte. (2008). Gene therapy for cystic fibrosis. *Clin. Rev. Allergy Immunol.* **35**, 164-178.
- Mul, Y. M. and P. C. van der Vliet. (1992). Nuclear factor I enhances adenovirus DNA replication by increasing the stability of a preinitiation complex. *EMBO J.* **11**, 751-760.

- Mul, Y. M., C. P. Verrijzer, and P. C. van der Vliet. (1990). Transcription factors NFI and NFIII/oct-1 function independently, employing different mechanisms to enhance adenovirus DNA replication. *J. Virol.* **64**, 5510-5518.
- Muller, U., T. Kleinberger, and T. Shenk. (1992). Adenovirus E4orf4 protein reduces phosphorylation of c-Fos and E1A proteins while simultaneously reducing the level of AP-1. *J. Virol.* **66**, 5867-5878.
- Murakami, P. and M. T. McCaman. (1999). Quantitation of adenovirus DNA and virus particles with the PicoGreen fluorescent Dye. *Anal. Biochem.* **274**, 283-288.
- Murray, P. G., D. Lissauer, J. Junying et al. (2003). Reactivity with A monoclonal antibody to Epstein-Barr virus (EBV) nuclear antigen 1 defines a subset of aggressive breast cancers in the absence of the EBV genome. *Cancer Res.* **63**, 2338-2343.
- Myhre, S., P. Henning, M. Friedman et al. (2009). Re-targeted adenovirus vectors with dual specificity; binding specificities conferred by two different Affibody molecules in the fiber. *Gene Ther.* **16**, 252-261.
- Myhre, S., P. Henning, O. Granio et al. (2007). Decreased immune reactivity towards a knobless, affibody-targeted adenovirus type 5 vector. *Gene Ther.* **14**, 376-381.
- Mysiak, M. E., P. E. Holthuizen, and P. C. van der Vliet. (2004a). The adenovirus priming protein pTP contributes to the kinetics of initiation of DNA replication. *Nucleic Acids Res.* **32**, 3913-3920.
- Mysiak, M. E., C. Wyman, P. E. Holthuizen et al. (2004b). NFI and Oct-1 bend the Ad5 origin in the same direction leading to optimal DNA replication. *Nucleic Acids Res.* **32**, 6218-6225.
- Nakai, H., E. Montini, S. Fuess et al. (2003). AAV serotype 2 vectors preferentially integrate into active genes in mice. *Nat. Genet.* **34**, 297-302.
- Nakai, M., K. Komiya, M. Murata et al. (2007). Expression of pIX gene induced by transgene promoter: possible cause of host immune response in first-generation adenoviral vectors. *Hum. Gene Ther.* **18**, 925-936.
- Nemerow, G. R., L. Pache, V. Reddy et al. (2009). Insights into adenovirus host cell interactions from structural studies. *Virology* **384**, 380-388.
- Nemunaitis, J., C. Cunningham, A. W. Tong et al. (2003). Pilot trial of intravenous infusion of a replication-selective adenovirus (ONYX-015) in combination with chemotherapy or IL-2 treatment in refractory cancer patients. *Cancer Gene Ther.* **10**, 341-352.
- Nemunaitis, J., N. Senzer, S. Sarmiento et al. (2007). A phase I trial of intravenous infusion of ONYX-015 and enbrel in solid tumor patients. *Cancer Gene Ther.* **14**, 885-893.
- Nemunaitis, J., A. W. Tong, M. Nemunaitis et al. (2009). A Phase I Study of Telomerase-specific Replication Competent Oncolytic Adenovirus (Telomelysin) for Various Solid Tumors. *Mol. Ther.*

- Nettelbeck, D. M., A. A. Rivera, C. Balague et al. (2002). Novel oncolytic adenoviruses targeted to melanoma: specific viral replication and cytolysis by expression of E1A mutants from the tyrosinase enhancer/promoter. *Cancer Res.* **62**, 4663-4670.
- Nevins, J. R. (1981). Mechanism of activation of early viral transcription by the adenovirus E1A gene product. *Cell* **26**, 213-220.
- Nevins, J. R. and J. E. Darnell, Jr. (1978). Steps in the processing of Ad2 mRNA: poly(A)+ nuclear sequences are conserved and poly(A) addition precedes splicing. *Cell* **15**, 1477-1493.
- Nevins, J. R. and M. C. Wilson. (1981). Regulation of adenovirus-2 gene expression at the level of transcriptional termination and RNA processing. *Nature* **290**, 113-118.
- Niidome, T. and L. Huang. (2002). Gene therapy progress and prospects: nonviral vectors. *Gene Ther.* **9**, 1647-1652.
- Nilsson, M., J. Ljungberg, J. Richter et al. (2004). Development of an adenoviral vector system with adenovirus serotype 35 tropism; efficient transient gene transfer into primary malignant hematopoietic cells. *J. Gene Med.* **6**, 631-641.
- Nupponen, N. and T. Visakorpi. (1999). Molecular biology of progression of prostate cancer. *Eur. Urol.* **35**, 351-354.
- O'Shea, C., K. Klupsch, S. Choi et al. (2005). Adenoviral proteins mimic nutrient/growth signals to activate the mTOR pathway for viral replication. *EMBO J.* **24**, 1211-1221.
- O'Shea, C. C., L. Johnson, B. Bagus et al. (2004). Late viral RNA export, rather than p53 inactivation, determines ONYX-015 tumor selectivity. *Cancer Cell* **6**, 611-623.
- Obert, S., R. J. O'Connor, S. Schmid et al. (1994). The adenovirus E4-6/7 protein transactivates the E2 promoter by inducing dimerization of a heteromeric E2F complex. *Mol. Cell Biol.* **14**, 1333-1346.
- Ohman, K., K. Nordqvist, and G. Akusjarvi. (1993). Two adenovirus proteins with redundant activities in virus growth facilitates tripartite leader mRNA accumulation. *Virology* **194**, 50-58.
- Okegawa, T., R. C. Pong, Y. Li et al. (2004). The role of cell adhesion molecule in cancer progression and its application in cancer therapy. *Acta Biochim. Pol.* **51**, 445-457.
- Ornelles, D. A. and T. Shenk. (1991). Localization of the adenovirus early region 1B 55-kilodalton protein during lytic infection: association with nuclear viral inclusions requires the early region 4 34-kilodalton protein. *J. Virol.* **65**, 424-429.
- Ostapchuk, P., M. E. Anderson, S. Chandrasekhar et al. (2006). The L4 22-kilodalton protein plays a role in packaging of the adenovirus genome. *J. Virol.* **80**, 6973-6981.
- Ostapchuk, P. and P. Hearing. (2005). Control of adenovirus packaging. *J. Cell Biochem.* **96**, 25-35.

Ostapchuk, P. and P. Hearing. (2008). Adenovirus IVa2 protein binds ATP. *J. Virol.* **82**, 10290-10294.

Ostapchuk, P., J. Yang, E. Auffarth et al. (2005). Functional interaction of the adenovirus IVa2 protein with adenovirus type 5 packaging sequences. *J. Virol.* **79**, 2831-2838.

Page, J. G., B. Tian, K. Schweikart et al. (2007). Identifying the safety profile of a novel infectivity-enhanced conditionally replicative adenovirus, Ad5-delta24-RGD, in anticipation of a phase I trial for recurrent ovarian cancer. *Am. J. Obstet. Gynecol.* **196**, 389.

Pagliario, L. C., A. Keyhani, D. Williams et al. (2003). Repeated intravesical instillations of an adenoviral vector in patients with locally advanced bladder cancer: a phase I study of p53 gene therapy. *J. Clin. Oncol.* **21**, 2247-2253.

Palmer, D. H., V. Mautner, D. Mirza et al. (2004). Virus-directed enzyme prodrug therapy: intratumoral administration of a replication-deficient adenovirus encoding nitroreductase to patients with resectable liver cancer. *J. Clin. Oncol.* **22**, 1546-1552.

Park, K., W. J. Kim, Y. H. Cho et al. (2008). Cancer gene therapy using adeno-associated virus vectors. *Front Biosci.* **13**, 2653-2659.

Parks, C. L. and T. Shenk. (1997). Activation of the adenovirus major late promoter by transcription factors MAZ and Sp1. *J. Virol.* **71**, 9600-9607.

Parks, R. J. (2005). Adenovirus protein IX: a new look at an old protein. *Mol. Ther.* **11**, 19-25.

Patel, P. Prostate cancer gene and immunotherapy. 2006.  
Ref Type: Thesis/Dissertation

Patel, P., J. G. Young, V. Mautner et al. (2009). A phase I/II clinical trial in localized prostate cancer of an adenovirus expressing nitroreductase with CB1954 [correction of CB1984]. *Mol. Ther.* **17**, 1292-1299.

Peng, Z. (2005). Current status of gendicine in China: recombinant human Ad-p53 agent for treatment of cancers. *Hum. Gene Ther.* **16**, 1016-1027.

Perez-Romero, P., K. E. Gustin, and M. J. Imperiale. (2006). Dependence of the encapsidation function of the adenovirus L1 52/55-kilodalton protein on its ability to bind the packaging sequence. *J. Virol.* **80**, 1965-1971.

Perez-Romero, P., R. E. Tyler, J. R. Abend et al. (2005). Analysis of the interaction of the adenovirus L1 52/55-kilodalton and IVa2 proteins with the packaging sequence in vivo and in vitro. *J. Virol.* **79**, 2366-2374.

Post, L. E. (2002). Selectively replicating adenoviruses for cancer therapy: an update on clinical development. *Curr. Opin. Investig. Drugs* **3**, 1768-1772.

Princen, F., P. Robe, C. Lechanteur et al. (1999). A cell type-specific and gap junction-independent mechanism for the herpes simplex virus-1 thymidine kinase gene/ganciclovir-mediated bystander effect. *Clin. Cancer Res.* **5**, 3639-3644.

Qasim, W., H. B. Gaspar, and A. J. Thrasher. (2009). Progress and prospects: gene therapy for inherited immunodeficiencies. *Gene Ther.* **16**, 1285-1291.

Querido, E., P. Blanchette, Q. Yan et al. (2001a). Degradation of p53 by adenovirus E4orf6 and E1B55K proteins occurs via a novel mechanism involving a Cullin-containing complex. *Genes Dev.* **15**, 3104-3117.

Querido, E., M. R. Morrison, H. Chu-Pham-Dang et al. (2001b). Identification of three functions of the adenovirus e4orf6 protein that mediate p53 degradation by the E4orf6-E1B55K complex. *J. Virol.* **75**, 699-709.

Quinn, D. I., S. M. Henshall, D. R. Head et al. (2000). Prognostic significance of p53 nuclear accumulation in localized prostate cancer treated with radical prostatectomy. *Cancer Res.* **60**, 1585-1594.

Rajecki, M., A. Kanerva, U. H. Stenman et al. (2007). Treatment of prostate cancer with Ad5/3Delta24hCG allows non-invasive detection of the magnitude and persistence of virus replication in vivo. *Mol. Cancer Ther.* **6**, 742-751.

Raper, S. E., N. Chirmule, F. S. Lee et al. (2003). Fatal systemic inflammatory response syndrome in a ornithine transcarbamylase deficient patient following adenoviral gene transfer. *Mol. Genet. Metab* **80**, 148-158.

Rauen, K. A., D. Sudilovsky, J. L. Le et al. (2002). Expression of the coxsackie adenovirus receptor in normal prostate and in primary and metastatic prostate carcinoma: potential relevance to gene therapy. *Cancer Res.* **62**, 3812-3818.

Raychaudhuri, P., S. Bagchi, and J. R. Nevins. (1989). DNA-binding activity of the adenovirus-induced E4F transcription factor is regulated by phosphorylation. *Genes Dev.* **3**, 620-627.

Raychaudhuri, P., R. Rooney, and J. R. Nevins. (1987). Identification of an E1A-inducible cellular factor that interacts with regulatory sequences within the adenovirus E4 promoter. *EMBO J.* **6**, 4073-4081.

Reid, T., E. Galanis, J. Abbruzzese et al. (2002). Hepatic arterial infusion of a replication-selective oncolytic adenovirus (dl1520): phase II viral, immunologic, and clinical endpoints. *Cancer Res.* **62**, 6070-6079.

Reid, T. R., S. Freeman, L. Post et al. (2005). Effects of Onyx-015 among metastatic colorectal cancer patients that have failed prior treatment with 5-FU/leucovorin. *Cancer Gene Ther.* **12**, 673-681.

Reynolds, M. A. (2008). Molecular alterations in prostate cancer. *Cancer Lett.* **271**, 13-24.

- Ring, C. J. (2002). Cytolytic viruses as potential anti-cancer agents. *J. Gen. Virol.* **83**, 491-502.
- Riordan, J. R., J. M. Rommens, B. Kerem et al. (1989). Identification of the cystic fibrosis gene: cloning and characterization of complementary DNA. *Science* **245**, 1066-1073.
- Robinson, M., Y. Ge, D. Ko et al. (2008). Comparison of the E3 and L3 regions for arming oncolytic adenoviruses to achieve a high level of tumor-specific transgene expression. *Cancer Gene Ther.* **15**, 9-17.
- Rodriguez, R., E. R. Schuur, H. Y. Lim et al. (1997). Prostate attenuated replication competent adenovirus (ARCA) CN706: a selective cytotoxic for prostate-specific antigen-positive prostate cancer cells. *Cancer Res.* **57**, 2559-2563.
- Roelvink, P. W., L. G. Mi, D. A. Einfeld et al. (1999). Identification of a conserved receptor-binding site on the fiber proteins of CAR-recognizing adenoviridae. *Science* **286**, 1568-1571.
- Roesen, N. Development of a conditionally replicating adenovirus with temporally-controlled expression of suicide gene. 2006.  
Ref Type: Thesis/Dissertation
- Rojas, J. J., M. Cascallo, S. Guedan et al. (2009). A modified E2F-1 promoter improves the efficacy to toxicity ratio of oncolytic adenoviruses. *Gene Ther.*
- Rooney, R. J., P. Raychaudhuri, and J. R. Nevins. (1990). E4F and ATF, two transcription factors that recognize the same site, can be distinguished both physically and functionally: a role for E4F in E1A trans activation. *Mol. Cell Biol.* **10**, 5138-5149.
- Rosa-Calatrava, M., L. Grave, F. Puvion-Dutilleul et al. (2001). Functional analysis of adenovirus protein IX identifies domains involved in capsid stability, transcriptional activity, and nuclear reorganization. *J. Virol.* **75**, 7131-7141.
- Rosa-Calatrava, M., F. Puvion-Dutilleul, P. Lutz et al. (2003). Adenovirus protein IX sequesters host-cell promyelocytic leukaemia protein and contributes to efficient viral proliferation. *EMBO Rep.* **4**, 969-975.
- Rothmann, T., A. Hengstermann, N. J. Whitaker et al. (1998). Replication of ONYX-015, a potential anticancer adenovirus, is independent of p53 status in tumor cells. *J. Virol.* **72**, 9470-9478.
- Rowe, W. P., R. J. Huebner, L. K. Gilmore et al. (1953). Isolation of a cytopathogenic agent from human adenoids undergoing spontaneous degeneration in tissue culture. *Proc. Soc. Exp. Biol. Med.* **84**, 570-573.
- Rudin, C. M., E. E. Cohen, V. A. Papadimitrakopoulou et al. (2003). An attenuated adenovirus, ONYX-015, as mouthwash therapy for premalignant oral dysplasia. *J. Clin. Oncol.* **21**, 4546-4552.

- Russell, W. C. (2009). Adenoviruses: update on structure and function. *J. Gen. Virol.* **90**, 1-20.
- Saban, S. D., M. Silvestry, G. R. Nemerow et al. (2006). Visualization of alpha-helices in a 6-angstrom resolution cryoelectron microscopy structure of adenovirus allows refinement of capsid protein assignments. *J. Virol.* **80**, 12049-12059.
- Sagawa, T., M. Takahashi, T. Sato et al. (2004). Prolonged survival of mice with multiple liver metastases of human colon cancer by intravenous administration of replicable E1B-55K-deleted adenovirus with E1A expressed by CEA promoter. *Mol. Ther.* **10**, 1043-1050.
- Sambrook, J., E. F. Fritsch, and T. Maniatis. 1989. *Molecular Cloning: A Laboratory Manual*. Cold Spring Harbor Press.
- Samulski, R. J., X. Zhu, X. Xiao et al. (1991). Targeted integration of adeno-associated virus (AAV) into human chromosome 19. *EMBO J.* **10**, 3941-3950.
- San Martin, C., J. N. Glasgow, A. Borovjagin et al. (2008). Localization of the N-terminus of minor coat protein IIIa in the adenovirus capsid. *J. Mol. Biol.* **383**, 923-934.
- Saphire, A. C., T. Guan, E. C. Schirmer et al. (2000). Nuclear import of adenovirus DNA in vitro involves the nuclear protein import pathway and hsc70. *J. Biol. Chem.* **275**, 4298-4304.
- Sargent, K. L., R. A. Meulenbroek, and R. J. Parks. (2004). Activation of adenoviral gene expression by protein IX is not required for efficient virus replication. *J. Virol.* **78**, 5032-5037.
- Schaack, J., W. Y. Ho, P. Freimuth et al. (1990). Adenovirus terminal protein mediates both nuclear matrix association and efficient transcription of adenovirus DNA. *Genes Dev.* **4**, 1197-1208.
- Schaley, J., R. J. O'Connor, L. J. Taylor et al. (2000). Induction of the cellular E2F-1 promoter by the adenovirus E4-6/7 protein. *J. Virol.* **74**, 2084-2093.
- Schaley, J. E., M. Polonskaia, and P. Hearing. (2005). The adenovirus E4-6/7 protein directs nuclear localization of E2F-4 via an arginine-rich motif. *J. Virol.* **79**, 2301-2308.
- Schmid, S. I. and P. Hearing. (1997). Bipartite structure and functional independence of adenovirus type 5 packaging elements. *J. Virol.* **71**, 3375-3384.
- Schneider-Brachert, W., V. Tchikov, O. Merkel et al. (2006). Inhibition of TNF receptor 1 internalization by adenovirus 14.7K as a novel immune escape mechanism. *J. Clin. Invest* **116**, 2901-2913.
- Schwiebert, L. M. (2004). Cystic fibrosis, gene therapy, and lung inflammation: for better or worse? *Am. J. Physiol Lung Cell Mol. Physiol* **286**, L715-L716.
- Segerman, A., J. P. Atkinson, M. Marttila et al. (2003). Adenovirus type 11 uses CD46 as a cellular receptor. *J. Virol.* **77**, 9183-9191.

Selley, S., J. Donovan, A. Faulkner et al. (1997). Diagnosis, management and screening of early localised prostate cancer. *Health Technol. Assess.* **1**, i, 1-i,96.

Sena-Esteves, M., Y. Saeki, C. Fraefel et al. (2000). HSV-1 amplicon vectors--simplicity and versatility. *Mol. Ther.* **2**, 9-15.

Seow, Y. and M. J. Wood. (2009). Biological gene delivery vehicles: beyond viral vectors. *Mol. Ther.* **17**, 767-777.

Shayakhmetov, D. M., A. Gaggar, S. Ni et al. (2005). Adenovirus binding to blood factors results in liver cell infection and hepatotoxicity. *J. Virol.* **79**, 7478-7491.

Shen, Y. and J. Nemunaitis. (2006). Herpes simplex virus 1 (HSV-1) for cancer treatment. *Cancer Gene Ther.* **13**, 975-992.

Shepard, R. N. and D. A. Ornelles. (2003). E4orf3 is necessary for enhanced S-phase replication of cell cycle-restricted subgroup C adenoviruses. *J. Virol.* **77**, 8593-8595.

Shimada, H., H. Matsubara, T. Shiratori et al. (2006). Phase I/II adenoviral p53 gene therapy for chemoradiation resistant advanced esophageal squamous cell carcinoma. *Cancer Sci.* **97**, 554-561.

Shirakawa, T., S. Terao, N. Hinata et al. (2007). Long-term outcome of phase I/II clinical trial of Ad-OC-TK/VAL gene therapy for hormone-refractory metastatic prostate cancer. *Hum. Gene Ther.* **18**, 1225-1232.

Short, J. J., A. V. Pereboev, Y. Kawakami et al. (2004). Adenovirus serotype 3 utilizes CD80 (B7.1) and CD86 (B7.2) as cellular attachment receptors. *Virology* **322**, 349-359.

Singleton, D. C., D. Li, S. Y. Bai et al. (2007). The nitroreductase prodrug SN 28343 enhances the potency of systemically administered armed oncolytic adenovirus ONYX-411(NTR). *Cancer Gene Ther.* **14**, 953-967.

Small, E. J., M. A. Carducci, J. M. Burke et al. (2006). A phase I trial of intravenous CG7870, a replication-selective, prostate-specific antigen-targeted oncolytic adenovirus, for the treatment of hormone-refractory, metastatic prostate cancer. *Mol. Ther.* **14**, 107-117.

Smith, T. A., N. Idamakanti, J. Marshall-Neff et al. (2003). Receptor interactions involved in adenoviral-mediated gene delivery after systemic administration in non-human primates. *Hum. Gene Ther.* **14**, 1595-1604.

Smitt, P. S., M. Driesse, J. Wolbers et al. (2003). Treatment of relapsed malignant glioma with an adenoviral vector containing the herpes simplex thymidine kinase gene followed by ganciclovir. *Mol. Ther.* **7**, 851-858.

Spaete, R. R. and N. Frenkel. (1982). The herpes simplex virus amplicon: a new eucaryotic defective-virus cloning-amplifying vector. *Cell* **30**, 295-304.

Spector, D. J., M. McGrogan, and H. J. Raskas. (1978). Regulation of the appearance of cytoplasmic RNAs from region 1 of the adenovirus 2 genome. *J. Mol. Biol.* **126**, 395-414.

- Sramkoski, R. M., T. G. Pretlow, J. M. Giaconia et al. (1999). A new human prostate carcinoma cell line, 22Rv1. *In Vitro Cell Dev. Biol. Anim* **35**, 403-409.
- Stephens, C. and E. Harlow. (1987). Differential splicing yields novel adenovirus 5 E1A mRNAs that encode 30 kd and 35 kd proteins. *EMBO J.* **6**, 2027-2035.
- Sterman, D. H., A. Recio, A. Vachani et al. (2005). Long-term follow-up of patients with malignant pleural mesothelioma receiving high-dose adenovirus herpes simplex thymidine kinase/ganciclovir suicide gene therapy. *Clin. Cancer Res.* **11**, 7444-7453.
- Sterman, D. H., J. Treat, L. A. Litzky et al. (1998). Adenovirus-mediated herpes simplex virus thymidine kinase/ganciclovir gene therapy in patients with localized malignancy: results of a phase I clinical trial in malignant mesothelioma. *Hum. Gene Ther.* **9**, 1083-1092.
- Stern, M., N. J. Caplen, J. E. Browning et al. (1998). The effect of mucolytic agents on gene transfer across a CF sputum barrier in vitro. *Gene Ther.* **5**, 91-98.
- Stewart, P. L., S. D. Fuller, and R. M. Burnett. (1993). Difference imaging of adenovirus: bridging the resolution gap between X-ray crystallography and electron microscopy. *EMBO J.* **12**, 2589-2599.
- Stone, K. R., D. D. Mickey, H. Wunderli et al. (1978). Isolation of a human prostate carcinoma cell line (DU 145). *Int. J. Cancer* **21**, 274-281.
- Stracker, T. H., C. T. Carson, and M. D. Weitzman. (2002). Adenovirus oncoproteins inactivate the Mre11-Rad50-NBS1 DNA repair complex. *Nature* **418**, 348-352.
- Strom, A. C., P. Ohlsson, and G. Akusjarvi. (1998). AR1 is an integral part of the adenovirus type 2 E1A-CR3 transactivation domain. *J. Virol.* **72**, 5978-5983.
- Strunze, S., L. C. Trotman, K. Boucke et al. (2005). Nuclear targeting of adenovirus type 2 requires CRM1-mediated nuclear export. *Mol. Biol. Cell* **16**, 2999-3009.
- Subramanian, T., B. Tarodi, and G. Chinnadurai. (1995). p53-independent apoptotic and necrotic cell deaths induced by adenovirus infection: suppression by E1B 19K and Bcl-2 proteins. *Cell Growth Differ.* **6**, 131-137.
- Sun, A., I. Shanmugam, J. Song et al. (2007). Lithium suppresses cell proliferation by interrupting E2F-DNA interaction and subsequently reducing S-phase gene expression in prostate cancer. *Prostate* **67**, 976-988.
- Sun, X., B. Pawlyk, X. Xu et al. (2010). Gene therapy with a promoter targeting both rods and cones rescues retinal degeneration caused by AIPL1 mutations. *Gene Ther.* **17**, 117-131.
- Sung, M. W., H. C. Yeh, S. N. Thung et al. (2001). Intratumoral adenovirus-mediated suicide gene transfer for hepatic metastases from colorectal adenocarcinoma: results of a phase I clinical trial. *Mol. Ther.* **4**, 182-191.

- Supiot, S., R. P. Hill, and R. G. Bristow. (2008). Nutlin-3 radiosensitizes hypoxic prostate cancer cells independent of p53. *Mol. Cancer Ther.* **7**, 993-999.
- Suzuki, K., R. Alemany, M. Yamamoto et al. (2002). The presence of the adenovirus E3 region improves the oncolytic potency of conditionally replicative adenoviruses. *Clin. Cancer Res.* **8**, 3348-3359.
- Swaminathan, S. and B. Thimmapaya. (1996). Transactivation of adenovirus E2-early promoter by E1A and E4 6/7 in the context of viral chromosome. *J. Mol. Biol.* **258**, 736-746.
- Symington, J. S., L. A. Lucher, K. H. Brackmann et al. (1986). Biosynthesis of adenovirus type 2 i-leader protein. *J. Virol.* **57**, 848-856.
- Tan, M. H., A. J. Smith, B. Pawlyk et al. (2009). Gene therapy for retinitis pigmentosa and Leber congenital amaurosis caused by defects in AIPL1: effective rescue of mouse models of partial and complete Aipl1 deficiency using AAV2/2 and AAV2/8 vectors. *Hum. Mol. Genet.* **18**, 2099-2114.
- Tannock, I. F., W. R. de, W. R. Berry et al. (2004). Docetaxel plus prednisone or mitoxantrone plus prednisone for advanced prostate cancer. *N. Engl. J. Med.* **351**, 1502-1512.
- Teh, B. S., E. Aguilar-Cordova, K. Kernen et al. (2001). Phase I/II trial evaluating combined radiotherapy and in situ gene therapy with or without hormonal therapy in the treatment of prostate cancer--a preliminary report. *Int. J. Radiat. Oncol. Biol. Phys.* **51**, 605-613.
- Teh, B. S., G. Ayala, L. Aguilar et al. (2004). Phase I-II trial evaluating combined intensity-modulated radiotherapy and in situ gene therapy with or without hormonal therapy in treatment of prostate cancer-interim report on PSA response and biopsy data. *Int. J. Radiat. Oncol. Biol. Phys.* **58**, 1520-1529.
- Temperley, S. M. and R. T. Hay. (1992). Recognition of the adenovirus type 2 origin of DNA replication by the virally encoded DNA polymerase and preterminal proteins. *EMBO J.* **11**, 761-768.
- Tenenbaum, L., E. Lehtonen, and P. E. Monahan. (2003). Evaluation of risks related to the use of adeno-associated virus-based vectors. *Curr. Gene Ther.* **3**, 545-565.
- Thomas, G. P. and M. B. Mathews. (1980). DNA replication and the early to late transition in adenovirus infection. *Cell* **22**, 523-533.
- Thomas, M. A., R. S. Broughton, F. D. Goodrum et al. (2009). E4orf1 limits the oncolytic potential of the E1B-55K deletion mutant adenovirus. *J. Virol.* **83**, 2406-2416.
- Tibbetts, C. and C. Z. Giam. (1979). In vitro association of empty adenovirus capsids with double-stranded DNA. *J. Virol.* **32**, 995-1005.

Tollefson, A. E., J. S. Ryerse, A. Scaria et al. (1996a). The E3-11.6-kDa adenovirus death protein (ADP) is required for efficient cell death: characterization of cells infected with adp mutants. *Virology* **220**, 152-162.

Tollefson, A. E., A. Scaria, T. W. Hermiston et al. (1996b). The adenovirus death protein (E3-11.6K) is required at very late stages of infection for efficient cell lysis and release of adenovirus from infected cells. *J. Virol.* **70**, 2296-2306.

Tollefson, A. E., A. Scaria, S. K. Saha et al. (1992). The 11,600-MW protein encoded by region E3 of adenovirus is expressed early but is greatly amplified at late stages of infection. *J. Virol.* **66**, 3633-3642.

Tollefson, A. E., A. Scaria, B. Ying et al. (2003). Mutations within the ADP (E3-11.6K) protein alter processing and localization of ADP and the kinetics of cell lysis of adenovirus-infected cells. *J. Virol.* **77**, 7764-7778.

Tollefson, A. E., A. R. Stewart, S. P. Yei et al. (1991). The 10,400- and 14,500-dalton proteins encoded by region E3 of adenovirus form a complex and function together to down-regulate the epidermal growth factor receptor. *J. Virol.* **65**, 3095-3105.

Tollefson, A. E., K. Toth, K. Doronin et al. (2001). Inhibition of TRAIL-induced apoptosis and forced internalization of TRAIL receptor 1 by adenovirus proteins. *J. Virol.* **75**, 8875-8887.

Tollefson, A. E., B. Ying, K. Doronin et al. (2007). Identification of a new human adenovirus protein encoded by a novel late 1-strand transcription unit. *J. Virol.* **81**, 12918-12926.

Tormanen, H., E. Backstrom, A. Carlsson et al. (2006). L4-33K, an adenovirus-encoded alternative RNA splicing factor. *J. Biol. Chem.* **281**, 36510-36517.

Toth, M., W. Doerfler, and T. Shenk. (1992). Adenovirus DNA replication facilitates binding of the MLTF/USF transcription factor to the viral major late promoter within infected cells. *Nucleic Acids Res.* **20**, 5143-5148.

Touraine, R. L., H. Ishii-Morita, W. J. Ramsey et al. (1998). The bystander effect in the HSVtk/ganciclovir system and its relationship to gap junctional communication. *Gene Ther.* **5**, 1705-1711.

Trask, T. W., R. P. Trask, E. Aguilar-Cordova et al. (2000). Phase I study of adenoviral delivery of the HSV-tk gene and ganciclovir administration in patients with current malignant brain tumors. *Mol. Ther.* **1**, 195-203.

Tribouley, C., P. Lutz, A. Staub et al. (1994). The product of the adenovirus intermediate gene IVa2 is a transcriptional activator of the major late promoter. *J. Virol.* **68**, 4450-4457.

Trotman, L. C., N. Mosberger, M. Fornerod et al. (2001). Import of adenovirus DNA involves the nuclear pore complex receptor CAN/Nup214 and histone H1. *Nat. Cell Biol.* **3**, 1092-1100.

Tsukuda, K., R. Wiewrodt, K. Molnar-Kimber et al. (2002). An E2F-responsive replication-selective adenovirus targeted to the defective cell cycle in cancer cells: potent antitumoral efficacy but no toxicity to normal cell. *Cancer Res.* **62**, 3438-3447.

Turnell, A. S., R. J. Grand, and P. H. Gallimore. (1999). The replicative capacities of large E1B-null group A and group C adenoviruses are independent of host cell p53 status. *J. Virol.* **73**, 2074-2083.

Turnell, A. S., G. S. Stewart, R. J. Grand et al. (2005). The APC/C and CBP/p300 cooperate to regulate transcription and cell-cycle progression. *Nature* **438**, 690-695.

Tyler, R. E., S. G. Ewing, and M. J. Imperiale. (2007). Formation of a multiple protein complex on the adenovirus packaging sequence by the IVa2 protein. *J. Virol.* **81**, 3447-3454.

Ullman, A. J., N. C. Reich, and P. Hearing. (2007). Adenovirus E4 ORF3 protein inhibits the interferon-mediated antiviral response. *J. Virol.* **81**, 4744-4752.

Vales, L. D. and J. E. Darnell, Jr. (1989). Promoter occlusion prevents transcription of adenovirus polypeptide IX mRNA until after DNA replication. *Genes Dev.* **3**, 49-59.

van Breukelen, B., P. N. Kanellopoulos, P. A. Tucker et al. (2000). The formation of a flexible DNA-binding protein chain is required for efficient DNA unwinding and adenovirus DNA chain elongation. *J. Biol. Chem.* **275**, 40897-40903.

Varga, M. J., C. Weibull, and E. Everitt. (1991). Infectious entry pathway of adenovirus type 2. *J. Virol.* **65**, 6061-6070.

Varghese, S. and S. D. Rabkin. (2002). Oncolytic herpes simplex virus vectors for cancer virotherapy. *Cancer Gene Ther.* **9**, 967-978.

Vasey, P. A., L. N. Shulman, S. Campos et al. (2002). Phase I trial of intraperitoneal injection of the E1B-55-kd-gene-deleted adenovirus ONYX-015 (dl1520) given on days 1 through 5 every 3 weeks in patients with recurrent/refractory epithelial ovarian cancer. *J. Clin. Oncol.* **20**, 1562-1569.

Vass, S. O. Increasing the Efficiency of Enzyme Prodrug Systems for Cancer Gene Therapy. 2007.

Ref Type: Thesis/Dissertation

Vass, S. O., D. Jarrom, W. R. Wilson et al. (2009). E. coli NfsA: an alternative nitroreductase for prodrug activation gene therapy in combination with CB1954. *Br. J. Cancer* **100**, 1903-1911.

Vellinga, J., J. de Vrij, S. Myhre et al. (2007). Efficient incorporation of a functional hyper-stable single-chain antibody fragment protein-IX fusion in the adenovirus capsid. *Gene Ther.* **14**, 664-670.

- Vellinga, J., M. J. Rabelink, S. J. Cramer et al. (2004). Spacers increase the accessibility of peptide ligands linked to the carboxyl terminus of adenovirus minor capsid protein IX. *J. Virol.* **78**, 3470-3479.
- Vellinga, J., H. S. Van der, and R. C. Hoeben. (2005). The adenovirus capsid: major progress in minor proteins. *J. Gen. Virol.* **86**, 1581-1588.
- Virtanen, A., P. Gilardi, A. Naslund et al. (1984). mRNAs from human adenovirus 2 early region 4. *J. Virol.* **51**, 822-831.
- Virtanen, A. and U. Pettersson. (1985). Organization of early region 1B of human adenovirus type 2: identification of four differentially spliced mRNAs. *J. Virol.* **54**, 383-391.
- Waddington, S. N., J. H. McVey, D. Bhella et al. (2008). Adenovirus serotype 5 hexon mediates liver gene transfer. *Cell* **132**, 397-409.
- Walters, R. W., P. Freimuth, T. O. Moninger et al. (2002). Adenovirus fiber disrupts CAR-mediated intercellular adhesion allowing virus escape. *Cell* **110**, 789-799.
- Wang, K., S. Huang, A. Kapoor-Munshi et al. (1998). Adenovirus internalization and infection require dynamin. *J. Virol.* **72**, 3455-3458.
- Wang, Q., X. C. Jia, and M. H. Finer. (1995). A packaging cell line for propagation of recombinant adenovirus vectors containing two lethal gene-region deletions. *Gene Ther.* **2**, 775-783.
- Weber, J. (1976). Genetic analysis of adenovirus type 2 III. Temperature sensitivity of processing viral proteins. *J. Virol.* **17**, 462-471.
- Weedon, S. J., N. K. Green, I. A. McNeish et al. (2000). Sensitisation of human carcinoma cells to the prodrug CB1954 by adenovirus vector-mediated expression of E. coli nitroreductase. *Int. J. Cancer* **86**, 848-854.
- Weiss, R. S. and R. T. Javier. (1997). A carboxy-terminal region required by the adenovirus type 9 E4 ORF1 oncoprotein for transformation mediates direct binding to cellular polypeptides. *J. Virol.* **71**, 7873-7880.
- Weiss, R. S., S. S. Lee, B. V. Prasad et al. (1997). Human adenovirus early region 4 open reading frame 1 genes encode growth-transforming proteins that may be distantly related to dUTP pyrophosphatase enzymes. *J. Virol.* **71**, 1857-1870.
- Whyte, P., K. J. Buchkovich, J. M. Horowitz et al. (1988). Association between an oncogene and an anti-oncogene: the adenovirus E1A proteins bind to the retinoblastoma gene product. *Nature* **334**, 124-129.
- Wickham, T. J., P. Mathias, D. A. Cheresch et al. (1993). Integrins alpha v beta 3 and alpha v beta 5 promote adenovirus internalization but not virus attachment. *Cell* **73**, 309-319.

Wiethoff, C. M., H. Wodrich, L. Gerace et al. (2005). Adenovirus protein VI mediates membrane disruption following capsid disassembly. *J. Virol.* **79**, 1992-2000.

Wilson, J. M., J. F. Engelhardt, M. Grossman et al. (1994). Gene therapy of cystic fibrosis lung disease using E1 deleted adenoviruses: a phase I trial. *Hum. Gene Ther.* **5**, 501-519.

Wilson-Rawls, J. and W. S. Wold. (1993). The E3-6.7K protein of adenovirus is an Asn-linked integral membrane glycoprotein localized in the endoplasmic reticulum. *Virology* **195**, 6-15.

Wodrich, H., A. Cassany, M. A. D'Angelo et al. (2006). Adenovirus core protein pVII is translocated into the nucleus by multiple import receptor pathways. *J. Virol.* **80**, 9608-9618.

Wodrich, H., T. Guan, G. Cingolani et al. (2003). Switch from capsid protein import to adenovirus assembly by cleavage of nuclear transport signals. *EMBO J.* **22**, 6245-6255.

Wohl, B. P. and P. Hearing. (2008). Role for the L1-52/55K protein in the serotype specificity of adenovirus DNA packaging. *J. Virol.* **82**, 5089-5092.

Wold, W. S. and L. R. Gooding. (1991). Region E3 of adenovirus: a cassette of genes involved in host immunosurveillance and virus-cell interactions. *Virology* **184**, 1-8.

Wolf, J. K., D. C. Bodurka, J. B. Gano et al. (2004). A phase I study of Adp53 (INGN 201; ADVEXIN) for patients with platinum- and paclitaxel-resistant epithelial ovarian cancer. *Gynecol. Oncol.* **94**, 442-448.

Work, L. M., N. Ritchie, S. A. Nicklin et al. (2004). Dual targeting of gene delivery by genetic modification of adenovirus serotype 5 fibers and cell-selective transcriptional control. *Gene Ther.* **11**, 1296-1300.

<http://www.cancer.gov/statistics/> (2009) U.S. National Cancer Institute Statistics

<http://www.ictvonline.org/virusTaxonomy.asp?version=2009> (2009) International Committee on Taxonomy of Viruses

<http://www.statistics.gov.uk/statbase/Product.asp?vlnk=15096> (2009) Office for National Statistics

<http://www.wiley.co.uk/genetherapy/clinical/> (2009) Gene Therapy Clinical Trials Worldwide

Xi, Q., R. Cuesta, and R. J. Schneider. (2005). Regulation of translation by ribosome shunting through phosphotyrosine-dependent coupling of adenovirus protein 100k to viral mRNAs. *J. Virol.* **79**, 5676-5683.

Xin, H. (2006). Chinese gene therapy. Gendicine's efficacy: hard to translate. *Science* **314**, 1233.

Xu, F., S. Li, X. L. Li et al. (2009). Phase I and biodistribution study of recombinant adenovirus vector-mediated herpes simplex virus thymidine kinase gene and ganciclovir

administration in patients with head and neck cancer and other malignant tumors. *Cancer Gene Ther.* **16**, 723-730.

Yalkinoglu, A. O., R. Heilbronn, A. Burkle et al. (1988). DNA amplification of adeno-associated virus as a response to cellular genotoxic stress. *Cancer Res.* **48**, 3123-3129.

Yang, C., C. Cirielli, M. C. Capogrossi et al. (1995). Adenovirus-mediated wild-type p53 expression induces apoptosis and suppresses tumorigenesis of prostatic tumor cells. *Cancer Res.* **55**, 4210-4213.

Yang, T. T., P. Sinai, and S. R. Kain. (1996a). An acid phosphatase assay for quantifying the growth of adherent and nonadherent cells. *Anal. Biochem.* **241**, 103-108.

Yang, Y., Q. Su, and J. M. Wilson. (1996b). Role of viral antigens in destructive cellular immune responses to adenovirus vector-transduced cells in mouse lungs. *J. Virol.* **70**, 7209-7212.

Yegnasubramanian, S., J. Kowalski, M. L. Gonzalgo et al. (2004). Hypermethylation of CpG islands in primary and metastatic human prostate cancer. *Cancer Res.* **64**, 1975-1986.

Ying, B., K. Toth, J. F. Spencer et al. (2009). INGN 007, an oncolytic adenovirus vector, replicates in Syrian hamsters but not mice: comparison of biodistribution studies. *Cancer Gene Ther.* **16**, 625-637.

Ying, B. and W. S. Wold. (2003). Adenovirus ADP protein (E3-11.6K), which is required for efficient cell lysis and virus release, interacts with human MAD2B. *Virology* **313**, 224-234.

Young, C. S. (2003). The structure and function of the adenovirus major late promoter. *Curr. Top. Microbiol. Immunol.* **272**, 213-249.

Yu, S. F., T. von Ruden, P. W. Kantoff et al. (1986). Self-inactivating retroviral vectors designed for transfer of whole genes into mammalian cells. *Proc. Natl. Acad. Sci. U. S. A* **83**, 3194-3198.

Yueh, A. and R. J. Schneider. (1996). Selective translation initiation by ribosome jumping in adenovirus-infected and heat-shocked cells. *Genes Dev.* **10**, 1557-1567.

Zeimet, A. G. and C. Marth. (2003). Why did p53 gene therapy fail in ovarian cancer? *Lancet Oncol.* **4**, 415-422.

Zhang, W. and M. J. Imperiale. (2000). Interaction of the adenovirus IVa2 protein with viral packaging sequences. *J. Virol.* **74**, 2687-2693.

Zhou, H., W. O'Neal, N. Morral et al. (1996). Development of a complementing cell line and a system for construction of adenovirus vectors with E1 and E2a deleted. *J. Virol.* **70**, 7030-7038.

Zou, A., I. Atencio, W. M. Huang et al. (2004). Overexpression of adenovirus E3-11.6K protein induces cell killing by both caspase-dependent and caspase-independent mechanisms. *Virology* **326**, 240-249.

Zubieta, C., G. Schoehn, J. Chroboczek et al. (2005). The structure of the human adenovirus 2 penton. *Mol. Cell* **17**, 121-135.